PNWD-3824
WTP-RPT-153 Rev. 0

Estimate of Hanford Waste Insoluble Solid Particle Size and Density Distribution

B. E. Wells
M. A. Knight

E. C. Buck
R. C. Daniel
P. A. Meyer
J. M. Tingey
W. S. Callaway III
M. E. Johnson
D. J. Washenfelder
M. N. Hall
S. L. Thomson

S. K. Cooley
L. A. Mahoney
A. P. Poloski

G. A. Cooke
M. G. Thien
J. J. Davis
G. L. Smith
Y. Onishi

February 2007

Prepared for Bechtel National, Inc.
under Contract No. 24590-101-TSA-W000-00004

LEGAL NOTICE

This report was prepared by Battelle – Pacific Northwest Division (Battelle) as an account of sponsored research activities. Neither Client nor Battelle nor any person acting on behalf of either:

MAKES ANY WARRANTY OR REPRESENTATION, EXPRESS OR IMPLIED, with respect to the accuracy, completeness, or usefulness of the information contained in this report, or that the use of any information, apparatus, process, or composition disclosed in this report may not infringe privately owned rights; or

Assumes any liabilities with respect to the use of, or for damages resulting from the use of, any information, apparatus, process, or composition disclosed in this report.

References herein to any specific commercial product, process, or service by trade name, trademark, manufacturer, or otherwise, does not necessarily constitute or imply its endorsement, recommendation, or favoring by Battelle. The views and opinions of authors expressed herein do not necessarily state or reflect those of Battelle.

Estimate of Hanford Waste Insoluble Solid Particle Size and Density Distribution

B. E. Wells, Chair, Particulate Characterization Working Group
Battelle – Pacific Northwest Division
M. A. Knight, Chair, Risk Assessment Working Group
CH2M HILL

E. C. Buck
S. K. Cooley
R. C. Daniel
L. A. Mahoney
P. A. Meyer
A. P. Poloski
J. M. Tingey
W. S. Callaway III[a]
G. A. Cooke[a]
M. E. Johnson[a]
M. G. Thien[a]
D. J. Washenfelder[a]
J. J. Davis[b]
M. N. Hall[c]
G. L. Smith[c]
S. L. Thomson[c]
Y Onishi[d]

February 2007

Subcontract No. 24590-101-TSA-W000-0004, SCN 63

for W. Tamosaitis 2/26/07
ACCEPTED FOR
WTP PROJECT USE

Battelle – Pacific Northwest Division
Richland, Washington, 99352

(a) CH2M HILL
(b) U.S. Department of Energy Office of River Protection
(c) Bechtel National Inc.
(d) Yasuo Onishi Consulting, LLC

Completeness of Testing

This report summarizes the results of analyses of data obtained from the referenced analyses of Hanford waste. The analyses and the report, which used data from, but did not involve laboratory testing, followed the quality assurance requirements outlined in Pacific Northwest Division's Waste Treatment Plant Support Project Quality Assurance Requirements and Description Manual.

The descriptions provided in this report are an accurate account of both the conduct of the work and the data analyses performed. A summary of the analysis results is reported. Also reported are any unusual or anomalous occurrences that are different from expected results. The analysis results and this report have been reviewed and verified.

Approved:

Gordon H. Beeman

Gordon H. Beeman, Manager
WTP R&T Support Project

2/6/07
Date

Testing Summary

The U.S. Department of Energy (DOE) Office of River Protection's Waste Treatment and Immobilization Plant (WTP) will process and treat radioactive waste that is stored in tanks at the Hanford Site. Piping and pumps have been selected to transport the high-level waste (HLW) slurries in the WTP.

This report addresses the analyses performed by the Particulate Characterization Working Group (PCWG) and Risk Assessment Working Group comprising Battelle – Pacific Northwest Division (PNWD), Bechtel National Inc. (BNI), CH2M HILL Hanford Group, Inc. (CH2M HILL), U.S. Department of Energy Office of River Protection (DOE ORP) and Yasuo Onishi Consulting, LLC staff on data obtained from documented Hanford waste analyses to determine a best-estimate insoluble solid particle size and density distribution (PSDD) and its relation to slurry transport.

The scope of the PCWG efforts is specified in the approved WTP Issue Response Plan (BNI 2006a). The actual testing activities were performed and reported separately in referenced documentation. Because of this, many of the required topics below do not apply and are so noted.

Test Objectives

This section is not applicable. No testing was performed for this investigation.

Test Exceptions

This section is not applicable. No testing was performed for this investigation.

Results and Performance Against Success Criteria

This section is not applicable. No testing was performed for this investigation.

Quality Requirements

PNWD's Quality Assurance Program is based on requirements defined in U.S. Department of Energy (DOE) Order 414.1C, Quality Assurance, and 10 CFR 830, Energy/Nuclear Safety Management, Subpart A–Quality Assurance Requirements (a.k.a. the Quality Rule). PNWD has chosen to implement the requirements of DOE Order 414.1C and 10 CFR 830 Subpart A by integrating them into the Laboratory's management systems and daily operating processes. The procedures necessary to implement the requirements are documented through PNWD's Standards-Based Management System.

PNWD implements the DOE River Protection Project (RPP) WTP quality requirements by performing work in accordance with the PNWD WTP Support Program (SP) quality assurance project plan (QAPjP) approved by the RPP-WTP Quality Assurance (QA) organization. This work was performed to the quality requirements of NQA-1-1989 Part I, Basic and Supplementary Requirements, NQA-2a-1990 Part 2.7 and DOE/RW-0333P Rev. 13. These quality requirements are implemented through PNWD's WTPSP Quality Assurance Requirements and Description Manual. The requirements of

DOE/RW-0333P, Rev 13, Quality Assurance Requirements and Descriptions (QARD) were not required for this work.

This report is based on data from testing as referenced. PNWD assumes that the data from these references have been fully reviewed and documented in accordance with the analysts' QA programs. PNWD only analyzed data from the referenced documentation. At PNWD, the performed calculations, the documentation, and reporting of results and conclusions were performed in accordance with the WTPSP QA program. Internal verification and validation activities were addressed by conducting an independent technical review of the final data report in accordance with PNWD procedure QA-RPP-WTP-604. This review verifies that the reported results are traceable, that inferences and conclusions are soundly based, and that the reported work satisfies the Test Plan objectives. This review procedure is part of PNWD's WTPSP Quality Assurance Requirements and Description Manual.

Test Conditions

This section is not applicable. No testing was performed for this investigation.

Simulant Use

This section is not applicable. No testing was performed for this investigation.

Results of Data Analysis

Representative particle size and density distributions (PSDDs) of Hanford waste insoluble solids have been developed based on a new approach for relating measured particle size distributions (PSDs) to solid-phase compounds. This work was achieved through extensive review of available Hanford waste PSDs and solid-phase compound data. Composite PSDs representing the waste in up to 19 Hanford waste tanks were developed, and the insoluble solid-phase compounds for the 177 Hanford waste tanks, their relative fractions, crystal densities, and particle size and shape were developed. The agglomeration of these compounds has been modeled with a fractal dimension analysis. A Monte Carlo simulation approach was used to model the PSDDs.

The solid-phase compound information was modeled with the best-estimate PSDs via Monte Carlo simulations into PSDDs such that:

- The composite PSDs are reproduced.
- The solid-phase compound mass fractions are reproduced.
- The expected in situ bulk-solids density is qualitatively reproduced.
- A representative fraction of the waste volume comprising agglomerates is qualitatively reproduced.

Four particle size and density distributions were developed and evaluated. The different cases considered are:

- Case 1. Sonicated PSD Case
  - Primary particles and hard agglomerates are assigned crystal density
- Case 2. Sonicated PSD Case
  - Primary particles are assigned crystal density
  - Density of hard agglomerates assigned via fractal relation
- Case 3. Minimal Disturbance PSD Case
  - Primary particles, soft and hard agglomerates are assigned crystal density
- Case 4. Minimal Disturbance PSD Case
  - Primary particles are assigned crystal density
  - Density of soft and hard agglomerates assigned via fractal relation

For each case, a representative PSDD for each case based on a deterministic calculation on the centroid input data (i.e., solid-phase compounds volume fraction, primary particle size, and PSD) values of the Monte Carlo simulation is provided as matrices of volume-based probability (i.e., the compound volume fraction) of each of the solid-phase compounds to exist in a PSD particle size bin and their associated density in that bin. The largest volume fraction of large-dense particulate is achieved for Case 3 and the minimum amount for Case 2. The specific largest volume fractions in the PSDDs, that is, the most likely particulate on a volume basis, 0.05 for Cases 1 and 3 and 0.03 for Cases 2 and 4, occurs at 7.7 μm for each case. The corresponding densities are 2.42 g/mL for Cases 1 and 3, and 1.44 g/mL for Cases 2 and 4.

The PSDDs resulting from this new approach provide a "best representation" of a volume-based probability for the Hanford waste insoluble solid particles in terms of particle size and density. Any application of the provided PSDDs must acknowledge the presented limitations of the available data. Additionally, given the composite nature of the approach, the PSDDs may be expected to vary within specific waste streams. The PSDDs provided herein are neither bounding nor conservative.

Critical velocity calculations have been conducted for each PSDD. The critical velocity equations specified by BNI (2006b) were employed. The applicability of these models to the current study conditions was not evaluated.

Recommendations are made regarding application the PSDDs to critical velocity calculations and validation thereof as well as waste sample analysis to address the current data limitations.

Discrepancies and Follow-on Tests

This section is not applicable. No testing was performed for this investigation.

Summary References

Bechtel National Inc. (BNI). 2006a. *Issue Response Plan for Implementation of External Flowsheet Review Team (EFRT) Recommendations - M1, Plugging in Process Piping*. 24590-WTP-PL-ENG-06-0010 Rev. 0, BNI, Richland, Washington.

Bechtel National Inc. (BNI). 2006b. *Minimum Flow Velocity for Slurry Lines*. 24590-WTP-GPG-M-0058 Rev. 0, BNI, Richland, Washington.

Acknowledgments

Bechtel National Inc., CH2M HILL, U.S. Department of Energy Office of River Protection, Yasuo Onishi Consulting LLC, and Battelle – Pacific Northwest Division staff provided critical expert elicitation to define pertinent parameters with available data.

Acronyms and Abbreviations

BBI	Best Basis Inventory
BNI	Bechtel National, Inc.
CDF	cumulative distribution plot
HLW	high-level waste
MW	molecular weight
PNWD	Battelle – Pacific Northwest Division
PSD	particle size distribution
PSDD	particle size and density distribution
QA	quality assurance
RSD	relative standard deviation
SEM	scanning electron microscopy
TEM	transmission electron microscopy
TRU	transuranic waste
WIPP	Waste Isolation Pilot Plant
WTP	Waste Treatment Plant
XRD	X-ray diffraction

Nomenclature

β	broadening of XRD peaks
$\delta M_{n,j}$	uncertainty in each individual-tank mass term
δm_j	error in the total mass (over all tanks) of each compound
δV	error in the total volume of each compound
δT	propagated error in the total volume
$\delta\phi_j$	propagated error in the volume fraction
$\delta\phi_j/\phi_j$	estimate of the relative uncertainty in the volume fractions
Θ	peak position
λ	X-ray wavelength
μ_L	liquid dynamic viscosity
υ	liquid kinematic viscosity
ρ_L	liquid density (kg/m^3)
ρ_S	density of solid
ρ_A	agglomerate density
ρ_{Aij}	agglomerate density of compound j for bin i
ρ_{Sj}	crystal density of compound j
ϕ_{ESP}	ESP-predicted dry solid fraction, average of all the waste in the tank
ϕ_j	volume fraction of each compound in the N-tank average composition

χ	fraction of eddies having velocities equal to or greater than settling velocity

a, b, c	longest, intermediate, and shortest mutually perpendicular axes of the particle
b_s	constant
C	volume fraction of undissolved solid in the flow
C_V	primary particle's volume fraction
$c_{n,j}$	ESP output providing a set of kg/L concentrations
D	fractal dimension
D_j	fractal dimension of compound j
D_p	pipe diameter (m)
d	particle diameter (m)
d_i	particle diameter for bin i
d_j	primary particle size of compound j
$\{d_i, f_i\}$	fractional counts versus particle diameter bins for i=1,N
E	mass fraction error
f_i	fractional abundance
$f_{ij,agg}$	fraction of agglomerates in bin *i* for chemical species *j* based on primary particle size $d_{j,}$
f_{ij}	volume fraction of material in bin *i* below maximum diameter for species *j*
g	gravitational acceleration
M_j	calculated mass of solid phase compound j
Mn_j	normalized mass of species j over the input PSD
$M_{j,0}$	input mass fraction of compound j
m_j	total mass of each compound over all tanks
m^*_j	non-normalized mass of species j over the PSD histogram
N	number of tanks
N_B	number of bins in the PSD histogram
N_C	number of solid-phase compounds
n_s	constant
n	tank the concentration is for
R	agglomerate size
R_i	particle size of bin i; agglomerate size
r	primary particle size
r_j	primary particle size of compound j
S	ratio of the solid density to liquid density, ρ_S/ρ_L
S_F	average dawsonite shape factor
s	cumulative distribution
T	total volume of all dry solids
U_c	critical velocity
V	total waste volume in the tank as defined by the BBI
V_i	volume fraction of overall PSD for bin i

V_S	dry solid volume in the tank
W_j	weighting vector
X	volume fraction or average density of case being considered

Contents

Figures

Tables

1.0 Introduction

The DOE Office of River Protection's Waste Treatment and Immobilization Plant (WTP) is being designed and built to pretreat and then vitrify a large portion of the wastes in Hanford's 177 underground waste storage tanks. Because of the variability of the waste, WTP process piping must be capable of transporting a wide range of materials, including Newtonian and non-Newtonian fluids, slurries with differing solids concentrations, and slurries with mechanical and chemical plugging potential.

A minimum pipeline velocity is required to avoid mechanical plugging for slurries. This minimum or critical velocity is a function of the solid particle size and morphology, particle density, solid concentration, the carrier fluid, and the pipeline configuration. It is defined as the minimum velocity demarcating flows in which the solids form a bed at the bottom of the pipe to fully suspended flow (Oroskar and Turian 1980). The analytical prediction method for the WTP critical velocities is provided in BNI (2006a). The Oroskar and Turian (1980) calculation for the critical velocity, U_c, listed in BNI (2006a) may be determined by

$$U_c = \sqrt{gd(S-1)}\left[1.85C^{0.1536}(1-C)^{0.3564}\left(\frac{D_p}{d}\right)^{0.378}\left(\frac{\rho_L D_p\sqrt{gd(S-1)}}{\mu_L}\right)^{0.09}\chi^{0.3}\right] \tag{1.1}$$

where

g = gravitational acceleration (m/s^2)
d = particle diameter (m)
S = ratio of the solid density to liquid density, ρ_S/ρ_L
C = volume fraction of undissolved solid in the flow
D_p = pipe diameter (m)
ρ_L = liquid density (kg/m^3)
μ_L = liquid dynamic viscosity (Pa s)
χ = fraction of eddies having velocities equal to or greater than the settling velocity (set to 0.96).

To calculate the velocity at which sliding bed will transition to a stationary bed, BNI (2006a) provides the Thomas equation (Thomas 1976, 1979) as

$$U_T = 9\left(\frac{g\mu_L(S-1)}{\rho_L}\right)^{0.37}\left(\frac{D_p\rho_L}{\mu_L}\right)^{0.11} \tag{1.2}$$

BNI (2006a) states that the lower limit of the median particle size for the experimental data used in the development of the Oroskar and Turian equation was 100 μm, while the Thomas equation is applicable if the fluid stream contains particles which are less than 74 μm in size.

The undissolved solids and therefore their size and density affect the critical velocity calculation. In the absence of specific WTP as-received process stream data, the physical properties of the insoluble solid waste in the Hanford tank farm are used as the initial condition of the waste received at the WTP.

Waste will be fed to the WTP by the Hanford waste feed delivery system. High-level waste (HLW) feed includes insoluble solids consisting primarily of oxides and hydroxides of metals used in the fabrication and reprocessing of nuclear fuels. These solid particles range in size and density from small, dense, primary particles to large, low-density, diffuse flocs or soft agglomerates and large, relatively dense, cemented aggregates and stable agglomerates (collectively termed hard agglomerates). Figure 1.1 depicts these different particles.

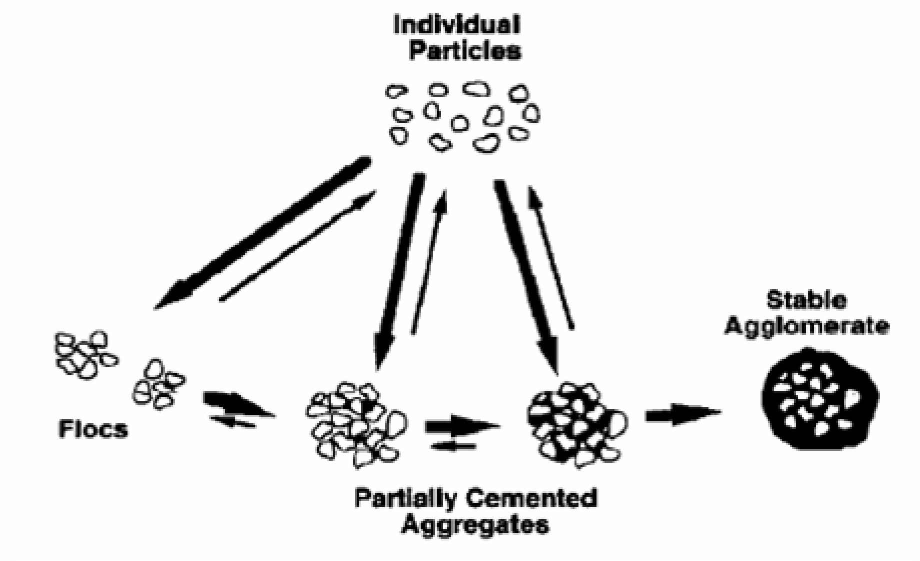

Figure 1.1. Solid Particles and Soft and Hard Agglomerates (from Ilievski and White 1994)

The individual particle size in a waste stream may vary by five orders of magnitude, and is affected by the constituents present. As stated by Jewett et al. (2002),

> …the smallest particles are many oxides and hydroxides, including ZrO_2 and FeOOH, whose diameters are in the 3 to 6 nm range. Other particles such as boehmite (AlOOH) and apatite are in the 0.1 to 1 μm size range. These submicron primary particles found in many HLW tanks form agglomerates typically 1 to 10 μm is size, but can reach 100 μm or more (Herting 1997, Bunker et al. 2000). Some of the largest primary particles are gibbsite ($Al(OH)_3$) and uranium phosphate, which can exceed 20 μm in size.

Because the individual primary particles vary in size and density, the agglomerates formed from them also vary in density.

Many studies have been conducted to determine the particle size and constituents of the undissolved solids in the Hanford waste. However, the available information relating the particle size and the constituents is limited. This report describes a new approach for relating measured particle size distribution (PSDs) to solid-phase compounds and generating expected particle size and density distributions (PSDDs).

Solid-phase compounds considered the most probable constituents of insoluble Hanford waste, their relative volume fractions, crystal density, maximum primary particle size, and maximum agglomeration size are identified. These compounds are then modeled with the best-estimate PSD such that the PSD probability is reproduced, and the in situ estimated bulk solid density and expected fraction of agglomerates are represented. The PSD and solid-phase compound data typically are not available for equivalent samples. Thus, data were combined that are not directly correlated.

The PSDDs resulting from this new approach provide a “best representation” of a volume-based probability for the Hanford waste insoluble solid particles in terms of particle size and density. Any application of the provided PSDDs must acknowledge the limitations of the available data. Additionally, given the composite nature of the approach, the PSDDs may be expected to vary with regard to specific waste streams. The PSDDs provided herein are neither bounding nor conservative.

Section 3 presents the data sources considered and the development of the best-estimate data sets for PSDs and solid-phase compounds. The relation of the available data sets with regard to the insoluble solid inventory at Hanford is discussed. Quantifiable uncertainties in the data are elucidated. The particle size and density distribution (PSDD) models are presented in Section 4, and the PSDD results and critical velocity criterion calculations are given in Section 5. Conclusions and recommendations are presented in Section 6, and references are listed in Section 7. Supporting information is included in the appendixes.

2.0 Quality Requirements

PNWD's Quality Assurance Program is based on requirements defined in U.S. Department of Energy (DOE) Order 414.1C, Quality Assurance, and 10 CFR 830, Energy/Nuclear Safety Management, Subpart A–Quality Assurance Requirements (a.k.a. the Quality Rule). PNWD has chosen to implement the requirements of DOE Order 414.1C and 10 CFR 830, Subpart A by integrating them into the Laboratory's management systems and daily operating processes. The procedures necessary to implement the requirements are documented through PNWD's Standards-Based Management System.

PNWD implements the RPP-WTP quality requirements by performing work in accordance with the PNWD WTPSP quality assurance project plan (QAPjP) approved by the RPP-WTP Quality Assurance (QA) organization. This work was performed to the quality requirements of NQA-1-1989 Part I, Basic and Supplementary Requirements, NQA-2a-1990 Part 2.7 and DOE/RW-0333P Rev. 13. These quality requirements are implemented through PNWD's WTPSP Quality Assurance Requirements and Description Manual. The requirements of DOE/RW-0333P, Rev 13, Quality Assurance Requirements and Descriptions (QARD) were not required for this work.

This report is based on data from testing as referenced. The PNWD assumes that the data from these references has been fully reviewed and documented in accordance with the analysts' QA Programs. PNWD only analyzed data from the referenced documentation. At PNWD, the performed calculations, the documentation and reporting of results and conclusions were performed in accordance with the WTPSP Quality Assurance Program. Internal verification and validation activities were addressed by conducting an independent technical review of the final data report in accordance with PNWD procedure QA-RPP-WTP-604. This review verifies that the reported results are traceable, that inferences and conclusions are soundly based, and that the reported work satisfies the Test Plan objectives. This review procedure is part of PNWD's WTPSP Quality Assurance Requirements and Description Manual.

3.0 Solid Particle Size and Density Data

This section describes the data sources considered and the development of the best-estimate data sets for measured PSDs (Section 3.1) and solid-phase compounds (Section 3.2). The relative volume fractions, crystal density, maximum primary particle size, and maximum agglomeration size are identified. The relation of both the measured PSDs and the solid-phase compound information to the insoluble solid inventory at Hanford is discussed. Quantifiable uncertainties in the data are considered. Data pertaining to the base liquid density and viscosity parameters required in the PSDD and critical velocity criterion calculations are presented in Section 3.3.

3.1 Basis and Criteria for Particulate Characterization Selection

The goal of the particulate characterization selection analysis was to review historical PSD measurements for tank waste samples and to develop a representative (composite) PSD or PSDs from those measurements. Particle size analysis has been performed on core and auger samples from the Hanford tanks as part of the Tank Waste Characterization, Retrieval, Safety, and Pretreatment projects at Hanford. A survey of these particle size analyses was performed to prepare a comprehensive data set from which a composite PSD could be developed for the sludge layers in the Hanford tanks. The references containing tank waste PSD measurements and considered in the literature survey are listed in Table 3.1.1. In total, 53 references with particle-size data for 49 tanks were evaluated for inclusion in the composite PSD set.

The composite PSD derived from these data is intended to provide a “best representation” of the size of insoluble particulate matter contained in all 177 tanks and is, in some sense, an “averaged” distribution. As such, and because it is generated from a limited data set, the composite PSD should be expected to differ from known PSDs for specific tanks. It should not be considered either bounding or conservative.

There is a larger base of references containing particle size measurements for various tank wastes. However, as with many of the reports, they are primarily concerned with the influence of post-retrieval treatment processes, such as caustic leaching, on the PSD. The reports listed in Table 3.1.1 were selected for consideration because they contained PSD measurements for “as-received” material. In some cases, these reports also present PSD for treated wastes; however, as the emphasis of the composite particle size analysis will be on waste conditions at retrieval, the effect of post-retrieval processing was not considered further.

The main difficulty in obtaining distributions representative of all tank wastes and waste types was that PSD measurements were not available for all tanks. In the cases where PSDs measurements were taken, such as those in the referenced reports, creation of a single representative distribution was further complicated by the fact that many of the measurements were not equivalent or comparable. But before discussing this in regard to the actual tank measurements, a general understanding of PSD sampling and analysis is discussed.

Table 3.1.1. References Considered for Inclusion in the Representative PSD

#	Reference	Tanks with PSD Data
1	7S110-WSC-03-002, 2003, “Particle Size Distribution Analysis Results: Tank-241-AN-102, Core 307.” Internal memo, WS Callaway to KG Carothers, October 7, 2003), CH2M HILL Hanford Group, Inc. (CH2M HILL), Richland, Washington.	AN-102
2	7S110-WSC-03-012, 2003, “Particle Size Distribution Analysis of Samples from Tank 241-AZ-102, Core 310,” (internal memorandum from WS Callaway to KG Carothers dated December 12), CH2M HILL, Richland, Washington.	AZ-102
3	7S110-WSC-05-011, 2005, “Particle Size Measurements in Support of the Tank 241-AN-102 Chemistry Control Recovery Plan,” (internal memorandum from WS Callaway, GA Cooke and DL Herting to KG Carothers dated March 18), CH2M HILL, Richland, Washington.	AN-102
4	7S110-WSC-06-148, 2006, “Particle Size Distribution Measurements on Samples from Tank 241-AY-102 Core 319,” (internal memorandum from WS Callaway to KG Carothers dated January 24), CH2M HILL, Richland, Washington.	AY-102
5	B3610-WSC-02-028, 2002, “Particle Size Distribution Analysis Results: Tank 241-AN-107, Core 304,” (internal memorandum from WS Callaway to HL Baker dated December 26), Fluor Hanford, Inc., Richland, Washington.	AN-107
6	BNFL-RPT-030, 2000, Characterization, Washing, Leaching, and Filtration of C-104 Sludge, Pacific Northwest National Laboratory, Richland, Washington	C-104
7	BNFL-RPT-038, 2000, Characterization, Washing, Leaching, and Filtration of AZ-102, Pacific Northwest National Laboratory, Richland, Washington	AZ-102
8	Brooks et al. 1996. “Sludge Pretreatment Studies Using Hanford Tank C-107.” Letter Report prepared for the Westinghouse Hanford Company by Pacific Northwest National Laboratory, Richland, Washington	C-107
9	CH2M-0400872, 2004, “Distribution of Plutonium-Rich Particles in Tank 241-SY-102 Sludge,” (external letter from WS Callaway and GA Cooke, CH2M HILL, to KH Abel, BNI, dated May 17), CH2M HILL, Richland, Washington.	SY-102
10	FH-0201635, 2002, “Particle Size Distribution Analysis Results: Tank 241-AY-101, Cores 275 and 277,” (external letter from WS Callaway, FH, to JH Baldwin, CH2M HILL, dated April 9), Fluor Hanford, Inc., Richland, Washington.	AY-101
11	FH-0201835, 2002, “Particle Size Distribution Analysis Results: Tank 241-C-107, Cores 287 and 288,” (external letter from WS Callaway, FH, to JH Baldwin, CH2M HILL, dated April 24), Fluor Hanford, Inc., Richland, Washington.	C-107
12	FH-0202775, 2002, “Particle Size Distribution Analysis Results: Tank 241-SY-102, Core 284,” (external letter from WS Callaway, FH, to JH Baldwin, CH2M HILL, dated June 18), Fluor Hanford, Inc., Richland, Washington.	SY-102
13	FH-0202392, 2002, “Particle Size Distribution Analysis Results: Tank 241-AY-102, Cores 289 and 290,” (external letter from WS Callaway, FH, to JH Baldwin, CH2M HILL, dated May 28), Fluor Hanford, Inc., Richland, Washington.	AY-102
14	Gray et al. 1993, “Characterization of the First Core Sample of Neutralized Current Acid Waste from Double-Shell Tank 102-AZ,” (unnumbered report), Pacific Northwest Laboratory, Richland, Washington.	AZ-102
15	Gray et al. 1993, “Characterization of the Second Core Sample of Neutralized Current Acid Waste from Double-Shell Tank 101-AZ.” Unnumbered report, Pacific Northwest National Laboratory, Richland, Washington	AZ-101
16	HNF-1647, 1999, Tank 241-S-l11, Core 237 Analytical Results for the Final Report, Rev. 0A, Waste Management of Hanford, Inc., for Fluor Daniel Hanford, Inc., Richland, Washington	S-101
17	HNF-1666, 1999, Tank 241-SY-101, Cores 255, 256, and 257, Analytical Results for the Final Report, Rev. 0A, Waste Management of Hanford, Inc., for Fluor Daniel Hanford, Inc., Richland, Washington.	SY-101
18	HNF-3352 Rev. 0, 1998, Results of Dilution Studies with Waste from Tank 241-AN-104, Fluor Daniel Hanford Inc., Richland, Washington.	AN-104
19	HNF-4964 Rev. OA, 2000, Results of Dilution Studies with Waste from Tank 211-AW-101, Fluor Hanford Inc., Richland, Washington.	AW-101

Table 3.1.1 (contd)

#	Reference	Tanks with PSD Data
20	HNF-7078 Rev. 0A, 2002, Results of Retrieval Testing of Sludge from Tank 241-AZ-101, Fluor Hanford, Inc., Richland, Washington.	AZ-101
21	HNF-8862 Rev. 0, 2002, Particle Property Analyses of High-Level Waste Tank Sludges, Fluor Hanford, Inc., Richland, Washington.	AW-103, AY-101, AY-102, AZ-102, C-104, C-107, SY-102
22	HNF-SD-WM-DTR-046 Rev. OA, 1999, Results of Dilution Studies with Waste from Tank 241-AN-I 05, Fluor Daniel Hanford Inc., Richland, Washington.	AN-105
23	LA-UR-95-2070, 1995, Sludge Washing and Alkaline Leaching Test son Actual Hanford Tank Sludge: A Status Report, Los Alamos National Laboratory, Los Alamos, New Mexico	B-202, BX-105, C-108, S-104, T-104, T-107
24	LA-UR-96-2839, 1996, Sludge Water Washing and Alkaline Tests on Actual Hanford Tank Sludge: FY 1996 Results, Los Alamos National Laboratory, Los Alamos, New Mexico.	B-104, BX-109, C-107, TY-104
25	LA-UR 97-2889, 1997, Sludge Water Washing and Alkaline Tests on Actual Hanford Tank Sludge: FY 1997 Results, Los Alamos National Laboratory, Los Alamos, New Mexico.	B-106, BX-103, C-104, C-105, SX-113
26	Peters, 1988, Tank 101-AY Sludge Particle Size Analysis, (unnumbered memorandum to RS Edrington, dated July 22), Westinghouse Hanford Company, Richland, Washington.	AY-101
27	Peterson, 1990, Preliminary Results—Analysis of Waste Layers from DST 101-AZ Core #2, (letter 9001040 to AJ DiLiberto and LM Sasaki, dated February 28), Pacific Northwest Laboratory, Richland, Washington.	AZ-101
28	PNL-10078, 1995, Washing and Alkaline Leaching of Hanford Tank Sludges: A Status Report, Pacific Northwest Laboratory, Richland, Washington	B-201, U-110
29	PNL-10099, 1994, Tank Characterization Report for Single-Shell Tank B-111, Pacific Northwest Laboratory, Richland, Washington	B-111
30	PNL-10101, 1994, Tank Characterization Report for Single-Shell Tank T-102, Pacific Northwest Laboratory, Richland, Washington	T-102
31	PNL-10175, 1994, Ferrocyanide Safety Project: Comparison of Actual and Simulated Ferrocyanide Waste Properties, Pacific Northwest Laboratory, Richland, Washington	C-109, C-112
32	PNL-10712, Washing and Caustic Leaching of Hanford Tank Sludges: Results of FY 1995 Studies, 1995, Pacific Northwest Laboratory, Richland, Washington	B-111, BX-107, C-103, S-104, SY-103, T-104, T-111
33	PNNL-11025, 1996, Comparison of Simulants to Actual Neutralized Current Acid Waste: Process and Product Testing of Three NCAW Core Samples from Tanks 101-AZ and 102-AZ, Pacific Northwest National Laboratory, Richland, Washington	AZ-101, AZ-102
34	PNNL-11098, 1996, Comparison of Simulants to Actual Neutralized Current Acid Waste: Process and Product Testing of Three NCAW Core Samples from Tanks 101-AZ and 102-AZ, Pacific Northwest National Laboratory, Richland, Washington	AZ-101, AZ-102
35	PNNL-11278 Rev. 1, 1996, Washing and Leaching of Hanford Sludges: Results of FY 1996 Studies, Pacific Northwest National Laboratory, Richland, Washington	BY-104, BY-110, C-107, S-107, SX-108
36	PNNL-11352, 1996, Tank SY-102 waste retrieval assessment: Rheological measurements and pump jet mixing simulations, Pacific Northwest National Laboratory, Richland, Washington.,	SY-102
37	PNNL-11381 Rev. 1, 1996, Washing and Caustic Leaching of Hanford Tank C-106 Sludge, Pacific Northwest National Laboratory, Richland, Washington	C-106
38	PNNL-11580, 1997, Caustic Leaching of Composite AZ-101/AZ-102 Hanford Tank Sludge, Pacific Northwest National Laboratory, Richland, Washington	AZ-101 / AZ-102 composition sample
39	PNNL-11636, 1997, Washing and Leaching of Hanford Sludges: Results of FY 1997 Studies, Pacific Northwest National Laboratory, Richland, Washington	AN-104, BY-108, S-101, S-111
40	PNNL-12010, 1998, Bench-Scale Enhanced Sludge Washing and Gravity Settling of Hanford Tank C-107 Sludge, Pacific Northwest National Laboratory, Richland, Washington	S-107
41	PNNL-13028, 1999, Characterization of the First Core Sample of Neutralized Current Acid Waste from Double-Shell Tank 101-AZ, Pacific Northwest National Laboratory, Richland, Washington	AZ-101
42	PNNL-16133, 2006, Characterization and Correlation of Particle-Level Interactions to the Macroscopic Rheology of Powders, Granular Slurries, and Colloidal Suspensions, Pacific Northwest National Laboratory, Richland, Washington	B-203, T-110, T-203, T-204

Table 3.1.1 (contd)

#	Reference	Tanks with PSD Data
43	RPP-5798 Rev. 0, 2002, Results of Retrieval Studies with Waste from Tank 241-C-104, Fluor Hanford, Inc., Richland, Washington.	C-104
44	RPP-9806 Rev. 0, 2002, Results of Retrieval Testing of Sludge from Tank 241-AZ-102, Fluor Hanford, Inc., Richland, Washington.	AZ-102
45	WHC-EP-0643, 1993, Tank characterization Report for Single-Shell Tank 241-U-110, Westinghouse Hanford Company, Richland, Washington.	U-110
46	WHC-EP-0668, 1993, Tank Characterization Report: Tank 241-C-109, Westinghouse Hanford Company, Richland, Washington.	C-109
47	WHC-EP-0739, 1994, Tank Characterization Report for Single-Shell Tank 241-BX-107, Westinghouse Hanford Company, Richland, Washington.	BX-107
48	WHC-SD-WM-ER-370, Tank Characterization Report for Single-Shell Tank 241-S-104, Westinghouse Hanford Company, Richland, Washington.	S-104
49	WHC-SD-WM-TI-540, 1992, Analysis Report for 241-BY-104 Auger Samples, Westinghouse Hanford Company, Richland, Washington.	BX-107
50	WTP-RPT-021, rev. 1, 2002, Chemical and Physical Properties Testing of 241-AN-102 Tank Waste Blended with 241-C-104 Wash/Leachate Solutions, Pacific Northwest National Laboratory, Richland, Washington	S-104
51	WTP-RPT-043 Rev. 1, 2003, Filtration, Washing, and Caustic Leaching of Hanford Tank AZ-101 Sludge, Pacific Northwest National Laboratory, Richland, Washington	BX-107
52	WTP-RPT-048 Rev. 1, 2004, Chemical Analysis and Physical Properties Testing of 241-AZ-101 Tank Waste Supernatant and Centrifuged Solids, Pacific Northwest National Laboratory	S-104
53	WTP-RPT-076, 2003, Chemical Analysis and Physical Properties Testing of 241-AZ-101 Tank Waste Supernatant and Centrifuged Solids, Pacific Northwest National Laboratory	BX-107

3.1.1 General Difficulties with PSD Measurements

The goal of any PSD analysis is to obtain a particle size measurement that is representative of the tested sample under specified conditions. Material collection must be controlled to eliminate bias in the sampling of the tank waste. However, the tank configuration and the chemistry and physical properties of the sludge contained therein makes representative sampling difficult, if not impossible.

To begin, tanks containing particulate matter generally contain a large volume of sludge, typically 10 to 1000 kiloliters, that can be sampled, whereas analytical testing (and the safety requirements tests) dictates tank sample volumes on the order of liters. Particle size analysis must, as a result, derive a representative size distribution from only a fraction of the tank material. Significant sampling difficulties derive from the fact that the sludge chemistry and physical properties within a given tank may not be uniform. Tank heterogeneity derives from a number of processes, including (but not limited to) the addition of different process wastes into the same tank over a number of years (resulting in layered waste types), uncontrolled precipitation of multiple chemical species, and continued chemical changes within the tank (which may also vary within the tank because of temperature differentials). The result is possible variation of solid species concentrations and particle sizes, among other things, with location in the tank.

Spatial variations make the definition of a representative material for a given tank relatively ambiguous, especially when the analysis is aimed at characterizing all the solid material in that tank. Under such circumstances, it would be ideal to homogenize the entire tank prior to sampling or to pull multiple samples and homogenize them prior to analysis. Because of their size, homogenization of entire tanks is not practical. In addition, tanks are configured such that there is limited control over where waste samples can be taken, so multiple sampling and subsequent homogenization also may not provide a means of obtaining a representative sample. With the acknowledgement of these factors, the PSDs for a waste sample may not be representative of the PSD of the waste in the tank as a whole.

Even if a representative sample is obtained through rigorous sampling, the testing protocol used in PSD analysis can influence the results dramatically. For example, the choice of suspending fluid can influence PSD results. If the suspending fluid viscosity is low, large or dense particles may settle out of suspension prior to analysis in static cells or may not be suspended in flow systems. In this case, a bias toward fine particles would be introduced to the PSD results. Additionally, the ionic strength and pH of the suspending medium may also alter the measured PSD through dissolution or precipitation or through changes in the interparticle forces that govern the formation and stability of flocs and/or aggregates. Shear forces applied to the sample during PSD measurement can also influence the measured distribution size. For example, weak flocs that exist under quiescent conditions may be disrupted under shear or by an applied ultrasonic field. Indeed, ultrasonic fields are usually used to break down weak flocs in samples where the distribution of primary particles or hard agglomerates is of interest. Shear and ultrasonics typically shift the PSD to lower particle diameters. The force required to disrupt the weak flocs depends strongly on the nature of forces holding the particles together. In some cases, the degree of agitation required to suspend the samples' particulate matter may also be sufficient to break weak flocs.

3.1.2 Selected Characterizations

Many of the concerns outlined in Section 3.1.1 apply to the PSD measurements considered for inclusion in the overall PSD. The documents referenced in Table 3.1.1 were prepared over a number of years and by different organizations, and, as a result, the PSD measurements given therein were not governed by a single universal procedure. Tank sampling methods differ from report to report in the location and method of extraction (e.g., rotary core, push-mode core, slurry grab samples, etc.). Some reports considered waste samples extracted from a single height in the tank, while others retrieved samples from multiple heights and homogenized them into a single sample. Differences in treatment of tank waste samples after extraction but before PSD analysis arise from different storage protocols after extraction and different experimental objectives. For example, some tank waste samples were reported to have dried during storage because of evaporation. To counteract evaporative losses, the original sample mass was restored by adding deionized water to the sample. In such cases, it would be difficult to evaluate what influence this process had on the size distribution of particles in the affected samples because the process of precipitation on drying may not be immediately reversible. Neglecting the influence of such pretreatments, PSD analyses were performed with a number of instruments that employ different measurement principles and flow geometries. The latter is especially significant because some instruments measure the dispersion under static/quiescent conditions, whereas others circulate and stir the dispersion during the analysis. Both correspond to dramatically different shear environments. Even where measurements have employed flow systems, differences in the circulation rate, line diameter, and presence of sample reservoir agitation (e.g., stirring or sonication) result in variations in the effective shear applied to the sample. These differences mean that the PSD measurements contained in the referenced reports are not always directly comparable.

Because of the wide differences in sampling and measurement of tank waste PSDs, several of the referenced PSD measurements in Table 3.1.1 were not included in the composite distributions generated by the Particulate Characterization Working Group. The final PSD measurements included in the compiled data set are considered to provide the most reliable assessments of the size of particles in a given tank. Exclusions were made with the intention of eliminating biased, flawed, or irrelevant PSD measurements and were based on tank waste type, treatment of the sample prior to PSD measurement, and method and instrument used for measuring the PSD. A detailed summary of the particle size analyses that have been performed on Hanford tank wastes is presented in Appendix A (Table A.38). This table is arranged by tank and includes primary and secondary sludge waste types, particle size analyzer, conditions under which the sample was analyzed, references, and comments about the measurements.

Of the 49 tanks with PSD available, data from 19 tanks were accepted for inclusion in the overall PSD. The breakdown of selected and excluded references along with a brief justification for each inclusion/exclusion is given in Table 3.1.2.

Table 3.1.2. List of References Included and Excluded from the Overall PSD

Reference	Tanks with PSD Data	Instrument	Status
7S110-WSC-03-002	AN-102	Horiba LA-910	Excluded – saltcake waste
7S110-WSC-03-012	AZ-102	Horiba LA-910 with flow cell	Included – sonicated data only
7S110-WSC-05-011	AN-102	Horiba LA-910 with flow cell	Excluded – saltcake waste
7S110-WSC-06-148	AY-102	Horiba LA-910 with flow cell	Excluded – low stir / pump speeds
B3610-WSC-02-028	AN-107	Horiba LA-910 with flow cell	Excluded – saltcake waste
BNFL-RPT-030	C-104	Microtrac X-100 & UPA	Excluded UPA data Included X-100 data
BNFL-RPT-038	AZ-102	Microtrac X-100 & UPA	Excluded UPA data Included X-100 data
Brooks C-107	C-107	Microtrac X-100	Excluded – insufficient PSD data reported
CH2M-0400872	SY-102	Horiba LA-910 with flow cell	Excluded – low stir / pump speeds
FH-0201635	AY-101	Horiba LA-910 with fraction cell	Excluded – non-flow cell, external sonication
FH-0201835	C-107	Horiba LA-910 with fraction cell	Excluded – non-flow cell, external sonication
FH-0202775	SY-102	Horiba LA-910 with fraction cell	Excluded – non-flow cell, external sonication
FH-0202392	AY-102	Horiba LA-910 with fraction cell	Excluded – non-flow cell, external sonication
Gray AZ-102	AZ-102	Brinkman PSA 2010	Excluded; non-flow cell
Gray AZ-101	AZ-101	Brinkman PSA 2010	Excluded; non-flow cell
HNF-1647	S-101	Horiba LA-910 with fraction cell	Excluded; non-flow cell
HNF-1666	SY-101	Horiba LA-910 with fraction cell	Excluded; non-flow cell
HNF-3352	AN-104	Brinkman PSA 2010	Excluded; saltcake waste, non-flow cell
HNF-4964	AW-101	Horiba LA-910 with fraction cell	Excluded; saltcake waste
HNF-7078	AZ-101	Horiba LA-910 with fraction cell	Excluded; non-flow cell, external sonication
HNF-8862	AW-103, AY-101, AY-102, AZ-102, C-104, C-107, SY-102	Microtrac X-100 and Horiba LA-910 with flow cell	Included
HNF-SD-WM-DTR-046	AN-105	Brinkman PSA 2010	Excluded; non-flow cell
LA-UR-95-2070	B-202, BX-105, C-108, S-104, T-104, T-107	Leeds & Northrup UPA	Excluded; limited range on UPA system
LA-UR-96-2839	B-104, BX-109, C-107, TY-104	Leeds & Northrup UPA	Excluded; limited range on UPA system
LA-UR-97-2889	B-106, BX-103, C-104, C-105, SX-113	Leeds & Northrup UPA	Excluded; limited range on UPA system
Peters AY-101	AY-101	Brinkman PSA 2010	Excluded; non-flow cell
Peterson AZ-101	AZ-101	Brinkman PSA 2010	Excluded; non-flow cell

Table 3.1.2 (contd)

Reference	Tanks with PSD Data	Instrument	Status
PNL-10078	B-201, U-110	Brinkman PSA 2010	Excluded; non-flow cell
PNL-10099	B-111	Brinkman PSA 2010	Excluded; non-flow cell
PNL-10101	T-102	Brinkman PSA 2010	Excluded; non-flow cell
PNL-10175	C-109, C-112	Brinkman PSA 2010	Excluded; non-flow cell
PNL-10712	B-111, BX-107, C-103, S-104, SY-103, T-104, T-111	Brinkman PSA 2010	Excluded; non-flow cell SY-103; saltcake waste
PNNL-11025	AZ-101, AZ-102	Brinkman PSA 2010	Excluded; non-flow cell
PNNL-11098	AZ-101, AZ-102	Brinkman PSA 2010	Excluded; non-flow cell
PNNL-11278	BY-104, BY-110, C-107, S-107, SX-108	Microtrac X-100 and Brinkmann PSA 2010	Excluded C-107 data; non-flow cell Included remaining data
PNNL-11352	SY-102	Microtrac X-100	Included
PNNL-11381	C-106	Microtrac X-100	Included
PNNL-11580	AZ-101/AZ-102 composition sample	Microtrac X-100	Excluded; composite waste
PNNL-11636	AN-104, BY-108, S-101, S-111	Microtrac X-100	Excluded AN-104; saltcake waste Excluded S-111 data; sample caustically leached Included remaining data
PNNL-12010	S-107	Microtrac X-100	Included
PNNL-13028	AZ-101	HIAC/ROYCO	Excluded; limited measuring range on HIAC/ROYCO
PNNL-16133	B-203, T-110, T-203, T-204	Malvern Mastersizer 2000	Included
RPP-5798	C-104	Horiba LA-910 with fraction cell	Excluded; non-flow cell, external sonication
RPP-9806	AZ-102	Horiba LA-910 with flow cell	Included
WHC-EP-0643	U-110	Brinkman PSA 2010	Excluded; non-flow cell
WHC-EP-0668	C-109	Brinkman PSA 2010	Excluded; non-flow cell
WHC-EP-0739	BX-107	Brinkman PSA 2010	Excluded; non-flow cell
WHC-SD-WM-ER-370	S-104	Brinkman PSA 2010	Excluded; non-flow cell
WHC-SD-WM-TI-540	BY-104	Brinkman PSA 2010	Excluded; non-flow cell
WTP-RPT-021 / WTP-RPT-076	AN-102	Microtrac X-100	Excluded; saltcake waste
WTP-RPT-043/WTP-RPT-048	AZ-101	Microtrac X-100	Included

From these 19 tanks, PSD measurements were further down-selected to generate two types of distributions:

- *Minimal Disturbance PSD:* the minimal disturbance PSDs correspond to the particle-size measurement data taken under flow conditions sufficient to suspend all of the particulate matter while minimizing any shear-induced breakage of flocs/aggregates. The goal was to evaluate the presence of flocs or soft agglomerates in the waste samples while maintaining favorable suspending flows for dense/large particles. These data would be expected to include individual primary particles and both soft and hard agglomerates.
- *Sonicated PSD:* the sonicated PSDs correspond to particle-size measurement data taken under flow conditions sufficient to suspend all particulate matter (similar to those of minimal disturbance). The primary difference is that the sample is sonicated immediately before and during measurement. The goal was to evaluate distribution under conditions of maximal agitation. The data would be expected to include individual primary particles and hard agglomerates but not flocs or soft agglomerates.

Certain particle size analyzers (e.g., Horiba LA-910 and Microtrac X-100) suspend and circulate solid samples within the instruments during PSD measurements. The solid suspension and circulation would exert shear forces on the solids containing agglomerates. Sonication also imposes strong shear force on them. Mixer pumps to suspend sludge deposited in double-shell tanks and transfer pumps for subsequent waste pipeline transfer would also impose shear forces on the sludge. The slurry pipeline flow itself also imposes shear forces on the sludge due to the pipe flow velocity gradient.

Shear force acts to restructure, fragment, and/or break up agglomerates (Kramer and Clark 1999, Selomnlya et al. 2003). These changes tend to result in an increase in the population of smaller size particles (Selomnlya et al. 2002, 2003). Thus, agglomerate size and density would change, depending on the magnitude of the shear force. In general, the more shear force, the more extensive the breakup of agglomerates. Because sonication is expected to exert additional shear force on the agglomerate, the PSD obtained with sonication is expected to show a higher population of fines relative to the PSD obtained without sonication. It is reasonable to expect that the shear force exerted on the agglomerates by mixer pumps is greater than that of the 3~5 ft/sec slurry pipeline flow.

Table 3.1.3 shows the list of tanks for which particle size measurements were included in Table 3.1.2 and further down-selected by type of disturbance as outlined above. In the following sections, the basis for inclusion and exclusion of data sets is outlined in detail.

Table 3.1.3. List of Tank Data Included in Composite PSD Analysis

Tank	Report(s)	Minimal Disturbance Data	Sonicated Data
AW-103	HNF-8862 (Bechtold et al. 2002)	X	X
AY-101	HNF-8862 (Bechtold et al. 2002)	X	X
AY-102	HNF-8862 (Bechtold et al. 2002)	X	X
AZ-101	WTP-RPT-043 (Geeting et al. 2002), WTP-RPT-048	X	X
AZ-102	7S110-WSC-03-012,[(a)] HNF-8862 (Bechtold et al. 2002), RPP-9806, BNFL-RPT-038 (Brooks et al. 2000b)	X	X
B-203	PNNL-16133 (Poloski et al. 2006)	X	X
BY-104	PNNL-11278 (Lumetta et al 1996a)	X	X
BY-108	PNNL-11636 (Lumetta et al. 1997)	X	X
BY-110	PNNL-11278 (Lumetta et al 1996a)	X	X
C-104	BNFL-RPT-030 (Brooks et al. 2000a), HNF-8862 (Bechtold et al. 2002)	X	X
C-106	PNNL-11381 (Lumetta et al. 1996b)	X	X
C-107	HNF-8862 (Bechtold et al. 2002)	X	X
S-101	PNNL-11636 (Lumetta et al. 1997)	X	
S-107	PNNL-11278 (Lumetta et al 1996a), PNNL-12010 (Brooks et al. 1998)	X	X
SX-108	PNNL-11278 (Lumetta et al 1996a)	X	X
SY-102	HNF-8862 (Bechtold et al. 2002), PNNL-11352 (Onishi et al. 1996)	X	X
T-110	PNNL-16133 (Poloski et al. 2006)	X	X
T-203	PNNL-16133 (Poloski et al. 2006)	X	X
T-204	PNNL-16133 (Poloski et al. 2006)	X	X
(a) Report only presents sonicated data for AZ-102.			

3.1.2.1 Types of PSD Considered

In the reports listed in Table 3.1.1, PSDs are often reported using both volume and number bases. Number distributions provide information on the number of particles in a given size range, whereas volume distributions relate the amount of material in a given size range. Because the current application is concerned with the volume of tank waste material that falls outside the handling capabilities of the WTP, only volume-based PSDs were included in the composite PSD data set. In the balance of this report, the term PSD indicates volume-based particle size distribution.

3.1.2.2 Tank Samples Considered

The influence of tank retrieval method and location of sample extraction was not considered. All "as-received" tanks wastes were treated equally and assumed to be sampled such that the particles and aggregates contained therein were equally representative of their source tank.

3.1.2.3 Waste Types Considered

The reports listed in Table 3.1.1 include PSD measurements for tank wastes spanning a number of different waste type designations. The waste types for all tanks considered for inclusion in the composite PSD are listed in Table 3.1.4. Definitions for the waste type acronyms are provided in Appendix B.

Of all the waste types considered, only PSD measurements corresponding to saltcake wastes (tanks AN-102, AN-104, AN-105, AN-107, AW-101, SY-101, and SY-103) were excluded from further consideration. These exclusions were based on the fact that particle size measurements for saltcake wastes are particularly susceptible to dissolution effects. For the samples in question, any lowering of the ionic strength of the suspending medium (either during retrieval or subsequent analysis) has the strong potential of dissolving the solids, altering it significantly from what would be considered an "as-received" PSD. These exclusions are also consistent with the specific PSDD task scope to consider only insoluble (loosely defined as non-sodium salt particulate).

The remainder of the tank waste types considered are sludge solid wastes. Because these wastes are composed of primarily insoluble solids, they are expected to be more robust and resistant to dissolution effects. Even though these types are considered resistant to dissolution, it is acknowledged that sodium-salt solid-phase compounds can still be present in these wastes. As a result, the potential influence of sample solid dissolution on the composite PSD cannot be entirely neglected. While it is difficult to quantify, the potential impact of these solubility issues on the resulting PSDs will be indirectly addressed in Section 5 through variation of the composite PSD.

Waste type definitions have evolved over time as additional information on the composition of wastes transferred to the Hanford tanks has been identified. The latest modifications were included in Revision 5 of the Hanford Defined Waste Model (Higley and Place 2004). Most of these changes are included in the 2006 Best Basis Inventory (BBI), which is the database provided in the Tank Waste Information System (TWINS) and used in this report to determine the sludge volumes associated with each waste type. In the 2006 BBI, waste types 1C1 and 1C2 are combined as 1C, and waste types 2C1 and 2C2 are combined as 2C. Several waste types defined in the model are not observed in the sludge fraction of the tank wastes and are not included in Appendix B (List of Waste Type Acronyms and Meanings).

Table 3.1.4. Primary and Secondary Solids Waste Types for Tanks Listed in Table 3.1.1[(a,b)]

Tank	Primary Waste Type	Secondary Waste Type
AN-102	A2-SltSlr	
AN-104	A2-SltSlr	
AN-105	A2-SltSlr	
AN-107	A2-SltSlr	
AW-101	A2-SltSlr	
AW-103	CWZr	A1-SltCk
AY-101	NA(c)	
AY-102	NA(c)	BL
AZ-101	P3	NA(c)
AZ-102	P3	SRR, PL2, NA(c)
B-104	2C	1C, B-SltCk
B-106	TBP	1C
B-111	2C	B
B-201	224	
B-202	224	
B-203	224	
BX-103	CWP	TBP
BX-105	CWP	BY-SltCk, TBP, MW
BX-107	1C	
BX-109	TBP	
BY-104	BY-SltCk	PFeCN
BY-108	BY-SltCk	PFeCN
BY-110	BY-SltCk	PFeCN
C-103	CWP	
C-104	CWP	CWZr, OWW, TH, NA(c)
C-105	CWP	TBP
C-106	NA(c)	
C-107	1C	SRR, CWP
C-108	1C	TBP, TFeCN
C-109	TFeCN	1C, CWP, HS
C-112	TFeCN	1C, CWP, HS
S-101	NA	S1-SltCk, S2-SltCk
S-104	R-SltCk	R (boiling), CWR
S-107	CWR	CWZr, R (boiling), S1-SltCk, S2-SltCk, T2-SltCk
S-111	S1-SltCk	R (non-boiling), CWR
SX-108	R (boiling)	
SX-113	Diatomaceous Earth	R (boiling)
SY-102	NA(c)	Z
SY-103	S2-SltSlr	
T-102	CWP	MW
T-104	1C	
T-107	1C	CWP, TBP
T-110	2C	224
T-111	224	2C
T-203	224	
T-204	224	
TY-104	1CFeCN	TBP
U-110	R (boiling)	CWR, 1C

(a) The primary waste type indicates which waste is present in the highest volumetric quantity for the listed tank.
(b) Secondary wastes are any other wastes present in that tank.
(c) Waste volume information indicates that this waste type is unclassified solid sludge.

The 2002 BBI is used in the current ESP model; therefore, some of the waste types in the 2006 BBI were combined to be consistent with the ESP model and previous reports. Waste types identified in the sludge layers in the 2006 BBI are compared with the waste types used in this report in Table 3.1.5. A few sludge layers in Hanford tanks have not been identified as a particular waste type and are listed as unclassified waste.

Table 3.1.5. Comparison of Waste Type Groups

2006 BBI	**This Report**
Bismuth Phosphate Process Waste Types	
MW1	MW
MW2	
1C	1C
2C	2C
224-1	224
224-2	
Uranium Recovery and Scavenging Waste Types	
TBP	TBP
PFeCN	PFeCN
TFeCN	TFeCN
1CFeCN	1CFeCN
REDOX Process Waste Types	
R1	R (boiling) or R (non-boiling)
R2	
CWR1	CWR
CWR2	
PUREX Process Waste Types	
P1	P1
P2	P2
P3AZ1	P3
P3AZ2	
CWP1	CWP
CWP2	
CWZr1	CWZr
CWZr2	
OWW3	OWW3
PL2	PL2
TH1	TH
TH2	
Cesium and Strontium Recovery Waste Types	
HS	HS
AR	AR
B	B
BL	BL
SRR	SRR
Other Process Facility Wastes	
Z	Z
Miscellaneous Wastes	
CEM	Portland Cement
DE	DE

REDOX HLW is classified as R1 and R2 in the 2006 BBI based on the date of waste generation, but these classifications do not indicate the thermal history of the REDOX waste, which is essential in determining whether gibbsite or boehmite is the predominate aluminum species in the waste. Therefore, REDOX HLW was reclassified into REDOX boiling and REDOX non-boiling waste types to provide definitions that segregated the aluminum-containing sludges based on the predominant aluminum phase (gibbsite or boehmite). This reclassification was based on thermal history and aluminum leaching factors in these wastes as described in Meacham (2003).

The 224 waste is currently in the Hanford baseline to be dried and transported to the Waste Isolation Pilot Plant (WIPP) as transuranic (TRU) waste. This waste is included as a contingency for processing these wastes in the WTP instead of the DOE/ORP baseline plan for sending these wastes to WIPP. Additionally, the waste in tanks T-104, T-107, and B-111 are also designated in the DOE/ORP baseline for treatment, packaging and disposal at WIPP. This includes waste types that will be processed in WTP (1C, 2C, B, CWP, and TBP).

3.1.2.4 Tank Waste Pretreatments Considered

While many of the reports listed in Table 3.1.1 examine the influence of post-retrieval treatment process such as caustic leaching on PSD, only PSDs corresponding to as-received material were considered for the composite PSD. Samples formed by compositing multiple tanks wastes into a single sample, such as the AZ-101/AZ-102 sludge composite studied in Rapko and Wagner (1997) were also excluded from the composite PSD data set.

When received for analysis, the tank material was often reported to have phase segregated into a clear supernatant layer over a dense settled sludge layer. Samples were typically homogenized to resuspend the solids before subsampling aliquots for PSD and other measurements. As with the method and location of sample retrieval from the source tank, the influence of mechanical pretreatments like homogenization and subsampling on the measured PSD and its quality are neglected. This does not extend to the mechanical operations to disperse the sample during the particle size measurement (e.g., measurement flow conditions). Exclusions made on this basis are described in Section 3.1.2.5.

Though chemically pretreated sample material is excluded, tank waste samples used for PSD analyses must sometimes be diluted with an additional suspending phase to meet maximum allowable dispersion obscuration requirements of the particle size analyzer employed for the measurement. Most commercially available analyzers have dispersion limits of approximately 1% solids (by volume), whereas tank waste samples range anywhere from 5–15% solids.

Dilution of the tank waste material to facilitate measurement will not be considered a chemical pretreatment. To minimize dissolution effects, preference is given to particle size measurements of tank waste diluted with actual waste supernatant for that tank or a high ionic strength suspending phase simulant (such as 1 M NaOH and 1 M $NaNO_3$). Particle size measurements of tank wastes diluted with inhibited water (0.01 M NaOH) or DI water are provisionally included if no acceptable high-ionic strength dilutions exist with the understanding that some salt solids may dissolve.

3.1.2.5 PSD Analyzers Considered

The PSD measurements included in the reports listed in Table 3.1.1 were carried out using several instruments. A complete list of the instruments used is given in Table 3.1.5. Within a particular report, most PSD analyses were carried out using a single instrument, although there were some exceptions. For example, Microtrac X-100 PSD measurements were accompanied by Microtrac UPA measurements (which provide additional resolution for submicron particles) in some reports. In Bechtold et al. (2002), PSD measurements of material from the same tanks were taken using both the Horiba LA-910 and Microtrac X-100/UPA systems. In Lumetta et al. (1996a), while most tank samples were sized using a Microtrac X-100 analyzer, the sample from Tank C-107 was only analyzed with a Brinkman PSA 2010.

Table 3.1.5. Instruments Used for PSD Analysis in Reports Listed in Table 3.1.1

Analyzer	Measurement Range (μm)	Stirring/Flow	Sonication	Status
Brinkman PSA 2010	0.7 – 150	Magnetic Stir Bar	None	Excluded
HIAC/ROYCO	4 – 225	NA[a]	NA	Excluded
Horiba LA-910	0.02 - 1020	Stir in Reservoir/Flow	External/Internal	Included – Flow Cell Excluded – Fraction Cell
Leeds & Northrup UPA	0.003 – 6.5	None	None	Excluded
Malvern Mastersizer 2000	0.02-2000	Flow Cell	Internal	Included
Microtrac UPA	0.003 - 6.5	Magnetic Stir Bar	None	Excluded
Microtrac X-100	0.04 - 700	Flow Cell	Internal	Included
(a) NA = information not available.				

The Microtrac UPA and Leeds & Northrup UPA are nonflow systems useful for characterizing submicron particles. Because the measuring range of nonflow systems (0.003 to 6.5 μm) does not fully encompass the spread of particle sizes for tank wastes as determined by microscopy, inclusion of any PSD data set measured using these systems would preferentially bias the fines fraction in the final composite distribution. Thus, all UPA measurements were excluded from the composite distribution data set.

The measurement range of the HIAC/ROYCO system is limited to 4.5 to 225 μm. PSDs for typical tank wastes, which are expected to contain particles smaller than 4.5 μm and/or larger than 225 μm, cannot be properly characterized using this system. As a result, all PSD measurement data obtained from this system were excluded from the composite distribution.

The Brinkman PSA 2010 employs minimal stirring during measurement. Because the mechanical agitation is weak relative to flow cell systems, there is some concern that large, dense particles may settle to the bottom of the cell prior to the start of the measurement. Based on these concerns, all PSDs obtained by the Brinkman PSA 2010 were excluded from the composite size distribution.

PSD measurements taken with the Horiba LA-910 have employed 1) a static fraction cell with external sample sonication and 2) a flow cell with internal sample sonication that continuously circulates the sample. For the first configuration, there is concern that large, dense particles may again settle to the bottom of the cell before measurement begins. All PSDs employing the fraction cell with external sonication were excluded from the composite size distribution.

The flow cell configuration for the Horiba LA-910 includes a sample reservoir that is mechanically mixed and a pump that flows a portion of the sample through the analyzer optics. This configuration also allows internal sonication during the measurement and control over the stirring and pumping speeds. Horiba LA-910 measurements in the reports referenced in Table 3.1.1 employ a diversity of pump and flow speeds. Like with the fraction cell, there is concern that the lower stir/pump speeds were not sufficient to suspend large, dense particles during the measurements. For the Horiba LA-910, the circulator pump speed setting is adjustable from 0-6 with '6' corresponding to a pump discharge rate of 14.4 mL/s. Stir speeds settings range from 0 to 6, with '6'corresponding to a stirring speed of 1000 rpm. Experience has found that pump settings of '5' or greater combined with stir speeds of '3' provide adequate suspension of particles. As such, measurements using pump/stir speeds of '6/3' or '5/3' were included in the composite size distribution. Both unsonicated (minimal disturbance) and sonicated data sets were considered. In most cases, the samples were sonicated at least two minutes prior to analysis. Measurements at lower pump/stir settings, such as '4/2' and '6/1', were excluded from the composite size distribution.

Like the Horiba LA-910, the Microtrac X-100 is equipped with a flow cell and internal sonication capabilities that continuously circulate and agitate the sample dispersion during measurement. The X-100 is typically operated at a flow rate of 40 or 60 mL/s. Both are assumed to provide adequate sample dispersion; however, all X-100 data sets included in the composite size distribution employ a pump speed of 60 mL/s with only one exception: the S-107 sonicated data set taken from PNNL-12010 (Brooks et al. 1998) (for which no 60 mL/s sonicated raw data set was available). X-100 measurements included in the composite PSD cover both unsonicated (minimal disturbance) and sonicated size-distributions.

The Malvern Mastersizer 2000 was used only in the analyses reported in (Poloski et al. 2006). It is equipped with a Hydro µP sample dispersion unit that allows for internal sample sonication and includes a flow cell with speed settings that range from 500–5000 rpm. A pump setting of 3000 rpm was used in all measurements provided in Poloski et al. (2006) and is considered to provide sufficient sample agitation to prevent the settling of large, dense particles. As such, most data from this instrument are included in the composite PSD data set. The Malvern Mastersizer 2000 measurements cover both unsonicated (minimal disturbance) and sonicated size-distributions.

3.1.2.6 Minimal Disturbance and Sonicated Measurements Considered

As discussed, PSD data sets considered for evaluation were further down-selected into minimal disturbance and sonicated data. All minimal disturbance sets derive from PSD measurements taken some time after sample load-in but prior to any sample sonication. Sonicated PSD data sets are typically taken after the first period of sonication. Depending on the experimental protocol followed, the period of sonication prior to measurement ranges between 60 and 300 seconds. All subsequent reported PSD measurements performed after initial sample sonication and PSD are discarded. In most cases, the reports referenced in Table 3.1.1 provide both minimal disturbance and sonicated data. Exceptions include a reference(a) that provides only sonicated PSD measurements for AZ-102 and (Lumetta et al. 1997), which provides the minimal disturbance PSD measurement for Tank S-101.

(a) Callaway WS. October 7, 2003. "Particle Size Distribution Analysis Results: Tank-241-AN-102, Core 307." 7S110-WSC-03-002, internal memorandum to KG Carothers, CH2M HILL, Richland, Washington.

3.1.2.7 Other Considerations

Additional PSD measurements were included or excluded on a case-by-case basis. Duplicate measurements, when available, were typically included in the compiled data set for each of the tanks listed in Table 3.1.3 as long as they satisfied the other criteria outlined above. The PSD data sets for some tanks comprise a large number of duplicates (e.g., there are 13 observations for minimal disturbance AZ-102). Other tank data sets, such as AZ-101, are composed of only one PSD observation. The intention of including duplicate measurements is to provide as much data as possible for subsequent statistical analysis. For a given report, PSDs for duplicate samples were only included if the sample dilution and treatment were equivalent to the primary sample.

Both sonicated and minimal disturbance data were examined for the presence of air bubbles. For flow systems, stirring, pumping, and sonication can generate or suck air bubbles into the measurement cell in the form of submillimeter- to millimeter-sized bubbles. The laser diffraction systems typically employed in these systems cannot distinguish air bubbles from actual particles in this size range. Even a single bubble can appreciably influence PSD measurements because of their large volume relative to micrometer-sized particles. For this reason, any transient peaks in the millimeter size range observed during the measurement should typically be noted and subsequently excluded. It is not known if this was the case for the measurements used herein. For this reason, any data showing large peaks around 1 mm are considered suspect (but not necessarily excluded). The following methodology is used to evaluate samples with large peaks:

- *Minimal disturbance data* showing peaks around 500–1000 μm are considered suspect. The corresponding sonicated data set is examined. If the peak remains both during and after the application of ultrasonics, the data set is included. If the peak vanishes upon application of ultrasonics and is not observed in duplicate measurements, the data are excluded. The underlying assumption is that sonication will dislodge any bubbles in the measurement cell. This is not always the best assumption; thus, exclusions based on suspicion of bubbles are made *only* if duplicate samples do not show the large peaks in either their minimal disturbance or sonicated data. This is done to avoid potential exclusion of particles and flocs in the 500–1000 μm range. If no duplicate measurements have been made or duplicates show the same behavior as the primary sample, the suspect sample is included.
- *Sonicated data* showing peaks around 1 mm are compared to the corresponding minimal disturbance data set. If no large peak exists in the minimal disturbance set, the sonicated data are excluded from further consideration.

If corresponding data are not available to validate suspect sets, they are provisionally excluded.

3.1.2.8 Significance of the Wastes Considered

Without regard to the quality of the PSD measurements, the reports listed in Table 3.1.1 contain PSD measurements for only a limited number of tanks at the Hanford Site. Exclusion of select PSD based on criteria outlined in the preceding sections only serves to further limit the number of tanks on which the composite PSD will be based. The significance of the composite PSD in relation to the actual tank inventory can be judged in terms of the fraction of the total tank volume (expressed by waste type) considered in the analysis herein. This is presented in Figure 3.1.1. In most cases, a substantial fraction of each waste type has had some form of particle size characterization performed. Exceptions include but

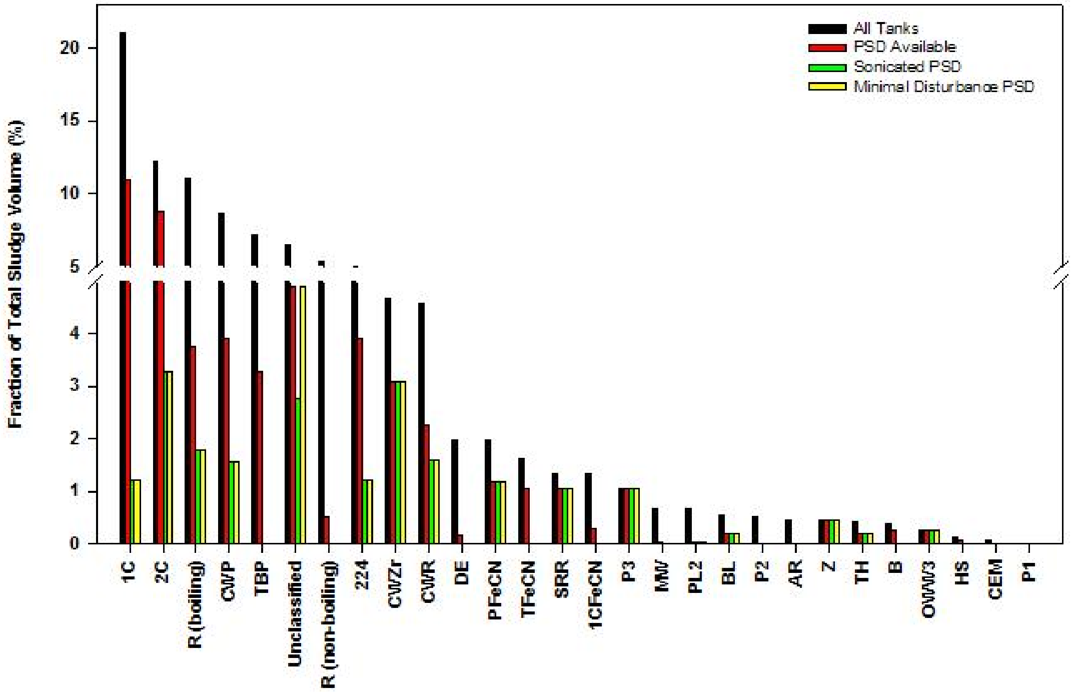

Figure 3.1.1. Volumetric Significance of Composite PSD Analysis. Here, the volume fraction of total sludge solids by waste types (black bars) is compared to the volume fraction with PSD measurements available (red bars), regardless of quality, and the volume fraction down selected for sonicated and minimal disturbance data sets (green and yellow, respectively).

are not limited to R (non-boiling), DE, and 1CFeCN wastes. In some cases, the PSD measurements selected for inclusion in the composite PSD capture a significant portion of the waste volume. For example, a significant fraction of the CWZr (greater than 50%) and all of the SRR and Z waste types are captured in the composite PSD. As such, these waste types are expected to be well represented in the composite analysis. Because of their limited inclusion, waste types such 1C and R (non-boiling) are not expected to be well represented by the composite PSD.

It is recognized that several waste types are missing from the composite PSD. However, the goal of this report is to create a more representative particle size and density distribution for the Hanford tank farm sludge as a whole using the available data. The chemical compositions used as input to this report do represent the entire Hanford tank farm sludge inventory (Section 3.2).

3.1.2.9 Final Form of the Down-Selected Data

Prior to analysis and creation of the composite PSDs, the final set of down-selected data are sorted into four following groups. These groups include:

- Minimal disturbance PSD measurements corresponding to waste samples whose PSDs have also been measured under sonicated conditions within the same report. PSDs in this data set will be referred to as MD PSD with corresponding sonicated PSDs.

- Sonicated PSD measurements corresponding to waste samples whose PSDs have also been measured under minimal disturbance conditions within the same report. PSDs in this data set will be referred to as Sonicated PSD that have corresponding MD PSDs.
- All minimal disturbance PSD measurements
- All sonicated PSD measurements.

The first two data sets listed above exclude PSD measurements for samples that do have a corresponding minimal disturbance or sonicated PSD measurement. This allows composite PSDs for both minimal disturbance and sonicated data sets to be created on an equivalent tank basis.

3.1.3 Format of the Extracted Data

Particle size measurements available in the referenced reports are presented in a large number of formats. These include:

- particle diameters corresponding to select cumulative percentiles (typically every 10% or 25% and sometimes including the 95% and 99%).
- raw histograms given as a function of counts versus particle diameter ranges
- plots of cumulative percentiles (or percent undersized) as a function of particle diameter.

To minimize the number of data maintained in the collected PSD database, raw histogram and cumulative percentiles as a function of particle diameter are recorded (transcribed) into particle diameters corresponding to select cumulative percentiles. The range of percentiles maintained is limited to 1, 5, 10, 20, 25, 30, 40, 50, 60, 70, 75, 80, 90, 95, and 99% (at the most).

When the source data are already in the form of percentiles, only the original percentiles are transcribed into the particle size database. Exceptions are made for 95 and 99% diameters, which are important in defining the upper limit of the PSD. Data from the Horiba LA-910 analyzer typically report 95 and 99% diameters; Microtrac X-100 data reports only include up to the 95% diameter. In the latter case, the 99% diameter is determined from log interpolation of the raw histogram (which is usually also reported).

Raw histograms are typically given as in fractional counts versus particle diameter bins [{d_i, f_i} for i=1, N_B, where d_i is particle diameter, f_i is the fractional abundance, and i and N_B are the bin index and total bin number]. These data may be compiled into a cumulative distribution using Eq. (3.1.1):

$$s = \sum_{1}^{j} f_i \qquad (3.1.1)$$

where s is the cumulative distribution (or percent undersize) for the particle diameter d_i. Once the cumulative distribution is determined, the particle diameters at the percentiles of interest are determined using log interpolation. If the cumulative distributions are provided in plots, the desired percentiles are read directly from plots of the cumulative percentiles. All of the reports referenced in Table 3.1.1 that included raw histogram data also gave the raw cumulative distributions. Thus, raw histogram data did not need to be converted to cumulative percentiles using Eq. (3.1.1).

A complete listing of the particle size data obtained from the referenced reports and included in the composite PSD is given in Appendix A.

3.1.4 Method Used to Generate Composite PSD

The final composite PSD data set breaks down the minimal disturbance and sonicated data into the four categories outlined in Section 3.1.2.6:

- minimal disturbance PSD that have corresponding (equivalent) sonicated PSD
- sonicated PSD that have corresponding (equivalent) minimal disturbance PSD
- all minimal disturbance PSD
- all sonicated PSD.

Distributions for a given sample include a particle diameter representing the 99th percentile by volume and particle diameters corresponding to several other percentiles. The number of PSD observations for a given tank is varied; some tanks have multiple PSD observations and others have only one. For each of the four categories, a composite simulated distribution was calculated by combining the individual data sets using the appropriate weighting factors. The following steps describe how the single composite distributions were generated:

Step 1: For each sample from a given tank, a particle size representing a maximum size for that sample was determined. This was done by multiplying the size from the 99th percentile for that sample by 1.1. Thus, the maximum particle size from each sample was assumed to be 10% larger than the size from the 99th percentile, the largest percentile listed in the data sets. This approach implies that 1% of the particles from the sample have sizes between the size from the 99th percentile and the maximum size.

Step 2: The cumulative probabilities listed in the data files were converted to noncumulative probabilities, which were used along with the corresponding particle sizes to form probability distributions for each sample from the different tanks. These probability distributions included maximum particle size values determined in Step 1 and had probabilities that summed to 1.

Step 3: The probability distributions (including particle sizes and corresponding noncumulative probabilities) were combined over the samples from a given tank. The probabilities were all divided by the number of samples from the given tanks to form a single probability distribution for each tank. The probabilities in the combined probability distributions summed to 1 for each tank.

Step 4: The probabilities in the probability distributions for the different tanks were multiplied by the volume weights for the different tanks (see Table 3.1.6, determined from Cowley et al. 2003) then combined over the different tanks to form a single probability distribution representing particle sizes for waste from the available collection of waste tanks.

Table 3.1.6. Weighting Factors Based on Volume of Dried Sludge Solids (reduced salt-free) Used for Combining Averaged Tank Distributions

Tank	Weighting Factor (volume fraction dried sludge solids)		
	Minimal Disturbance and Sonicated Compilation	Sonicated Only Compilation	Minimal Disturbance Only Compilation
AW-103	0.0897	0.0897	0.0760
AY-101	0.0495	0.0495	0.0419
AY-102	0.0742	0.0742	0.0629
AZ-101	0.0393	0.0393	0.0333
AZ-102	0.0438	0.0438	0.0371
B-203	0.0033	0.0033	0.0028
BY-104	0.0861	0.0861	0.0729
BY-108	0.1041	0.1041	0.0883
BY-110	0.0572	0.0572	0.0485
C-104	0.1410	0.1410	0.1195
C-106	0.0047	0.0047	0.0040
C-107	0.1027	0.1027	0.0871
S-101	-- --	-- --	0.1525
S-107	0.0867	0.0867	0.0735
SX-108	0.0160	0.0160	0.0135
SY-102	0.0839	0.0839	0.0711
T-110	0.0130	0.0130	0.0110
T-203	0.0021	0.0021	0.0018
T-204	0.0028	0.0028	0.0023

Step 5: The particle sizes contained in the combined probability distribution formed in Step 4 were resampled 10,000 times (with replacement) with the probability of selection equal to corresponding probabilities from the combined probability distribution to form a vector of 10,000 simulated realizations (simulated distribution) of particle sizes for a nominal volume percent.

Step 6: The simulated distributions were summarized by determining key quantiles of the resulting simulated particle sizes and by constructing a histogram to visually describe the simulated distribution.

Using this methodology, the sample data were composited into combined PSD for all sonicated data, all minimal disturbance data, and sonicated and minimal disturbance with corresponding PSD (see Section 3.1.6).

As outlined in Step 3, multiple PSD observations for a single tank were weighted equally when combining the distributions. This step generated an averaged PSD for each tank. The averaged tank distributions were then combined into a composite distribution, as described in Step 4. Here, single-tank distributions were weighted with the volume fraction of dried sludge solids (reduced salt-free) of that tank waste within the composite PSD tank matrix. The weighting factors used are listed in Table 3.1.6. Because not all tanks have both minimal disturbance and sonicated distributions, a separate set of weighting factors must be used when combining minimal disturbance/sonicated data sets with corresponding sonicated/minimal disturbance data, sonicated-only data, and minimal disturbance-only data.

3.1.5 Method Used to Generate PSDs for Variability Studies

Another goal of this analysis was to illustrate the variability introduced into the composite PSD by the select removal and/or recombination (using different weighting factors) of the individual tank averaged PSD. Rather than approach this problem through the removal or recombination of tank PSDs using systematically or randomly varied tank bases or weighting factors, the variation analysis is accomplished by generating “pseudo-waste-type” PSDs.

The composition of each tank within in the PSD tank matrix may be expressed in terms of its volumetric fractional contributions of the constituent waste types present, such as CWZr and OWW3. In the simplest case, tanks are composed of a single sludge solids waste type. One example is AW-103, which is composed of only CWZr (neglecting the soluble salt solids). In other cases, tanks incorporate multiple waste types; AZ-102, which includes P3, PL2, and SRR wastes, is one such example.

For tanks whose sludge volume solely or overwhelmingly consists of a single waste type, it is possible to associate the averaged tank PSD with a PSD for that particular waste type. Of the tanks considered, 11 satisfy this requirement: AW-103, AY-101, B-203, BY-104, BY-108, BY-110, C-106, S-101, SX-108, T-203, and T-204. From these tanks, distributions for waste types 224, CWZr, PFeCN, and R (boiling) could be unambiguously derived. Determination of waste-type PSDs for tanks comprising multiple waste types is possible under the assumption that the particles from different waste types are noninteracting—provided particle size information is available on a sufficient number of tank and/or waste types. The approach would involve simultaneous solution of the unknown waste type PSDs and known tank/type PSDs and is akin to solving a set of N equations with N unknowns.

Because this analysis aims to understand PSD variation, not to generate actual waste-type PSDs, the proper waste-type analysis described above is foregone. Instead, the waste types will be used as a basis for estimating variability. To differentiate the results of the variability study from the actual waste-type PSDs, the former will be referred to as pseudo-waste-type PSDs.

Sixteen new combinations of averaged tank PSDs are considered using the weighting factors listed in Table 3.1.7. For a given pseudo-waste type, the factors used to weight each averaged tank PSD correspond to the volume fraction of dried sludge solids (salt-free) appearing in a particular tank relative to other tanks containing that waste type. If the tank is free of a given pseudo-waste type, its weighting factor is zero. For example, the waste type CWZr appears in AW-103, C-104, and S-107. The volume of dried solids present in these tanks is 87, 137, and 84 kL, respectively, and the total volume of dried solids is 309 kL. Insight into PSD variability within a waste type may be gained by considering the tank-by-tank PSDs provided in Appendix A. A composite PSD for the CWZr pseudo-waste type is calculated by weighting the averaged tank PSDs for AW-103, C-104, and S-107 by 0.28, 0.44, and 0.27, respectively.

The pseudo-waste-type PSDs should be considered only for the purpose of evaluating PSD variation. They should not be considered as representative PSDs for their associated waste type because some of the tank PSDs used in their generation comprise multiple waste types.

Table 3.1.7. Weighting Factors Used for Tanks when Calculating Simulated PSD for the Pseudo-Waste-Type Variation Analysis

Waste Type	Constituent Tanks	Sonicated Only Compilation
224	B-203 T-110 T-203 T-204	0.1546 0.6139 0.1011 0.1304
1C	C-107	1.0000
2C	T-110	1.0000
BL	AY-102	1.0000
CWP	C-104 C-107	0.5785 0.4215
CWR	S-107	1.0000
CWZr	AW-103 C-104 S-107	0.2825 0.4442 0.2733
OWW3	C-104	1.0000
P3	AZ-101 AZ-102	0.4729 0.5271
PFeCN	BY-104 BY-108 BY-110	0.3479 0.4209 0.2312
PL2	AZ-102	1.0000
R (boiling)	S-107 SX-108	0.8445 0.1555
SRR	AZ-102 C-107	0.2989 0.7011
TH	C-104	1.0000
Z	SY-102	1.0000
Unclassified[(a)]	AY-101 AY-102 AZ-101 AZ-102 C-104 C-106 SY-102	0.1133 0.1701 0.0900 0.1003 0.3231 0.0108 0.1923
(a) TWINS no classification for certain tank sludge volumes.		

3.1.6 Composite PSD Results

In this section, the composite PSD for the various waste types and states of agitation are discussed. Figure 3.1.2 shows the probability and cumulative distributions for 1) a composite minimal disturbance PSD based on minimal disturbance waste samples whose PSDs have also been measured under sonicated conditions and 2) a composite sonicated PSDs derived from samples whose PSDs have also been measured under minimal disturbance conditions within the same report. The PSD shown in Fig. 3.1.2 cover the first two sets discussed in Section 3.1.2.9. Because both composite PSDs derive from the same tank basis, it is appropriate to directly compare these two. The minimal disturbance data show a broad distribution ranging from approximately 0.5 to 300 μm. The first approximately 90% of the distribution encompasses particle sizes from 0.5 to 20 μm with the remainder forming a long tail from 20 to 300 μm.

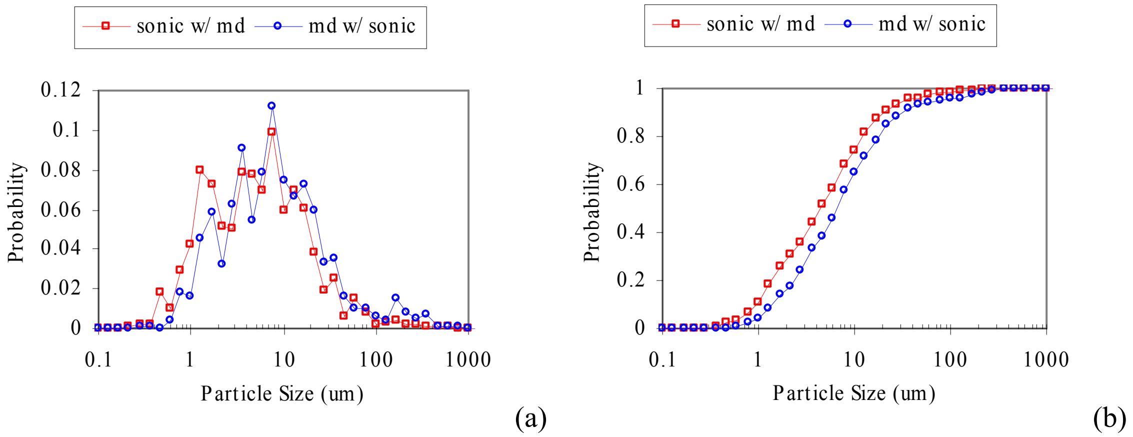

Figure 3.1.2. Probability (a) and Cumulative (b) Composite PSDs Derived from Minimal Disturbance PSD Data Sets (blue circles) and Sonicated PSD Data Sets (red squares). These distributions are calculated on a same-tank basis and correspond to the first two cases outlined (see section 3.1.2.9).

As expected, sonication shifts the PSD to lower particle diameters. The shift appears to be uniform across the entire range of sizes observed, although the PSD tail between 100 and 300 μm appears to be appreciably reduced. After sonication, 90% of the material falls below 20 μm. The shift to lower particle sizes is not dramatic—less than an order of magnitude. The small difference between the sonicated and minimal disturbance may indicate that much of the material is either primary particles or hard agglomerates; it could also suggest that, were any large flocs present in the waste samples prior to analysis, the shear required to suspend the particles and obtain representative measurements was also sufficient to break those flocs.

Composite PSDs generated using all available minimal disturbance and sonicated data are presented in Figure 3.1.3. Because only a single tank does not have both sonicated and minimal disturbance distributions, there are very few differences between Figures 3.1.2 and 3.1.3. Quantiles of the PSDs provided in the figures are provided in Table 3.1.8. The distribution characteristics noted with regard to the figures are apparent.

Table 3.1.9 provides the results of the pseudo-waste type composite sonicated PSD analysis. Because of the number of waste types examined, the results are expressed in terms of particle diameters at select cumulative percentiles to ease comparison. Like the composite distribution, the pseudo-waste-type sonicated PSDs show a broad range of particle diameters spanning both submicron and supramicron particle ranges. The 50th percentile particle size ranges from approximately 3 to 11 μm. Disparity in the PSDs increases beyond this point.

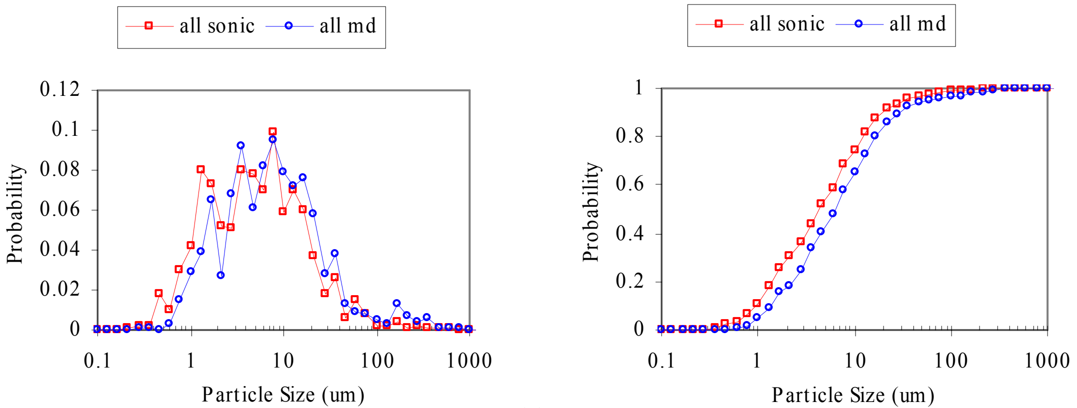

(a) (b)

Figure 3.1.3. Probability (a) and Cumulative (b) Composite PSDs for all Minimal Disturbance Data and all Sonicated Data. These distributions employ different tank bases.

Table 3.1.8. PSD Quantiles (μm)

Quantile	**1%**	**5%**	**25%**	**50%**	**75%**	**95%**	**99%**	**100%**
All Sonicated	0.39	0.70	1.63	4.39	10.1	33.4	112	774
All Minimal Disturbance	0.65	1.00	2.80	6.31	14.0	58.6	256	1000
Sonicated[(a)]	0.39	0.70	1.63	4.42	10.2	33.9	129	599
Minimal Disturbance[(a)]	0.64	1.06	2.88	6.59	14.7	74.2	280	1000
(a) Data include tanks with both sonicated and minimal disturbance PSDs.								

Table 3.1.9. Results of the Pseudo-Waste-Type Composite Analysis Expressed as Particle Size at Select Cumulative Percentiles from Sonicated PSDs

Psuedo-Waste Type	**PSD Percentiles (μm)**						
	1%	**5%**	**25%**	**50%**	**75%**	**95%**	**99%**
224	0.60	1.05	3.52	8.90	20.9	395	546
1C	0.77	1.00	2.15	4.64	7.24	12.3	15.6
2C	0.36	1.00	3.60	10.00	27.8	360	464
BL	0.61	0.77	1.29	2.78	8.13	16.2	23.6
CWP	0.36	0.71	1.54	4.64	9.37	32.9	57.9
CWR	0.82	1.00	2.79	6.87	14.8	46.4	71.6
CWZr	0.34	0.73	1.78	5.02	14.2	53.3	139
OWW3	0.32	0.60	1.37	4.64	15.4	48.8	60.7
P3	0.64	1.00	2.88	7.07	16.1	121	269
PFeCN	0.38	0.51	1.25	3.35	7.40	30.8	52.2
PL2	1.30	1.89	4.62	10.78	27.5	180	337
R (boiling)	0.43	0.91	2.53	6.73	15.4	43.6	70.5
SRR	0.80	1.11	2.79	5.58	10.1	52.5	210
TH	0.32	0.60	1.37	4.64	15.4	48.8	60.8
Unclassified	0.38	0.69	1.62	4.69	10.7	33.1	117
Z	0.37	0.89	1.62	3.46	7.31	12.9	19.1

3.2 Solid-Phase Compounds and Characteristics

This section describes identification, sizes, and shapes of solid phases in the sludge waste. It also presents a functional relationship between sizes and densities of agglomerates based on a fractal analysis.

3.2.1 Identity of Solid Phases in Sludge

A hybrid approach was taken to identify and quantify the compounds present in the solid phase of Hanford tank sludges. The solids predicted by the ESP[a] chemical thermodynamic model were taken as a first approximation. The sodium salts were removed from the ESP prediction, reflecting the dilution of tank waste that would occur before the waste reaches the WTP process. The non-salt predictions were then reviewed and revised by a panel of experts (Appendix E) who compared the compounds to observations made on sludge solids, typically by microscopic analysis techniques. In some cases, non-salt compounds not predicted in ESP but observed by microscopic analysis were added in a manner that maintained the mass balances on the main analytes in the compounds. In other cases, non-salt compounds were removed because they were present only in trace quantities. The most significant added compound was boehmite, which was added as the aluminum hydroxide/oxide phase in the tanks containing REDOX boiling waste. All aluminum hydroxide predicted by ESP in tanks containing REDOX boiling waste was assigned as boehmite. Aluminum hydroxide/oxide predicted in other tanks is assigned as gibbsite. The end result is shown in Table 3.2.1.

Table 3.2.1. Estimated Composition of Solid Phase in Hanford Sludges

ID of Assigned Compound	Crystal Density (kg/m^3)	Mass Percent of Total	Vol% of Total
Gibbsite	2420	44.9%	51.5%
$(NaAlSiO_4)_6 \cdot (NaNO_3)_{1.6} \cdot 2H_2O$	2365	14.2%	16.6%
Boehmite	3010	11.5%	10.6%
$NaAlCO_3(OH)_2$	2420	8.3%	9.5%
Fe_2O_3	5240	7.8%	4.1%
$Ca_5OH(PO_4)_3$	3140	2.3%	2.0%
$Na_2U_2O_7$	5617	3.2%	1.6%
ZrO_2	5680	2.2%	1.1%
Bi_2O_3	8900	2.6%	0.81%
SiO_2	2600	0.65%	0.69%
$Ni(OH)_2$	4100	0.81%	0.55%
MnO_2	5026	0.98%	0.54%
CaF_2	3180	0.27%	0.23%
$LaPO_4 \cdot 2H_2O$	6510	0.31%	0.13%
Ag_2CO_3	6077	0.021%	0.0094%
PuO_2	11430	0.0054%	0.0013%

(a) ESP was supplied and developed by OLI Systems, Inc., Morris Plains, New Jersey.

3.2.1.1 ESP Model Predictions

In May 2002 the BBIs for all 177 tanks were used to provide whole-tank-average composition inputs to the ESP model, which uses thermodynamic data to calculate the liquid and solid phase compositions at equilibrium. This modeling effort (Cowley et al. 2003) was carried out to support development of a tank-by-tank toxic source term for use in tank farm safety analyses.

The ESP predictions constitute the only phase composition information that 1) is available for all 177 tanks and 2) was prepared using a consistent method for all 177 tanks. It was therefore appropriate and advantageous to draw on this database in devising a sludge phase composition for transfer system design. However, this application of ESP had certain characteristics that should be noted:

- Compositions were calculated on a whole-tank basis, as if all the different layers of waste had been mixed and allowed to come to equilibrium.
- ESP is an equilibrium model and is not expected to predict the correct concentration of any compounds that have not yet come to equilibrium with an in-tank chemical environment different from those in which they formed (e.g., different temperature, pH, etc.).
- In the 2002 study, certain compounds were excluded from precipitating to reflect kinetic limitations, or sometimes to reduce computational time or avoid nonconvergence of the solution algorithm. As one significant example, boehmite was excluded because, had it been included, it would have been thermodynamically preferred to gibbsite in all wastes. Because gibbsite is actually dominant due to kinetic constraints that prevent boehmite from forming at lower temperatures, the databank excluded boehmite from forming at a temperature less than 100°C.
- Because of computational time constraints, REDOX equilibrium was not calculated on a tank-by-tank basis in the 2002 study; rather, expert judgment and generic-composition runs of ESP were used to fix the metal oxidation states in all tanks. Iron was fixed as Fe^{+3}, manganese as Mn^{+2}, chromium as Cr^{+3} or Cr^{+6}, and so forth. Thus, the ESP predictions could not include compounds formed by metals in any other oxidation states.
- The study assigned compounds to the trace analytes (including thorium, cadmium, copper, tin, and many others) without employing the ESP model; thus, these metals are not present in the compounds in the ESP-predictions database.
- Thermodynamic data were not available for all the compounds that could potentially form in the tank waste, which led to the omission of some compounds.

The ESP model, as used, predicted the normalized concentration of each solid in the waste. In other words, the model predicted the relative masses of different solids, and the relative volumes and masses of total liquid and total solid, but not the absolute masses or volumes in a tank. The absolute volume of dry solid phase in a tank was calculated for the present study by combining the ESP results with BBI volumes, using the following equation:

$$V_S = V\phi_{ESP} \tag{3.2.1}$$

where

V_S = dry solid volume in the tank

ϕ_{ESP}= ESP-predicted dry solid fraction, average of all the waste in the tank
V = the total waste volume in the tank as defined by the BBI.

The solid volume calculated by the above equation contains some uncertainty because of uncertainty in the parameters and because potential retained gas volume is not accounted for.

3.2.1.2 Description of Sludge

Because the main design concern was transport and mixing of the waste after it had been diluted, it was necessary to remove all salt compounds from all of the solids predicted by ESP for the 177 tanks on the assumption that they would have been leached out by dilution. Only the insoluble metal compounds were retained. However, it is possible that some portion of the least soluble salts, e.g. sodium fluoride phosphate ($Na_7F(PO_4)_2{\bullet}19H_2O$) and sodium oxalate ($Na_2C_2O_4$), would still be present during transport and handling. Some uncertainty in the solids density and size distribution is therefore present.

Table 3.2.2 shows the ESP-predicted solid-phase composition for the average waste (salts included) in all 177 tanks. Table 3.2.3 shows the ESP-based solid-phase composition on a salt-free basis.

Table 3.2.2. ESP-Predicted Composition of Volume-Weighted Average Solid Phase in Waste from the 177 Tanks

Molecular Formula	Crystal Density (kg/m^3)	Mass Percent of Total	Vol% of Total
$NaNO_3$	2260	43.7	44.0
$Na_7F(PO_4)_2{\bullet}19H_2O$	1750	10.4	13.5
$Al(OH)_3$	2420	14.2	13.4
$Na_2CO_3{\bullet}H_2O$	2250	7.5	7.6
$Na_3PO_4{\bullet}0.25NaOH{\bullet}12H_2O$	1620	2.4	3.4
$NaAlSiO_4$	2590	2.8	2.5
$Na_2C_2O_4$	2340	2.3	2.2
$NaAlCO_3(OH)_2$	2420	2.0	1.9
Na_3FSO_4	2650	2.1	1.8
$Na_4P_2O_7{\bullet}10H_2O$	1830	1.4	1.8
$Na_6(SO_4)_2CO_3$	2640	1.9	1.7
FeOOH	4260	2.1	1.1
$Na_2SO_4.10H_2O$	1464	0.59	0.91
$Na_3NO_3SO_4{\bullet}H_2O$	2300	0.80	0.79
NaF	2780	0.91	0.74
$NaNO_2$	2168	0.48	0.50
$Ca_5OH(PO_4)_3$	3140	0.51	0.37
$Na_2U_2O_7$	5617	0.76	0.31
CrOOH	5220	0.68	0.30
ZrO_2	5680	0.53	0.21
$NaHCO_3$	2159	0.15	0.16
Bi_2O_3	8900	0.56	0.14
SiO_2	2600	0.15	0.13
$Mn(OH)_2$	3260	0.17	0.12
KNO_3	2109	0.098	0.11
$Ni(OH)_2$	4100	0.19	0.10

Table 3.2.2 (contd)

Molecular Formula	Crystal Density (kg/m^3)	Mass Percent of Total	Vol% of Total
$KAlSiO_4$	2610	0.076	0.067
$Mn_3(PO_4)_2$	3102	0.065	0.048
CaF_2	3180	0.063	0.045
$SrCO_3$	3500	0.066	0.043
$Pb(OH)_2$	7590	0.093	0.028
$LaPO_4 \bullet 2H_2O$	6510	0.070	0.024
$(NaAlO_2)_2 \bullet 2.5H_2O$	2500	0.026	0.024
$CaCO_3$	2710	0.025	0.021
BiOCl	7720	0.062	0.018
$MnCO_3$	3125	0.022	0.016
Na_2SO_4	2680	0.017	0.014
$NiC_2O_4 \bullet 2H_2O$	1798	0.0058	0.0074
$Na_3PO_4.8H_2O$	1800	0.0041	0.0052
$Ca(OH)_2$	2240	0.0029	0.0029
$Sr_3(PO_4)_2$	3500	0.0040	0.0026
$La(OH)_3$	2300	0.0022	0.0022
Ag_2CO_3	6077	0.0049	0.0018
$PbCO_3$	6600	0.0049	0.0017
$Ni_3(PO_4)_2$	3930	0.0026	0.0015
$Pb_3(PO_4)_2$	7100	0.0034	0.0011
$Pu(OH)_4$	5926	0.0015	0.00056
$CaC_2O_4 \bullet H_2O$	2200	0.00034	0.00035
HgO	11100	0.0012	0.00024
TcO_2	11400	0.00038	0.000075

Table 3.2.3. ESP-Predicted Composition of Volume-Weighted Average Salt-Free Solid Phase in Waste from the 177 Tanks

Molecular Formula	Crystal Density (kg/m^3)	Mass Percent of Total	Vol% of Total
$Al(OH)_3$	2420	56.4%	64.2%
$NaAlSiO_4$	2590	11.1%	11.8%
$NaAlCO_3(OH)_2$	2420	7.8%	8.9%
FeOOH	4260	8.2%	5.3%
$Ca_5OH(PO_4)_3$	3140	2.0%	1.8%
$Na_2U_2O_7$	5617	3.0%	1.5%
CrOOH	5220	2.7%	1.4%
ZrO_2	5680	2.1%	1.0%
Bi_2O_3	8900	2.2%	0.69%
SiO_2	2600	0.61%	0.65%
$Mn(OH)_2$	3260	0.68%	0.58%
$Ni(OH)_2$	4100	0.74%	0.50%
$KAlSiO_4$	2610	0.30%	0.32%
$Mn_3(PO_4)_2$	3102	0.26%	0.23%
CaF_2	3180	0.25%	0.22%
$SrCO_3$	3500	0.26%	0.20%

Table 3.2.3 (contd)

Molecular Formula	Crystal Density (kg/m^3)	Mass Percent of Total	Vol% of Total
$Pb(OH)_2$	7590	0.37%	0.13%
$LaPO_4 \cdot 2H_2O$	6510	0.28%	0.12%
$(NaAlO_2)_2 \cdot 2.5H_2O$	2500	0.10%	0.11%
$CaCO_3$	2710	0.098%	0.099%
BiOCl	7720	0.25%	0.088%
$MnCO_3$	3125	0.086%	0.075%
$NiC_2O_4 \cdot 2H_2O$	1798	0.023%	0.036%
$Ca(OH)_2$	2240	0.011%	0.014%
$Sr_3(PO_4)_2$	3500	0.016%	0.012%
$La(OH)_3$	2300	0.0086%	0.010%
Ag_2CO_3	6077	0.020%	0.0088%
$PbCO_3$	6600	0.019%	0.0081%
$Ni_3(PO_4)_2$	3930	0.010%	0.0073%
$Pb_3(PO_4)_2$	7100	0.013%	0.0052%
$Pu(OH)_4$	5926	0.0058%	0.0027%
$CaC_2O_4 \cdot H_2O$	2200	0.0014%	0.0017%
HgO	11100	0.0046%	0.0011%
TcO_2	11400	0.0015%	0.00036%

The existing database of sludge-solid identifications was derived by X-ray diffraction (XRD), transmission electron microscopy (TEM) coupled with electron diffraction, and scanning electron microscopy (SEM) combined with electron-dispersive X-ray. The observations indicate the presence in Hanford wastes of a variety of compounds not modeled in the 2002 ESP runs. Appendix C contains a detailed summary of the observations of non-salt compounds that have been made and the sludge waste layers that have been included in the observed samples.

3.2.1.3 Final Selection of Phases

The set of solid compounds predicted by the ESP model was recognized to be incomplete, as discussed in Section 3.2.1.1 and illustrated in Appendix C. An improved selection of compounds was arrived at through review by an expert panel (Appendix E) and by comparison with a wide range of observations and microscopic analyses. As a result of the review effort, the ESP-predicted solids set was modified and reduced in number. The progression from ESP solids set to final set is tabulated in Table 3.2.4. The sludge (non-salt) compounds that were omitted from the final set (as distinct from those that were treated as being present in some other form) constitute 2.1% of the non-salt solid volume predicted by the ESP model. Thus, about 98 vol% of the predicted non-salt solids is included.

The final sludge composition produced by making the changes described in Table 3.2.4 is the one given in Table 3.2.1. Generally speaking, compounds were removed (or converted to others) because they were trace contributors and/or had no images to provide a size distribution and shape factor. A more detailed discussion of the changes in compound selection follows. All of the densities discussed are reported in the *Handbook of Chemistry and Physics* (CRC 1975) except where otherwise noted.

Table 3.2.4. Relationship of ESP-Predicted Solid Set to Final Solid Set

Molecular Formula of ESP-Predicted Compound	**Volume Fraction (%) (in salt-free ESP-predicted basis)**	**Assigned to the Compound**
Ag_2CO_3	0.0088	Ag_2CO_3
Bi_2O_3	0.69	Bi_2O_3; this compound, not $BiPO_4$, is considered to be the predominant form of Bi
BiOCl	0.088	Bi_2O_3
$Ca_5OH(PO_4)_3$	1.8	$Ca_5OH(PO_4)_3$
$CaCO_3$	0.099	$Ca_5OH(PO_4)_3$
$Ca(OH)_2$	0.014	$Ca_5OH(PO_4)_3$
$CaC_2O_4 \bullet H_2O$	0.0017	$Ca_5OH(PO_4)_3$
CaF_2	0.22	CaF_2
FeOOH	5.3	Fe_2O_3
$Al(OH)_3$	64.2	gibbsite, unless tank contains any REDOX (boiling) type; in that case, all $Al(OH)_3$ in the tank is considered to be boehmite
$(NaAlO_2)_2 \bullet 2.5H_2O$	0.11	gibbsite, unless tank contains any REDOX (boiling) type; in that case, all aluminate in the tank is considered to be boehmite
$NaAlCO_3(OH)_2$	8.9	$NaAlCO_3(OH)_2$
$NaAlSiO_4$	11.8	$(NaAlSiO_4)_6 \bullet (NaNO_3)_{1.6} \bullet 2H_2O$, nitrate cancrinite
$LaPO_4 \bullet 2H_2O$	0.12	$LaPO_4 \bullet 2H_2O$
$La(OH)_3$	0.010	$LaPO_4 \bullet 2H_2O$
$Mn_3(PO_4)_2$	0.23	MnO_2, based on observation that Mn in process waste precipitates as sodium birnesite
$Mn(OH)_2$	0.58	MnO_2
$MnCO_3$	0.075	MnO_2
$Ni(OH)_2$	0.50	$Ni(OH)_2$
$NiC_2O_4 \bullet 2H_2O$	0.036	$Ni(OH)_2$
$Ni_3(PO_4)_2$	0.007	$Ni(OH)_2$
$Pu(OH)_4$	0.0027	PuO_2 was the dominant compound found in SY-102 sludge
SiO_2	0.65	SiO_2
$Na_2U_2O_7$	1.5	$Na_2U_2O_7$; $Na_4(UO_2)(CO_3)_3$ has also been observed but is rarer and tends to dissolve when waste is diluted
ZrO_2	1.0	ZrO_2
$Pb(OH)_2$	0.13	removed (Pb may be an artifact of sample handling)
$PbCO_3$	0.0081	removed
$Pb_3(PO_4)_2$	0.0052	removed
CrOOH	1.4	removed (trace)
$KAlSiO_4$	0.32	removed (trace)
$SrCO_3$	0.20	removed (trace)
$Sr_3(PO_4)_2$	0.012	removed (trace)
HgO	0.0011	removed (trace)
TcO_2	0.00036	removed (trace)

Ag compounds. Silver is a small trace contributor to sludge solids but was retained in the distribution because images of Ag-rich particles were available for three different tank wastes (AY-102, C-106, and SY-102). The ESP-predicted compound silver carbonate, with a crystal density of 6.077 g/mL, was considered a reasonable representative of silver compounds.

Al compounds. Aluminum compounds make up almost 90 vol% of the sludge solids. The compounds predicted by ESP in the 2002 study are known to be an incomplete set, excluding boehmite for the reasons given. In addition, the forms of cancrinite that are present in tank waste were not available in the ESP databank in 2002. Certain other aluminosilicates were present in the ESP databank but were excluded from the runs as a way of saving run time, since the exact form of aluminosilicate that was present was not important for the purposes of the 2002 study.

Gibbsite and boehmite are among the primary aluminum phases observed in the Hanford tanks. The relative amounts of gibbsite and boehmite that are present in the tanks can be approximated by considering the tank waste temperature history. Boehmite was primarily produced in the tanks containing REDOX HLW at elevated temperatures (denoted as REDOX boiling waste compared with REDOX non-boiling waste). This additional heat allowed the gibbsite to be converted to boehmite. Boehmite is more stable than gibbsite, but the conversion from gibbsite to boehmite is slow at temperatures below 100ºC. At 150ºC, temperatures commonly achieved in sludge layers in the boiling tanks, and 4 M NaOH the conversion of gibbsite to boehmite is 85% complete within 6 to 10 hours (Russell et al. 1955). The conversion rate of boehmite to gibbsite increases with increasing temperature and NaOH concentration.

Microscopic and XRD analysis of wastes from Hanford tanks have indicated the presence of several other less common aluminum phases along with boehmite and gibbsite. These other aluminum phases were observed before and after caustic leaching. The tanks in which they were observed are discussed in Appendix C.

To approximately reflect the distribution of aluminum among solid-phase compounds, the following rules were used:

- The dawsonite ($NaAlCO_3(OH)_2$) predicted by ESP was left as is to reflect the chemical environment that made the carbonate thermodynamically possible.
- The Al in the predicted $Al(OH)_3$ was divided between gibbsite and boehmite (with the appropriate stoichiometric conversion to boehmite), depending on whether REDOX boiling waste had ever been added to the tank. It was assumed for simplicity that all aluminum hydroxide in the tank, whether part of the REDOX waste or not, would have been converted to boehmite before the waste in the tank cooled.(a) These tanks were S-101, S-104, S-107, S-110, SX-103, SX-104, SX-107 through SX-115, and U-110 (Meacham 2003). In all other tanks, those without REDOX boiling waste, $Al(OH)_3$ was considered to be gibbsite.

(a) The estimated boehmite/gibbsite split could be refined by using the aluminum leaching factors in the TWINS database. In this approach, the $NaAlSiO_4$ and $NaAlCO_3(OH)_2$ predicted in the boiling tanks by ESP would be considered non-leachable, the remainder of the non-leachable fraction of the aluminum would be considered to be boehmite, and the leachable fraction would be considered gibbsite. This would probably give a low estimate of boehmite in the 177 tanks, since none of the boehmite in non-boiling tanks is included.

- Sodium aluminate, $(NaAlO_2)_2•2.5H_2O$, was predicted in one tank (AN-103). It was assumed that on dilution this compound would be transformed to gibbsite, the form present in wastes with lower hydroxide concentrations.
- The predicted sodium aluminosilicate ($NaAlSiO_4$) was treated as being nitrate cancrinite ($(NaAlSiO_4)_6•(NaNO_3)_{1.6}•2H_2O$), a compound whose composition is very similar.(a) Potassium aluminosilicate ($KAlSiO_4$) was omitted, being a trace contributor.

The densities of the aluminum oxide and hydroxide compounds (Wefers and Misra 1987) vary significantly (Table 3.2.5). Gibbsite has the lowest density of the aluminum oxides and hydroxides (2.42 g/mL). Dawsonite and cancrinite densities are comparable to that of gibbsite. Nordstrandite, another form of aluminum hydroxide, has the same measured density as gibbsite. The measured density for bayerite (2.53 g/mL) is slightly higher than the density of gibbsite. Boehmite has an intermediate density (3.01 g/mL) which is about 25% higher than the gibbsite density. The highest density of the aluminum oxides and hydroxides is found in corundum, at 3.98 g/mL.

Table 3.2.5. Densities of Aluminum Oxides and Hydroxides

Phase	Formula	Density (g/mL)
Gibbsite	$Al(OH)_3$	2.42
Bayerite		2.53
Nordstrandite		2.42(a)
Boehmite	AlOOH	3.01
Diaspore		3.44
Corundum	Al_2O_3	3.98
(a) Density of nordstrandite was obtained from Roberts et al. (1990).		

Bi compounds. The ESP model, as used in the 2002 study, predicted bismuth precipitation primarily as Bi_2O_3, with small amounts of BiOCl in some tanks. While Bi_2O_3 (and similar compounds) and $BiPO_4$ have been observed in Hanford tank wastes, BiOCl has not. Bismuth phosphate has been identified in relatively few of the tank sludges examined by microscopic or XRD examination. Specific Bi phases and the tank in which they were observed were listed in Appendix C.

For the purpose of the particle size correlation with density, it was assumed that the Bi_2O_3 represented all the Bi phases present in the tank. The stoichiometry of the bismuth and oxygen in the oxide phases incorporating other metals ($Bi_{38}CrO_{60}$, $Bi_{24}Al_2O_{39}$, and $Bi_{36}Fe_2O_{57}$) is similar to that of Bi_2O_3. The density of Bi_2O_3 and $BiPO_4$ are 8.9 and 6.323 g/mL, respectively, while their sizes are similar. Bi_2O_3 is selected.

(a) The nitrate form of cancrinite has only been observed in evaporated waste from tank AP-101, though it may also be present in in-situ waste. The carbonate cancrinite, $(NaAlSiO_4)_6•(CaCO_3)_2$, has been observed in in-situ waste. The densities of the two forms are very similar (2.4 to 2.5 g/cc for the carbonate, versus 2.365 g/cc for the nitrate) as are the molecular weights. Using carbonate cancrinite instead of nitrate would change the volume fraction of cancrinite by about 3% of its value. The particle sizes and shapes of the two forms are also much the same.

Ca compounds. The Ca compounds predicted by ESP are $Ca_5OH(PO_4)_3$ (density 3.14 g/mL), CaF_2 (density 3.18 g/mL), $CaCO_3$ (density 2.71 g/mL), $Ca(OH)_2$ (density 2.24 g/mL), and $CaC_2O_4•H_2O$ (density 2.20 g/mL), in order of decreasing concentration. Of these, $Ca_5OH(PO_4)_3$ and $CaCO_3$ have been observed in the waste. Because of their predominance in the waste and somewhat higher density, the species $Ca_5OH(PO_4)_3$ and CaF_2 were used to represent calcium compounds.

Cr compounds. Chromium oxyhydroxide (CrOOH) was the only Cr(III) compound predicted by ESP to exist in the solid phase. Because no images of Cr compounds were available, no Cr compounds were included in the final solids composition.

Fe compounds. ESP uniformly predicted that Fe would precipitate as goethite (FeOOH); this prediction resulted from excluding Fe_2O_3 from the potential precipitates modeled by ESP because of the expectation that FeOOH was more common. Rapko and Lumetta (2000) showed iron compounds in the waste; of these, FeOOH appeared commonly. Fe_2O_3 also appeared in images and its density (5.24 g/mL) was comparable to that of FeOOH (4.26 g/mL); Fe_2O_3 was selected to represent iron in the sludge solids.

La compounds. Lanthanum was predicted to exist in solid form as the phosphate ($LaPO_4•2H_2O$) or hydroxide ($La(OH)_3$). The phosphate being more prevalent, it was chosen to represent La compounds.

Mn compounds. Three manganese compounds were predicted by ESP: $Mn_3(PO_4)_2$ (density 3.102 g/mL), $Mn(OH)_2$ (density 3.26 g/mL), and $MnCO_3$ (density 3.125 g/mL). However, denser Mn compounds have been observed, including MnOOH (4.3 g/cc) and Mn-containing spinels such as Mn_2MnO_4 (5 g/cc). In the WTP process, the manganese added as permanganate, a major source of in-process Mn, precipitates as sodium birnesite,(a) whose chemical formula is nearly that of MnO_2 (density 5.026 g/cc). Thus Mn compounds predicted by ESP are treated as MnO_2 (converted on moles-Mn basis).

Pb compounds. The lead compounds are removed from the sludge solids as trace contributors. In addition, it is possible that Pb in Hanford tank waste samples may have been partly an artifact, having been added to the core samples by leaching from containers in which they were stored.

Pu compounds. The ESP-predicted plutonium solid was plutonium hydroxide, $Pu(OH)_4$. For comparison, more than 70% of the Pu mass found in the solids in SY-102 samples contained only Pu and O, and was considered to be PuO_2.(b) The remainder of the Pu-bearing solids had a variety of compositions, frequently including bismuth, phosphorus, and/or aluminum. Based on these data, all Pu in the sludge solids is considered to be PuO_2.

Si compounds. As seen in Table 3.2.2, most of the Si present in solids was predicted to take the form of aluminosilicate; the remainder was predicted to be SiO_2. This prediction was considered acceptable because the local sand, quartz, feldspars, and other minerals, is known to have entered tanks. Depending on its form, silicon dioxide may have a density of 2.17 g/mL (natural opal) to 2.66 g/mL (natural quartz). A density of 2.60 g/cc was selected based on quartz.

(a) Personal communication from JG Reynolds (Bechtel National, Inc.) to LA Mahoney (Pacific Northwest National Laboratory) during expert elicitation meeting on November 27, 2006.

(b) Callaway WS and GA Cooke. 5/17/2004. "Distribution of Plutonium-Rich Particles in Tank 241-SY-102 Sludge." CH2M-0400872, CH2M HILL, Richland, Washington.

U compounds. A variety of uranium compounds have been observed in sludge wastes, including sodium diuranate ($Na_2U_2O_7$), uranium oxides, and cejkaite ($Na_4UO_2(CO_3)_3$). Of these, ESP predicted only $Na_2U_2O_7$. Sodium diuranate has a density of 5.617 g/mL and was selected as the representative uranium compound.

Zr compounds. The ESP model predicted ZrO_2 as the sole solid compound. This compound has been observed in several tank wastes and was therefore used in this study to represent Zr solids.

Other compounds. Although mercury, technetium, and strontium compounds were also included in the ESP modeling results from the 2002 study, they were considered to be trace contributors and were omitted from the composition. As already noted, a number of other trace constituents (including thorium, cadmium, copper, tin, and many others) were not included in the ESP model inputs or outputs in 2002. These also were omitted from the present study.

3.2.1.4 Propagation of Composition Uncertainty

A variety of sources of uncertainty were mentioned in Section 3.2.1, all of which contribute to uncertainty in the final volume-fraction composition (Table 3.2.1). Expressions can be derived to estimate this uncertainty in the calculated volume fractions of solid compounds (J of them) in the average waste from some number N of tanks.

ESP output provides a set of kg/L concentrations $c_{n,j}$ (where j denotes which of J compounds the concentration is for, and n denotes which of N tanks) for the concentrations of each precipitated compound in the dry solid phase. The uncertainty in these ESP-predicted concentrations comes from the BBI-based inputs, the ESP-predicted analyte solubility, and the choice of precipitated compounds.

The uncertainty in the concentrations that were taken from BBI and used as ESP input is stated in the TWINS database, expressed as the relative standard deviation (RSD) of the concentration.[a] The median values of RSD for all major sludge analytes in all the sludge layers in the 177 tanks are given in Table 3.2.6.[b] The uncertainty that comes from variability of the waste in the tank, which affects the representativeness of samples taken from the waste, is not considered. The RSDs of the concentrations of sludge-type analytes present in salt layers also were not considered.

The ESP prediction uncertainty can be considered in terms of what fraction of the analyte in the BBI inventory ends up in solid phase. (The uncertainty in the identity of the compound is a separate issue, discussed later.) The analytes that are important to sludge solid phases are almost entirely precipitated, except in a few tanks where chelator concentrations are high, e.g., AN-107. Chemical analyses of the waste agree with ESP predictions in this respect. Because the analyte solubilities are so low and the extent of precipitation so great, uncertainties in the ESP-predicted solubility of sludge solids are not likely to be significant compared with the input RSD.

---

[a] The RSD is defined as the standard deviation divided by the mean.

[b] BBI data for all 177 tanks were downloaded on November 27, 2006 from BBI Calculation Details on TWINS (http://twinsweb.pnl.gov/twinsdata/forms/bbiRequiredReading.asp?bbiSrc=autotcr.dbo.v_calc_detail&srcName=Best+Basis+Calculation+Detail).

Table 3.2.6. Median RSD for Analytes in Sludge Layers

Sludge Analyte	Median RSD in BBI Analyte Concentration
Ag	0.19
Al	0.12
Bi	0.090
Ca	0.17
Fe	0.12
La	0.74
Mn	0.21
Ni	0.14
Pu	0
Si	0.15
U	0.14
Zr	0.43

The uncertainty in compound assignment is present whether compounds are identified by ESP predictions or by subsequent expert judgment based on observations. The compound identity determines properties such as the molecular weight (MW). An uncertainty in the MW representing the range of possible compounds containing an analyte can be estimated by finding the standard deviation of the formula weights of several possible compounds.[a] This is not a rigorous uncertainty, in part because the selected compound is not necessarily the one with the median MW of the set, but may be at one end or the other, and because the values are not weighted by the relative probability of precipitation of the compounds. However, the approach does give a rough idea of the effect of compound identity.

Table 3.2.7 shows the relative uncertainties in MW that were used and lists the compounds that were considered in estimating the MW uncertainty. The table also shows the relative uncertainties in the final set of compound mass concentrations that result from BBI inputs and compound selection. These mass-concentration uncertainties are found as the square root of the sum of the squares of the relative uncertainties[b] in BBI concentration and MW.

The mass of each compound in each tank, m_j, is obtained by multiplying the final mass concentrations by the volume of dry solids in each tank, S_n. This volume contains error that comes from the BBI total volume (possibly including retained gas, which is not accounted for) and the ESP-predicted ratio of dry solid volume to total waste volume. A value of 0.2 is assigned to the relative volume uncertainty, $\delta S_n/S_n$, based on the 20% uncertainty in volume that it is reasonable to expect from the BBI. The uncertainty in ESP-predicted solid volume fraction is derived from compound choice and solubility and already accounted for.

---

[a] The formula weight is the MW of the compound divided by the number of moles of analyte that one mole of the compound contains.

[b] The relative uncertainty in MW is defined, for the present purpose, as the standard deviation in the set of MW divided by the mean value. The same definition is used for "relative uncertainty" in other variables, as well.

Table 3.2.7. Uncertainty in Molecular Weight of Assigned Compounds

Sludge Analyte	Compounds Considered	Relative Uncertainty in the Compound MW	Resulting Relative Uncertainty in the Compound Mass
Ag	Ag_2CO_3, AgCl, AgOH	0.070	0.21
Al	$Al(OH)_3$, AlOOH, $(NaAlO_2)_2$•$2.5H_2O$, $NaAlCO_3(OH)_2$, $(NaAlSiO_4)_6$•$(NaNO_3)_{1.6}$•$2H_2O$, $AlPO_4$	0.36	0.38
Bi	Bi_2O_3, BiOCl, $BiPO_4$, $Bi_{38}CrO_{60}$	0.13	0.16
Ca	$Ca_5OH(PO_4)_3$, CaF_2, $Ca_3(PO_4)_2$, $Ca(OH)_2$, $CaCO_3$, $CaC_2O_4.2H_2O$	0.31	0.36
Fe	Fe_2O_3, FeOOH, $Fe(OH)_3$, $FePO_4$	0.30	0.32
La	$LaPO_4.2H_2O$, $La(OH)_3$	0.20	0.76
Mn	MnO_2, $Mn_3(PO_4)_2$, MnOOH, $MnCO_3$, $Mn(OH)_2$, Mn_2MnO_4	0.18	0.27
Ni	$Ni(OH)_2$, $Ni_3(PO_4)_2$, NiC_2O_4•$2H_2O$	0.35	0.37
Pu	PuO_2, $Pu(OH)_4$	0.088	0.088
Si	$(NaAlSiO_4)_6$•$(NaNO_3)_{1.6}$•$2H_2O$, SiO_2, $NaAlSi_3O_8$	0.54	0.56
U	$Na_2U_2O_7$, UO_2, UO_3, $Na_4(UO_2)(CO_3)_3$	0.36	0.38
Zr	ZrO_2, $Zr(OH)_4$	0.18	0.46

The total mass m_j of each compound j, over all N tanks, is

$$m_j = \sum_{n=1}^{N} S_n c_{n,j} = \sum_{n=1}^{N} M_{n,j} \tag{3.2.2}$$

The uncertainty in each individual-tank mass term, $\delta M_{n,j}$, is

$$\delta M_{n,j} = M_{n,j} \sqrt{\left(\frac{\delta S_n}{S_n}\right)^2 + \left(\frac{\delta c_{n,j}}{c_{n,j}}\right)^2} \tag{3.2.3}$$

The error in the total mass (over all tanks) of each compound, δm_j, is

$$\delta m_j = \sqrt{\sum_{n=1}^{N} \left(\delta M_{n,j}\right)^2}$$

$$\delta m_j = \sqrt{\sum_{n=1}^{N} \left[\left(c_{n,j}\delta S_n\right)^2 + \left(S_n \delta c_{n,j}\right)^2\right]} \tag{3.2.4}$$

The relative error in the total compound mass is

$$\frac{\delta m_j}{m_j} = \frac{\sqrt{\sum_{n=1}^{N}\left[\left(c_{n,j}\delta S_n\right)^2 + \left(S_n \delta c_{n,j}\right)^2\right]}}{\sum_{n=1}^{N} c_{n,j} S_n} \tag{3.2.5}$$

The volume V_j of each compound is

$$V_j = \frac{m_j}{\rho_j} \tag{3.2.6}$$

The uncertainty in the density comes largely from the uncertainty in compound identity and is calculated the same way as MW—as the standard deviation in the densities of compounds in which the analytes appear. Table 3.2.8 lists the uncertainties in the compound density for each analyte.

The error in the total volume of each compound, δV_j, can be found as

$$\delta V_j = V_j \sqrt{\left(\frac{\delta m_j}{m_j}\right)^2 + \left(\frac{\delta \rho_j}{\rho_j}\right)^2} \tag{3.2.7}$$

Table 3.2.8. Uncertainty in Density of Assigned Compounds

Sludge Analyte	Compounds Considered	Relative Uncertainty in Compound Density
Ag	Ag_2CO_3 (6.077 g/mL); AgCl (5.56 g/mL)	0.063
Al	Gibbsite (2.42 g/mL); boehmite (3.01 g/mL); diaspore (3.3 g/mL, 3.5 g/mL); $(NaAlO_2)_2$•$2.5H_2O$ (2.5 g/mL); $(NaAlSiO_4)_6$•$(NaNO_3)_{1.6}$•$2H_2O$ (2.365 g/mL); $AlPO_4$ (2.566 g/mL)	0.16
Bi	Bi_2O_3 (8.9 g/mL); BiOCl (7.72 g/mL); $BiPO_4$ (6.323 g/mL)	0.17
Ca	$Ca_5OH(PO_4)_3$ (3.14 g/mL); CaF_2 (3.18 g/mL); $Ca(OH)_2$ (2.24 g/mL); $CaCO_3$ (2.71 g/mL); $CaC_2O_4.2H_2O$ (2.2 g/mL)	0.17
Fe	Fe_2O_3 (5.24 g/mL); FeOOH (4.26 g/mL); $Fe(OH)_3$ (3.4 g/mL, $Fe(OH)_2$); $FePO_4$ (2.74 g/mL, dihydrate)	0.28
La	$LaPO_4.2H_2O$ (6.51 g/mL); $LaCO_3$ (2.65 g/mL, octahydrate)	0.60
Mn	MnO_2 (5.026 g/mL); $Mn_3(PO_4)_2$ (3.102 g/mL, trihydrate); MnOOH (4.35 g/mL); $MnCO_3$ (3.125 g/mL); $Mn(OH)_2$ (3.26 g/mL); Mn_2MnO_4 (5.0 g/mL, as for other spinels)	0.23
Ni	$Ni(OH)_2$ (4.1 g/mL); $Ni_3(PO_4)_2$ (3.93 g/mL); NiC_2O_4•$2H_2O$ (1.798 g/mL)	0.025
Pu	PuO_2 (11.43 g/mL); $Pu(OH)_4$ (5.926 g/mL)	0.45
Si	$(NaAlSiO_4)_6$•$(NaNO_3)_{1.6}$•$2H_2O$ (2.365 g/mL); SiO_2 (2.6 g/mL quartz, 2.19 g/mL lechatelierite); $NaAlSi_3O_8$ (2.61 g/mL)	0.083
U	$Na_2U_2O_7$ (5.617 g/mL); UO_2 (10.96 g/mL); UO_3 (7.29 g/mL); $Na_4(UO_2)(CO_3)_3$ (3 g/mL, estimated)	0.50
Zr	ZrO_2 (5.68 g/mL); $Zr(OH)_4$ (3.25 g/mL)	0.38

The total volume of all dry solids, *T*, is the sum of the volumes of all compounds. The propagated error in the total volume, δT, is

$$\delta T = \sqrt{\sum_{j=1}^{J} \left(\delta V_j\right)^2} = \sqrt{\sum_{j=1}^{J} \left[\left(\frac{\delta m_j}{\rho_j} \right)^2 + \left(m_j \delta \rho_j \right)^2 \right]} \tag{3.2.8}$$

The volume fraction ϕ_j of each compound in the N-tank average composition is

$$\phi_j = \frac{V_j}{T} \tag{3.2.9}$$

The propagated error in the volume fraction, $\delta\phi_j$, is

$$\delta\phi_j = \phi_j \sqrt{\left(\frac{\delta V_j}{V_j} \right)^2 + \left(\frac{\delta T}{T} \right)^2} \tag{3.2.10}$$

The final product of the above derivation, an estimate of the relative uncertainty in the volume fractions, $\delta\phi_j/\phi_j$, is given in Table 3.2.9 with the volume-based composition.

Table 3.2.9. Relative Uncertainty of the 177-Tank Sludge Solid-Phase Composition

ID of Assigned Compound	Volume Percent of Total	Relative Uncertainty in Volume Fraction
Gibbsite	51.5%	0.20
$(NaAlSiO_4)_6 \cdot (NaNO_3)_{1.6} \cdot 2H_2O$	16.6%	0.22
Boehmite	10.6%	0.23
$NaAlCO_3(OH)_2$	9.5%	0.22
Fe_2O_3	4.1%	0.30
$Ca_5OH(PO_4)_3$	2.0%	0.22
$Na_2U_2O_7$	1.6%	0.51
ZrO_2	1.1%	0.48
Bi_2O_3	0.81%	0.20
SiO_2	0.69%	0.30
$Ni(OH)_2$	0.55%	0.12
MnO_2	0.54%	0.26
CaF_2	0.23%	0.22
$LaPO_4 \cdot 2H_2O$	0.13%	0.64
Ag_2CO_3	0.0094%	0.16
PuO_2	0.0013%	0.46

3.2.2 Solid-Phase Compound Particle Size Estimates

The particle size estimates for the pertinent compounds are based on scanning electron microscope images provided in Appendix D. The spatial resolution of the SEM instrument used in these analyses was ~0.5 μm, which sets a lower limit on the size range that can be accurately recorded. Furthermore, the visibility of surface features varies with beam voltage. Most of the analyses are performed with backscattered imaging at 20–30 kV, further reducing the ability to define individual crystallites. TEM images permit much lower limits and a more accurate assessment of the actual crystal size; however, few TEM analyses of Hanford tank waste have been conducted. The error in the SEM and TEM calibrations is likely to be 10 to 20%. Additional uncertainties will result from orientation of particles relative to the probe, which may affect their apparent size under the microscope. XRD can be used to examine the crystallite size by examining the degree of peak broadening.

3.2.2.1 PSDs for Solid-Phase Compounds

PSDs have been reported as either cumulative distribution plots (CDF) or simple triangular distributions with maximum and minimum values as well as an average expected value. For the more common phases, enough data were available for a CDF. Images were analyzed with Gatan Digital Micrograph DM 3.9.2 and calibrated to the micron-bar visible on the images. As many measurements as possible were made. Identifying the individual length is a judgment call. The microscope can reveal the individual grains but the strength of the agglomerates may make this type of assessment irrelevant.

The presented PSDs only illustrate the distribution of the viewed images. On the order of 10,000 images may need to be analyzed to establish a statistically significant PSD (Jillaventesa et al. 2001). A best estimate for PSDs is listed in Table 3.2.10. This table is, in effect, an expansion of Table 3.2.1. For comparison, the particles have been classified into larger groups in Table 3.2.11 and given a range of particle sizes.

Table 3.2.10. Solid Characteristics

Mol. Formula	**Mineral Name**	ρ . **(g/cm^3)**	**Vol. Fract. Tot.**	**Triangular Distribution of Primary Particles (μm)**			**Source**
				Max	**Mode**	**Min**	
$Al(OH)_3$	gibbsite	2.44	0.516	20	4.4	0.8	(see CDF); Bechtold et al. 2003 (a, b, c, d)
$Al(O)OH$(e)	boehmite	3.07	TBD	0.5	0.1	0.02	(see CDF); Lumetta et al. 1997, 1996b), SY-103 (Liu et al. 1995)
$Na_{7.6}[AlSiO_4]_6(NO_3)_{1.6}\bullet(H_2O)_2$	NO_3-cancrinite	2.365	0.195	8	2.5	1	(see CDF); Buck and McNamara 2004(f)
Fe_2O_3/ $FeOOH$	hematite	5.240	0.108	4.3	2.4	0.1	(see CDF); Bechtold et al. 2003; Herting et al. 2004; Buck et al. 2003 (a, c, d, g)
$NaAlCO_3(OH)_2$	dawsonite	2.46	0.069	15	3.4	0.5	(see CDF); Bechtold et al. 2003; Herting et al. 2004 (d, h)
$Na_2U_2O_7$ / U_3O_8	clarkeite, oxide	6.61 / 10.97	0.022	15	0.1	0.05	(see CDF); Lumetta et al. 1997; Warrant and Cooke 2003; Buck et al. 2003(a, b, g, h)
$Ca_5OH(PO_4)_3$	hydroxyapatite	3.140	0.020	0.1		0.05	Lumetta et al. 1997(f)

Table 3.2.10 (contd)

Mol. Formula	Mineral Name	ρ . (g/cm^3)	Vol. Fract. Tot.	Triangular Distribution of Primary Particles (μm)			Source
				Max	Mode	Min	
Na Phosphates				1000	60	15	see CDF; Herting et al. 2004 (a, f, g)
SiO_2	quartz sand	2.600	0.016	100			Assumed as sand source
ZrO_2		5.680	0.015	50	0.2	0.05	Lumetta et al. 1997, 1996c; [a, d, j]
MnO_2	birnesite	5026	0.0053	10	1.3	0.3	Bechtold et al. 2003; Buck et al. 2003
$Ni(OH)_2$		4.100	0.007	0.5	0.2	0.005	Lumetta et al. 1997
CaF_2		3.180	0.004	15			No data available
$LaPO_4 \bullet 2H_2O$		6.510	0.003	3	0.2	0.1	TEM(d)
$CaCO_3$		2.710	0.001	14			Herting et al. 2004(a)
Ag_2CO_3		6.077	0.0002	4			Bechtold et al. 2003(a, d)
Pu solids (varied composition)		11.430	0.00002	40	8	1	(a) (see CDF in Figure 1)
Addition Minor Phases							
Al-Silicates	"zeolites"	~2.5	TBD	20	5	0.1	Lumetta et al. 1997; Buck et al. 2003
Al-Silicates	"clays"	*2.3*	TBD	0.6	0.3	0.1	SX-108
$Mn_3(PO_4)_2$	sidorenkite	3.102	0.006	8		8	(k)
$Na_4(UO_2)(CO_3)_3$	cejkaite	3.76	TBD	50	7.5	2	(see CDF); Krupka et al. 2006
$Pb_5(OH)(PO_4)_3$	Pb phosphate		TDB	0.4		0.05	C-107(g)
$BiPO_4$	Biphosphate		TBD	10	2	1	(g)
Zr-Fe phase	Fe-Zirc		TBD	2		0.5	
$(Ca,Sr)_3(Cr,Al)_2(OH)_2$	hydrouvarite		TBD	10		5	Warrant and Cooke 2003
$Cr(OH)_3$			TBD	10	0.2	0.15	(d)

(a) Callaway WS and GA Cooke. 5/17/2004. "Distribution of Plutonium-Rich Particles in Tank 241-SY-102 Sludge." CH2M-0400872, CH2M HILL, Richland, Washington.

(b) Callaway WS, GA Cooke, and DL Herting. 3/18/2005. "Particle Size Measurements in Support of the Tank 241-AN-102 Chemistry Control Recovery Plan." 7S110-WSC-05-011, CH2M HILL, Richland, Washington.

(c) Herting DL and GA Cooke. 5/5/2004. "Caustic Demand Test Results for Tank 241-C-103 Sludge." 7S110-DLH-04-015, CH2M HILL, Richland, Washington.

(d) Warrant RW. November 2006. "Results of Caustic Testing of Tank 241-AY-102 Core 319 Sludge Solids." 7S110-RWW-06-080, CH2M HILL, Richland, Washington.

(e) Additional Al-phases include diaspore (25 μm long x 1 μm thick), Al-phosphate, $Ca_3Al_2O_6$.

(f) Herting DL. 7/28/2005. "Tank 241-AN-102 Process Chemistry Test Results." 7S110-DLH-05-028, CH2M HILL, Richland, Washington.

(g) Frye JM. 4/29/2005. "Results of Caustic Testing of 241-C-101 & 241-C-107." 7S110-JMF-05-015, CH2M HILL, Richland, Washington.

(h) Herting DL. 8/28/2003. "Caustic Demand Test Results, Tank 241-AN-102 Sludges." FH-0303343, Fluor Hanford, Inc., Richland, Washington.

(i) Values calculated from XRD broadening shown below.

(j) Herting DL. 9/15/2005, "Tank AY-102 Centrifuged Solids Analysis Results." 7S110-DLH-05-040, CH2M HILL, Richland, Washington.

(k) $Fe_2Bi(SiO_4)_2OH$, $Bi_{38}CrO_{60}$, and $Bi_2Fe_4O_9$ reported by Cooke and coworkers.

Table 3.2.11. Grouped Primary Particle Characteristics

Groups	Maximum Observed Length (μm)	Mode Size (μm)	Minimum Observed Length (μm)
Aluminum oxides	20	4	0.02
Al-Silicates	20	4.5	0.1
Transition metal oxides	25	0.35	0.02
P-Block oxides	10	2	0.05
Phosphates[(a)]	1000	15	0.05
Uranium oxides[(b)]	5	0.1	0.05
Plutonium oxides	40	8	1

(a) Minimum phosphate size from bismuth phosphate, large sizes observed for Na phosphates.
(b) Largest uranium phases observed for cejkaite (rod-like particle); these were ignored in this analysis because they should be unstable in solution.

3.2.2.2 Determination of Particle Size from XRD

When crystals are less than 0.1 mm in diameter, significant broadening of XRD peaks can occur; it is possible to extract information on the crystallites size based on this broadening. Using the Scherrer equation,

$$D \cong \frac{0.9\lambda}{\beta \cos\Theta} \tag{3.2.11}$$

where

λ = x-ray wavelength (0.154178 nm)
β = broadening (FWHM•180/2π, radians)
Θ = peak position (degrees).

Broadening in peaks is listed in Table 3.2.12 for AN-102 and AZ-101, respectively, in Buck et al. (2003) as FWHM values. FWHM is the width of the XRD peaks at the full-width half-maximum point. The x-ray anodes were Cu-K-alpha. The boehmite phase did exhibit significant broadening; however, as the boehmite particles are hexagonal plates, this analysis may not represent the actual particle size. It is likely that the values with the small 2Θ values are the most accurate as these were from isolated peaks that permitted the most accurate measurements.(a) The XRD results suggest very small crystallite sizes.

High fluoride content in BY-109 leads to formation of fluoride sulfate double salts, not included in this analysis. These include Na_3FSO_4, $Na_7(PO_4)_2{\bullet}19H_2O$, $Na_2C_2O_4$, and NaF. The phase termed cejkaite may also fall into this group as it will have very high solubility. Both bismuth oxides and phosphates were observed in the same samples.(b)

(a) 2Θ is reported as this is the measurement obtained from the XRD plots.
(b) Poloski AP, R Daniels, and EC Buck. 2005. Environmental Management Science Program (unpublished data), Pacific Northwest National Laboratory, Richland, Washington.

Table 3.2.12. Determination of Boehmite Particle Size from XRD

Sample	2-Theta	FHWM Adjusted[(a)]	Est. Size (nm)
AN-102	14.601	0.517	8
AN-102	28.155	0.299	15
AN-102	49.15	0.386	18
AN-102	51.719	0.204	31
AN-102	55.406	0.167	42
AZ-101	14.52	0.454	9
AZ-101	28.181	0.270	17
AZ-101	38.38	0.285	18
AZ-101	48.98	0.573	11
Washed			
AZ-101	14.52	0.315	13
AZ-101	28.199	0.241	19
AZ-101	38.36	0.147	34
AZ-101	48.777	0.155	38

(a) The value was reduced slightly based on examination of the spectrum from a corundum compound that was used as an internal standard.

The size distribution of cejkaite (uranium), plutonium phase particles, aluminum phases, cancrinite (zeolitic) phases, and iron oxide phases is shown below (see Figures 3.2.1 to 3.2.4). The two actinide phases have similar size ranges. However, cejkaite, the uranyl carbonate phase, is considered stable under evaporative conditions and; hence, the large particle sizes observed for this phase are unlikely to occur during waste processing.

In the aluminum phases, boehmite particles are considerably smaller than either gibbsite or dawsonite which both exhibit similar size ranges. In the case of dawsonite and other elongated (acicular) particles, the largest length was used in the data plots.

Cancrinite crystals consist of agglomerates that look like balls of wool. With very high-resolution microscopy the true nature of the bent crystallites can be seen. In this case the reported particle size is biased towards the individual ball size.

The distribution of sodium phosphate phases ($Na_4P_2O_7 \cdot 10H_2O$ and $Na_7F(PO_4)_2 \cdot 19H_2O$) exhibited the largest particle sizes in this investigation. Other phosphates are reported but no image data was available from these for analysis. In Figure 3.2.5 the distribution of these sodium phosphate phases is shown.

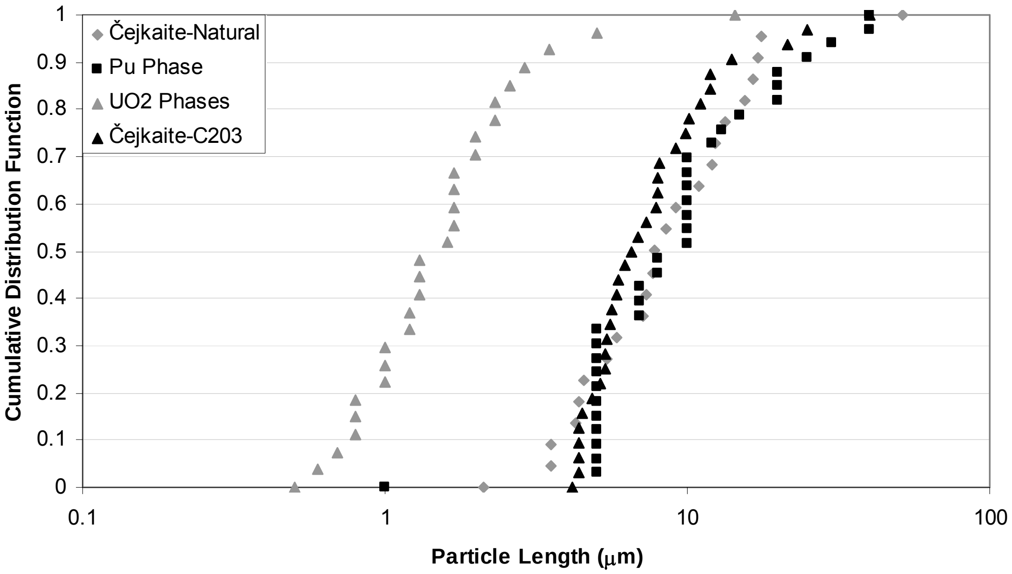

Figure 3.2.1. Cumulative PSDs for Actinide Phases (Cejkaite, Krupka et al. 2006; Pu phases,[(a)] U oxide phases[(a,b,c,d)], Lumetta et al. 1996, 1997)

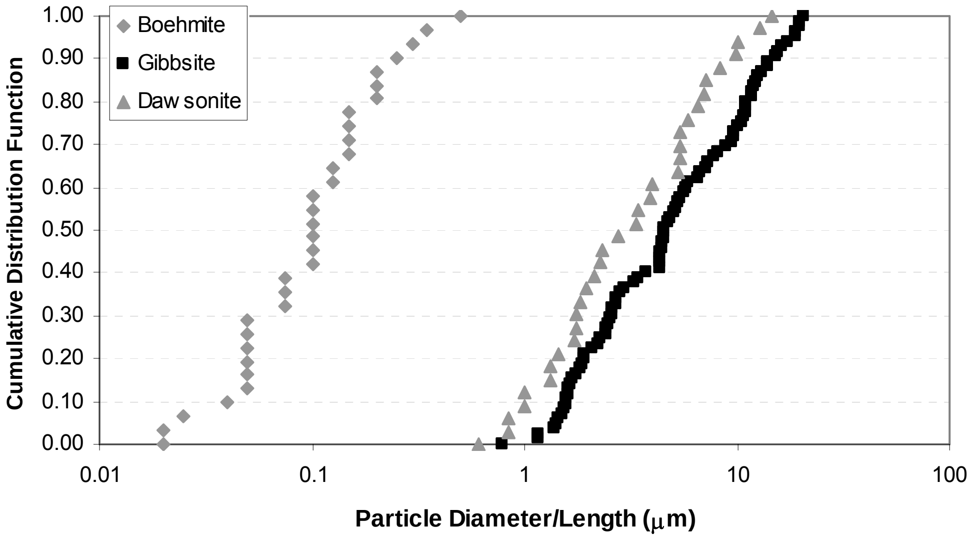

Figure 3.2.2. PSDs for Aluminum Phases (boehmite data from Lumetta et al. 1996c, 1997; gibbsite images from[(a,b,c,d)], Bechtold et al. 2003; dawsonite images from[(b,c)], Bechtold et al. 2003, Herting et al. 2004)

(a) Callaway WS and GA Cooke. 5/17/2004. "Distribution of Plutonium-Rich Particles in Tank 241-SY-102 Sludge." CH2M-0400872, CH2M HILL, Richland, Washington.

(b) Frye JM. 4/29/2005. "Results of Caustic Testing of 241-C-101 & 241-C-107." 7S110-JMF-05-015, CH2M HILL, Richland, Washington.

(c) Herting DL. 8/28/2003, "Caustic Demand Test Results, Tank 241-AN-102 Sludges." FH-0303343, Fluor Hanford, Inc., Richland, Washington.

(d) Callaway WS, GA Cooke, and DL Herting. 3/18/2005, "Particle Size Measurements in Support of the Tank 241-AN-102 Chemistry Control Recovery Plan." 7S110-WSC-05-011, CH2M HILL, Richland, Washington.

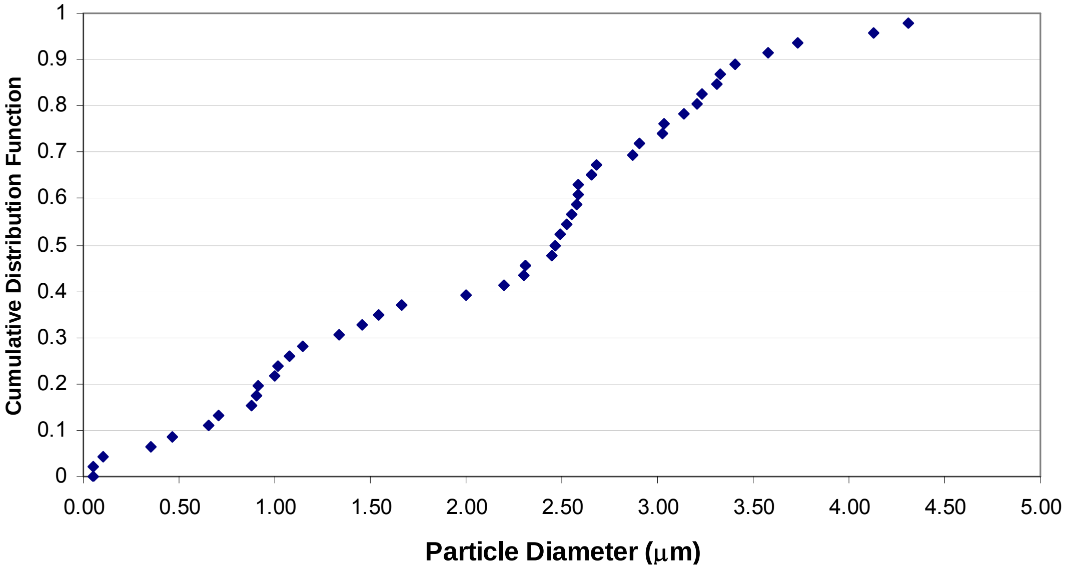

Figure 3.2.3. PSDs for Hematite/Ferrihydrite Phases(a,b,c,e) (Bechtold et al. 2003, Herting et al. 2004, Buck et al. 2003)

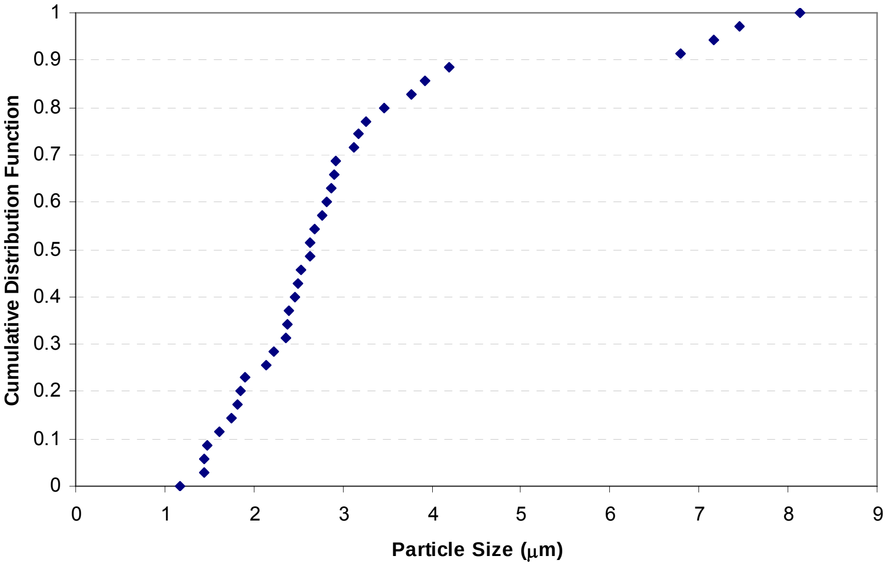

Figure 3.2.4. PSD for Cancrinite Phases

(a) Callaway WS and GA Cooke. 5/17/2004. "Distribution of Plutonium-Rich Particles in Tank 241-SY-102 Sludge." CH2M-0400872, CH2M HILL, Richland, Washington.

(b) Warrant RW. November 2006. "Results of Caustic Testing of Tank 241-AY-102 Core 319 Sludge Solids." 7S110-RWW-06-080, CH2M HILL, Richland, Washington.

(c) Herting DL and GA Cooke. 5/5/2004. "Caustic Demand Test Results for Tank 241-C-103 Sludge." 7S110-DLH-04-015, CH2M HILL, Richland, Washington.

(d) Callaway WS, GA Cooke, and DL Herting. 3/18/2005. "Particle Size Measurements in Support of the Tank 241-AN-102 Chemistry Control Recovery Plan." 7S110-WSC-05-011, CH2M HILL, Richland, Washington.

(e) Frye JM. 4/29/2005. "Results of Caustic Testing of 241-C-101 & 241-C-107." 7S110-JMF-05-015, CH2M HILL, Richland, Washington.

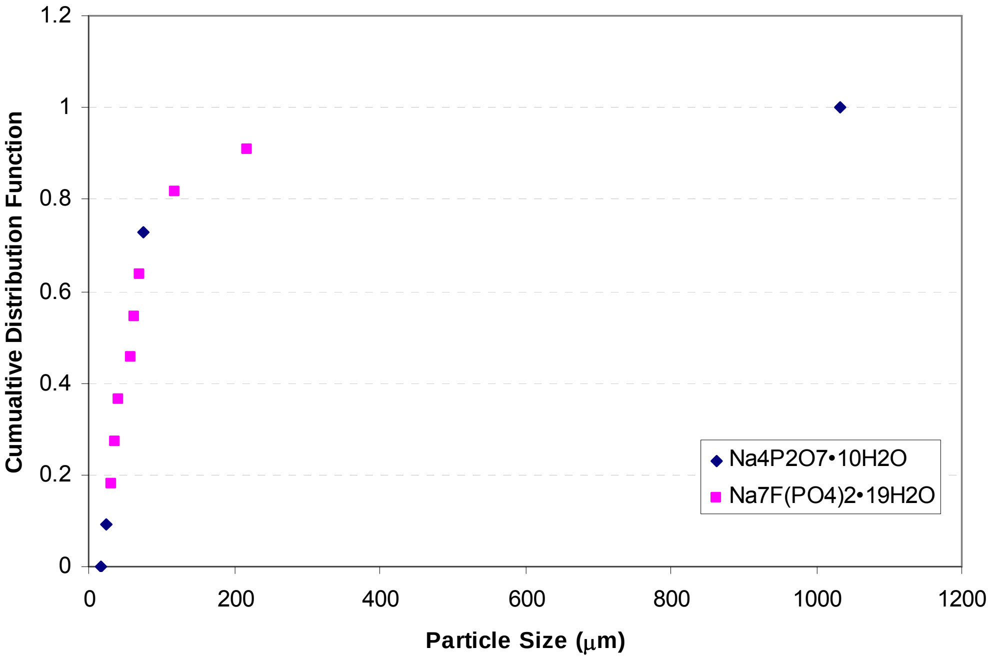

Figure 3.2.5. PSD for Sodium Phosphate Particles

3.2.3 Particle Shapes

One of the major factors affecting solid transport is the solid settling velocity; particle shape, a key solid characteristic beside the solid size and density, affects the settling velocity. As will be discussed, some of primary particles of sludge are not spherical. Because most settling velocity and sediment transport formulas and models have been developed for spherical particles, there is a need to make shape factor corrections for non-spherical particles (Vanoni 1975).

Several approaches are available to express the shape factor of an arbitrarily-shaped solid for use in calculating the settling velocity, including the following (McNown et al. 1951, Vanoni 1975, Lansen et al. 1979, Simons and Senturk 1977):

- Corey's shape factor

$$S_F = \frac{c}{\sqrt{ab}} \tag{3.2.12}$$

where a, b, c = the longest, intermediate and shortest mutually perpendicular axes of the particle.

- Sphericity is the ratio of the surface area of a sphere with equal volume as a particle to the surface area of the particle considered (or the ratio of the diameter of a sphere with equivalent volume to the diameter of circumscribed sphere)
- Roundness is the ratio of the average radius of curvature to a radius of circle inscribed in the maximum projected area of a particle.

Because the Corey's shape factor approach is most practical to use, this approach has been used to estimate the settling velocity of a non-spherical particles by Eq. 3.2.13 (Wu and Wang 2006)

$$w_S = \frac{M\nu}{Nd}\left[\sqrt{\frac{1}{4}+\left(\frac{4N}{3M^2}D_*^{\;3}\right)^{\frac{1}{n}}}-\frac{1}{2}\right]^n \tag{3.2.13}$$

where

$$d = \sqrt[3]{abc} \tag{3.2.14}$$

$$M = 53.5e^{-0.65S_F} \tag{3.2.15}$$

$$N = 5.65e^{-2.5S_F} \tag{3.2.16}$$

$$n = 0.7 + 0.9S_F \tag{3.2.17}$$

$$D_* = d\left[\frac{\left(\frac{\rho_S}{\rho_L}-1\right)g}{\nu^2}\right]^{\frac{1}{3}} \tag{3.2.18}$$

where

ρ_L and ρ_S = densities of liquid and solid, respectively

υ = liquid kinematic viscosity.

An equivalent sphere of an arbitrarily-shaped solid is defined here as a sphere whose settling velocity is the same as that of the arbitrarily-shaped solid. The diameter of the equivalent sphere, d_E, is calculated by solving the following equation with known values of w_S, ρ, ρ_S, and υ (Wu and Wang 2006):

$$\left[\left(\frac{w_S d_E}{60.22\nu}\right)^{0.625}+0.5\right]^2 = 0.25+\frac{1}{86.69}d_E^{\;1.875}\left\{\left(\frac{\rho_S}{\rho_L}-1\right)\frac{g}{\nu^2}\right\}^{0.625} \tag{3.2.19}$$

where g = gravitational acceleration.

Using the Corey's shape factor, the nature of some acicular particles was explored. Cejkaite, boehmite, hematite, dawsonite, and sodium phosphates exhibited very elongated crystals (see Tables 3.2.13 to 3.2.18). Note that b and c in Table 3.2.14 are the intermediate and shortest lengths used in the Corey's shape factor (see Eq. 3.2.12). The thickness of the boehmite crystals is based on their apparent transparency in TEM images obtained at ~100 kV, suggesting that they cannot be much thicker than 30 nm.

Table 3.2.13. Feature Dimensions from Image of Cejkaite (Krupka et al. 2006)

Length (μm)	Thickness (μm)	Shape Factor
2.13	2.45	1.07
3.55	0.82	0.48
3.55	0.82	0.48
4.29	1.64	0.62
4.37	0.98	0.47
4.55	0.90	0.44
5.41	1.42	0.51
5.86	1.47	0.50
7.11	2.12	0.55
7.31	2.46	0.58
7.70	1.39	0.43
7.77	3.67	0.69
8.50	1.10	0.36
9.11	3.82	0.65
10.93	2.36	0.47
12.06	2.48	0.45
12.31	3.00	0.49
13.40	4.26	0.56
15.41	2.60	0.41
16.45	2.88	0.42
17.10	2.19	0.36
17.65	2.37	0.37
51.52	10.70	0.46

Table 3.2.14. Dimensions from TEM Image of Boehmite (measurements in nm)

Boehmite		**Thickness, a (nm)**		**Shape Factor**	
c (nm)	**b (nm)**	**Min**	**Max**	**Min**	**Max**
245.49	183.63	5	30	0.02	0.14
96.31	78.53	5	30	0.06	0.34
197.52	176.58	5	30	0.03	0.16
192.59	163.58	5	30	0.03	0.17
105.1	100.56	5	30	0.05	0.29
175.12	117.58	5	30	0.03	0.21
69.88	53.56	5	30	0.08	0.49
Mean Shape factor				0.04	0.26
	Stdev			0.02	0.13

Table 3.2.15. Dimensions from SEM Image of Hematite (measurements in μm)

Length (μm)	Thickness (μm)	Shape Factor
2.55	0.71	0.53
3.23	1.18	0.60
0.71	0.68	0.50
2.53	0.48	0.43
3.73	0.41	0.33
2.59	0.54	0.46
1.46	0.29	0.44
3.58	0.54	0.39
1.15	0.56	0.70
1.24	0.51	0.64
2.54	1.00	0.63

Table 3.2.16. Dimensions from SEM Image of Dawsonite (measurements in μm)

Length (μm)	Thickness (μm)	Shape Factor
10.01	0.87	0.29
12.93	0.82	0.25
14.69	0.78	0.23
3.877	0.67	0.42
5.9	0.93	0.40
9.86	1.14	0.34
3.36	0.70	0.46
7.01	1.01	0.38
6.54	1.20	0.43
1.97	0.55	0.53
8.24	1.03	0.35
5.40	0.98	0.43
5.39	0.70	0.36
7.17	0.77	0.33
3.40	0.77	0.48
1.77	0.71	0.63
5.27	0.74	0.38
2.73	0.95	0.59
2.32	0.63	0.52
4.00	0.64	0.40
1.43	0.48	0.58
2.12	0.50	0.49
5.38	0.65	0.35

Table 3.2.17. Dimensions from SEM Image of Sodium Phosphates (measurements in μm)

Length (μm)	Width (μm)	Shape Factor
15.9	2.4	0.39
23.1	2.3	0.32
76.1	7.7	0.32
1033.8	41.2	0.20

For the current evaluation, all solid phases listed in Table 3.2.1 were assumed to be spherical except for dawsonite ($NaAlCO_3(OH)_2$), boehmite (AlOOH), and hematite (Fe_2O_3):

- The average dawsonite shape factor, S_F, is equal to 0.42 from Table 3.2.16. Assuming that the intermediate and minimum diameters are the same, Eq. 3.2.19 and sizes listed in Table 3.2.10 yield the maximum, mode, and minimum sizes of dawsonite of 4.2, 0.94, and 0.14 μm, respectively.
- With the average shape factor of 0.18 from Table 3.2.14 and the smallest diameter (i.e., its thickness) assigned as 0.018 μm, Eq. 3.2.19 and Table 3.2.10 yield the maximum and mode sizes of boehmite to be 0.052 and 0.048 μm, respectively. The minimum boehmite particle of 0.02 μm was assumed to have a shape factor of 0.26 and its thickness of 0.005 μm. These values yield the diameter of an equivalent sphere as 0.015 μm. Thus, all the maximum, mode, and minimum sizes of boehmite are very small, below 0.1 μm.
- For hematite, the average shape factor in Table 3.2.15 is 0.514. Assuming the intermediate and minimum diameters are the same, Eq. 3.2.19 and Table 3.2.10 yield the maximum, mode, and minimum sizes of hematite to be 1.6, 0.88, and 0.037 μm, respectively.

Thus, replacing particle sizes of these three solid phases in Table 3.2.10, the final primary solid characteristics of the sludge were selected, as shown in Table 3.2.18. The values indicated in this table were used for the subsequent modeling to determine the particulate size and density distributions.

Table 3.2.18. Primary Particle Characteristics of Hanford Sludge Waste

Solid Phase	**Density, kg/m^3**	**Amount**		**Maximum Particle Size, μm**
		wt%	**vol%**	
Gibbsite	2420	44.9	51.5	20
$(NaAlSiO_4)_6$•$(NaNO_3)_{1.6}$•$2H_2O$	2365	14.2	16.6	8
Boehmite	3010	11.5	10.6	0.05
$NaAlCO_3(OH)_2$	2420	8.3	9.5	4.2
Fe_2O_3	5240	7.8	4.1	1.6
$Ca_5OH(PO_4)_3$	3140	2.3	2.0	0.1
$Na_2U_2O_7$	5617	3.2	1.6	15
ZrO_2	5680	2.2	1.1	50
Bi_2O_3	8900	2.6	0.81	10
SiO_2	2600	0.6	0.69	100
$Ni(OH)_2$	4100	0.8	0.55	0.5
MnO_2	5026	1.0	0.54	10
CaF_2	3180	0.27	0.23	15
$LaPO_4$•$2H_2O$	6510	0.31	0.13	3
Ag_2CO_3	6077	0.021	0.0094	4
PuO_2	11430	0.0054	0.0013	40

3.2.4 Agglomeration

Hanford sludge waste contains many oxides and hydroxides of primary (crystal) particles of Al, Fe, U, Zr, Mn, Ni, and others (Jewett et al. 2002, Rector and Bunker 1995a), as discussed in Section 3.2.1. Many of these primary particles are attached to each other, resulting in extensive formation of fractal agglomerates[(a)] (Bunker et al. 2000). Thus, tank waste usually contains mixtures of primary particles and their composite agglomerates, and most sludge consists of 1- to 100-μm agglomerates of submicron primary particles[(a)] (Bunker et al. 2000). Primary particles greater than approximately 10- to 20-μm typically do not form agglomerates in the tank waste. Hard agglomerates, such as hematite, are always observed regardless of solution pH, salt content, and agitation conditions (Bunker et al. 2000). Thus, it is reasonable to account for both primary particles and agglomerates to evaluate the sludge particulate characteristics. This section provides a functional relationship between the agglomerate size and its density. This relationship was used to determine the sludge size and density distributions through Monte Carlo modeling.

The volume fraction occupied by primary particles within agglomerate is (Bunker et al. 2000)[(a)]

$$C_V = \left(\frac{R}{r}\right)^{D-3} \tag{3.2.20}$$

where

C_V = primary particle's volume fraction
D = fractal dimension
R = agglomerate size
r = primary particle size.

The agglomerate density is estimated by

$$\rho_A = C_V \rho_S + (1 - C_V)\rho_L \tag{3.2.21}$$

where

ρ_A = agglomerate density
ρ_L = liquid density
ρ_S = primary particle density.

Substituting Eq. 3.2.20 into Eq. 3.2.21 yields

$$\rho_A = \left(\frac{R}{r}\right)^{D-3} \left(\rho_S - \rho_L\right) + \rho_L \tag{3.2.22}$$

Equation 3.2.22 provides a relationship between the agglomerate size and its density. Agglomerate density decreases as the size increases, for a constant value of D. The fractal dimension, D, is between 0 and 3. At D=3, the particulate is a primary particle or an agglomerate without any pore space. Ilievski et al. (2003) determined the void fraction of stable agglomerate gibbsite to be 0 ± 0.03.

In general, a higher solid concentration forms larger agglomerates, but not in all cases (Selomnlya et al. 2002). When the driving force for agglomeration is very high (diffusion-limited aggregation),

---

(a) Bunker BC, PJ Bruinsma, GL Gruff, CR Hymas, XS Li, JR Phillips, DR Rector, PA Smith, L Song, JM Tingey, and Y Wang. 1995. "Colloidal Studies for Solid/Liquid Separation." TWRSPP-95-045, PNNL, Richland, Washington.

agglomerates are not very dense, having D ≈ 1.6 ~ 1.8. When the driving force for agglomeration is weak (reaction-limited aggregation), agglomerates are more dense, with D = 1.8 ~ 2.25. High-packing dense agglomerates may have D ≥ 2.5.

Hanford tank waste conditions with high pH and ion strength favor reaction-limited agglomeration. Only limited evaluations of the fractal dimension relevant to Hanford tank waste are available (Bunker et al. 2000). Rector and Bunker (1995b) reported that most colloidal agglomerates form a fractal structure with a fractal dimension, D, of 1.6 ~ 2.5. A colloidal study assumed 1.8 ~ 2.5 for the fractal dimension of an agglomerate of $Fe(OH)_3$.[a] Rector and Bunker (1995b) simulated the agglomeration process, resulting in a fractal dimension of 2.25. Bunker et al. (2000) also used the fractal dimension of 2.25 for an experimental study conducted to provide insight into the Hanford tank waste.

Table 3.2.19 presents some measured fractal dimension values reported in literature ranging from 1.6 to 2.8 (Kramer and Clark 1999, Kim and Kramer 2005). Most of these experiments have been performed on agglomerates with single-sized primary particles.

Table 3.2.19. Some Measured Fractal Dimensions

System	Fractal Dimension
Ferric sulfate flocs	
< 0.65 μm	2.3
> 0.65 μm	2.8
Ferric chloride (< 0.75 μm)	2.3
α-FeOOH	
(a) Diffusion limited aggregation	1.6
(b) Reaction limited aggregation	2.0
Kaolin with aluminum sulfate	1.6 ~ 1.95
Nickel hydrocarbonate microsphere	
without shear	1.7 ~ 1.8
with shear	2.2 ~ 2.7
Latex sphere	
(a) Small flocs	2.1
(b) large flocs	2.5
Latex sphere with sodium chloride	1.75 ~ 2.25
Polystyrene spheres	2.48

Bunker et al. (2000) reported that Hanford sludge waste has a wide range of primary particles forming agglomerates and the overlaying solids in the sediment layer exerts the normal and shear force that rearrange the agglomerates, possibly increasing their fractal dimension. Thus, the fractal dimension value may be greater than 2.25 ~ 2.5. There is also a study indicating that in some cases the fractal dimension decreases as the agglomerate size increases (Khelifa and Hill 2006). However, because a fractal analysis is usually based on the “self similitude” concept imposing constant fractal dimension, and because there is a lack of specific Hanford waste data to support the different or varying fractal dimensions for the sludge agglomerates, the current evaluation assumed that the fractal dimension is uniform and constant over the entire range of compounds and primary particle sizes forming agglomerates.

(a) Bunker BC, PJ Bruinsma, GL Gruff, CR Hymas, XS Li, JR Phillips, DR Rector, PA Smith, L Song, JM Tingey, and Y Wang. 1995. “Colloidal Studies for Solid/Liquid Separation.” TWRSPP-95-045, PNNL, Richland, Washington.

When there is shear force, agglomerates will undergo restructuring, fragmentation/breakup, and rearrangement, usually results in increased agglomerate density (Selomnlya et al. 2003). Beside shear stress, normal stress and distortion energy also cause agglomerate to reform and breakup (Kramer and Clark 1999). Under low to moderate shearing (strain rate of 32 ~ 100 s^{-1}), agglomerates of different particle sizes (0.38 to 0.81 μm) of latex exhibit different behavior (i.e., restructuring, fragmentation/breakup, reformulation) of their changes, depending on the primary particle sizes. Note that the expected strain rate of the 4-ft/sec slurry flow in a 3-inch pipeline is 130 s^{-1}. Experiments with latex indicate this restructuring occurs rather quickly; reaching its maximum size in 10 minutes and arriving at the final, somewhat smaller, equilibrium size in about 30 minutes (Selomnlya et al. 2002). With higher shear, agglomerate compaction occurs due to breakup and reformation in a similar manner for primary particle of different sizes. Flocs of larger primary particles tend to be more susceptible to breakage than dense agglomerates, thus they can increase in density through restructuring (Selomnlya et al. 2003). Smaller primary particles tend to form agglomerates with greater strength (Selomnlya et al. 2002).

There is a maximum agglomerate size that can be attained under shear (Selomnlya et al. 2003). The effect of shearing on the maximum agglomerate size is expressed by (Sonntag and Russel 1987, Bunker et al. 2000)

$$R = b_s \gamma^{\frac{D-1}{2n_s(D-3)}} \tag{3.2.23}$$

where b_s and n_s are constants.

The ratio of maximum agglomerate sizes at two different strain rates may be obtained from Eq. (3.2.23) by

$$\frac{R_1}{R_2} = \left(\frac{\gamma_1}{\gamma_2} \right)^{\frac{D-1}{2n(D-3)}} \tag{3.2.24}$$

Equations 3.2.23 and 3.2.24 may be used to estimate the maximum agglomerate sizes under another strain rate if the maximum agglomerate size under one strain rate and values of n and D are known. Equation 3.2.22 was used to compute the agglomerate density of a given agglomerate size to reproduce the known sludge particulate size distribution and expected density of average sludge solids consisting of primary particles and agglomerates.

Based on the studies of Rector and Bunker (1995b) and Bunker et al. (2000) and an expected range of the fractal dimension for reaction limited aggregation (the Hanford sludge condition), the selection of the fractal dimension of D = 2.6 may be appropriate. Application of this value in determination of the sludge particle size and density distribution through Monte Carlo modeling qualitatively reproduced the expected volume-weighted average solid density and total agglomerate volume fraction (Section 5.2.2).

Substituting D=2.25, Eq. 3.2.22 becomes

$$\rho_A = \left(\frac{R}{r}\right)^{-0.4} \left(\rho_S - \rho_L\right) + \rho_L \tag{3.2.25}$$

This fractal analysis is rather preliminary and has several limitations and assumptions, including:

- Each primary particle forms its own agglomerates.
- A single fractal dimension value was used for agglomerates of different compounds and primary particle sizes.
- The same single fractal dimension value was used for all agglomerate sizes.
- The diameter of an equilibrium sphere was used to represent a non-spherical primary particle.
- All primary particles form agglomerates of any size within a measured solid size range, regardless of the size of primary particles.
- Due to shear and normal forces acting on it, sludge may have different agglomerate sizes and associated fractal dimensions during the slurry pipeline transfer and for those sitting in a tank before and after the pipeline transfer.

3.3 Liquid Properties

The average liquid density in sludge waste, another property needed for PSDD and critical velocity criterion calculations, was calculated from the ESP modeling results for appropriate tanks, those that contained only sludge. The first step in identifying these tanks was the data in Table D-13 of Barker (2006). The table indicates, with an SL identifier, which waste tanks were defined as containing solids that were predominantly sludge. This SL set was further reduced by removing all tanks that in the 2002 BBI (the version used for the ESP runs) contained even a small layer of saltcake solids (tanks AW-103, B-104, S-107, SX-107, SX-110, SX-111, SX-112, SX-114, and TX-101). The remaining 70 tanks of the SL set were used to represent all sludge waste in the 177 waste tanks, with the average liquid density for the set of tanks being calculated in three different ways:

- The ESP-modeled liquid densities for the tanks were averaged according to the total volume of liquid layer(s) in each tank in the 2002 BBI. The volume-weighting therefore includes only the drainable liquid. The resulting average liquid density was 1.172 g/L.
- The BBI-defined liquid densities for the liquid layers in the tanks were averaged according to the total volume of liquid layer(s) in each tank in the 2002 BBI. The resulting average liquid density was 1.185 g/L.
- The ESP-modeled liquid densities for the tanks were averaged according to the total volume of liquid in each tank as predicted by multiplying the ESP-predicted tank waste liquid times the total waste volume in the 2002 BBI. This volume-weighting includes both drainable and non-drainable liquid. The resulting average liquid density was 1.198 g/L.

Based on these calculations, a value of 1.2 g/L was used to represent the liquid density in tanks that contain sludge solids as well as liquid. A representative median liquid viscosity for the five HLW waste tanks listed in Table 3.3.1 is nominally 2 mPa s.

Table 3.3.1. Hanford HLW Liquid Viscosity

Tank	**Liquid Viscosity (mPa s) [Sample Temperature (˚C)]**	**Reference**
AZ-101	2.25 [27.7]	Callaway (2000)
AZ-102	1.46 [27]	Warrant (2002)
AY-102	1.78 [27]	Warrant (2001)
C-104	1.7 [27][a]	O'Rourke (2000)
C-107	1.0 [25]	Warrant (2004)
(a) Temperature reported as ambient; assumed equivalent to prevalent ambient conditions for other samples.		

4.0 Approaches to Define the Solid Particle Size and Density Distribution

The data presented in Section 3 are used to calculate the composite insoluble solid PSDD. The approaches taken to relate measured PSDs to solid-phase compounds and generate expected PSDDs are summarized in Section 4.1, and the modeling approach is presented in Section 4.2.

4.1 Particle Size and Density Distribution Approaches

As described in Section 3.1, the sonicated PSD is assumed to represent the PSD for the individual primary particles and the hard agglomerates, while the minimal disturbance PSD is assumed to represent the PSD for the individual primary particles and both the soft and hard agglomerates. In lieu of data sets representing more complete sampling of Hanford waste, these PSDs are used as representations of the combined insoluble solid-phase inventory. The solid-phase compounds for the insoluble Hanford waste, their relative volume fractions, crystal density, maximum primary particle size, and maximum agglomeration size have also been identified as described in Section 3.2. To define the insoluble solid PSDD, the solid-phase compound data is modeled into the sonicated and minimal disturbance PSDs as will be described below.

Quantifying the fractal dimension relating the agglomerate size to its density for the Hanford waste is subject to uncertainty as described in Section 3. Thus, although assigning a crystal density to all of the waste particulate is not supported by any Hanford waste knowledge, a case with the agglomerates set to the crystal density is considered for each PSD modeled. Cases in which the fractal dimension is adjusted such that the resulting volume-weighted average density of the bulk solids (primary particles and agglomerates) approximates that estimated for in situ conditions in individual waste tanks (see Jewett et al. 2002 for example) are also evaluated. Four PSDD modeling approaches were considered:

- Case 1. Sonicated PSD
  - Primary particles and hard agglomerates were assigned crystal density
- Case 2. Sonicated PSD
  - Primary particles were assigned crystal density
  - Density of hard agglomerates assigned via fractal relation
- Case 3. Minimal Disturbance PSD
  - Primary particles, soft and hard agglomerates were assigned crystal density
- Case 4. Minimal Disturbance PSD
  - Primary particles were assigned crystal density
  - Densities of soft and hard agglomerates were assigned via fractal relation.

Cases 1 and 3 have all of the particulate assigned a crystal density; higher density for a given particle is not achievable within a given solid-phase compound. Thus, for the given PSD and solid-phase compounds, the Case 1 and Case 3 PSDDs provide an upper bound. Cases 2 and 4 are expected to be more representative of actual Hanford waste conditions given the observed pervasiveness of agglomerate particulate and their expected fractal dimensions (Section 3). The considered cases are not in any way bounding to the range of actual waste that might be received by the WTP.

The modeling approach is illustrated with a simple example. Consider hypothetical solid-phase compounds A, B, C, and D as described in Table 4.1.1. 50% of the solid particles by volume are compound A, which has a density of 2.4 g/mL, primary particles up to 10 μm, and a maximum agglomeration size of 1,000 μm. Compound A information is represented with an example PSD as shown in Figure 4.1.1. The "A" label in the 50% "box" for the waste composition is located at the limit of the primary particle size, 10 μm. Because the expected maximum agglomeration size is the PSD limit, the compound A "box" spans the entire PSD. Thus, for Case 1, 50% of the solid particles by volume for the entire PSD have a density of 2.4 g/mL. The probability of each size particle is dictated by the probability of the PSD itself. The frequency at a particle size of 4 μm, for example, is 4% by volume. Therefore, 50% of the 4 μm particles, that have a probability of occurrence of 4%, have a density of 2.4 g/mL. The remaining 50% of the particles at 4 μm is composed of 25% at 6.5 g/mL, 15% at 3.0 g/mL, and 10% at 5.6 g/mL. This procedure is applied across the PSD, and in application, as will be described in Section 4.2, mass is conserved such that the integrity of the PSD is retained.

Table 4.1.1. Example Solid-Phase Compound Parameters

Solid-Phase Compound	Crystal Density (g/mL)	Volume Fraction	Maximum Observed Particle Size (μm)	Maximum Agglomeration Size (μm)
A	2.4	0.50	10	PSD Limit
B	6.5	0.25	2	PSD Limit
C	3.0	0.15	20	PSD Limit
D	5.6	0.10	5	PSD Limit

For Case 2, 50% of the solid particles by volume at each size, as dictated by the probability of occurrence of the PSD, up 10 μm has a density of 2.4 g/mL, and beyond this limit of the primary particles for compound A, the density is assigned via fractal relation. The remaining compounds are treated similarly.

4.2 Modeling

The composite PSD is deconvoluted into PSDs for each solid -phase compound by solving a least squares optimization problem. For each realization (i.e., set of parametric variations performed), the optimization problem is formulated by finding a set of weighting factors, W_j, that minimizes the error, ε, between the input mass fraction (e.g., see Table 3.2.18) of a compound and the calculated mass fraction of the compound.

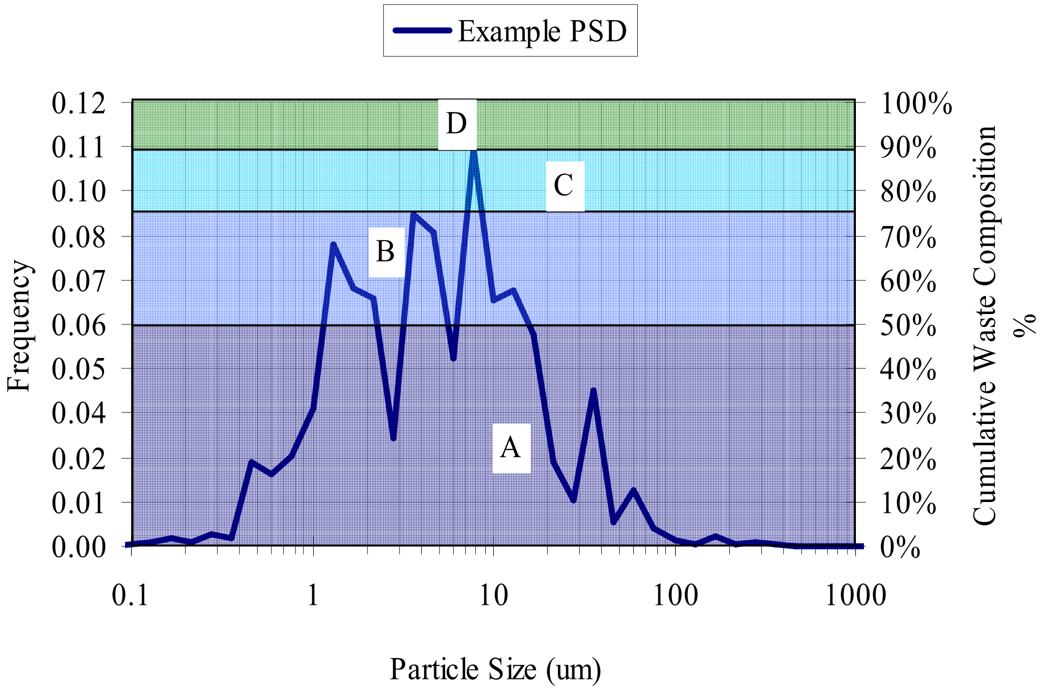

Figure 4.1.1. Example Solid-Phase Compounds from Table 4.1.1 with Example PSD

The error is defined as the square of the relative error between the input mass composition of the solid-phase compounds and the mass composition of compounds calculated in this deconvolution exercise:

$$\varepsilon = \sum_j \left(\frac{M_{j,0} - M_j}{M_{j,0}} \right)^2 \tag{4.2.1}$$

where M_j is the calculated mass fraction of solid-phase compound j and $M_{j,0}$ is the input mass fraction of compound j.

The mass fraction of a particular compound is determined similar to that described in the example in Section 4.1. The PSD is described as a series of bins of particle size. For each bin/compound combination, the volume fraction of that bin that falls below the maximum observed size for the given compound is defined. The volume fraction of a compound present in a particular bin is proportional to the number of compounds present in that size range. The volume fraction is then converted to a mass by multiplying this value by the density of the compounds in that bin.

The density can be defined as either crystalline or fractal. Crystals can exist from the minimal bin size to a defined input value (see Section 3.2). Agglomerates can exist from a minimal value that represents the agglomerate "building block" primary particle size to the specified limit. The fractal dimension relation provided in Eq. (3.2.22) is used to relate the crystalline primary particle density to the agglomerate as

$$\rho_{Aij} = \left(\frac{R_i}{r_j}\right)^{D_j-3} (\rho_{Sj} - \rho_L) + \rho_L \tag{4.2.2}$$

where

ρ_{Aij} = agglomerate density of compound j for bin i
ρ_{Sj} = crystal density of compound j
ρ_L = liquid density
D_j = fractal dimension of compound j
R_i = particle size of bin i; agglomerate size
r_j = primary particle size of compound j.

In this model, the threshold between crystals and agglomerates for a particular compound, r_j, is the primary particle building block size. The total mass of each compound can then be calculated through the following equation:

$$m^*_j = \sum_{i=1}^{N_B} \left[\frac{W_j f_{ij}}{\sum_{k=1}^{N_C} W_k f_{ik}} V_i \right] \left[\left\{ (1 - f_{ij,agg}) + (f_{ij,agg}) \left(\frac{R_i}{r_j}\right)^{D_j-3} \right\} \rho_{Sj} \right] \tag{4.2.3}$$

where

m^*_j = non-normalized mass of compound j over the PSD histogram
N_B = number of bins in the PSD histogram
N_C = number of solid-phase compounds
$f_{ij,agg}$ = fraction of agglomerates in bin i for chemical compound j set to 0 or 1 based on the primary particle size $d_{j,}$
f_{ij} = volume fraction of material in a given bin i falling below the maximum observed diameter for a chemical compound j
V_i = volume fraction of the overall PSD for bin i.

These values can be converted to a mass fraction through the following normalization:

$$Mn_j = \frac{m^*_j}{\sum_{k=1}^{N_{species}} m_k} \tag{4.2.4}$$

where Mn_j is the normalized mass of compound j over the input PSD.

This optimization problem was implemented in an Excel® spreadsheet. For a given realization, the weighting vector W_j was solved to close the mass balance on the model problem. The result is a PSD where each size bin is deconvoluted by crystals and agglomerates. Densities are known for each solid-phase compound in each particle size bin, and thus a PSDD is created.

The PSDD may then be used as input to critical velocity equation calculations. Critical velocities are determined for each chemical compound in each particle size bin using the equations referenced in BNI

(2006a). The critical velocity equations, Oroskar and Turian equation (1980), and Thomas equation (1976, 1979) are provided in Section 1. The mass fraction of the solids in the flow for each size and density "pair" in the PSDD matrix is was set to the total flow value. Critical velocity values are thus assigned to the chemical compound present in each bin in the PSD. The applicability of these models to the current study conditions was not evaluated. Results are obtained for the following cases:

- Oroskar and Turian equation over entire particle size range
- Thomas equation for fine particles, Oroskar and Turian (1980) equation for coarse particles, interpolation of Thomas and Oroskar and Turian equations for transition region

Thomas (1979) states that his equation is valid for particle sizes smaller than 0.3 times the viscous sublayer thickness while conventional critical velocity relations such as the Oroskar and Turian equation can be used for particle sizes above the boundary layer thickness. The viscous sublayer thickness was calculated at approximately 130 μm for the flow of water at 4 ft/sec in a 3-inch ID pipe. Therefore, for the second approach described above, the Thomas equation is used for particles smaller than 40 μm, and the Oroskar and Turian equation is used for particles above 130 μm. A log interpolation between the Thomas and Oroskar and Turian equations is used to determine the critical velocity in the transition region between 40 and 130 μm.

Given a threshold design velocity value, the fraction of the PSD having critical velocities above the threshold design value can be determined via a simple summation.

5.0 Results

The purpose of this investigation is to provide estimates of the Hanford waste insoluble solid PSDD. The PSDD approaches taken to relate measured PSDs to solid-phase compounds as described in Section 4 were applied to the data sets provided in Section 3 and summarized in Tables 5.0.1 and 5.0.2.

In Section 5.1, the method of application of the PSDD models is described. Representative PSDDs are provided in Section 5.2, and critical velocity criterion and calculation results are presented in Section 5.3. Effects of the modeling approach on these results are considered in Section 5.4.

Table 5.0.1. PSDs (μm)

Quantile	1%	5%	25%	50%	75%	95%	99%	100%
Sonicated[(a)]	0.39	0.70	1.63	4.39	10.1	33.4	112	774
Minimal Disturbance[(b)]	0.65	1.00	2.80	6.31	14.0	58.6	256	1000

(a) Combined data from 18 sludge tanks.
(b) Combined data from 19 sludge tanks.

Table 5.0.2. Solid-Phase Compound Parameters

Solid-Phase Compound	Crystal Density (g/mL)	Volume Fraction	Maximum Observed Particle Size (μm)
$Al(OH)_3$, Gibbsite	2.42	0.515	20
$(NaAlSiO_4)_6 \bullet (NaNO_3)_{1.6} \bullet 2H_2O$	2.365	0.166	8
AlOOH, Boehmite	3.01	0.106	0.05
$NaAlCO_3(OH)_2$	2.42	0.095	4.2
Fe_2O_3	5.24	0.041	1.6
$Ca_5OH(PO_4)_3$	3.14	0.020	0.1
$Na_2U_2O_7$	5.617	0.016	15
ZrO_2	5.68	0.011	50
Bi_2O_3	8.9	0.0081	10
SiO_2	2.6	0.0069	100
$Ni(OH)_2$	4.1	0.0055	0.5
MnO_2	5.026	0.0054	10
CaF_2	3.18	0.0023	15
$LaPO_4 \bullet 2H_2O$	6.51	0.0013	3
Ag_2CO_3	6.077	0.000094	4
PuO_2	11.43	0.000013	40

5.1 PSDD Model Application Method

The model inputs required to calculate the PSDDs have significant uncertainties that must be considered in the evaluation of the results. As presented in Section 3, some uncertainties may be approximately quantified (e.g., solid compound volume fraction relative errors, etc.), while others may not (e.g., waste sampling effects on PSDs, waste type coverage, etc.).

5.1.1 Quantified Data Uncertainty

Quantifiable parameter uncertainties are used to establish overall probability distributions for the model predictions. However, rather than performing a deterministic calculation with all inputs set to bounding values, which has no physical or statistical meaning, uncertainties can be propagated through the calculation accurately using a Monte Carlo simulation. In this method, a number of model simulations are run with input sets selected from their respective distributions. The collection of output values from all the model simulations then forms the overall probability distribution of the result.

A Monte Carlo simulation approach was used to derive the representative PSDDs for each PSDD approach as well as investigate the uncertainty in critical velocity criterion calculations. For each PSDD approach modeled, 500 simulations were conducted. The result is a set of 500 model outputs that constitutes a probability distribution over those results, and the probability of a given result given the input probability distributions may be determined.

Each input value used for a simulation is randomly sampled from an infinite population based on the specified distribution, as will be described. The commercial code R(a) was used to generate these inputs. A Visual Basic code written around the Excel-based model was used to generate results for each of the 500 simulations. These PSDD and critical velocity criterion results are then considered.

The PSDD results must be interpreted with regards to what is being represented. For example, from Section 4, it may be inferred that for each particle size, a distribution of solid density (or, exactly equivalently, the solid-phase compound) exists. That is, referring to the Section 4.1 example at a particle size of 4 μm, 50% of the particles of that size have a density of 2.4 g/mL, 25% have a density of 6.5 g/mL, and so on.

For the PSDD approach results, matrices of probability and density as functions of the solid-phase compound and particle size bin are generated (see Section 4.2). It is not physically meaningful to consider a specific quantile of these results in and of themselves because the integrity of the mass balance of the individual PSDD must be maintained. A representative PSDD result is therefore defined by the PSDD determined at the centroid (normalized average) input values.

The critical velocity criterion (Section 5.3) provides a single result in terms of the volume of particulate that does not meet the criterion for each PSDD result in a simulation. Necessarily, the single "pass" or "fail" result is composed of the "pass" or "fail" information for each solid-phase compound.

(a) R Version 2.1.0, R Development Core Team (2005). *R: A language and environment for statistical computing*. R Foundation for Statistical Computing, Vienna, Austria. URL http://www.R-project.org.

These fractions of the waste volume that fail the criteria results constitute a probability distribution and can be evaluated as such. Specific quantile results can be considered, and the uncertainty of the results, based on the applied input uncertainty, is quantifiable. Each critical velocity criterion result is associated with a specific realization of the PSDD. Thus, the PSDDs associated with a criterion quantile of the distribution of critical velocity criteria can be identified for consideration if desired.

Data uncertainties associated with each parameter in the input data sets from Tables 5.0.1 and 5.0.2 are described as follows:

- PSDs. Sampling of the PSD via the methodology described in Section 3.1.4 is performed for each simulation (i.e., the combined PSD is sampled 500 times for 500 unique realizations).
- Crystal density and volume fraction. As described in Section 3.2.1.3, the volume fractions of the solid-phase compounds as well as their relative errors are determined from a mass basis. Thus the uncertainty in the compound densities has been accounted for by using the computed relative errors in solid phase volume fractions. The volume fraction for each compound is sampled from a normal distribution about the best-estimate value with a standard deviation equal to the relative error divided by three (i.e., the relative error is assumed to represent 3 standard deviations or approximately a 99% confidence bound). These volume fractions are then normalized to unity within a given simulation.
- Maximum observed particle size. The maximum observed particle size is fixed for this analysis. The Case 1 and Case 3 results, which are generated by assigning the crystal density to the primary particles and agglomerates, necessarily bound the effect of altering this parameter.
- Primary particle size. The primary particle size is varied uniformly between 0.25 μm (selected as a lower bound accounting for less than 1% of the waste by volume) and the maximum observed particle size. While a skewed-normal distribution may be expected, insufficient data is available to accurately assign a specific distribution. Thus, uniform distributions are specified. Those compounds with a maximum particle size less than 0.25 μm are fixed at their respective sizes. The primary particle size variation affects Cases 2 and 4 which use the fractal relation of Section 3 to determine the agglomerate density, and is not meant to account for the unquantifiable uncertainty of the estimated values themselves. Rather, through the Monte Carlo approach, it allows for variation in the acknowledged but not quantifiable fraction of the particulate for a given compound that is less than the maximum particle size but still an agglomerate. The validity of this approach is evaluated qualitatively through consideration of the resulting volume-weighted density average of the bulk solids and the volume fraction of the waste that is composed of agglomerates.

The solid-phase compound quantity and size uncertainties used in the Monte Carlo simulations are summarized in Table 5.1.1. Specifying the maximum agglomeration size as the PSD limit indicates that all compounds may from agglomerates to the largest measured particle size (as discussed in Section 3.2).

Table 5.1.1. Solid-Phase Compound Uncertainties

Solid-Phase Compound	Volume Fraction	Relative Error in Volume Fraction	Maximum Observed Particle Size (μm)	Primary Particle Size (μm)	Maximum Agglomeration Size (μm)
$Al(OH)_3$, Gibbsite	0.515	0.20	20	[(a)]	PSD Limit
$(NaAlSiO_4)_6$•$(NaNO_3)_{1.6}$•$2H_2O$	0.166	0.22	8	[(a)]	PSD Limit
AlOOH, Boehmite	0.106	0.23	0.05	0.05	PSD Limit
$NaAlCO_3(OH)_2$	0.095	0.22	4.2	[(a)]	PSD Limit
Fe_2O_3	0.041	0.30	1.6	[(a)]	PSD Limit
$Ca_5OH(PO_4)_3$	0.020	0.22	0.1	0.1	PSD Limit
$Na_2U_2O_7$	0.016	0.51	15	[(a)]	PSD Limit
ZrO_2	0.011	0.48	50	[(a)]	PSD Limit
Bi_2O_3	0.0081	0.20	10	[(a)]	PSD Limit
SiO_2	0.0069	0.30	100	[(a)]	PSD Limit
$Ni(OH)_2$	0.0055	0.12	0.5	[(a)]	PSD Limit
MnO_2	0.0054	0.26	10	[(a)]	PSD Limit
CaF_2	0.0023	0.22	15	[(a)]	PSD Limit
$LaPO_4$•$2H_2O$	0.0013	0.64	3	[(a)]	PSD Limit
Ag_2CO_3	0.000094	0.16	4	[(a)]	PSD Limit
PuO_2	0.000013	0.46	40	[(a)]	PSD Limit

(a) Primary particle size for Monte Carlo simulation distributed as discussed with the exception of fixed values for AlOOH (boehmite) and $Ca_5OH(PO_4)_3$ as indicated.

5.1.2 Qualitative Uncertainty and Effect of Modeling Approach

As described, there may be specific uncertainty in the PSDs as a result of waste sampling technique, location, and handling. Further, not all waste types have been sampled. These considerations apply equally well to the solid-phase compound information, specifically impacting maximum primary particle size. While these effects cannot be quantified precisely, some information on the waste type sampling error can be garnered by evaluating PSDDs and the critical velocity criterion for PSDs from individual waste types. The variations determined in Section 5.4 illustrate potential uncertainty but do not quantify the uncertainty associated with the waste type coverage.

The predominant areas in which the modeling approach can affect the results are the binning of the PSD and number of simulation conducted for a given approach. Each of these areas is evaluated with respect to its impact on the results in Section 5.4.

5.2 Particle Size and Density Distributions

Representative PSDDs described in Section 5.1 are presented in Section 5.2.1 for each modeling approach. The effects of the qualitative uncertainty and modeling approach are evaluated. The PSDD approaches are summarized in Table 5.2.1; the fractal dimension for Cases 2 and 4 (2.6) is assigned based on the discussion in Section 3.2. Qualitative comparison of calculated and expected in situ volume-weighted average solid density and total agglomerate volume fraction is presented in Section 5.2.2.

Table 5.2.1. PSDD Approach Parameter Summary

Case	PSD	Liquid Density (g/mL)	Assigned Solid Density				
			Crystals (g/mL)	**Hard Agglomerates (g/mL)**	**Fractal Dimension**	**Soft Agglomerates (g/mL)**	**Fractal Dimension**
1	All sonicated	1.2	Crystal density	Fractal relation	3	N/A	N/A
2	All sonicated	1.2	Crystal density	Fractal relation	2.6	N/A	N/A
3	All min. disturbance	1.2	Crystal density	Fractal relation	3	Fractal relation	3
4	All min. disturbance	1.2	Crystal density	Fractal relation	2.6	Fractal relation	2.6

5.2.1 Representative PSDDs

Representative PSDDs for each PSDD approach case have been determined via 500-realization Monte Carlo simulations. The volume fraction and density for each compound in each particle size bin of the representative PSDDs is computed from the centroid inputs of the respective Monte Carlo simulations. For each case, the sum of the volume fractions over all bins and all compounds is unity. The resulting representative distribution is essentially the volume-based probability of each of the solid-phase compounds, and the density associated with that compound, predicted to exist in a PSD bin. The bin size represents the upper size limit of the particles associated with a given bin. For example, for consecutive bins sized 6 and 7.7 μm, the 7.7 μm bin includes a particle size range from 6 to 7.7 μm. The volume fraction and density of a compound with particles ranging in size from 6 to 7.7 μm thus resides in this bin. Index numbers for the solid-phase compounds of Table 5.0.2 are given in Table 5.2.2.

Table 5.2.2. Solid-Phase Compound Numerical Identification for PSDD Presentation

Solid-Phase Compound	Numerical Identification
$Al(OH)_3$, Gibbsite	1
$(NaAlSiO_4)_6 \cdot (NaNO_3)_{1.6} \cdot 2H_2O$	2
AlOOH, Boehmite	3
$NaAlCO_3(OH)_2$	4
Fe_2O_3	5
$Ca_5OH(PO_4)_3$	6
$Na_2U_2O_7$	7
ZrO_2	8
Bi_2O_3	9
SiO_2	10
$Ni(OH)_2$	11
MnO_2	12
CaF_2	13
$LaPO_4 \cdot 2H_2O$	14
Ag_2CO_3	15
PuO_2	16

The representative volume fraction of each compound by particle size for Case 1 is presented in Table 5.2.3 and the representative density of each compound by size in Table 5.2.4. To interpret, consider the example of compound $NaAlCO_3(OH)_2$ at a particle size of 36 µm. The compound $NaAlCO_3(OH)_2$ has a numerical ID of 4 from Table 5.2.2, and thus nominally 0.2% of the solid particulate by volume (Table 5.2.3) is between 28 and 36 µm with a density of 2.42 g/mL (Table 5.2.4). Because Case 1 does not allow agglomerates, the particle density does not vary with particle size.

The representative PSDD for Case 2 is provided in Tables 5.2.5 and 5.2.6. Again considering the example of compound $NaAlCO_3(OH)_2$ at a particle size of 36 µm, approximately 0.2% of the solid particulate by volume (Table 5.2.5) is between 28 and 36 µm with a density of 1.60 g/ml (Table 5.2.6). Since Case 2 considers agglomerates, the particle density decreases with increasing particle size.

The representative PSDDs for Cases 1 and 2 (data from Tables 5.2.3 - 5.2.6) are presented graphically in Figures 5.2.1 and 5.2.2. For Case 1, the particle size and density "pairs" are plotted in Fig. 5.2.1 with their respective volume fractions. The largest volume fraction, 0.05, occurs at 7.7 µm, 2.42 g/mL, corresponding to gibbsite, Tables 5.2.3 and 5.2.4. Note that $NaAlCO_3(OH)_2$ is equivalent in density, thus increasing the volume fraction of particulate at that specific size and density. The volume fractions across any particle size and density plane illustrate that particles of a given size may have a broad density range. This effect is limited in Case 2, Fig. 5.2.2. The effect of the fractal relation on the density is apparent, as the limited probability, i.e. low cumulative volume fraction, of large size and high density particles for Case 1 is "removed". The largest volume fraction, 0.03, occurs at 7.7 µm, 1.44 g/mL, corresponding to boehmite, Tables 5.2.5 and 5.2.6.

The representative PSDDs for Cases 3 and 4 are provided in Tables 5.2.7 and 5.2.8 and Tables 5.2.9 and 5.2.10, respectively. Figures 5.2.3 and 5.2.4 graphically present the PSDDs for Cases 3 and 4. The largest volume fractions, 0.05 and 0.03 for gibbsite and boehmite, respectively, again occur at 7.7 µm, 2.42 g/mL and 1.44 g/mL respectively.

Comparison of the PSDDs for Case 1 through 4 illustrates the impacts of treating all agglomerates as having the same density as their respective assigned primary particles and allowing for the presence of agglomerates via consideration of both the sonicated and minimal disturbance PSDs. These approaches provide a progression of the relative volume fraction of large dense particulate with the maximum amount for Case 3 and the minimum amount for Case 2.

Table 5.2.3. Representative PSDD Case 1, Volume Fraction of Solid-Phase Compounds

Particle Size (µm)	**Solid-Phase Compound Volume Fraction (refer to Table 5.2.2 for compound identification)**															
	1	**2**	**3**	**4**	**5**	**6**	**7**	**8**	**9**	**10**	**11**	**12**	**13**	**14**	**15**	**16**
0.22	4E-04	1E-04	8E-05	7E-05	3E-05	1E-05	1E-05	8E-06	6E-06	5E-06	4E-06	4E-06	2E-06	1E-06	7E-08	1E-08
0.28	9E-04	3E-04	2E-04	2E-04	7E-05	3E-05	3E-05	2E-05	1E-05	1E-05	1E-05	9E-06	4E-06	2E-06	2E-07	2E-08
0.36	1E-03	4E-04	2E-04	2E-04	9E-05	4E-05	3E-05	2E-05	2E-05	1E-05	1E-05	1E-05	5E-06	3E-06	2E-07	3E-08
0.46	9E-03	3E-03	2E-03	2E-03	8E-04	4E-04	3E-04	2E-04	1E-04	1E-04	1E-04	1E-04	4E-05	2E-05	2E-06	2E-07
0.60	5E-03	2E-03	1E-03	1E-03	4E-04	2E-04	2E-04	1E-04	8E-05	7E-05	6E-05	6E-05	2E-05	1E-05	1E-06	1E-07
0.77	2E-02	5E-03	3E-03	3E-03	1E-03	6E-04	5E-04	3E-04	2E-04	2E-04	2E-04	2E-04	7E-05	4E-05	3E-06	4E-07
1.0	2E-02	7E-03	4E-03	4E-03	2E-03	8E-04	7E-04	5E-04	3E-04	3E-04	2E-04	2E-04	1E-04	6E-05	4E-06	6E-07
1.3	4E-02	1E-02	8E-03	8E-03	3E-03	2E-03	1E-03	9E-04	7E-04	6E-04	4E-04	4E-04	2E-04	1E-04	8E-06	1E-06
1.7	4E-02	1E-02	8E-03	7E-03	3E-03	1E-03	1E-03	8E-04	6E-04	5E-04	4E-04	4E-04	2E-04	9E-05	7E-06	1E-06
2.2	3E-02	9E-03	6E-03	5E-03	2E-03	1E-03	8E-04	6E-04	4E-04	4E-04	3E-04	3E-04	1E-04	7E-05	5E-06	7E-07
2.8	3E-02	9E-03	5E-03	5E-03	2E-03	1E-03	8E-04	6E-04	4E-04	4E-04	3E-04	3E-04	1E-04	7E-05	5E-06	7E-07
3.6	4E-02	1E-02	8E-03	8E-03	3E-03	2E-03	1E-03	9E-04	7E-04	6E-04	4E-04	4E-04	2E-04	1E-04	8E-06	1E-06
4.6	4E-02	1E-02	8E-03	7E-03	3E-03	2E-03	1E-03	9E-04	6E-04	5E-04	4E-04	4E-04	2E-04	1E-04	7E-06	1E-06
6.0	4E-02	1E-02	7E-03	7E-03	3E-03	1E-03	1E-03	8E-04	6E-04	5E-04	4E-04	4E-04	2E-04	9E-05	7E-06	9E-07
7.7	5E-02	2E-02	1E-02	9E-03	4E-03	2E-03	2E-03	1E-03	8E-04	7E-04	5E-04	5E-04	2E-04	1E-04	9E-06	1E-06
10	3E-02	1E-02	6E-03	6E-03	2E-03	1E-03	9E-04	6E-04	5E-04	4E-04	3E-04	3E-04	1E-04	8E-05	6E-06	8E-07
13	4E-02	1E-02	7E-03	7E-03	3E-03	1E-03	1E-03	8E-04	6E-04	5E-04	4E-04	4E-04	2E-04	9E-05	7E-06	9E-07
17	3E-02	1E-02	6E-03	6E-03	2E-03	1E-03	1E-03	7E-04	5E-04	4E-04	3E-04	3E-04	1E-04	8E-05	6E-06	8E-07
22	2E-02	6E-03	4E-03	4E-03	2E-03	7E-04	6E-04	4E-04	3E-04	3E-04	2E-04	2E-04	9E-05	5E-05	4E-06	5E-07
28	9E-03	3E-03	2E-03	2E-03	8E-04	4E-04	3E-04	2E-04	2E-04	1E-04	1E-04	1E-04	4E-05	2E-05	2E-06	2E-07
36	1E-02	4E-03	3E-03	2E-03	1E-03	5E-04	4E-04	3E-04	2E-04	2E-04	1E-04	1E-04	6E-05	3E-05	2E-06	3E-07
46	3E-03	1E-03	7E-04	6E-04	3E-04	1E-04	1E-04	7E-05	5E-05	4E-05	3E-05	3E-05	1E-05	8E-06	6E-07	8E-08
60	8E-03	3E-03	2E-03	1E-03	6E-04	3E-04	2E-04	2E-04	1E-04	1E-04	8E-05	8E-05	3E-05	2E-05	1E-06	2E-07
77	4E-03	1E-03	8E-04	7E-04	3E-04	2E-04	1E-04	8E-05	6E-05	5E-05	4E-05	4E-05	2E-05	1E-05	7E-07	1E-07
100	1E-03	4E-04	3E-04	2E-04	1E-04	5E-05	4E-05	3E-05	2E-05	2E-05	1E-05	1E-05	5E-06	3E-06	2E-07	3E-08
129	1E-03	3E-04	2E-04	2E-04	8E-05	4E-05	3E-05	2E-05	2E-05	1E-05	1E-05	1E-05	4E-06	2E-06	2E-07	2E-08
167	2E-03	6E-04	4E-04	3E-04	2E-04	7E-05	6E-05	4E-05	3E-05	3E-05	2E-05	2E-05	8E-06	5E-06	3E-07	5E-08
215	6E-04	2E-04	1E-04	1E-04	5E-05	2E-05	2E-05	1E-05	1E-05	8E-06	7E-06	7E-06	3E-06	2E-06	1E-07	2E-08
278	8E-04	3E-04	2E-04	1E-04	6E-05	3E-05	3E-05	2E-05	1E-05	1E-05	9E-06	8E-06	4E-06	2E-06	1E-07	2E-08
359	4E-04	1E-04	9E-05	8E-05	3E-05	2E-05	1E-05	9E-06	7E-06	6E-06	4E-06	4E-06	2E-06	1E-06	8E-08	1E-08
464	5E-04	2E-04	1E-04	9E-05	4E-05	2E-05	1E-05	1E-05	7E-06	6E-06	5E-06	5E-06	2E-06	1E-06	9E-08	1E-08
599	3E-04	1E-04	7E-05	6E-05	3E-05	1E-05	1E-05	7E-06	5E-06	4E-06	4E-06	3E-06	1E-06	8E-07	6E-08	8E-09
774	6E-05	2E-05	1E-05	1E-05	5E-06	2E-06	2E-06	1E-06	9E-07	8E-07	6E-07	6E-07	3E-07	1E-07	1E-08	2E-09

Table 5.2.4. Representative PSDD Case 1, Density of Solid-Phase Compounds

Particle Size (µm)	Solid-Phase Compound Density (g/mL) (refer to Table 5.2.2 for compound identification)															
	1	2	3	4	5	6	7	8	9	10	11	12	13	14	15	16
0.22	2.42	2.365	3.01	2.42	5.24	3.14	5.617	5.68	8.9	2.6	4.1	5.026	3.18	6.51	6.077	11.43
0.28	2.42	2.365	3.01	2.42	5.24	3.14	5.617	5.68	8.9	2.6	4.1	5.026	3.18	6.51	6.077	11.43
0.36	2.42	2.365	3.01	2.42	5.24	3.14	5.617	5.68	8.9	2.6	4.1	5.026	3.18	6.51	6.077	11.43
0.46	2.42	2.365	3.01	2.42	5.24	3.14	5.617	5.68	8.9	2.6	4.1	5.026	3.18	6.51	6.077	11.43
0.60	2.42	2.365	3.01	2.42	5.24	3.14	5.617	5.68	8.9	2.6	4.1	5.026	3.18	6.51	6.077	11.43
0.77	2.42	2.365	3.01	2.42	5.24	3.14	5.617	5.68	8.9	2.6	4.1	5.026	3.18	6.51	6.077	11.43
1.0	2.42	2.365	3.01	2.42	5.24	3.14	5.617	5.68	8.9	2.6	4.1	5.026	3.18	6.51	6.077	11.43
1.3	2.42	2.365	3.01	2.42	5.24	3.14	5.617	5.68	8.9	2.6	4.1	5.026	3.18	6.51	6.077	11.43
1.7	2.42	2.365	3.01	2.42	5.24	3.14	5.617	5.68	8.9	2.6	4.1	5.026	3.18	6.51	6.077	11.43
2.2	2.42	2.365	3.01	2.42	5.24	3.14	5.617	5.68	8.9	2.6	4.1	5.026	3.18	6.51	6.077	11.43
2.8	2.42	2.365	3.01	2.42	5.24	3.14	5.617	5.68	8.9	2.6	4.1	5.026	3.18	6.51	6.077	11.43
3.6	2.42	2.365	3.01	2.42	5.24	3.14	5.617	5.68	8.9	2.6	4.1	5.026	3.18	6.51	6.077	11.43
4.6	2.42	2.365	3.01	2.42	5.24	3.14	5.617	5.68	8.9	2.6	4.1	5.026	3.18	6.51	6.077	11.43
6.0	2.42	2.365	3.01	2.42	5.24	3.14	5.617	5.68	8.9	2.6	4.1	5.026	3.18	6.51	6.077	11.43
7.7	2.42	2.365	3.01	2.42	5.24	3.14	5.617	5.68	8.9	2.6	4.1	5.026	3.18	6.51	6.077	11.43
10	2.42	2.365	3.01	2.42	5.24	3.14	5.617	5.68	8.9	2.6	4.1	5.026	3.18	6.51	6.077	11.43
13	2.42	2.365	3.01	2.42	5.24	3.14	5.617	5.68	8.9	2.6	4.1	5.026	3.18	6.51	6.077	11.43
17	2.42	2.365	3.01	2.42	5.24	3.14	5.617	5.68	8.9	2.6	4.1	5.026	3.18	6.51	6.077	11.43
22	2.42	2.365	3.01	2.42	5.24	3.14	5.617	5.68	8.9	2.6	4.1	5.026	3.18	6.51	6.077	11.43
28	2.42	2.365	3.01	2.42	5.24	3.14	5.617	5.68	8.9	2.6	4.1	5.026	3.18	6.51	6.077	11.43
36	2.42	2.365	3.01	2.42	5.24	3.14	5.617	5.68	8.9	2.6	4.1	5.026	3.18	6.51	6.077	11.43
46	2.42	2.365	3.01	2.42	5.24	3.14	5.617	5.68	8.9	2.6	4.1	5.026	3.18	6.51	6.077	11.43
60	2.42	2.365	3.01	2.42	5.24	3.14	5.617	5.68	8.9	2.6	4.1	5.026	3.18	6.51	6.077	11.43
77	2.42	2.365	3.01	2.42	5.24	3.14	5.617	5.68	8.9	2.6	4.1	5.026	3.18	6.51	6.077	11.43
100	2.42	2.365	3.01	2.42	5.24	3.14	5.617	5.68	8.9	2.6	4.1	5.026	3.18	6.51	6.077	11.43
129	2.42	2.365	3.01	2.42	5.24	3.14	5.617	5.68	8.9	2.6	4.1	5.026	3.18	6.51	6.077	11.43
167	2.42	2.365	3.01	2.42	5.24	3.14	5.617	5.68	8.9	2.6	4.1	5.026	3.18	6.51	6.077	11.43
215	2.42	2.365	3.01	2.42	5.24	3.14	5.617	5.68	8.9	2.6	4.1	5.026	3.18	6.51	6.077	11.43
278	2.42	2.365	3.01	2.42	5.24	3.14	5.617	5.68	8.9	2.6	4.1	5.026	3.18	6.51	6.077	11.43
359	2.42	2.365	3.01	2.42	5.24	3.14	5.617	5.68	8.9	2.6	4.1	5.026	3.18	6.51	6.077	11.43
464	2.42	2.365	3.01	2.42	5.24	3.14	5.617	5.68	8.9	2.6	4.1	5.026	3.18	6.51	6.077	11.43
599	2.42	2.365	3.01	2.42	5.24	3.14	5.617	5.68	8.9	2.6	4.1	5.026	3.18	6.51	6.077	11.43
774	2.42	2.365	3.01	2.42	5.24	3.14	5.617	5.68	8.9	2.6	4.1	5.026	3.18	6.51	6.077	11.43

Table 5.2.5. Representative PSDD Case 2, Volume Fraction of Solid-Phase Compounds

Particle Size (μm)	Solid-Phase Compound Volume Fraction (refer to Table 5.2.2 for compound identification)															
	1	**2**	**3**	**4**	**5**	**6**	**7**	**8**	**9**	**10**	**11**	**12**	**13**	**14**	**15**	**16**
0.22	2E-04	9E-05	3E-04	6E-05	3E-05	4E-05	8E-06	5E-06	4E-06	3E-06	6E-06	3E-06	1E-06	8E-07	6E-08	6E-09
0.28	6E-04	2E-04	6E-04	1E-04	7E-05	9E-05	2E-05	1E-05	1E-05	7E-06	1E-05	6E-06	3E-06	2E-06	1E-07	1E-08
0.36	7E-04	3E-04	7E-04	2E-04	9E-05	1E-04	2E-05	1E-05	1E-05	9E-06	2E-05	8E-06	3E-06	2E-06	2E-07	2E-08
0.46	6E-03	2E-03	6E-03	1E-03	8E-04	9E-04	2E-04	1E-04	1E-04	7E-05	1E-04	7E-05	3E-05	2E-05	1E-06	1E-07
0.60	3E-03	1E-03	4E-03	8E-04	4E-04	5E-04	1E-04	7E-05	6E-05	4E-05	8E-05	4E-05	2E-05	1E-05	8E-07	8E-08
0.77	9E-03	3E-03	1E-02	2E-03	1E-03	1E-03	3E-04	2E-04	2E-04	1E-04	2E-04	1E-04	4E-05	3E-05	2E-06	2E-07
1.0	1E-02	5E-03	1E-02	3E-03	2E-03	2E-03	4E-04	3E-04	2E-04	2E-04	3E-04	2E-04	6E-05	5E-05	3E-06	3E-07
1.3	3E-02	9E-03	3E-02	6E-03	3E-03	4E-03	8E-04	5E-04	4E-04	3E-04	6E-04	3E-04	1E-04	9E-05	6E-06	6E-07
1.7	2E-02	9E-03	3E-02	6E-03	3E-03	4E-03	8E-04	5E-04	4E-04	3E-04	6E-04	3E-04	1E-04	8E-05	6E-06	6E-07
2.2	2E-02	6E-03	2E-02	4E-03	2E-03	3E-03	5E-04	3E-04	3E-04	2E-04	4E-04	2E-04	8E-05	6E-05	4E-06	4E-07
2.8	2E-02	6E-03	2E-02	4E-03	2E-03	3E-03	5E-04	3E-04	3E-04	2E-04	4E-04	2E-04	8E-05	6E-05	4E-06	4E-07
3.6	3E-02	9E-03	3E-02	6E-03	3E-03	4E-03	8E-04	5E-04	4E-04	3E-04	6E-04	3E-04	1E-04	9E-05	6E-06	6E-07
4.6	3E-02	9E-03	3E-02	6E-03	3E-03	4E-03	8E-04	5E-04	4E-04	3E-04	6E-04	3E-04	1E-04	9E-05	6E-06	6E-07
6.0	2E-02	8E-03	2E-02	5E-03	3E-03	3E-03	7E-04	5E-04	4E-04	3E-04	6E-04	3E-04	1E-04	8E-05	5E-06	6E-07
7.7	3E-02	1E-02	3E-02	8E-03	4E-03	5E-03	1E-03	6E-04	5E-04	4E-04	8E-04	4E-04	1E-04	1E-04	8E-06	8E-07
10	2E-02	7E-03	2E-02	5E-03	3E-03	3E-03	6E-04	4E-04	3E-04	2E-04	5E-04	2E-04	9E-05	7E-05	5E-06	5E-07
13	2E-02	8E-03	2E-02	5E-03	3E-03	3E-03	7E-04	5E-04	4E-04	3E-04	6E-04	3E-04	1E-04	8E-05	5E-06	6E-07
17	2E-02	7E-03	2E-02	5E-03	3E-03	3E-03	6E-04	4E-04	3E-04	2E-04	5E-04	2E-04	9E-05	7E-05	5E-06	5E-07
22	1E-02	4E-03	1E-02	3E-03	2E-03	2E-03	4E-04	2E-04	2E-04	2E-04	3E-04	1E-04	6E-05	4E-05	3E-06	3E-07
28	6E-03	2E-03	6E-03	1E-03	8E-04	9E-04	2E-04	1E-04	1E-04	8E-05	1E-04	7E-05	3E-05	2E-05	1E-06	1E-07
36	8E-03	3E-03	9E-03	2E-03	1E-03	1E-03	3E-04	2E-04	1E-04	1E-04	2E-04	9E-05	4E-05	3E-05	2E-06	2E-07
46	2E-03	7E-04	2E-03	5E-04	3E-04	3E-04	6E-05	4E-05	3E-05	3E-05	5E-05	2E-05	9E-06	7E-06	5E-07	5E-08
60	5E-03	2E-03	5E-03	1E-03	7E-04	7E-04	2E-04	1E-04	8E-05	6E-05	1E-04	6E-05	2E-05	2E-05	1E-06	1E-07
77	2E-03	9E-04	3E-03	6E-04	3E-04	4E-04	8E-05	5E-05	4E-05	3E-05	6E-05	3E-05	1E-05	9E-06	6E-07	6E-08
100	8E-04	3E-04	8E-04	2E-04	1E-04	1E-04	2E-05	2E-05	1E-05	1E-05	2E-05	9E-06	4E-06	3E-06	2E-07	2E-08
129	6E-04	2E-04	6E-04	1E-04	8E-05	9E-05	2E-05	1E-05	1E-05	8E-06	2E-05	7E-06	3E-06	2E-06	1E-07	1E-08
167	1E-03	4E-04	1E-03	3E-04	2E-04	2E-04	4E-05	2E-05	2E-05	1E-05	3E-05	1E-05	5E-06	4E-06	3E-07	3E-08
215	4E-04	1E-04	4E-04	9E-05	5E-05	6E-05	1E-05	8E-06	7E-06	5E-06	1E-05	5E-06	2E-06	1E-06	9E-08	1E-08
278	5E-04	2E-04	5E-04	1E-04	7E-05	8E-05	2E-05	1E-05	9E-06	6E-06	1E-05	6E-06	2E-06	2E-06	1E-07	1E-08
359	3E-04	1E-04	3E-04	6E-05	4E-05	4E-05	8E-06	5E-06	5E-06	3E-06	7E-06	3E-06	1E-06	9E-07	6E-08	6E-09
464	3E-04	1E-04	3E-04	7E-05	4E-05	5E-05	9E-06	6E-06	5E-06	4E-06	7E-06	3E-06	1E-06	1E-06	7E-08	7E-09
599	2E-04	8E-05	2E-04	5E-05	3E-05	3E-05	7E-06	4E-06	4E-06	3E-06	5E-06	2E-06	9E-07	7E-07	5E-08	5E-09
774	4E-05	1E-05	4E-05	9E-06	5E-06	6E-06	1E-06	8E-07	6E-07	5E-07	9E-07	4E-07	2E-07	1E-07	9E-09	9E-10

Table 5.2.6. Representative PSDD Case 2, Density of Solid-Phase Compounds

Particle Size (µm)	Solid-Phase Compound Density (g/mL) (refer to Table 5.2.2 for compound identification)															
	1	2	3	4	5	6	7	8	9	10	11	12	13	14	15	16
0.22	2.42	2.37	2.21	2.42	5.24	2.63	5.62	5.68	8.90	2.60	4.10	5.03	3.18	6.51	6.08	11.43
0.28	2.42	2.37	2.11	2.42	5.24	2.49	5.62	5.68	8.90	2.60	4.10	5.03	3.18	6.51	6.08	11.43
0.36	2.42	2.37	2.02	2.42	5.24	2.36	5.62	5.68	8.90	2.60	4.10	5.03	3.18	6.51	6.08	11.43
0.46	2.42	2.37	1.94	2.42	5.24	2.25	5.62	5.68	8.90	2.60	4.10	5.03	3.18	6.51	6.08	11.43
0.60	2.42	2.37	1.87	2.42	5.24	2.15	5.62	5.68	8.90	2.60	3.60	5.03	3.18	6.51	6.08	11.43
0.77	2.42	2.37	1.80	2.42	5.24	2.06	5.62	5.68	8.90	2.60	3.37	5.03	3.18	6.51	6.08	11.43
1.0	2.42	2.37	1.75	2.42	5.24	1.97	5.62	5.68	8.90	2.60	3.16	5.03	3.18	6.51	6.08	11.43
1.3	2.42	2.37	1.69	2.42	4.71	1.90	5.62	5.68	8.90	2.60	2.97	5.03	3.18	6.51	6.08	11.43
1.7	2.42	2.37	1.65	2.42	4.37	1.83	5.62	5.68	8.90	2.60	2.80	5.03	3.18	6.51	6.08	11.43
2.2	2.42	2.37	1.60	2.42	4.06	1.77	5.62	5.68	8.90	2.60	2.64	5.03	3.18	5.95	6.08	11.43
2.8	2.42	2.37	1.56	2.42	3.78	1.71	5.62	5.68	8.90	2.60	2.50	5.03	3.18	5.48	5.58	11.43
3.6	2.42	2.37	1.53	2.20	3.53	1.66	5.62	5.68	8.90	2.60	2.37	5.03	3.18	5.07	5.15	11.43
4.6	2.42	2.37	1.50	2.10	3.31	1.62	5.62	5.68	8.90	2.60	2.26	5.03	3.18	4.69	4.77	11.43
6.0	2.42	2.20	1.47	2.02	3.10	1.58	5.62	5.68	8.90	2.60	2.16	5.03	3.18	4.35	4.42	11.43
7.7	2.42	2.10	1.44	1.94	2.92	1.54	5.62	5.68	7.71	2.60	2.06	4.42	3.18	4.05	4.11	11.43
10	2.42	2.01	1.42	1.86	2.75	1.51	5.18	5.68	7.08	2.60	1.98	4.11	3.18	3.77	3.83	11.43
13	2.42	1.93	1.40	1.80	2.60	1.48	4.80	5.68	6.51	2.60	1.90	3.82	2.82	3.52	3.57	11.43
17	2.20	1.86	1.38	1.74	2.46	1.45	4.45	5.68	5.99	2.60	1.84	3.57	2.66	3.29	3.34	11.43
22	2.10	1.80	1.36	1.69	2.34	1.43	4.13	5.68	5.52	2.60	1.77	3.34	2.52	3.09	3.13	11.43
28	2.01	1.74	1.34	1.64	2.23	1.40	3.84	5.68	5.10	2.60	1.72	3.13	2.39	2.91	2.94	10.22
36	1.93	1.69	1.33	1.60	2.13	1.38	3.59	5.10	4.72	2.60	1.67	2.94	2.27	2.74	2.77	9.34
46	1.86	1.64	1.32	1.56	2.04	1.37	3.36	4.72	4.38	2.60	1.62	2.77	2.17	2.59	2.62	8.55
60	1.80	1.60	1.31	1.52	1.96	1.35	3.15	4.38	4.07	2.60	1.58	2.62	2.07	2.45	2.48	7.83
77	1.74	1.56	1.30	1.49	1.88	1.34	2.96	4.07	3.79	2.38	1.54	2.48	1.99	2.33	2.36	7.19
100	1.69	1.52	1.29	1.46	1.82	1.32	2.79	3.79	3.54	2.26	1.51	2.36	1.91	2.22	2.25	6.61
129	1.64	1.49	1.28	1.44	1.76	1.31	2.63	3.54	3.31	2.16	1.48	2.24	1.84	2.12	2.14	6.08
167	1.60	1.46	1.27	1.42	1.70	1.30	2.49	3.31	3.11	2.06	1.45	2.14	1.78	2.03	2.05	5.60
215	1.56	1.44	1.26	1.39	1.65	1.29	2.37	3.11	2.92	1.98	1.43	2.05	1.72	1.95	1.97	5.18
278	1.52	1.41	1.26	1.38	1.61	1.28	2.25	2.92	2.75	1.90	1.41	1.97	1.67	1.88	1.89	4.79
359	1.49	1.39	1.25	1.36	1.57	1.27	2.15	2.75	2.60	1.84	1.39	1.89	1.63	1.81	1.83	4.44
464	1.46	1.37	1.25	1.34	1.53	1.27	2.06	2.60	2.47	1.77	1.37	1.83	1.59	1.75	1.77	4.13
599	1.44	1.36	1.24	1.33	1.50	1.26	1.97	2.47	2.34	1.72	1.35	1.77	1.55	1.70	1.71	3.84
774	1.41	1.34	1.24	1.32	1.47	1.25	1.90	2.34	2.23	1.67	1.34	1.71	1.51	1.65	1.66	3.58

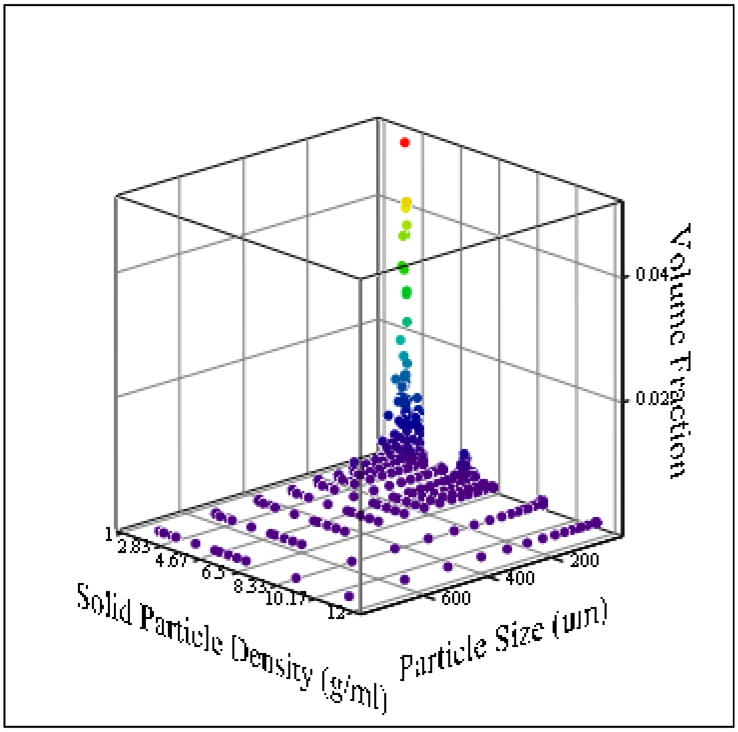

(X, Y, Z)

Figure 5.2.1. Case 1 Representative PSDD

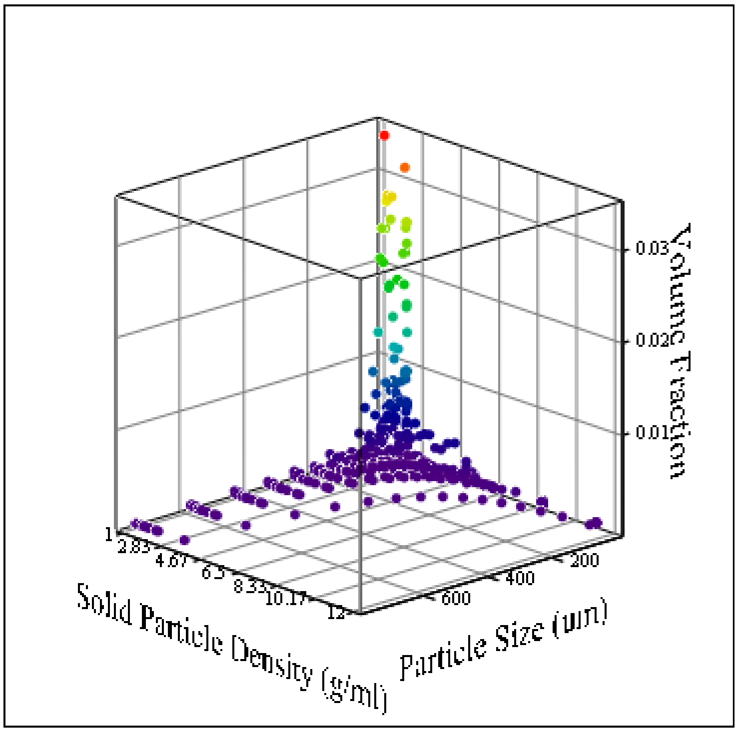

(X, Y, Z)

Figure 5.2.2. Case 2 Representative PSDD

Table 5.2.7. Representative PSDD Case 3, Volume Fraction of Solid-Phase Compounds

Particle Size (μm)	Solid-Phase Compound Volume Fraction (refer to Table 5.2.2 for compound identification)															
	1	2	3	4	5	6	7	8	9	10	11	12	13	14	15	16
0.22	1E-04	5E-05	3E-05	3E-05	1E-05	6E-06	5E-06	3E-06	2E-06	2E-06	2E-06	2E-06	7E-07	4E-07	3E-08	4E-09
0.28	3E-04	1E-04	6E-05	6E-05	2E-05	1E-05	9E-06	6E-06	5E-06	4E-06	3E-06	3E-06	1E-06	8E-07	5E-08	8E-09
0.36	6E-04	2E-04	1E-04	1E-04	5E-05	2E-05	2E-05	1E-05	1E-05	8E-06	7E-06	7E-06	3E-06	2E-06	1E-07	2E-08
0.46	5E-05	2E-05	1E-05	1E-05	4E-06	2E-06	2E-06	1E-06	9E-07	7E-07	6E-07	6E-07	2E-07	1E-07	1E-08	1E-09
0.60	2E-03	5E-04	3E-04	3E-04	1E-04	6E-05	5E-05	3E-05	2E-05	2E-05	2E-05	2E-05	7E-06	4E-06	3E-07	4E-08
0.77	8E-03	3E-03	2E-03	1E-03	6E-04	3E-04	2E-04	2E-04	1E-04	1E-04	8E-05	8E-05	3E-05	2E-05	1E-06	2E-07
1.0	2E-02	5E-03	3E-03	3E-03	1E-03	6E-04	5E-04	3E-04	2E-04	2E-04	2E-04	2E-04	7E-05	4E-05	3E-06	4E-07
1.3	2E-02	6E-03	4E-03	4E-03	2E-03	8E-04	6E-04	4E-04	3E-04	3E-04	2E-04	2E-04	9E-05	5E-05	4E-06	5E-07
1.7	3E-02	1E-02	7E-03	6E-03	3E-03	1E-03	1E-03	7E-04	5E-04	4E-04	4E-04	3E-04	1E-04	8E-05	6E-06	8E-07
2.2	1E-02	5E-03	3E-03	3E-03	1E-03	5E-04	4E-04	3E-04	2E-04	2E-04	1E-04	1E-04	6E-05	4E-05	3E-06	4E-07
2.8	4E-02	1E-02	7E-03	6E-03	3E-03	1E-03	1E-03	7E-04	6E-04	5E-04	4E-04	4E-04	2E-04	9E-05	6E-06	9E-07
3.6	5E-02	2E-02	1E-02	9E-03	4E-03	2E-03	1E-03	1E-03	7E-04	6E-04	5E-04	5E-04	2E-04	1E-04	9E-06	1E-06
4.6	3E-02	1E-02	6E-03	6E-03	3E-03	1E-03	1E-03	7E-04	5E-04	4E-04	3E-04	3E-04	1E-04	8E-05	6E-06	8E-07
6.0	4E-02	1E-02	9E-03	8E-03	3E-03	2E-03	1E-03	9E-04	7E-04	6E-04	5E-04	4E-04	2E-04	1E-04	8E-06	1E-06
7.7	5E-02	2E-02	1E-02	9E-03	4E-03	2E-03	2E-03	1E-03	8E-04	7E-04	5E-04	5E-04	2E-04	1E-04	9E-06	1E-06
10	4E-02	1E-02	8E-03	7E-03	3E-03	2E-03	1E-03	9E-04	6E-04	5E-04	4E-04	4E-04	2E-04	1E-04	7E-06	1E-06
13	4E-02	1E-02	8E-03	7E-03	3E-03	1E-03	1E-03	8E-04	6E-04	5E-04	4E-04	4E-04	2E-04	9E-05	7E-06	9E-07
17	4E-02	1E-02	8E-03	7E-03	3E-03	2E-03	1E-03	8E-04	6E-04	5E-04	4E-04	4E-04	2E-04	1E-04	7E-06	1E-06
22	3E-02	1E-02	6E-03	6E-03	2E-03	1E-03	9E-04	6E-04	5E-04	4E-04	3E-04	3E-04	1E-04	8E-05	5E-06	8E-07
28	1E-02	5E-03	3E-03	3E-03	1E-03	6E-04	4E-04	3E-04	2E-04	2E-04	2E-04	2E-04	6E-05	4E-05	3E-06	4E-07
36	2E-02	6E-03	4E-03	4E-03	2E-03	8E-04	6E-04	4E-04	3E-04	3E-04	2E-04	2E-04	9E-05	5E-05	4E-06	5E-07
46	7E-03	2E-03	1E-03	1E-03	6E-04	3E-04	2E-04	1E-04	1E-04	9E-05	7E-05	7E-05	3E-05	2E-05	1E-06	2E-07
60	5E-03	1E-03	9E-04	8E-04	4E-04	2E-04	1E-04	1E-04	7E-05	6E-05	5E-05	5E-05	2E-05	1E-05	8E-07	1E-07
77	4E-03	1E-03	9E-04	8E-04	3E-04	2E-04	1E-04	9E-05	7E-05	6E-05	5E-05	4E-05	2E-05	1E-05	8E-07	1E-07
100	3E-03	9E-04	5E-04	5E-04	2E-04	1E-04	8E-05	6E-05	4E-05	4E-05	3E-05	3E-05	1E-05	7E-06	5E-07	7E-08
129	2E-03	6E-04	4E-04	3E-04	1E-04	7E-05	5E-05	4E-05	3E-05	2E-05	2E-05	2E-05	8E-06	4E-06	3E-07	4E-08
167	7E-03	2E-03	1E-03	1E-03	5E-04	3E-04	2E-04	1E-04	1E-04	9E-05	7E-05	7E-05	3E-05	2E-05	1E-06	2E-07
215	4E-03	1E-03	7E-04	7E-04	3E-04	1E-04	1E-04	8E-05	6E-05	5E-05	4E-05	4E-05	2E-05	9E-06	7E-07	9E-08
278	2E-03	7E-04	4E-04	4E-04	2E-04	8E-05	6E-05	4E-05	3E-05	3E-05	2E-05	2E-05	9E-06	5E-06	4E-07	5E-08
359	3E-03	1E-03	6E-04	5E-04	2E-04	1E-04	9E-05	6E-05	5E-05	4E-05	3E-05	3E-05	1E-05	7E-06	5E-07	8E-08
464	6E-04	2E-04	1E-04	1E-04	5E-05	2E-05	2E-05	1E-05	1E-05	9E-06	7E-06	7E-06	3E-06	2E-06	1E-07	2E-08
599	4E-04	1E-04	8E-05	7E-05	3E-05	1E-05	1E-05	8E-06	6E-06	5E-06	4E-06	4E-06	2E-06	1E-06	7E-08	1E-08
774	4E-04	1E-04	9E-05	8E-05	3E-05	2E-05	1E-05	9E-06	7E-06	6E-06	4E-06	4E-06	2E-06	1E-06	8E-08	1E-08
1000	3E-05	9E-06	6E-06	5E-06	2E-06	1E-06	8E-07	6E-07	4E-07	4E-07	3E-07	3E-07	1E-07	7E-08	5E-09	7E-10

Table 5.2.8. Representative PSDD Case 3, Density of Solid-Phase Compounds

Particle Size (µm)	Solid-Phase Compound Density (g/mL) (refer to Table 5.2.2 for compound identification)															
	1	2	3	4	5	6	7	8	9	10	11	12	13	14	15	16
0.22	2.42	2.365	3.01	2.42	5.24	3.14	5.617	5.68	8.9	2.6	4.1	5.026	3.18	6.51	6.077	11.43
0.28	2.42	2.365	3.01	2.42	5.24	3.14	5.617	5.68	8.9	2.6	4.1	5.026	3.18	6.51	6.077	11.43
0.36	2.42	2.365	3.01	2.42	5.24	3.14	5.617	5.68	8.9	2.6	4.1	5.026	3.18	6.51	6.077	11.43
0.46	2.42	2.365	3.01	2.42	5.24	3.14	5.617	5.68	8.9	2.6	4.1	5.026	3.18	6.51	6.077	11.43
0.60	2.42	2.365	3.01	2.42	5.24	3.14	5.617	5.68	8.9	2.6	4.1	5.026	3.18	6.51	6.077	11.43
0.77	2.42	2.365	3.01	2.42	5.24	3.14	5.617	5.68	8.9	2.6	4.1	5.026	3.18	6.51	6.077	11.43
1.0	2.42	2.365	3.01	2.42	5.24	3.14	5.617	5.68	8.9	2.6	4.1	5.026	3.18	6.51	6.077	11.43
1.3	2.42	2.365	3.01	2.42	5.24	3.14	5.617	5.68	8.9	2.6	4.1	5.026	3.18	6.51	6.077	11.43
1.7	2.42	2.365	3.01	2.42	5.24	3.14	5.617	5.68	8.9	2.6	4.1	5.026	3.18	6.51	6.077	11.43
2.2	2.42	2.365	3.01	2.42	5.24	3.14	5.617	5.68	8.9	2.6	4.1	5.026	3.18	6.51	6.077	11.43
2.8	2.42	2.365	3.01	2.42	5.24	3.14	5.617	5.68	8.9	2.6	4.1	5.026	3.18	6.51	6.077	11.43
3.6	2.42	2.365	3.01	2.42	5.24	3.14	5.617	5.68	8.9	2.6	4.1	5.026	3.18	6.51	6.077	11.43
4.6	2.42	2.365	3.01	2.42	5.24	3.14	5.617	5.68	8.9	2.6	4.1	5.026	3.18	6.51	6.077	11.43
6.0	2.42	2.365	3.01	2.42	5.24	3.14	5.617	5.68	8.9	2.6	4.1	5.026	3.18	6.51	6.077	11.43
7.7	2.42	2.365	3.01	2.42	5.24	3.14	5.617	5.68	8.9	2.6	4.1	5.026	3.18	6.51	6.077	11.43
10	2.42	2.365	3.01	2.42	5.24	3.14	5.617	5.68	8.9	2.6	4.1	5.026	3.18	6.51	6.077	11.43
13	2.42	2.365	3.01	2.42	5.24	3.14	5.617	5.68	8.9	2.6	4.1	5.026	3.18	6.51	6.077	11.43
17	2.42	2.365	3.01	2.42	5.24	3.14	5.617	5.68	8.9	2.6	4.1	5.026	3.18	6.51	6.077	11.43
22	2.42	2.365	3.01	2.42	5.24	3.14	5.617	5.68	8.9	2.6	4.1	5.026	3.18	6.51	6.077	11.43
28	2.42	2.365	3.01	2.42	5.24	3.14	5.617	5.68	8.9	2.6	4.1	5.026	3.18	6.51	6.077	11.43
36	2.42	2.365	3.01	2.42	5.24	3.14	5.617	5.68	8.9	2.6	4.1	5.026	3.18	6.51	6.077	11.43
46	2.42	2.365	3.01	2.42	5.24	3.14	5.617	5.68	8.9	2.6	4.1	5.026	3.18	6.51	6.077	11.43
60	2.42	2.365	3.01	2.42	5.24	3.14	5.617	5.68	8.9	2.6	4.1	5.026	3.18	6.51	6.077	11.43
77	2.42	2.365	3.01	2.42	5.24	3.14	5.617	5.68	8.9	2.6	4.1	5.026	3.18	6.51	6.077	11.43
100	2.42	2.365	3.01	2.42	5.24	3.14	5.617	5.68	8.9	2.6	4.1	5.026	3.18	6.51	6.077	11.43
129	2.42	2.365	3.01	2.42	5.24	3.14	5.617	5.68	8.9	2.6	4.1	5.026	3.18	6.51	6.077	11.43
167	2.42	2.365	3.01	2.42	5.24	3.14	5.617	5.68	8.9	2.6	4.1	5.026	3.18	6.51	6.077	11.43
215	2.42	2.365	3.01	2.42	5.24	3.14	5.617	5.68	8.9	2.6	4.1	5.026	3.18	6.51	6.077	11.43
278	2.42	2.365	3.01	2.42	5.24	3.14	5.617	5.68	8.9	2.6	4.1	5.026	3.18	6.51	6.077	11.43
359	2.42	2.365	3.01	2.42	5.24	3.14	5.617	5.68	8.9	2.6	4.1	5.026	3.18	6.51	6.077	11.43
464	2.42	2.365	3.01	2.42	5.24	3.14	5.617	5.68	8.9	2.6	4.1	5.026	3.18	6.51	6.077	11.43
599	2.42	2.365	3.01	2.42	5.24	3.14	5.617	5.68	8.9	2.6	4.1	5.026	3.18	6.51	6.077	11.43
774	2.42	2.365	3.01	2.42	5.24	3.14	5.617	5.68	8.9	2.6	4.1	5.026	3.18	6.51	6.077	11.43
1000	2.42	2.365	3.01	2.42	5.24	3.14	5.617	5.68	8.9	2.6	4.1	5.026	3.18	6.51	6.077	11.43

Table 5.2.9. Representative PSDD Case 4, Volume Fraction of Solid-Phase Compounds

Particle Size (μm)	Solid-Phase Compound Volume Fraction (refer to Table 5.2.2 for compound identification)															
	1	**2**	**3**	**4**	**5**	**6**	**7**	**8**	**9**	**10**	**11**	**12**	**13**	**14**	**15**	**16**
0.22	9E-05	3E-05	1E-04	2E-05	1E-05	2E-05	3E-06	2E-06	2E-06	1E-06	2E-06	1E-06	4E-07	3E-07	2E-08	2E-09
0.28	2E-04	7E-05	2E-04	4E-05	3E-05	3E-05	6E-06	3E-06	3E-06	2E-06	5E-06	2E-06	8E-07	7E-07	4E-08	4E-09
0.36	4E-04	1E-04	5E-04	9E-05	6E-05	6E-05	1E-05	7E-06	7E-06	5E-06	1E-05	4E-06	2E-06	1E-06	9E-08	9E-09
0.46	3E-05	1E-05	4E-05	8E-06	5E-06	5E-06	1E-06	6E-07	6E-07	4E-07	9E-07	4E-07	1E-07	1E-07	8E-09	8E-10
0.60	9E-04	4E-04	1E-03	2E-04	1E-04	2E-04	3E-05	2E-05	2E-05	1E-05	3E-05	1E-05	4E-06	4E-06	2E-07	2E-08
0.77	5E-03	2E-03	6E-03	1E-03	7E-04	8E-04	1E-04	9E-05	8E-05	6E-05	1E-04	5E-05	2E-05	2E-05	1E-06	1E-07
1.0	9E-03	3E-03	1E-02	2E-03	1E-03	2E-03	3E-04	2E-04	2E-04	1E-04	3E-04	1E-04	4E-05	3E-05	2E-06	2E-07
1.3	1E-02	4E-03	1E-02	3E-03	2E-03	2E-03	4E-04	2E-04	2E-04	1E-04	3E-04	1E-04	5E-05	5E-05	3E-06	3E-07
1.7	2E-02	7E-03	2E-02	5E-03	3E-03	3E-03	6E-04	4E-04	3E-04	2E-04	6E-04	2E-04	9E-05	8E-05	5E-06	5E-07
2.2	8E-03	3E-03	1E-02	2E-03	1E-03	1E-03	3E-04	2E-04	1E-04	1E-04	2E-04	1E-04	4E-05	3E-05	2E-06	2E-07
2.8	2E-02	8E-03	3E-02	5E-03	3E-03	4E-03	7E-04	4E-04	4E-04	3E-04	6E-04	2E-04	1E-04	8E-05	5E-06	5E-07
3.6	3E-02	1E-02	3E-02	7E-03	4E-03	5E-03	9E-04	6E-04	5E-04	3E-04	8E-04	3E-04	1E-04	1E-04	7E-06	7E-07
4.6	2E-02	7E-03	2E-02	5E-03	3E-03	3E-03	6E-04	4E-04	3E-04	2E-04	5E-04	2E-04	9E-05	7E-05	5E-06	4E-07
6.0	2E-02	9E-03	3E-02	6E-03	4E-03	4E-03	8E-04	5E-04	4E-04	3E-04	7E-04	3E-04	1E-04	1E-04	6E-06	6E-07
7.7	3E-02	1E-02	3E-02	7E-03	4E-03	5E-03	9E-04	6E-04	5E-04	4E-04	8E-04	3E-04	1E-04	1E-04	7E-06	7E-07
10	2E-02	9E-03	3E-02	6E-03	4E-03	4E-03	8E-04	5E-04	4E-04	3E-04	7E-04	3E-04	1E-04	9E-05	6E-06	6E-07
13	2E-02	8E-03	3E-02	6E-03	3E-03	4E-03	7E-04	4E-04	4E-04	3E-04	6E-04	3E-04	1E-04	8E-05	6E-06	5E-07
17	2E-02	9E-03	3E-02	6E-03	3E-03	4E-03	7E-04	5E-04	4E-04	3E-04	7E-04	3E-04	1E-04	9E-05	6E-06	6E-07
22	2E-02	7E-03	2E-02	4E-03	3E-03	3E-03	6E-04	4E-04	3E-04	2E-04	5E-04	2E-04	8E-05	7E-05	5E-06	4E-07
28	8E-03	3E-03	1E-02	2E-03	1E-03	1E-03	3E-04	2E-04	2E-04	1E-04	2E-04	1E-04	4E-05	3E-05	2E-06	2E-07
36	1E-02	4E-03	1E-02	3E-03	2E-03	2E-03	4E-04	2E-04	2E-04	1E-04	3E-04	1E-04	5E-05	4E-05	3E-06	3E-07
46	4E-03	2E-03	5E-03	1E-03	6E-04	7E-04	1E-04	8E-05	7E-05	5E-05	1E-04	5E-05	2E-05	2E-05	1E-06	1E-07
60	3E-03	1E-03	3E-03	7E-04	4E-04	5E-04	9E-05	5E-05	5E-05	3E-05	8E-05	3E-05	1E-05	1E-05	7E-07	6E-08
77	2E-03	9E-04	3E-03	6E-04	4E-04	4E-04	8E-05	5E-05	4E-05	3E-05	7E-05	3E-05	1E-05	1E-05	6E-07	6E-08
100	2E-03	6E-04	2E-03	4E-04	2E-04	3E-04	5E-05	3E-05	3E-05	2E-05	4E-05	2E-05	7E-06	6E-06	4E-07	4E-08
129	1E-03	4E-04	1E-03	3E-04	2E-04	2E-04	3E-05	2E-05	2E-05	1E-05	3E-05	1E-05	5E-06	4E-06	3E-07	2E-08
167	4E-03	1E-03	5E-03	1E-03	6E-04	7E-04	1E-04	8E-05	7E-05	5E-05	1E-04	5E-05	2E-05	1E-05	1E-06	9E-08
215	2E-03	8E-04	3E-03	5E-04	3E-04	4E-04	7E-05	4E-05	4E-05	3E-05	6E-05	2E-05	1E-05	8E-06	5E-07	5E-08
278	1E-03	4E-04	1E-03	3E-04	2E-04	2E-04	4E-05	2E-05	2E-05	1E-05	3E-05	1E-05	6E-06	5E-06	3E-07	3E-08
359	2E-03	7E-04	2E-03	4E-04	3E-04	3E-04	6E-05	3E-05	3E-05	2E-05	5E-05	2E-05	8E-06	7E-06	4E-07	4E-08
464	4E-04	1E-04	5E-04	1E-04	6E-05	7E-05	1E-05	8E-06	7E-06	5E-06	1E-05	4E-06	2E-06	1E-06	1E-07	9E-09
599	2E-04	8E-05	3E-04	6E-05	3E-05	4E-05	7E-06	4E-06	4E-06	3E-06	6E-06	3E-06	1E-06	9E-07	6E-08	5E-09
774	2E-04	9E-05	3E-04	6E-05	4E-05	4E-05	8E-06	5E-06	4E-06	3E-06	7E-06	3E-06	1E-06	9E-07	6E-08	6E-09
1000	2E-05	6E-06	2E-05	4E-06	2E-06	3E-06	5E-07	3E-07	3E-07	2E-07	5E-07	2E-07	7E-08	6E-08	4E-09	4E-10

Table 5.2.10. Representative PSDD Case 4, Density of Solid-Phase Compounds

Particle Size (μm)	Solid-Phase Compound Density (g/mL) (refer to Table 5.2.2 for compound identification)															
	1	**2**	**3**	**4**	**5**	**6**	**7**	**8**	**9**	**10**	**11**	**12**	**13**	**14**	**15**	**16**
0.22	2.42	2.37	2.21	2.42	5.24	2.63	5.62	5.68	8.90	2.60	4.10	5.03	3.18	6.51	6.08	11.43
0.28	2.42	2.37	2.11	2.42	5.24	2.49	5.62	5.68	8.90	2.60	4.10	5.03	3.18	6.51	6.08	11.43
0.36	2.42	2.37	2.02	2.42	5.24	2.36	5.62	5.68	8.90	2.60	4.10	5.03	3.18	6.51	6.08	11.43
0.46	2.42	2.37	1.94	2.42	5.24	2.25	5.62	5.68	8.90	2.60	4.10	5.03	3.18	6.51	6.08	11.43
0.60	2.42	2.37	1.87	2.42	5.24	2.15	5.62	5.68	8.90	2.60	3.60	5.03	3.18	6.51	6.08	11.43
0.77	2.42	2.37	1.80	2.42	5.24	2.06	5.62	5.68	8.90	2.60	3.37	5.03	3.18	6.51	6.08	11.43
1.0	2.42	2.37	1.75	2.42	5.24	1.97	5.62	5.68	8.90	2.60	3.16	5.03	3.18	6.51	6.08	11.43
1.3	2.42	2.37	1.69	2.42	4.71	1.90	5.62	5.68	8.90	2.60	2.97	5.03	3.18	6.51	6.08	11.43
1.7	2.42	2.37	1.65	2.42	4.37	1.83	5.62	5.68	8.90	2.60	2.80	5.03	3.18	6.51	6.08	11.43
2.2	2.42	2.37	1.60	2.42	4.06	1.77	5.62	5.68	8.90	2.60	2.64	5.03	3.18	5.94	6.08	11.43
2.8	2.42	2.37	1.56	2.42	3.78	1.71	5.62	5.68	8.90	2.60	2.50	5.03	3.18	5.48	5.57	11.43
3.6	2.42	2.37	1.53	2.20	3.53	1.66	5.62	5.68	8.90	2.60	2.37	5.03	3.18	5.07	5.15	11.43
4.6	2.42	2.37	1.50	2.10	3.31	1.62	5.62	5.68	8.90	2.60	2.26	5.03	3.18	4.69	4.76	11.43
6.0	2.42	2.20	1.47	2.02	3.10	1.58	5.62	5.68	8.90	2.60	2.16	5.03	3.18	4.35	4.42	11.43
7.7	2.42	2.10	1.44	1.94	2.92	1.54	5.62	5.68	7.71	2.60	2.06	4.42	3.18	4.04	4.10	11.43
10	2.42	2.01	1.42	1.87	2.75	1.51	5.18	5.68	7.08	2.60	1.98	4.11	2.99	3.77	3.82	11.43
13	2.42	1.93	1.40	1.80	2.60	1.48	4.79	5.68	6.51	2.60	1.90	3.83	2.81	3.52	3.57	11.43
17	2.20	1.86	1.38	1.74	2.46	1.45	4.44	5.68	5.99	2.60	1.84	3.57	2.66	3.29	3.34	11.43
22	2.10	1.80	1.36	1.69	2.34	1.43	4.13	5.68	5.53	2.60	1.77	3.34	2.51	3.09	3.13	11.43
28	2.02	1.74	1.34	1.64	2.23	1.40	3.84	5.68	5.10	2.60	1.72	3.13	2.39	2.90	2.94	10.24
36	1.94	1.69	1.33	1.60	2.13	1.38	3.59	5.10	4.72	2.60	1.67	2.94	2.27	2.74	2.77	9.36
46	1.86	1.64	1.32	1.56	2.04	1.37	3.35	4.72	4.38	2.60	1.62	2.77	2.17	2.59	2.62	8.56
60	1.80	1.60	1.31	1.52	1.96	1.35	3.14	4.38	4.07	2.60	1.58	2.62	2.07	2.45	2.48	7.85
77	1.74	1.56	1.30	1.49	1.88	1.34	2.95	4.07	3.79	2.38	1.54	2.48	1.99	2.33	2.36	7.20
100	1.69	1.52	1.29	1.46	1.82	1.32	2.78	3.79	3.54	2.26	1.51	2.36	1.91	2.22	2.24	6.62
129	1.64	1.49	1.28	1.44	1.76	1.31	2.63	3.54	3.31	2.16	1.48	2.25	1.84	2.12	2.14	6.09
167	1.60	1.46	1.27	1.42	1.70	1.30	2.49	3.31	3.11	2.06	1.45	2.14	1.78	2.03	2.05	5.61
215	1.56	1.44	1.26	1.39	1.65	1.29	2.37	3.10	2.92	1.98	1.43	2.05	1.72	1.95	1.97	5.18
278	1.52	1.41	1.26	1.38	1.61	1.28	2.25	2.92	2.75	1.90	1.41	1.97	1.67	1.88	1.89	4.80
359	1.49	1.39	1.25	1.36	1.57	1.27	2.15	2.75	2.60	1.84	1.39	1.89	1.63	1.81	1.83	4.45
464	1.46	1.37	1.25	1.34	1.53	1.27	2.06	2.60	2.47	1.77	1.37	1.83	1.58	1.75	1.76	4.13
599	1.44	1.36	1.24	1.33	1.50	1.26	1.97	2.46	2.34	1.72	1.35	1.77	1.55	1.70	1.71	3.85
774	1.42	1.34	1.24	1.32	1.47	1.25	1.90	2.34	2.23	1.67	1.34	1.71	1.51	1.65	1.66	3.59
1000	1.39	1.33	1.23	1.31	1.45	1.25	1.83	2.23	2.13	1.62	1.32	1.66	1.48	1.61	1.62	3.36

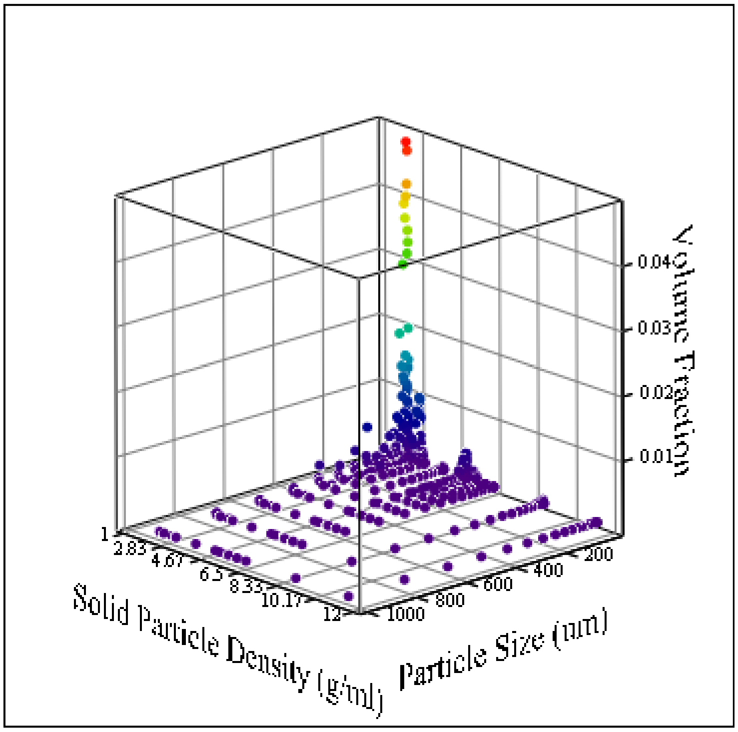

(X, Y, Z)

Figure 5.2.3. Case 3 Representative PSDD

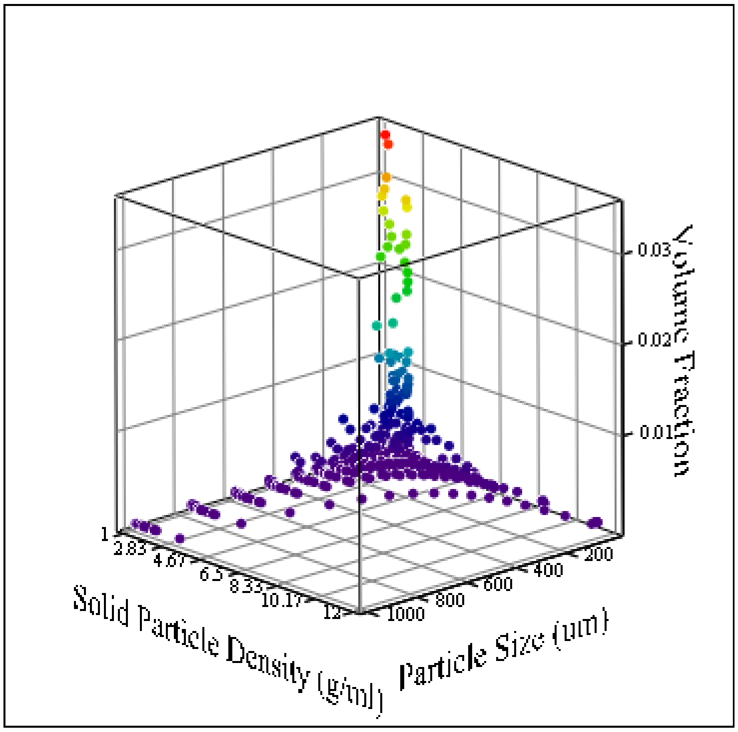

(X, Y, Z)

Figure 5.2.4. Case 4 Representative PSDD

The % difference of the volume fraction and density, represented for illustrative purposes as volume weighted average density per bin, is considered for the four PSDDs. Case 3, resulting in the largest volume fraction of large and dense particulate, is used for comparison. The % difference results are computed as

$$\% \,\mathrm{Difference} = \frac{X_{\mathrm{Case}} - X_{\mathrm{Case3}}}{X_{\mathrm{Case3}}} \tag{5.2.1}$$

where X is the volume fraction or average density (g/mL) of case being considered, subscript "Case" denotes considered PSDD case, and subscript "Case3" denotes Case 3 PSDD. Thus, a positive result indicates that the considered PSDD case has a larger volume fraction for a specific compound in a given bin or a higher average density per bin than Case 3, and vice-versa.

PSDD comparison results for Case 3 to Case 1 are provided in Table 5.2.11. As expected due to the input PSDs (Table 5.0.1), it is evident that Case 3 has larger particulate. Given that both Case 1 and 3 relate all constituent densities to the crystal densities, there is no difference in the average bulk density per bin. Similar disparity is observed between Cases 2 and 3, Table 5.2.12, with the addition of increasing density difference as the particle size increases due to the fractal relation in Case 2.

Comparison of Cases 3 and 4 is provided in Table 5.2.13. Although the same PSD is used in each case, the volume fraction of the constituents along the probability of the PSD is redistributed through the optimization process on the mass (Section 4.2). This effect is overwhelmed by the PSD differences in Cases 1 and 2 to Cases 3 and 4 as indicated by the relative similarity of the % differences by compound and bin in Tables 5.2.11 and 5.2.12. That is, the difference in Case 3 to Case 4 due to the fractal relation does not appear to have the same impact on the differences between Cases 2 and 3 (fractal and PSD case differences) as indicated by the similarity of this result to the Cases 1 and 3 comparison (PSD case difference only).

5.2.2 Comparison of Representative PSDDs to Expected Waste Conditions

Qualitative comparison of the representative PSDDs presented in Section 5.2.1 to in situ waste conditions is made by considering:

- The PSD of the PSDD
- The solid-phase compound mass fractions
- The volume-weighted average density of the bulk solids
- The fraction of the waste volume composed of agglomerates.

The PSD quantiles of the representative PSDDs can be determined by summing the volume-based probability of each of the solid-phase compounds over each particle size bin. As can be seen by comparing the results in Table 5.2.14 with the PSDs of Table 5.0.1, the input PSDs are reproduced exactly.

Table 5.2.11. Comparison of Representative PSDDs, Case 1 to Case 3

Particle Size (μm)	**Percent Difference (refer to Table 5.2.2 for compound identification)**																
	1	2	3	4	5	6	7	8	9	10	11	12	13	14	15	16	Bulk Density
0.22	155	155	155	155	155	155	155	155	155	155	155	155	155	155	155	155	0
0.28	197	197	197	197	197	197	197	197	197	197	197	197	197	197	197	197	0
0.36	74	74	74	74	74	74	74	74	74	74	74	74	74	74	74	74	0
0.46	2E+4	2E+4	2E+4	2E+4	2E+4	2E+4	2E+4	2E+4	2E+4	2E+4	2E+4	2E+4	2E+4	2E+4	2E+4	2E+4	0
0.60	242	242	242	242	242	242	242	242	242	242	242	242	242	242	242	242	0
0.77	95	95	95	95	95	95	95	95	95	95	95	95	95	95	95	95	0
1.0	45	45	45	45	45	45	45	45	45	45	45	45	45	45	45	45	0
1.3	106	106	106	106	106	106	106	106	106	106	106	106	106	106	106	106	0
1.7	13	13	13	13	13	13	13	13	13	13	13	13	13	13	13	13	0
2.2	93	93	93	93	93	93	93	93	93	93	93	93	93	93	93	93	0
2.8	-25	-25	-25	-25	-25	-25	-25	-25	-25	-25	-25	-25	-25	-25	-25	-25	0
3.6	-13	-13	-13	-13	-13	-13	-13	-13	-13	-13	-13	-13	-13	-13	-13	-13	0
4.6	28	28	28	28	28	28	28	28	28	28	28	28	28	28	28	28	0
6.0	-15	-15	-15	-15	-15	-15	-15	-15	-15	-15	-15	-15	-15	-15	-15	-15	0
7.7	4	4	4	4	4	4	4	4	4	4	4	4	4	4	4	4	0
10	-25	-25	-25	-25	-25	-25	-25	-25	-25	-25	-25	-25	-25	-25	-25	-25	0
13	-3	-3	-3	-3	-3	-3	-3	-3	-3	-3	-3	-3	-3	-3	-3	-3	0
17	-21	-21	-21	-21	-21	-21	-21	-21	-21	-21	-21	-21	-21	-21	-21	-21	0
22	-36	-36	-36	-36	-36	-36	-36	-36	-36	-36	-36	-36	-36	-36	-36	-36	0
28	-34	-34	-34	-34	-34	-34	-34	-34	-34	-34	-34	-34	-34	-34	-34	-34	0
36	-32	-32	-32	-32	-32	-32	-32	-32	-32	-32	-32	-32	-32	-32	-32	-32	0
46	-54	-54	-54	-54	-54	-54	-54	-54	-54	-54	-54	-54	-54	-54	-54	-54	0
60	71	71	71	71	71	71	71	71	71	71	71	71	71	71	71	71	0
77	-8	-8	-8	-8	-8	-8	-8	-8	-8	-8	-8	-8	-8	-8	-8	-8	0
100	-54	-54	-54	-54	-54	-54	-54	-54	-54	-54	-54	-54	-54	-54	-54	-54	0
129	-45	-45	-45	-45	-45	-45	-45	-45	-45	-45	-45	-45	-45	-45	-45	-45	0
167	-72	-72	-72	-72	-72	-72	-72	-72	-72	-72	-72	-72	-72	-72	-72	-72	0
215	-82	-82	-82	-82	-82	-82	-82	-82	-82	-82	-82	-82	-82	-82	-82	-82	0
278	-60	-60	-60	-60	-60	-60	-60	-60	-60	-60	-60	-60	-60	-60	-60	-60	0
359	-86	-86	-86	-86	-86	-86	-86	-86	-86	-86	-86	-86	-86	-86	-86	-86	0
464	-27	-27	-27	-27	-27	-27	-27	-27	-27	-27	-27	-27	-27	-27	-27	-27	0
599	-13	-13	-13	-13	-13	-13	-13	-13	-13	-13	-13	-13	-13	-13	-13	-13	0
774	-86	-86	-86	-86	-86	-86	-86	-86	-86	-86	-86	-86	-86	-86	-86	-86	0
1000	N/A	N/A	N/A	N/A	N/A	N/A	N/A	N/A	N/A	N/A	N/A	N/A	N/A	N/A	N/A	N/A	N/A

N/A indicates that at least one case has no data for the given bin due to different PSDs.

Table 5.2.12. Comparison of Representative PSDDs, Case 2 to Case 3

Particle Size (µm)	Percent Difference (refer to Table 5.2.2 for compound identification)																
	1	**2**	**3**	**4**	**5**	**6**	**7**	**8**	**9**	**10**	**11**	**12**	**13**	**14**	**15**	**16**	**Bulk Density**
0.22	59	81	741	106	168	537	65	52	74	50	275	74	63	124	109	53	-7
0.28	85	111	879	140	213	642	92	77	103	75	336	103	90	161	144	79	-8
0.36	9	24	476	41	84	336	13	4	19	3	156	19	12	53	43	5	-9
0.46	1E+4	1E+4	6E+4	1E+4	2E+4	4E+4	1E+4	1E+4	1E+4	1E+4	3E+4	1E+4	1E+4	2E+4	1E+4	1E+4	-11
0.60	114	143	1029	177	261	756	121	105	134	102	403	134	120	201	181	106	-12
0.77	22	39	544	58	106	388	26	17	33	15	187	34	25	71	60	17	-13
1.0	-10	3	378	17	53	262	-6	-13	-1	-14	113	-1	-7	27	19	-13	-14
1.3	29	46	580	67	117	415	33	23	41	22	203	41	32	81	69	24	-16
1.7	-30	-20	272	-9	19	182	-27	-33	-23	-33	66	-23	-28	-1	-8	-32	-17
2.2	20	37	535	56	103	381	24	15	31	14	183	32	23	69	58	16	-18
2.8	-53	-47	148	-39	-21	88	-51	-55	-49	-56	10	-49	-52	-34	-38	-55	-19
3.6	-46	-38	187	-30	-8	118	-44	-48	-41	-49	28	-41	-44	-24	-29	-48	-21
4.6	-20	-9	321	3	35	219	-18	-24	-13	-25	88	-13	-18	12	5	-23	-22
6.0	-47	-40	180	-31	-10	113	-45	-49	-42	-50	25	-42	-45	-25	-30	-49	-24
7.7	-35	-26	244	-16	10	160	-33	-38	-29	-39	53	-29	-33	-9	-15	-37	-25
10	-53	-46	148	-39	-21	88	-51	-55	-49	-56	11	-49	-52	-34	-38	-55	-27
13	-40	-31	219	-22	2	142	-37	-42	-34	-43	42	-34	-38	-15	-21	-42	-28
17	-51	-44	161	-36	-17	98	-49	-53	-46	-53	16	-46	-49	-31	-35	-52	-32
22	-60	-54	112	-48	-32	61	-59	-62	-56	-62	-6	-56	-59	-44	-47	-61	-34
28	-59	-53	117	-47	-31	64	-58	-61	-55	-61	-4	-55	-58	-42	-46	-61	-36
36	-58	-52	123	-45	-29	69	-56	-60	-54	-60	-1	-54	-57	-41	-45	-59	-38
46	-71	-67	53	-62	-51	16	-70	-72	-68	-73	-32	-68	-70	-59	-62	-72	-40
60	7	21	463	38	80	327	10	2	16	1	151	17	9	50	40	3	-42
77	-43	-35	203	-26	-3	130	-41	-45	-37	-46	35	-37	-41	-19	-25	-45	-43
100	-72	-68	50	-63	-52	14	-71	-73	-69	-73	-33	-69	-71	-60	-63	-73	-45
129	-66	-61	82	-55	-42	38	-64	-67	-62	-68	-19	-62	-65	-52	-55	-67	-46
167	-82	-80	-6	-77	-70	-29	-82	-83	-81	-83	-58	-81	-82	-75	-77	-83	-47
215	-89	-87	-41	-86	-81	-56	-89	-89	-88	-90	-74	-88	-89	-84	-85	-89	-48
278	-75	-72	32	-68	-58	0	-74	-76	-73	-76	-41	-73	-74	-65	-67	-76	-49
359	-91	-90	-54	-89	-85	-65	-91	-92	-90	-92	-79	-90	-91	-88	-88	-92	-49
464	-54	-48	141	-41	-23	83	-53	-56	-50	-57	7	-50	-53	-36	-40	-56	-50
599	-46	-38	186	-30	-9	117	-44	-48	-41	-49	27	-41	-44	-24	-29	-48	-51
774	-91	-90	-53	-88	-85	-64	-91	-91	-90	-92	-79	-90	-91	-87	-88	-91	-51
1000	N/A	N/A	N/A	N/A	N/A	N/A	N/A	N/A	N/A	N/A	N/A	N/A	N/A	N/A	N/A	N/A	N/A

N/A indicates that at least one case has no data for the given bin due to different PSDs.

Table 5.2.13. Comparison of Representative PSDDs, Case 4 to Case 3

Particle Size	Percent Difference (refer to Table 5.2.2 for compound identification)																
(μm)	1	2	3	4	5	6	7	8	9	10	11	12	13	14	15	16	Bulk Density
0.22	-41	-31	250	-19	10	165	-39	-45	-34	-46	56	-34	-39	-10	-17	-44	-7
0.28	-42	-31	248	-19	10	164	-39	-45	-35	-46	56	-34	-39	-11	-18	-45	-8
0.36	-42	-31	249	-19	10	164	-39	-45	-34	-46	56	-34	-39	-11	-18	-45	-10
0.46	-42	-32	245	-20	8	161	-39	-46	-35	-47	54	-35	-40	-12	-18	-45	-11
0.60	-41	-31	250	-19	10	165	-39	-45	-34	-46	56	-34	-39	-10	-17	-44	-12
0.77	-42	-31	249	-19	10	164	-39	-45	-34	-46	56	-34	-39	-11	-18	-45	-13
1.0	-41	-31	249	-19	10	165	-39	-45	-34	-46	56	-34	-39	-10	-17	-45	-14
1.3	-42	-31	249	-19	10	164	-39	-45	-34	-46	56	-34	-39	-11	-18	-45	-16
1.7	-41	-31	249	-19	10	164	-39	-45	-34	-46	56	-34	-39	-11	-18	-45	-18
2.2	-41	-31	249	-19	10	164	-39	-45	-34	-46	56	-34	-39	-11	-18	-45	-19
2.8	-41	-31	249	-19	10	164	-39	-45	-34	-46	56	-34	-39	-10	-18	-45	-20
3.6	-42	-31	249	-19	10	164	-39	-45	-34	-46	56	-34	-39	-11	-18	-45	-22
4.6	-41	-31	249	-19	10	164	-39	-45	-34	-46	56	-34	-39	-10	-17	-45	-23
6.0	-42	-31	249	-19	10	164	-39	-45	-34	-46	56	-34	-39	-11	-18	-45	-25
7.7	-42	-31	249	-19	10	164	-39	-45	-34	-46	56	-34	-39	-11	-18	-45	-26
10	-41	-31	249	-19	10	164	-39	-45	-34	-46	56	-34	-39	-10	-18	-45	-28
13	-42	-31	249	-19	10	164	-39	-45	-34	-46	56	-34	-39	-11	-18	-45	-29
17	-42	-31	249	-19	10	164	-39	-45	-34	-46	56	-34	-39	-11	-18	-45	-33
22	-41	-31	249	-19	10	164	-39	-45	-34	-46	56	-34	-39	-11	-18	-45	-35
28	-42	-31	249	-19	10	164	-39	-45	-34	-46	56	-34	-39	-11	-18	-45	-37
36	-42	-31	249	-19	10	164	-39	-45	-34	-46	56	-34	-39	-11	-18	-45	-39
46	-41	-31	249	-19	10	165	-39	-45	-34	-46	56	-34	-39	-10	-17	-45	-41
60	-42	-31	249	-19	10	164	-39	-45	-34	-46	56	-34	-39	-11	-18	-45	-42
77	-41	-31	249	-19	10	165	-39	-45	-34	-46	56	-34	-39	-10	-17	-45	-44
100	-42	-31	249	-19	10	164	-39	-45	-34	-46	56	-34	-39	-11	-18	-45	-45
129	-42	-31	249	-19	10	164	-39	-45	-34	-46	56	-34	-39	-11	-18	-45	-46
167	-41	-31	249	-19	10	164	-39	-45	-34	-46	56	-34	-39	-11	-18	-45	-47
215	-41	-31	249	-19	10	165	-39	-45	-34	-46	56	-34	-39	-10	-17	-45	-48
278	-42	-31	249	-19	10	164	-39	-45	-34	-46	56	-34	-39	-11	-18	-45	-49
359	-42	-31	249	-19	10	164	-39	-45	-34	-46	56	-34	-39	-11	-18	-45	-50
464	-41	-31	250	-19	10	165	-38	-45	-34	-46	57	-34	-39	-10	-17	-44	-50
599	-41	-31	250	-19	10	165	-39	-45	-34	-46	56	-34	-39	-10	-17	-44	-51
774	-41	-31	250	-19	10	165	-39	-45	-34	-46	56	-34	-39	-10	-17	-45	-52
1000	-41	-31	249	-19	10	164	-39	-45	-34	-46	56	-34	-39	-11	-18	-45	-52
N/A indicates that at least one case has no data for the given bin due to different PSDs.																	

Table 5.2.14. Representative PSDDs of PSDs (μm)

Quantile	1%	5%	25%	50%	75%	95%	99%	100%
Case 1	0.39	0.70	1.63	4.38	10.2	33.4	112	774
Case 2	0.39	0.70	1.63	4.38	10.2	33.4	112	774
Case 3	0.65	1.00	2.80	6.31	14.0	58.6	256	1000
Case 4	0.65	1.00	2.80	6.31	14.0	58.6	256	1000

Through the mass-based optimization process, the input solid-phase compound mass fractions are preserved in the Monte Carlo simulations. The mass fraction error, E, over the solid-phase compounds is defined by

$$E = \frac{\sum_{j} \left| M_{j,0} - M_{j} \right|}{\sum_{j} M_{j,0}} \tag{5.2.2}$$

where M_j is the calculated mass fraction of chemical compound j and $M_{j,0}$ is the mass fraction of compound j. For Cases 1 and 3, zero error in the mass fraction is achieved. For Cases 2 and 4, 95% of the simulations have a mass fraction error less than 0.00 and 0.02 respectively. All representative PSDDs have mass fraction errors of 0.00.

The volume-weighted average density of the bulk solids (primary particles and agglomerates) for Cases 2 and 4 with a fractal dimension of 2.6 is considered. The average density over the 500 Monte Carlo simulations for Case 2 is 2.1 g/mL, ranging from approximately 1.7 to 2.2 g/mL, and 2.0 g/mL, approximately 1.7 to 2.1 g/mL for Case 4. The average density for the representative PSDDs for Cases 2 and 4 are 2.12 g/mL and 2.03 g/mL respectively. With the higher preponderance of agglomerates in Case 4 (see input PSDs, Table 5.0.1), the comparatively higher density of Case 2 is expected. The average density from Jewett et al. (2002) for nine HLW tanks is approximately 2.08 g/mL. For both Case 1 and 3, the volume-weighted average density of the bulk solids is approximately 2.8 g/mL as compared to 2.9 g/mL for the crystal-density basis value from Jewett et al. (2002). These differences are expected given the different solid-phase compound bases; 177 waste tanks in the current analysis to nine and eight tanks respectively in Jewett et al.

A significant fraction of the waste volume, at least 50%, is expected to be composed of agglomerates, Section 3.2. It is further to be expected that the volume fraction of agglomerates in the sonicated PSD (Case 2) is reduced as compared to the minimal disturbance PSD (Case 4). The representative PSDD results for Cases 2 and 4 are considered with respect to these expectations. The volume fraction of each compound for each particle size bin less than the compound's centroid primary particle size is summed. This provides an estimate of the average volume fraction of the total solids that are represented for the representative PSDD as agglomerates. Volume fractions of approximately 0.66 and 0.73 are achieved for Cases 2 and 4, respectively. These results are in reasonable agreement with expectations in terms of magnitude as well as the relation between the sonicated and minimal disturbance PSDs.

The upper limit for agglomeration in the Monte Carlo simulations is essentially 100% if all primary particles were set to their minimum size. The lower limit can be determined similarly by setting the compounds' primary particle size to their respective maximum particle sizes for the representative PSDDs. Volume fraction results of 0.57 and 0.64 are achieved for Cases 2 and 4, respectively.

The volume fraction of agglomerates in the representative PSDDs is necessarily a function of the conservation of particulate mass approach. Increasing the fractal dimension reduces the volume fraction of agglomerates while the volume-weighted average density of the bulk solids increases. That is, when the density of the agglomerate particulate increases, a lower agglomerate volume is needed to conserve mass.

Consideration regarding the volume fraction of agglomerates is made with respect to the volume fraction of the constituents resulting from the mass-based optimization process. The respective volume fractions of the solid-phase compounds for the Case 2 and 4 representative PSDDs, presented in Table 5.2.15, may be determined by summing across the PSDs (Tables 5.2.5 and 5.2.9). The input mass fractions are conserved, Table 5.2.15. The relatively large mass fraction of boehmite, which, due to its small primary particle size, is always agglomerate, requires a substantial increase in volume fraction to conserve its particulate mass. Thus, the determined compound volume fractions are shifted from the particulate-basis input values, and the results are sensitive to the fraction of boehmite determined in Section 3.2. In addition to the boehmite, an increase in the volume fraction of $Ca_5OH(PO_4)_3$ may also be observed, again attributable to its relatively small primary particle size.

Table 5.2.15. Solid-Phase Compounds Mass and Volume Percent

Solid Phase	**Density, kg/m^3**	**Input**		**Case 2**		**Case 4**	
		wt%	**vol%**	**wt%**	**vol%**	**wt%**	**vol%**
Gibbsite	2420	44.9	51.5	44.9	32.1	44.9	30.1
$(NaAlSiO_4)_6 \cdot (NaNO_3)_{1.6} \cdot 2H_2O$	2365	14.2	16.6	14.2	11.8	14.2	11.5
Boehmite	3010	11.5	10.6	11.5	34.9	11.5	36.9
$NaAlCO_3(OH)_2$	2420	8.3	9.5	8.3	7.7	8.3	7.7
Fe_2O_3	5240	7.8	4.1	7.8	4.3	7.8	4.5
$Ca_5OH(PO_4)_3$	3140	2.3	2.0	2.3	5.0	2.3	5.3
$Na_2U_2O_7$	5617	3.2	1.6	3.2	1.0	3.2	0.98
ZrO_2	5680	2.2	1.1	2.2	0.65	2.2	0.60
Bi_2O_3	8900	2.6	0.81	2.6	0.56	2.6	0.54
SiO_2	2600	0.65	0.69	0.65	0.41	0.65	0.37
$Ni(OH)_2$	4100	0.81	0.55	0.81	0.81	0.81	0.86
MnO_2	5026	0.98	0.54	0.98	0.37	0.98	0.35
CaF_2	3180	0.27	0.23	0.27	0.15	0.27	0.14
$LaPO_4 \cdot 2H_2O$	6510	0.31	0.13	0.30	0.11	0.31	0.12
Ag_2CO_3	6077	0.021	0.0094	0.021	0.0077	0.021	0.0078
PuO_2	11430	0.0054	0.0013	0.0054	0.00079	0.0054	0.00073

5.3 Critical Velocity Criterion

Critical velocity calculations have been conducted for each PSDD. The Oroskar and Turian (1980) and Thomas (1976, 1979) equations specified in BNI (2006a) were employed. The applicability of these models to the current study conditions was not evaluated. Results are obtained for the following cases, as described in Section 4.2:

- Oroskar and Turian equation over entire particle size range
- Thomas equation for fine particles, Oroskar and Turian equation for coarse particles, interpolation of Thomas and Oroskar and Turian equations for transition region.

The mass fraction of the solids in the flow for each size and density pair in the PSDD matrices was set to 0.154, approximating the maximum solids loading, 200 g/L, specified in BNI (2006a). For the general calculations, the liquid density and viscosity were assigned as 1.2 g/mL and 2 mPa s, respectively. The pipe diameter was set to 3 inches. Criterion results are presented in Section 5.3.1. The flow parameters are briefly exercised in Section 5.3.2 to illustrate their impact on the results.

5.3.1 Critical Velocity Criterion Results

Critical velocity criterion results for each of the PSDD approaches are provided in Table 5.3.1. Four threshold design velocities are evaluated for the volume percent of solid particulate that requires a critical velocity above these thresholds. No design margin is applied to the threshold design velocities. The current waste feed delivery system has a minimum flow rate of 90 gpm, which translates to approximately 4 ft/sec in a 3-inch-diameter pipe. The threshold design velocity of 3.07 ft/sec represents the velocity required if the threshold of 4 ft/sec is assigned the typical 30% design margin (BNI 2006a).

Maximum results are achieved for Cases 1 and 3 with the sonicated and minimal disturbance PSDs, respectively. The maximum volume exceeding the criterion occurs for Case 3 as expected (see Section 5.2). The mass fraction of particulate, including the liquid mass in the agglomerates, necessarily flows the same trends (Table 5.3.1). The maximum relative difference is 183% for Case 4 at 4 ft/sec. The volume of particulate exceeding the criteria determined with the Oroskar and Turian equation decreases exponentially with the threshold design velocity (Figure 5.3.1).

The particle size and density pairs (Figures 5.2.1 through 5.2.4) that exceed the threshold design velocity of 3.07 ft/sec are provided in Figures 5.3.2 through 5.3.5 for the representative PSDDs of Cases 1 through 4, respectively. It is apparent that the particulate exceeding the criterion is spread over the possible particle size and density ranges with the largest contribution to the failure volume typically at a density of about 5.2 g/mL.

Table 5.3.1. PSDD Critical Velocity Criterion Results

Case	**Criterion(a)**	**Median Volume (%)** **(maximum to minimum range)** **[representative PSDD result: volume/mass(b)]**			
		Threshold Design Velocity (ft/sec)			
		3.07	**4**	**5**	**6**
1	OT	7.6 (6.5 - 8.8) [7.6/14.5]	2.4 (2.0 - 2.9) [2.5/5.7]	0.6 (0.5 - 0.8) [0.6/1.7]	0.2 (0.1 - 0.2) [0.2/0.5]
2	OT	1.8 (0.1 - 2.6) [2.0/5.7]	0.6 (0.0 - 0.9) [0.7/2.1]	0.1 (0.0 - 0.2) [0.0/0.0]	0.0 (0.0) [0.0/0.0]
3	OT	10.7 (9.2 - 12.2) [10.8/18.3]	3.5 (3.0 - 4.1) [3.6/7.7]	0.9 (0.8 - 1.1) [0.9/2.3]	0.4 (0.3 - 0.5) [0.4/1.0]
4	OT	1.9 (0.0 - 2.7) [2.1/5.9]	0.6 (0.0 - 1.1) [0.7/2.4]	0.0 (0.0 - 0.3) [0.0/0.0]	0.0 (0.0) [0.0/0.0]
1	OT and T	2.1 (1.8 - 2.6) [2.1/4.3]	0.3 (0.2 - 0.4) [0.3/0.5]	0.1 (0.1 - 0.2) [0.1/0.2]	0.1 (0.1 - 0.1) [0.1/0.2]
2	OT and T	0.5 (0.1 - 0.6) [0.5/2.0]	0.0 (0.0) [0.0/0.0]	0.0 (0.0) [0.0/0.0]	0.0 (0.0) [0.0/0.0]
3	OT and T	4.6 (4.0 - 5.2) [4.6/6.7]	0.8 (0.7 - 0.9) [0.8/1.3]	0.4 (0.3 - 0.4) [0.4/0.7]	0.3 (0.2 - 0.4) [0.3/0.6]
4	OT and T	0.4 (0.1 - 0.6) [0.5/1.8]	0.0 (0.0 - 0.1) [0.0/0.0]	0.0 (0.0) [0.0/0.0]	0.0 (0.0) [0.0/0.0]

(a) Criterion indicates equation(s) used to determine critical velocity. OT denotes Oroskar and Turian equation, T the Thomas equation. The applicability of these models to current study conditions was not evaluated.

(b) Reported mass fraction is the mass of primary particles and agglomerates (for Cases 2 and 4). The liquid mass in the agglomerates is included.

The specific particulate that exceeds the threshold design velocity criterion is examined to illustrate that a broad range of material in terms of particle size and density, and thus a range of solid-phase compounds, is represented. Therefore, consideration of a single particulate does not reflect the PSDDs. The particulate that exceeds the 3.07 ft/sec Oroskar and Turian criterion, in terms of particle size and density, is presented for Case 1 as an example in Table 5.3.2. The density of the particulate that exceeds the threshold design velocity criterion ranges from 2.365 g/mL to 11.43 g/mL; different solid-phase compounds are represented.

Examination of the specific solid-phase compounds that exceed the threshold design velocity criterion allows for two considerations. First, illustration of the relative impact of the compounds considered is provided. Second, this information provides insight into the potential impacts of specific waste streams. The Case 1 representative PSDD percentage (relative to initial volume fraction) of each solid-phase compound that exceeds the 3.07 ft/sec Oroskar and Turian criterion is presented in Table 5.3.3. The percent exceedance is, as expected, correlated with the compound densities.

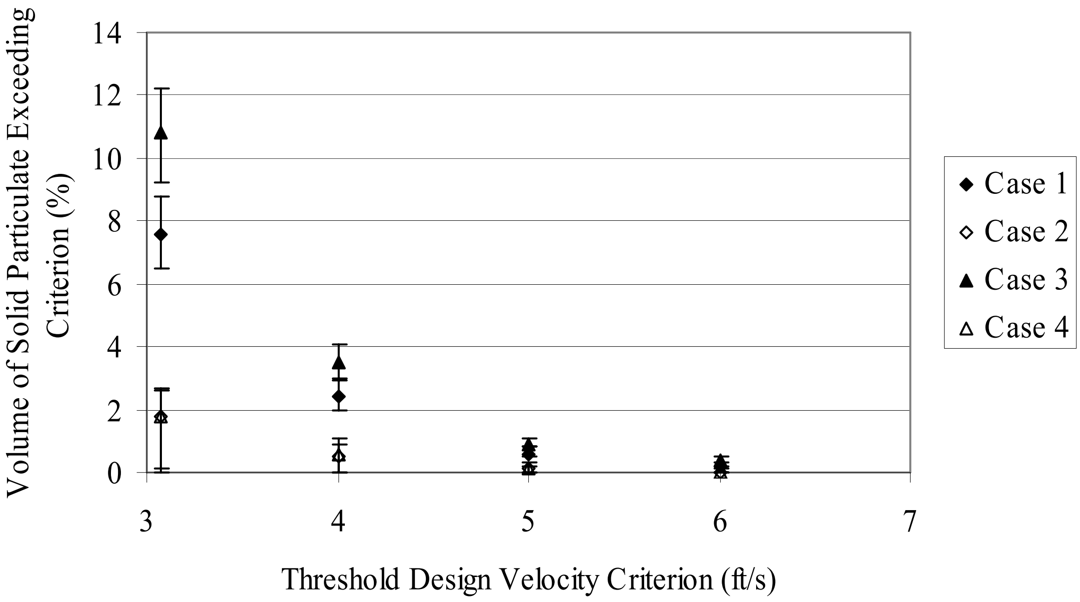

Figure 5.3.1. Volume of Solid Particulate Exceeding Threshold Design Velocity Criterion (Oroskar and Turian Equation)

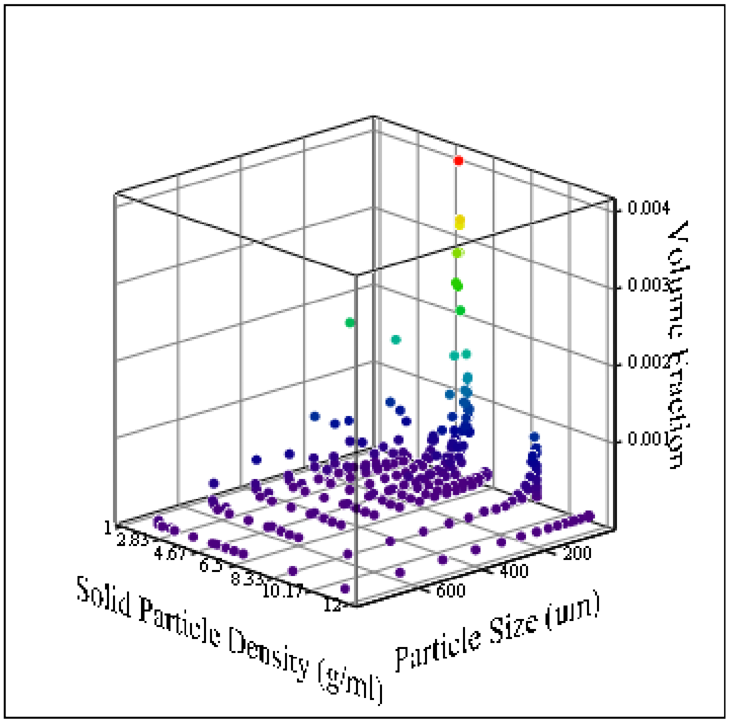

(X,Y,Z)

Figure 5.3.2. Case 1 Representative PSDD Particulate Exceeding 3.07 ft/sec Threshold Design Velocity (Oroskar and Turian Equation)

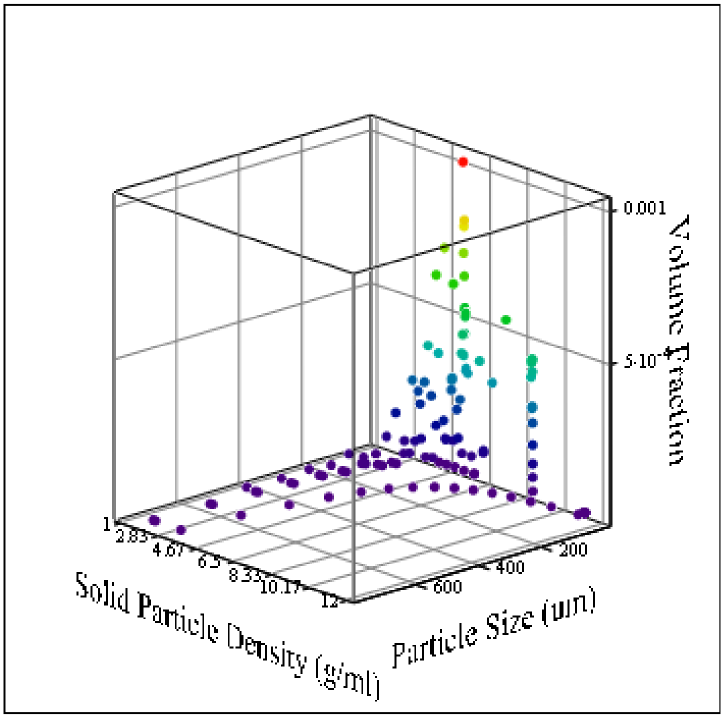

(X, Y, Z)

Figure 5.3.3. Case 2 Representative PSDD Particulate Exceeding 3.07 ft/sec Threshold Design Velocity (Oroskar and Turian Equation)

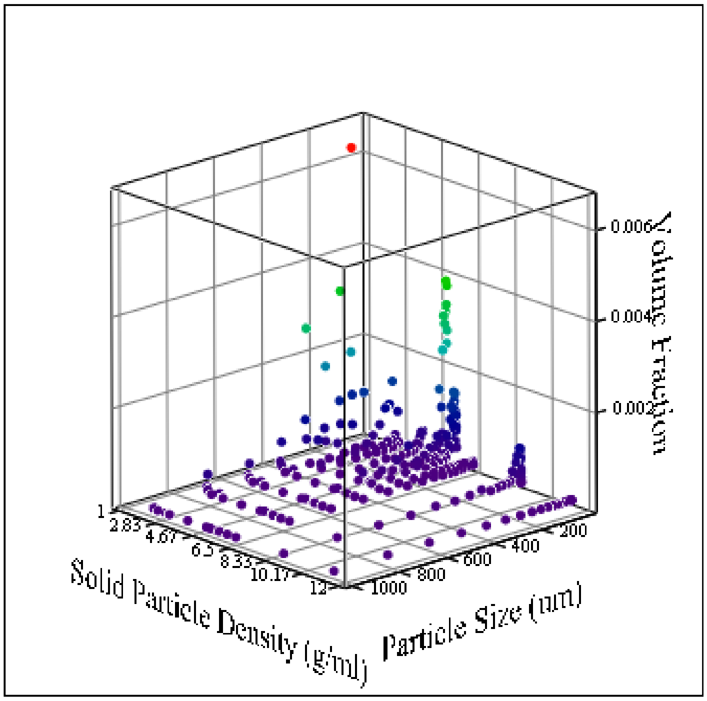

(X, Y, Z)

Figure 5.3.4. Case 3 Representative PSDD Particulate Exceeding 3.07 ft/sec Threshold Design Velocity (Oroskar and Turian Equation)

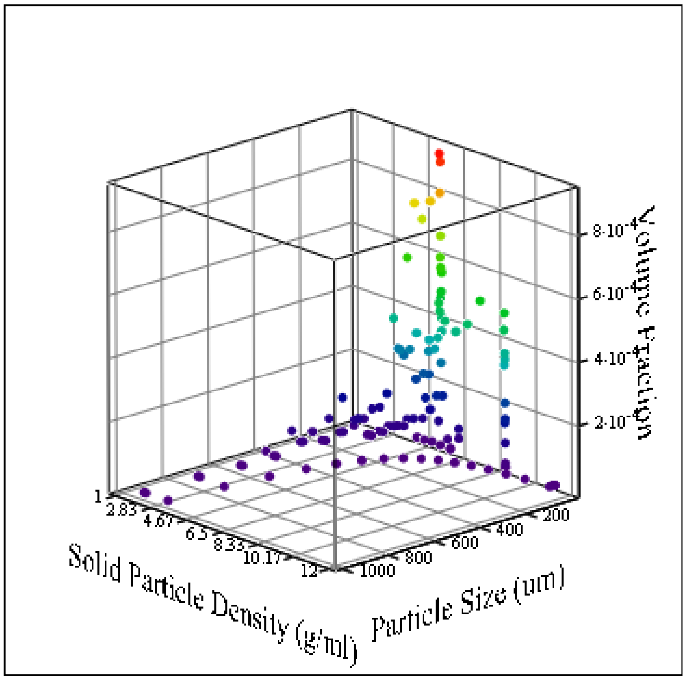

(X, Y, Z)

Figure 5.3.5. Case 4 Representative PSDD Particulate Exceeding 3.07 ft/sec Threshold Design Velocity (Oroskar and Turian Equation)

A specific conclusion on pipeline transportability of PuO_2 in this study should not be used for a criticality analysis. The critical velocity criterion analyses indicate that most of PuO_2 and its agglomerates (applicable to Cases 2 and 4) will not be suspended. However, the plutonium oxide in Tank SY-102 most likely came from tanks in the 241-Z Building through a 3-inch pipeline via Double-Contained Receiver Tank 244-TX (Douglas 1998). The transfer pump at Tank 244-TX is rated at 100 gpm (approximately 4.5 ft/sec through a 3-inch pipe). This apparent modeling inaccuracy on PuO_2 may be attributed to setting the solids loading in the slurry to the maximum specified in BNI (2006a) for each size and density pair in the PSDD, while PuO_2 actually only comprises approximately 0.00131 vol% of the solid particulate for Cases 1 and 3 and 0.00541 vol% of the solid particulate and Cases 2 and 4. In addition, all Pu compounds are represented by PuO_2 in this analysis (Section 3.2.1.3).

Table 5.3.2. Case 1 Representative PSDD Particulate Exceeding 3.07 ft/sec Threshold Design Velocity (Oroskar and Turian)

Particle Size (µm)	Solid-Phase Compound Density (g/mL) (refer to Table 5.2.2 for compound identification)															
	1	2	3	4	5	6	7	8	9	10	11	12	13	14	15	16
0.22	Pass	Pass	Pass	Pass	Pass	Pass	Pass	Pass	Pass	Pass	Pass	Pass	Pass	Pass	Pass	11.43
0.28	Pass	Pass	Pass	Pass	Pass	Pass	Pass	Pass	Pass	Pass	Pass	Pass	Pass	Pass	Pass	11.43
0.36	Pass	Pass	Pass	Pass	Pass	Pass	Pass	Pass	8.9	Pass	Pass	Pass	Pass	Pass	Pass	11.43
0.46	Pass	Pass	Pass	Pass	Pass	Pass	Pass	Pass	8.9	Pass	Pass	Pass	Pass	Pass	Pass	11.43
0.60	Pass	Pass	Pass	Pass	Pass	Pass	Pass	Pass	8.9	Pass	Pass	Pass	Pass	Pass	Pass	11.43
0.77	Pass	Pass	Pass	Pass	Pass	Pass	Pass	Pass	8.9	Pass	Pass	Pass	Pass	Pass	Pass	11.43
1.0	Pass	Pass	Pass	Pass	Pass	Pass	Pass	Pass	8.9	Pass	Pass	Pass	Pass	Pass	Pass	11.43
1.3	Pass	Pass	Pass	Pass	Pass	Pass	Pass	Pass	8.9	Pass	Pass	Pass	Pass	6.51	Pass	11.43
1.7	Pass	Pass	Pass	Pass	Pass	Pass	Pass	Pass	8.9	Pass	Pass	Pass	Pass	6.51	6.077	11.43
2.2	Pass	Pass	Pass	Pass	Pass	Pass	5.617	5.68	8.9	Pass	Pass	Pass	Pass	6.51	6.077	11.43
2.8	Pass	Pass	Pass	Pass	5.24	Pass	5.617	5.68	8.9	Pass	Pass	Pass	Pass	6.51	6.077	11.43
3.6	Pass	Pass	Pass	Pass	5.24	Pass	5.617	5.68	8.9	Pass	Pass	5.026	Pass	6.51	6.077	11.43
4.6	Pass	Pass	Pass	Pass	5.24	Pass	5.617	5.68	8.9	Pass	Pass	5.026	Pass	6.51	6.077	11.43
6.0	Pass	Pass	Pass	Pass	5.24	Pass	5.617	5.68	8.9	Pass	Pass	5.026	Pass	6.51	6.077	11.43
7.7	Pass	Pass	Pass	Pass	5.24	Pass	5.617	5.68	8.9	Pass	Pass	5.026	Pass	6.51	6.077	11.43
10	Pass	Pass	Pass	Pass	5.24	Pass	5.617	5.68	8.9	Pass	4.1	5.026	Pass	6.51	6.077	11.43
13	Pass	Pass	Pass	Pass	5.24	Pass	5.617	5.68	8.9	Pass	4.1	5.026	Pass	6.51	6.077	11.43
17	Pass	Pass	Pass	Pass	5.24	Pass	5.617	5.68	8.9	Pass	4.1	5.026	Pass	6.51	6.077	11.43
22	Pass	Pass	Pass	Pass	5.24	Pass	5.617	5.68	8.9	Pass	4.1	5.026	Pass	6.51	6.077	11.43
28	Pass	Pass	Pass	Pass	5.24	Pass	5.617	5.68	8.9	Pass	4.1	5.026	Pass	6.51	6.077	11.43
36	Pass	Pass	Pass	Pass	5.24	3.14	5.617	5.68	8.9	Pass	4.1	5.026	3.18	6.51	6.077	11.43
46	Pass	Pass	3.01	Pass	5.24	3.14	5.617	5.68	8.9	Pass	4.1	5.026	3.18	6.51	6.077	11.43
60	Pass	Pass	3.01	Pass	5.24	3.14	5.617	5.68	8.9	Pass	4.1	5.026	3.18	6.51	6.077	11.43
77	Pass	Pass	3.01	Pass	5.24	3.14	5.617	5.68	8.9	Pass	4.1	5.026	3.18	6.51	6.077	11.43
100	Pass	Pass	3.01	Pass	5.24	3.14	5.617	5.68	8.9	2.6	4.1	5.026	3.18	6.51	6.077	11.43
129	Pass	Pass	3.01	Pass	5.24	3.14	5.617	5.68	8.9	2.6	4.1	5.026	3.18	6.51	6.077	11.43
167	2.42	2.365	3.01	2.42	5.24	3.14	5.617	5.68	8.9	2.6	4.1	5.026	3.18	6.51	6.077	11.43
215	2.42	2.365	3.01	2.42	5.24	3.14	5.617	5.68	8.9	2.6	4.1	5.026	3.18	6.51	6.077	11.43
278	2.42	2.365	3.01	2.42	5.24	3.14	5.617	5.68	8.9	2.6	4.1	5.026	3.18	6.51	6.077	11.43
359	2.42	2.365	3.01	2.42	5.24	3.14	5.617	5.68	8.9	2.6	4.1	5.026	3.18	6.51	6.077	11.43
464	2.42	2.365	3.01	2.42	5.24	3.14	5.617	5.68	8.9	2.6	4.1	5.026	3.18	6.51	6.077	11.43
774	2.42	2.365	3.01	2.42	5.24	3.14	5.617	5.68	8.9	2.6	4.1	5.026	3.18	6.51	6.077	11.43

Shaded cells labeled "Pass" indicate that particulate did not exceed critical velocity criterion.

Table 5.3.3. Percentage of Case 1 Representative PSDD Particulate Exceeding 3.07 ft/sec Threshold Design Velocity by Solid-Phase Compound (Oroskar and Turian)

Solid-Phase Compound	Density, g/mL	Representative Case 1 PSDD Volume %	Percent Exceedance
$Al(OH)_3$, Gibbsite	2.42	51.5	1%
$(NaAlSiO_4)_6•(NaNO_3)_{1.6}•2H_2O$	2.365	16.6	1%
AlOOH, Boehmite	3.01	10.6	4%
$NaAlCO_3(OH)_2$	2.42	9.5	1%
Fe_2O_3	5.24	4.1	69%
$Ca_5OH(PO_4)_3$	3.14	2.0	7%
$Na_2U_2O_7$	5.617	1.6	74%
ZrO_2	5.68	1.1	74%
Bi_2O_3	8.9	0.81	100%
SiO_2	2.6	0.69	1%
$Ni(OH)_2$	4.1	0.55	31%
MnO_2	5.026	0.54	64%
CaF_2	3.18	0.23	7%
$LaPO_4•2H_2O$	6.51	0.13	89%
Ag_2CO_3	6.077	0.0094	81%
PuO_2	11.43	0.0013	100%

The "limit" of the particulate that meets the critical velocity criterion of 3.07 ft/sec by solid-phase compound, in terms of particle size and density, is defined for the representative Case 1 PSDD in Table 5.3.2. From Table 5.3.1, 7.6% of the particulate volume for Case 1 exceeds the 3.07 ft/sec criterion. Thus, the "Pass" area of Table 5.3.2 represents 92.4% of the particulate volume. That is, the maximum particle size and density "pairs" that "Pass" for each compound, by the particle size and particle density functional relation in the Oroskar and Turian equation (1980), bound 92.4% of the representative PSDD solid particulate by volume. These solid-phase compound particle size and density limits thus can be used to define quantiles of the particulate volume, similar to the PSD quantiles (Table 5.0.1).

By combining the specific PSDD parameters input to the critical velocity calculations, particle size and density, the Oroskar and Turian equation (1980), Eq. (1.1), can be written as

$$U_c = 1.85 g^{0.545} C_v^{\ 0.1536} \left(1 - C_v\right)^{0.3564} D^{0.468} \left(\frac{\rho_L}{\mu_L}\right)^{0.09} \beta \tag{5.3.1}$$

where

$$\beta = \left[d^{0.167} \left(S - 1\right)^{0.545}\right] \tag{5.3.2}$$

β is computed for the representative Case 1 PSDD (Tables 5.2.3 and 5.2.4) with liquid density of 1.2 g/mL. The cumulative solid volume as a function of β may then be determined (Figure 5.3.6).

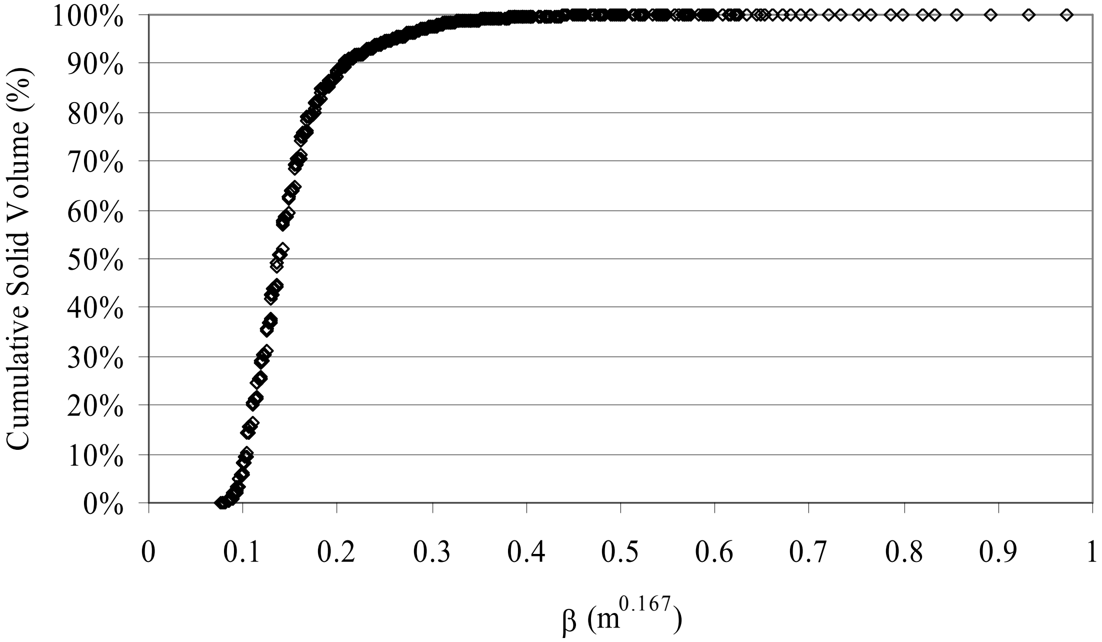

Figure 5.3.6. Case 1 Representative PSDD Cumulative Solid Volume as a Function of Particle Size and Density (Oroskar and Turian Equation)

The β values at each solid volume percentile represent the particle size and density relation, as defined by the Oroskar and Turian equation (1980), that encompasses a volume of solid particulate, independent of an actual critical velocity criterion calculation. For example, from Figure 5.3.6, nominally 20% by volume of the solid particulate of Case 1 has a β value of approximately 0.2.

The volume percent of solid particulate that requires a critical velocity above the threshold design velocities evaluated in Table 5.3.1 are associated with a constant β value. Figure 5.3.7 depicts the solid particle density as a function of particle size for Case 1 determined via Eq. (5.3.2). The constant β or constant solid particulate volume exceeding the velocity criteria represent the density "limits" for a given particle size, and, for 3.07 ft/sec, define the "pass/fail" boundary of Table 5.3.2. Thus, the particulate depicted in Figure 5.3.2 would be above the 3.07 ft/sec, 7.6% line in Figure 5.3.7.

Also included in Figure 5.3.7 are particle size and density relations for threshold design velocities 3.5 and 4.7 ft/sec. Five percent and 1% of the particulate volume exceed these criteria, respectively, and provide the "pass/fail" particle size and density boundaries representing 95% and 99% of the particulate volume for the representative Case 1 PSDD.

The particle size and density "pairs" for the solid-phase compounds that represent 95% and 99% of the solid particulate volume are provided in Tables 5.3.4 through 5.3.7 for each representative PSDD Case (Tables 5.2.3 trough 5.2.10). As discussed, these percentages, although defined by the functionality of the Oroskar and Turian equation (1980), are independent of the critical velocity calculation with regard to the flow parameters of mass fraction of solids, liquid viscosity, and pipe diameter.

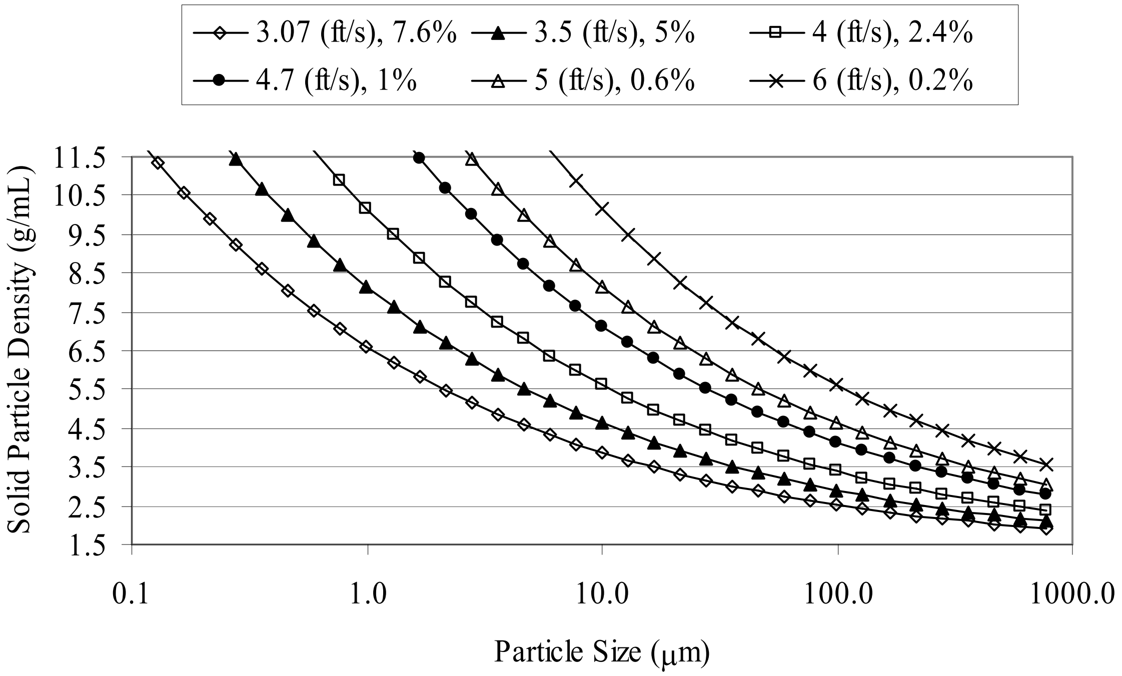

Figure 5.3.7. Case 1 Representative PSDD Particle Size and Density Relations at Specified Threshold Design Velocities. Percentages indicate the volume of particulate exceeding the respective velocity criterion (Oroskar and Turian equation, refer to Table 5.3.1)

Table 5.3.4. Case 1 Representative PSDD Particle Size and Density Limits at 95% and 99% of the Solid Particulate by Volume (Oroskar and Turian equation)

Solid-Phase Compound	**95% of Solid Particulate**		**99% of Solid Particulate**	
	Density, g/mL	**Particle Size (μm)**	**Density, g/mL**	**Particle Size (μm)**
$Al(OH)_3$, Gibbsite	2.42	278	2.42	774
$(NaAlSiO_4)_6 \bullet (NaNO_3)_{1.6} \bullet 2H_2O$	2.365	278	2.365	774
AlOOH, Boehmite	3.01	77.4	3.01	464
$NaAlCO_3(OH)_2$	2.42	278	2.42	774
Fe_2O_3	5.24	4.64	5.24	35.9
$Ca_5OH(PO_4)_3$	3.14	59.9	3.14	359
$Na_2U_2O_7$	5.617	3.59	5.617	21.5
ZrO_2	5.68	3.59	5.68	21.5
Bi_2O_3	8.9	0.60	8.9	3.59
SiO_2	2.6	167	2.6	774
$Ni(OH)_2$	4.1	16.7	4.1	100
MnO_2	5.026	5.99	5.026	35.9
CaF_2	3.18	46.4	3.18	359
$LaPO_4 \bullet 2H_2O$	6.51	2.154	6.51	12.9
Ag_2CO_3	6.077	2.783	6.077	16.7
PuO_2	11.43	0.215	11.43	1.67

Table 5.3.5. Case 2 Representative PSDD Particle Size and Density Limits at 95% and 99% of the Solid Particulate by Volume (Oroskar and Turian Equation)

Solid-Phase Compound	95% of Solid Particulate		99% of Solid Particulate	
	Density, g/mL	**Particle Size (μm)**	**Density, g/mL**	**Particle Size (μm)**
$Al(OH)_3$, Gibbsite	1.39	774	1.39	774
$(NaAlSiO_4)_6{\bullet}(NaNO_3)_{1.6}{\bullet}2H_2O$	1.33	774	1.33	774
AlOOH, Boehmite	1.23	774	1.23	774
$NaAlCO_3(OH)_2$	1.31	774	1.31	774
Fe_2O_3	5.24	0.46	1.45	774
$Ca_5OH(PO_4)_3$	1.25	774	1.25	774
$Na_2U_2O_7$	5.617	0.36	5.617	5.99
ZrO_2	5.68	0.36	5.68	4.64
Bi_2O_3	8.9	0.17	8.9	1.00
SiO_2	2.6	12.9	1.62	774
$Ni(OH)_2$	1.32	774	1.32	774
MnO_2	5.026	0.60	1.66	774
CaF_2	3.18	4.6	1.48	774
$LaPO_4{\bullet}2H_2O$	6.51	0.17	1.61	774
Ag_2CO_3	6.077	0.28	1.62	774
PuO_2	11.43	0.17	11.43	0.36

Table 5.3.6. Case 3 Representative PSDD Particle Size and Density Limits at 95% and 99% of the Solid Particulate by Volume (Oroskar and Turian equation)

Solid-Phase Compound	95% of Solid Particulate		99% of Solid Particulate	
	Density, g/mL	**Particle Size (μm)**	**Density, g/mL**	**Particle Size (μm)**
$Al(OH)_3$, Gibbsite	2.42	359	2.42	1000
$(NaAlSiO_4)_6{\bullet}(NaNO_3)_{1.6}{\bullet}2H_2O$	2.365	464	2.365	1000
AlOOH, Boehmite	3.01	100	3.01	599
$NaAlCO_3(OH)_2$	2.42	359	2.42	1000
Fe_2O_3	5.24	7.74	5.24	46.4
$Ca_5OH(PO_4)_3$	3.14	77	3.14	464
$Na_2U_2O_7$	5.617	5.99	5.617	35.9
ZrO_2	5.68	5.99	5.68	35.9
Bi_2O_3	8.9	1.00	8.9	5.99
SiO_2	2.6	278	2.6	1000
$Ni(OH)_2$	4.1	21.5	4.1	129
MnO_2	5.026	10.0	5.026	59.9
CaF_2	3.18	77.4	3.18	464
$LaPO_4{\bullet}2H_2O$	6.51	3.59	6.51	21.5
Ag_2CO_3	6.077	4.64	6.077	27.8
PuO_2	11.43	0.36	11.43	2.15

Table 5.3.7. Case 4 Representative PSDD Particle Size and Density Limits at 95% and 99% of the Solid Particulate by Volume (Oroskar and Turian equation)

Solid-Phase Compound	95% of Solid Particulate		99% of Solid Particulate	
	Density, g/mL	Particle Size (μm)	Density, g/mL	Particle Size (μm)
$Al(OH)_3$, Gibbsite	1.39	1000	1.39	1000
$(NaAlSiO_4)_6{\bullet}(NaNO_3)_{1.6}{\bullet}2H_2O$	1.33	1000	1.33	1000
AlOOH, Boehmite	1.23	1000	1.23	1000
$NaAlCO_3(OH)_2$	1.31	1000	1.31	1000
Fe_2O_3	5.24	0.46	1.45	1000
$Ca_5OH(PO_4)_3$	1.25	1000	1.25	1000
$Na_2U_2O_7$	5.617	0.36	5.617	5.99
ZrO_2	5.68	0.28	5.68	5.99
Bi_2O_3	8.9	0.17	8.9	1.00
SiO_2	2.6	12.9	1.62	1000
$Ni(OH)_2$	1.32	1000	1.32	1000
MnO_2	5.026	0.46	1.66	1000
CaF_2	3.18	4.64	1.48	1000
$LaPO_4{\bullet}2H_2O$	6.51	0.17	1.61	1000
Ag_2CO_3	6.077	0.22	1.62	1000
PuO_2	11.43	0.17	11.43	0.46

5.3.2 Effect of Flow Parameters on Critical Velocity Criterion Results

The flow parameters, mass fraction of solids, liquid density and viscosity, and pipe diameter, are briefly described to illustrate their impact on the results. Case 1 is again used as the example, and the Oroskar and Turian equation (1980) is considered. The applicability of this model to the current study conditions was not evaluated.

The results presented in Section 5.3.1 used a mass fraction of the solids in the flow as 0.154, approximating the maximum solids loading, 200 g/L, specified in BNI (2006a). The liquid density and viscosity were assigned as 1.2 g/mL and 2 mPa s, respectively, and the pipe diameter was set to 3 inches. These parameters were varied as presented in Table 5.3.8, representing reasonably realistic flow conditions.

The volume fraction of the particulate that exceeds the threshold design velocity criterion of 3.07 ft/sec from Table 5.3.8 is plotted as a function of the mass fraction of solids (Figure 5.3.8), liquid density and viscosity (Figure 5.3.9), and pipe diameter (Figure 5.3.10). As expected (Eq. 1.1), the volume fraction of the particulate that exceeds the threshold design velocity criterion increases with increasing mass fraction of solids in the flow and pipe diameter and decreases with increasing liquid density and viscosity. For the parameter variations considered, the pipe diameter had the most significant impact.

Table 5.3.8. Flow Parameter Variation, Case 1 Representative PSDD 3.07 ft/sec Velocity Criterion Results

Pipe Diameter (in.)	Mass Fraction of Solids	Liquid Density (g/mL)	Liquid Viscosity (mPa s)	Exceedance Volume Fraction
3	0.05	1.2	2	4.4
3	0.1	1.2	2	6.2
3	0.154	1.2	2	7.6
3	0.2	1.2	2	8.3
3	0.154	1	1	14.5
3	0.154	1	2	11.7
3	0.154	1	10	6.6
3	0.154	1.2	1	9.0
3	0.154	1.2	2	7.6
3	0.154	1.2	10	4.5
3	0.154	1.4	1	6.7
3	0.154	1.4	2	5.8
3	0.154	1.4	10	3.1
4	0.154	1.2	2	11.3
6	0.154	1.2	2	24.2
12	0.154	1.2	2	71.4

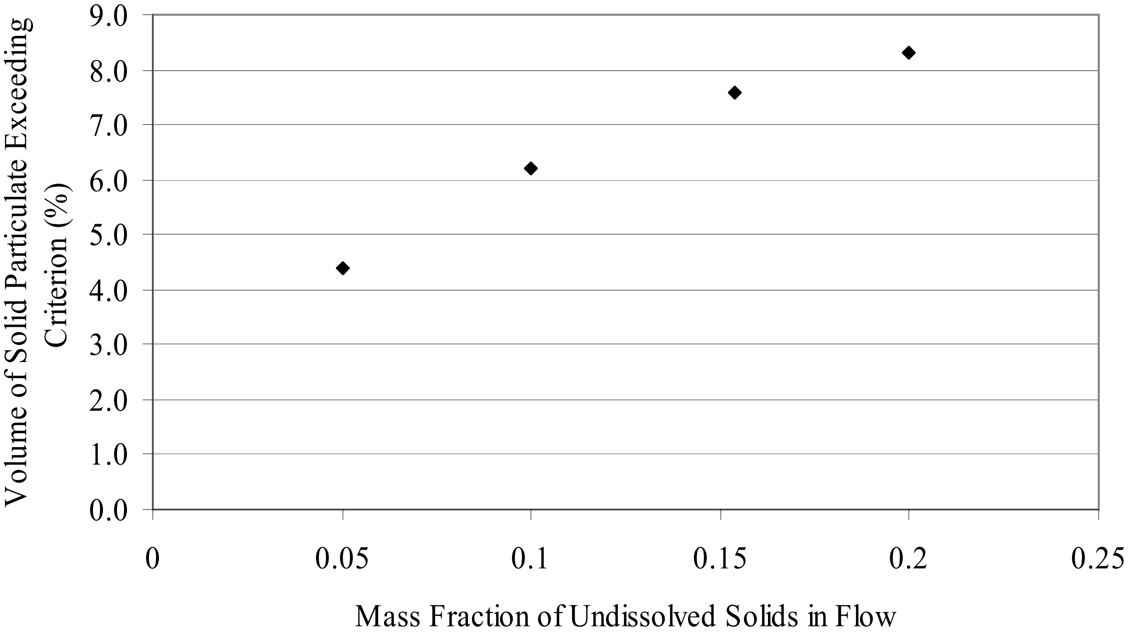

Figure 5.3.8. Volume of Solid Particulate Exceeding Threshold Design Velocity Criterion as a Function of the Mass Fraction of Solids in the Flow. Case 1 Representative PSDD, Oroskar and Turian Equation.

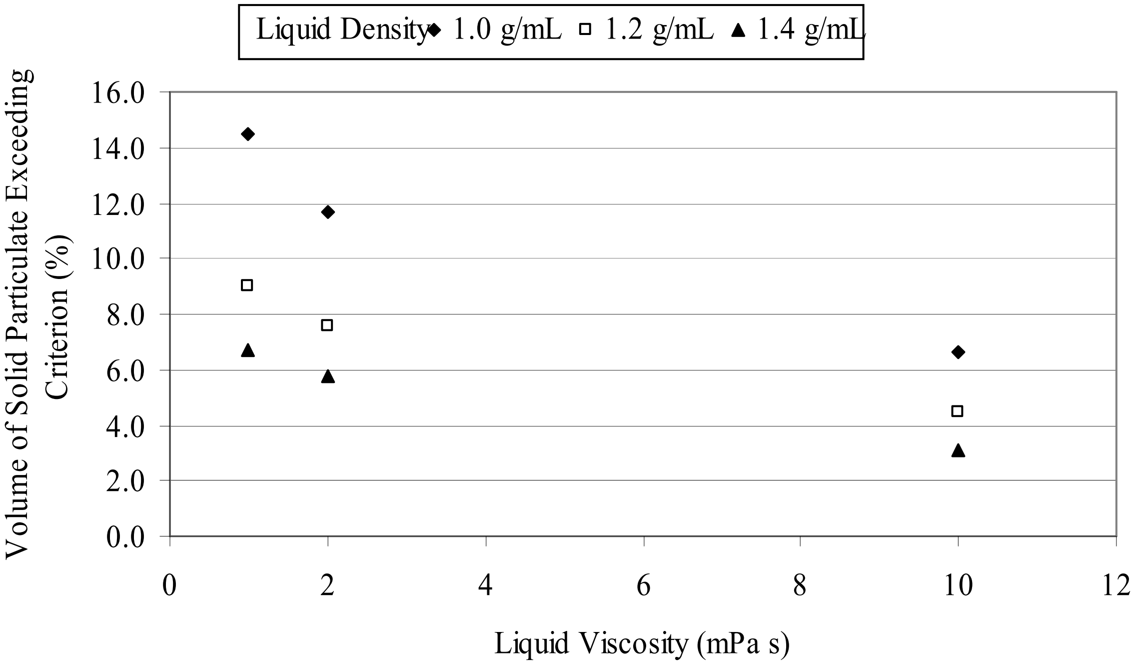

Figure 5.3.9. Volume of Solid Particulate Exceeding Threshold Design Velocity Criterion as a Function of the Liquid Viscosity and Density. Case 1 Representative PSDD, Oroskar and Turian Equation.

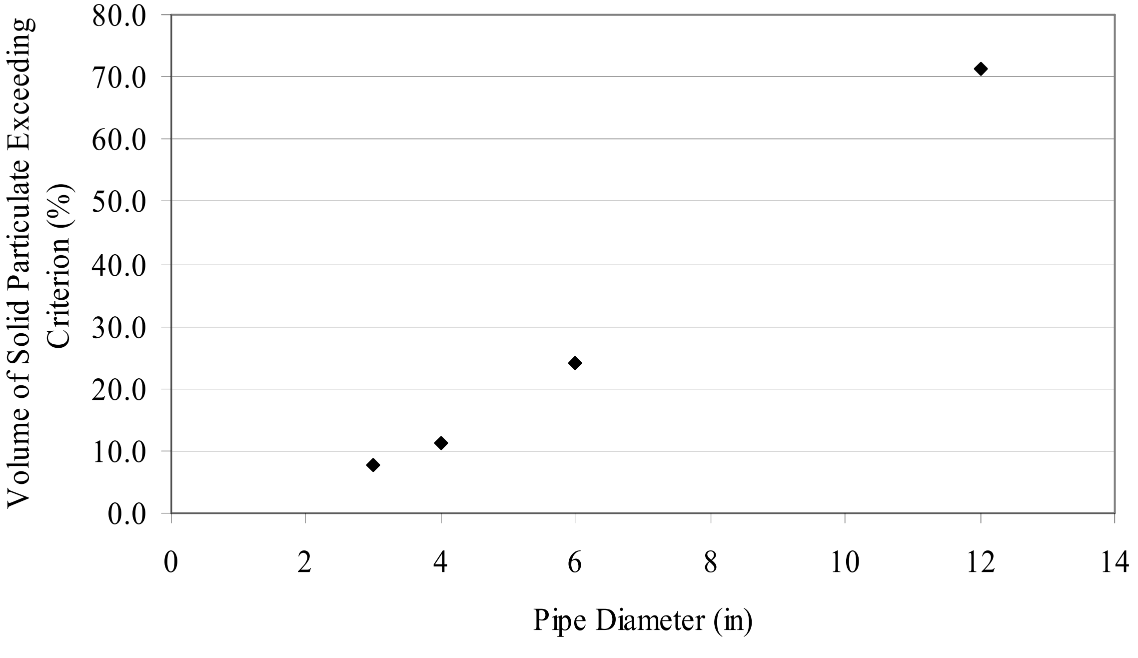

Figure 5.3.10. Volume of Solid Particulate Exceeding Threshold Design Velocity Criterion as a Function of the Pipe Diameter. Case 1 Representative PSDD, Oroskar and Turian Equation.

5.4 Effect of Qualitative Data Uncertainty and Modeling

Variation of the representative PSDDs (Section 5.2) and the critical velocity criterion results (Section 5.3) due to pseudo-waste-type differentiation in PSDs (see Section 3.1), PSD binning, and Monte Carlo simulation count are investigated in terms of the average percent difference of the volume fraction of the solid phase compounds at each particle size bin and median volume fraction of particulate exceeding the critical velocity criterion. The Oroskar and Turian equation (1980) results for Case 1 at a threshold design velocity of 3.07 ft/sec are considered as examples. The applicability of this model to the current study conditions was not evaluated. The Case 1 results are compared as follows:

- PSD differentiation. One PSD realization per pseudo-waste type is binned as for Case 1. The results are evaluated with all other variable parameters set to the centroid of the Case 1 inputs.
- PSD binning. The sonicated PSD was sampled once and binned 100 different ways. Bins were created by a uniform selection of the upper bin particle size limit between 1,000 and 10,000 μm. Between this randomly selected upper limit and a lower bin limit of 0.01 μm, a geometric progression was used to create 55 individual bins. A Monte Carlo simulation of this single PSD binned 100 different ways was then conducted with all other parameters set to the centroid of the Case 1 inputs.
- Simulation count. Case 1 results for 100 and 500 simulations are compared.

5.4.1 PSD Differentiation

The effect on the fraction of particulate that exceeds a threshold design velocity of 3.07 ft/sec of varying the input PSD for Case 1 has been evaluated by considering the pseudo-waste-type PSDs provided in Section 3.1. The volume of the solid particulate exceeding the threshold design velocity criteria varies from 5.9 to 17.5% (150%, relative difference), Table 5.4.1. The median value is 7.8% compared to 7.6% for the representative Case 1 PSDD (Table 5.3.1). This evaluation illustrates the sensitivity of the criterion results to the input PSD, and underscores the necessity of acknowledging that the composite PSD is from a limited data set. Results should be expected to vary as the data set is expanded or specific waste streams are studied. Similar comparison with regards to specific tanks can be made by considering the pseudo waste-type PSD quantiles in Table 3.1.9, the associated results, Table 5.4.1, and the tank by tank PSD quantiles provided in Appendix A. The PSDDs provided herein are neither bounding nor conservative given the variability of the PSDs.

A PSD based on the minimal disturbance data reported in Jewett et al. (2002) was analyzed similarly though the particle size data were affected by instrumentation operation (see Section 3.1). The volume of solids exceeding the velocity criterion was 19.4% was achieved, compared to 10.7% for Case 3 from Table 5.3.1.

Table 5.4.1. Critical Velocity Criterion Results for Varied PSDs

Pseudo-Waste-Type PSD	Volume of Solid Particulate Exceeding Criteria (%)
CWZr	8.4
Unclassified	7.6
BL	6.0
P3	12.2
PL2	17.5
SRR	9.8
PFeCN	5.9
CWP	6.7
OWW3	6.9
TH	6.9
1C	6.5
CWR	8.2
RBoiling	8.0
Z	6.3
224	15.4
2C	14.4

5.4.2 PSD Binning

The effect of PSD binning on the critical velocity criterion results for Case 1 was evaluated. Direct comparison of the representative PSDD resulting from the 100-iteration Monte Carlo simulation to the representative Case 1 PSDD of Section 5.2.1 via Eq. 5.2.1 is precluded by the dissimilar bin limits and bin count. The median volume of particulate that exceeds a threshold design velocity of 3.07 ft/sec is 7.6% (7.3 to 7.8%). These results show five times less relative difference; 6% versus 30% for Case 1 in Table 5.3.1. The indication is that the PSD binning has less impact on the modeling results than the variability of the data itself.

5.4.3 Simulation Count

PSDD and critical velocity criterion result impact of the Monte Carlo simulation count was considered. Comparison results for the representative PSDD Case 1 with 500 simulations (Tables 5.2.3 and 5.2.4) and representative PSDD Case 1 with 100 simulations are provided in Table 5.4.2. The comparison was made as described in Section 5.2 and indicates minimal difference (<4%) with the maximum difference, as would be expected, at the low-probability tails of the PSD.

The volume of the solid particulate exceeding a threshold design velocity criteria of 3.07 ft/sec varies from 6.7 to 8.5% for Case 1 with 100 simulations. The average value is 7.6%, which compares exactly with the 500 simulation Case 1 result of 7.6% in Table 5.3.1. The relative difference of the Case 1 500-simulation result, 32%, is thus much larger than the difference of the average results. Therefore, the effect of simulation count on the critical velocity criterion, dictated by the PSDD, is less than the uncertainty of the input data accounted for in the Monte Carlo simulations themselves.

Table 5.4.2. Comparison of Representative PSDDs, Case 1, 500 to 100 Simulation Iterations

Particle Size	Percent Difference (refer to Table 5.2.2 for compound identification)																
(µm)	1	2	3	4	5	6	7	8	9	10	11	12	13	14	15	16	Bulk Density
0.22	2	3	2	3	3	2	1	2	3	3	3	3	3	1	2	3	0
0.28	0	0	0	1	1	0	-1	-1	1	1	0	1	0	-1	0	1	0
0.36	-3	-2	-3	-2	-2	-3	-4	-3	-2	-2	-2	-2	-2	-4	-3	-2	0
0.46	0	1	0	1	1	0	-1	0	1	1	0	1	0	-1	0	1	0
0.60	1	1	1	1	2	1	0	0	1	2	1	2	1	0	1	2	0
0.77	0	0	0	0	1	0	-1	-1	0	1	0	1	0	-2	0	1	0
1.0	-1	0	-1	0	0	-1	-2	-1	0	0	0	0	0	-2	-1	0	0
1.3	0	1	0	1	1	0	-1	-1	1	1	0	1	0	-1	0	1	0
1.7	0	0	0	1	1	0	-1	-1	1	1	0	1	0	-1	0	1	0
2.2	1	1	1	1	2	1	0	0	1	2	1	2	1	0	1	2	0
2.8	0	0	0	0	1	0	-1	-1	0	1	0	1	0	-1	0	1	0
3.6	0	0	0	1	1	0	-1	-1	1	1	0	1	0	-1	0	1	0
4.6	0	0	0	1	1	0	-1	-1	1	1	0	1	0	-1	0	1	0
6.0	0	0	0	0	1	0	-1	-1	0	1	0	1	0	-1	0	1	0
7.7	0	0	0	1	1	0	-1	-1	1	1	0	1	0	-1	0	1	0
10	0	0	0	1	1	0	-1	-1	1	1	0	1	0	-1	0	1	0
13	0	0	-1	0	1	-1	-1	-1	0	1	0	0	0	-2	0	1	0
17	0	1	0	1	1	0	-1	0	1	1	0	1	1	-1	0	1	0
22	-2	-1	-2	-1	-1	-2	-3	-2	-1	0	-1	-1	-1	-3	-2	0	0
28	1	2	1	2	2	1	0	1	2	2	2	2	2	0	1	3	0
36	-1	0	-1	0	0	-1	-2	-1	0	1	0	0	0	-2	-1	1	0
46	-1	-1	-2	-1	-1	-2	-2	-2	-1	0	-1	-1	-1	-3	-2	0	0
60	-1	-1	-1	-1	0	-1	-2	-2	-1	0	-1	0	-1	-2	-1	0	0
77	1	1	0	1	2	0	0	0	1	2	1	1	1	-1	0	2	0
100	-1	-1	-2	-1	0	-2	-2	-2	-1	0	-1	-1	-1	-3	-2	0	0
129	6	6	6	7	7	6	5	5	7	7	6	7	6	5	6	7	0
167	-4	-4	-4	-3	-3	-4	-5	-5	-3	-3	-4	-3	-4	-5	-4	-3	0
215	1	1	1	1	2	1	0	0	1	2	1	2	1	0	1	2	0
278	0	0	0	1	1	0	-1	-1	1	1	0	1	0	-1	0	1	0
359	-3	-3	-3	-2	-2	-3	-4	-4	-2	-2	-3	-2	-3	-4	-3	-2	0
464	0	1	0	1	1	0	-1	0	1	1	1	1	1	-1	0	1	0
599	3	3	3	4	4	3	2	2	4	4	3	4	3	2	3	4	0
774	1	1	1	1	2	1	0	0	1	2	1	2	1	0	1	2	0

6.0 Conclusions and Recommendations

Representative PSDDs of Hanford waste insoluble solids were developed based on a new approach for relating measured PSDs to solid-phase compounds. This work was achieved through extensive review of available Hanford waste PSDs and solid-phase compound data. Composite PSDs representing the waste in up to 19 Hanford waste tanks were developed, and the insoluble solid-phase compounds for the 177 Hanford waste tanks, their relative fractions, crystal densities, and particle size and shape were developed. The agglomeration of these compounds has been modeled with a fractal dimension analysis. A Monte Carlo simulation approach was used to model the PSDDs.

Limitations of the analysis are summarized in Section 6.1. Particle size and density distribution results are summarized in Section 6.2, and critical velocity criterion results are presented in Section 6.3. Recommendations are provided in Section 6.4.

6.1 Limitations of Analysis

The following list of limitations of this analysis must be acknowledged with any application of the presented results:

- PSDs
    - Waste samples may not accurately represent process streams.
    - Waste samples represent only the sampled region of the waste.
    - Sample handling prior to analysis may affect results.
    - Conditions at which sample is analyzed may not represent in situ conditions.
    - Instrumentation used to measure the PSDs and the operation thereof may affect results.
    - All waste types do not have data.
    - Analyzed samples may not contain all constituents accounted for.
    - Analyzed samples may contain constituents in addition to those accounted for.
    - It is assumed that the sonicated data represents individual particles and hard agglomerates.
    - It is assumed that the minimal disturbance data represent individual particles and both soft and hard agglomerates.
- Solid-phase compounds; identity, fraction of waste
    - All known compounds are not explicitly accounted for.
    - Multi-component agglomerates are not explicitly accounted for.
    - Waste samples for chemical analysis and observation may not accurately represent process streams.
    - Waste samples represent only the sampled region of the waste.
    - Sample handling prior to analysis may affect results.
    - Conditions at which sample is analyzed may not represent in situ conditions.
    - Instrumentation used to analyze the samples and the operation thereof may affect results.
    - All waste types do not have data.

- Particle size and density distribution modeling
  - Data generated from different waste samples were combined.
  - Assigning crystal density to the entire spectrum of particle sizes is not supported by any Hanford waste knowledge.
  - The fractal relation for agglomeration for Hanford waste was not specifically determined.
  - Each primary particle forms its own agglomerates.
  - Waste as a "whole" (within the data limitations) is considered; specific tanks or waste streams may have unique characteristics.
- Critical velocity criterion
  - Models not validated for Hanford waste.

The effect of these limitations on the presented results is not quantified.

6.2 Particle Size and Density Distributions

Solid-phase compounds that are considered the most probable constituents of insoluble Hanford waste, their relative volume fractions, crystal density, maximum primary particle size, and agglomeration characteristics were identified. These compounds were then modeled with the best-estimate PSDs via Monte Carlo simulations into PSDDs such that:

- The composite PSDs were reproduced.
- The solid-phase compound mass fractions were reproduced.
- The expected in situ bulk-solids density was qualitatively reproduced.
- A representative fraction of the waste volume comprising agglomerates was qualitatively reproduced.

Four particle size and density distributions were developed and evaluated. The cases considered were:

- Case 1. Sonicated PSD
  - Primary particles and hard agglomerates were assigned crystal density
- Case 2. Sonicated PSD
  - Primary particles were assigned crystal density
  - Density of hard agglomerates assigned via fractal relation
- Case 3. Minimal Disturbance PSD
  - Primary particles, soft and hard agglomerates were assigned crystal density
- Case 4. Minimal Disturbance PSD
  - Primary particles were assigned crystal density
  - Densities of soft and hard agglomerates were assigned via fractal relation.

For each case, a representative PSDD based on a deterministic calculation on the centroid input data (i.e., solid-phase compound volume fraction, primary particle size, and PSD) values of the Monte Carlo simulation is provided in Section 5.2 as a matrix of volume-based probability (i.e., the compound volume fraction) of each solid-phase compound in a PSD bin and its associated density in that bin. The bins represent the upper and lower size limit of the particles associated with a given bin. Thus, the volume fraction of particulate at a given size and density was specified over the entire waste volume.

The largest volume fraction of large-dense particulate was achieved for Case 3 and the minimum amount for Case 2. The specific largest volume fractions in the PSDDs, that is, the most likely particulate on a volume basis, 0.05 for Cases 1 and 3 and 0.03 for Cases 2 and 4, occurs at 7.7 μm for each case. The corresponding densities are 2.42 g/mL for Cases 1 and 3 and 1.44 g/mL for Cases 2 and 4.

The PSDDs resulting from this approach provide a best representation of a volume-based probability for the Hanford waste insoluble solid particles in terms of particle size and density. Any application of the provided PSDDs must acknowledge the limitations of the available data, as summarized in Section 6.1. Additionally, given the composite nature of the approach, the PSDDs can be expected to vary with specific waste streams. The PSDDs provided herein are neither bounding nor conservative.

6.3 Critical Velocity Criterion

Critical velocity calculations have been conducted for each PSDD. The Oroskar and Turian and Thomas equations specified in BNI (2006a) were employed. The applicability of these models to the current study conditions was not evaluated.

Application of the critical velocity calculations to a PSDD was accomplished by:

- Computing a critical velocity for each particle size and density "pair" with all other calculation parameters held constant.
- Comparing the calculated critical velocity for each particle size and density "pair" to the threshold design velocity and assigning each result for a respective volume fraction to a "pass" or "fail" vector.
- Summing the "pass" and "fail" vectors of volume fraction to indicate the volume fraction of solid particulate that will pass or fail the threshold design velocity.

The mass fraction of the solids in the flow for each size and density "pair" in the PSDD matrixes was set to 0.154. The liquid density and viscosity were assigned as 1.2 g/mL and 2 mPa s, respectively. The pipe diameter was set to 3 inches.

With no design margin on the Oroskar and Turian equation (1980), a threshold design velocity of 5 ft/sec is required to calculate less than 1% of the solid particulate by volume to exceed the critical velocity criterion with no agglomeration accounted for. When agglomeration is accounted for, less than 1% of the solid particulate by volume is calculated to exceed the critical velocity criterion when the threshold design velocity is set to 4 ft/sec. For the combined Oroskar and Turian and Thomas equations with no design margin, the no-agglomeration and agglomeration PSDDs are calculated to require approximately 4 and 3.07 ft/sec, respectively, for less than 1% exceedance. These results should not be used for design calculations until the additional analyses described below are accomplished.

6.4 Recommendations

As will be addressed below, there are four general recommendations:

1. Address limitations of the input data (i.e. PSDs, solid-phase compound parameters).
2. Validate the PSDD modeling methodology.
3. Address homogeneous and heterogeneous suspension of the slurry.
4. Conduct experimental testing to select the appropriate critical velocity correlations.

Defining an acceptable threshold design velocity for pipeline transfer of Hanford waste will require a combined applicable critical velocity equation and accurate characterization of the Hanford solid particulate and rheology. Many slurry transfer models, including the Oroskar and Turian model, have been developed and applied to pipeline transfer of particulates that tend to have larger particles than most Hanford waste. Therefore, additional experimental testing is recommended to evaluate the Oroskar and Turian model and others, and to select appropriate approaches and associated models for the critical velocity correlations used for the WTP design.

One of the ways to determine the amount of solids that will not be carried through a pipeline at a specific velocity is to use the particle size and density distributions obtained in this study. It is recommended that slurry transport satisfy the following two requirements:

1. The slurry pipe flow is turbulent.
2. All solids are suspended during the transport.

The transported solids are in either homogeneous or heterogeneous suspension. By using the Wasp slurry pipeline pressure drop model (Wasp et al. 1963), Onishi et al. (2002) predicted that solids are in 99.7% homogeneity at 2.5 ft/sec in a 3-inch diameter pipeline when the particle sizes vary from 0.7 to 33.5 μm with 50th, 75th, and 95th quantiles of approximately of 3.5 μm, 7.5 μm, and 31 μm respectively. The solid size distribution of the minimal disturbance has 95 vol% of the solids as finer than 58.6 μm (see Table 5.0.1, minimal disturbance PSD). The fine particles shown in Table 5.0.1 may thus be expected to be mostly in homogeneous suspension. The homogeneous part of the slurry would carry the large particles in heterogeneous suspension. Thus, the solids would be in "hetero-homogeneous" suspension with most solids in homogeneous suspension.

For this type of slurry, there are two critical velocities, one for homogeneous suspension to satisfy the turbulence flow requirement (Requirement 1), and the other for heterogeneous suspension to satisfy the no-solid-deposition (Requirement 2). The larger of these two velocities should be selected as the overall critical velocity. The current study addresses the second requirement with the use of the Oroskar and Turian and Thomas models.

The critical velocity for a homogeneous suspension is the transition velocity, below which a laminar flow exists. Suspended solids are known to suppress turbulence. Thus, the slurry flow transition from a laminar to a turbulent flow is different from that of a liquid flow and varies with the slurry properties and pipeline operational conditions. Under a laminar flow condition, the slurry pipeline transport operation may have a pipeline plugging problem and would be unstable over time because particles tend to deposit, albeit slowly, resulting in the increased pressure over time (Wasp et al. 1977). Additionally, solids moving on the pipe bottom would erode the lower portion of the pipe. Thus, industry does not usually operate slurry transport under a laminar condition (Wasp et al. 1977).

To obtain the transition and deposition velocities, and thus the transferable solid amount, the transition velocity must first be determined, and then the deposition velocity. To determine the transition velocity, the carrier fluid, consisting of the liquid and homogeneously suspended solid particulate, must be identified. With this approach, the amount of solids which would not be transported as suspended solids for a given slurry velocity may be estimated. If one needs to determine the critical velocity for a given slurry, the required critical velocity is the greater of the transition and deposition velocities.

As indicated, there are several possible approaches and models to determine the deposition velocity. Therefore, experimental testing is recommended to evaluate the appropriate approaches and associated models for critical velocity correlations. The recommended experimental testing should employ pipe runs representative of typical layouts to exist in the WTP including critical components such as short elbows, miter bends, and vertical risers. Testing should also subject the pipe flow to the same inlet (feed) conditions that will exist during plant operations. Testing should be conducted to evaluate:

- Whether the design velocities predicted by correlations for the range of anticipated PSDs are sufficient to maintain fully suspended slurry flow.
- What the critical velocity is for initiation of solid settling.
- If the specified flush flow rate and volume are sufficient to re-suspend and clear settled solids from the pipe runs.

Simulants for this testing initially should be designed based on the current state of knowledge from the PSDDs contained in this report. As described however, the data used to develop these PSDDs have limitations. Further, the PSDD modeling methodology itself should be validated.

Validation of the PSDD modeling methodology is recommended and could be accomplished by using simulants with known PSDDs, analyzing samples of the simulant for PSDs, observed size ranges, etc., and comparing the known PSDD to a PSDD modeled from the sample analysis.

Specific data limitations include: entire waste types are not characterized for PSDs, SEM images used to define the solid-phase compound sizes do not represent all of the Hanford waste types, and lack of correlation between the PSDs and SEM images. Considering a wider range of Hanford wastes with correlated analyses would increase confidence in the generated PSDDs. It is recommended therefore that characterization testing be performed on composite samples representing different major Hanford waste types.

Samples should be analyzed to determine the size and density of the solid particles, and rheology characteristics. Seven composite samples prepared by the external flowsheet review team (EFRT) M12 task (BNI 2006b) include the following waste types: 1C, 2C, CWP, CWR, R (boiling), TBP, and PFeCN. Additional archived samples, outside the scope of the M12 testing, may be available and consist of the following waste types: R (non-boiling), 224, and CWZr. Analysis of the listed samples would result in a waste type profile that covers the major volume of Hanford sludge. Deliverables of the sample characterization should include the following:

- Sonicated and minimal disturbance PSDs
- Solid-phase compound identification and sample fraction
- Size range observed for particles of a specific compound
- Whether the particles are crystalline or agglomerates
- Shape of the particles from a certain compound
- Slurry rheology.

7.0 References

Arey BW, HT Schaef, KM Krupka, and WJ Deutsch. 2005. "Application of Scanning Electron Microscopy to Characterization of Radioactive Solid Waste from Underground Storage Tanks." *Micros. Microanal*, 11(2005):1768-1769.

Barker SA. 2006. *Methodology and Calculations for the Assignment of Waste Groups for the Large Underground Waste Storage Tanks at the Hanford Site*. RPP-10006 Rev. 5. CH2M HILL, Richland, Washington.

Bechtel National Inc. (BNI). 2006a. *Minimum Flow Velocity for Slurry Lines*. 24590-WTP-GPG-M-0058 Rev. 0, BNI, Richland, Washington.

Bechtel National Inc. (BNI). 2006b. *Issue Response Plan for Implementation of External Flowsheet Review Team (EFRT) Recommendations - M12, Undemonstrated Leaching Processes*. 24590-WTP-PL-ENG-06-0024, Rev. 0, BNI, Richland, Washington.

Bechtold, DB, Callaway WS, Cooke GA, Duncan JB, Herting DL, Jewett JR, Person JC, and JM Tingey. 2002. *Particle Property Analyses of High-Level Waste Tank Sludges*. HNF-8862 Rev. 0, Fluor Hanford, Inc., Richland, Washington.

Bechtold DB, GA Cooke, DL Herting, JC Person, RS Viswanath, and RW Warrant. 2003. *Laboratory Testing of Oxalic Acid Dissolution of Tank 241-C-106 Sludge*. RPP-17158 Rev. 0, Fluor Hanford, Inc., Richland, Washington.

Bredt PR, BW Arey, EC Buck, ED Jenson, BK McNamara, AP Poloski, and RG Swoboda. 2003. *Rheological and Physical Properties of AP-101 LAW Pretreated Waste and Melter Feed*. PNWD-3279, Battelle – Pacific Northwest Division, Richland, Washington.

Brooks KP, JR Bontha, GR Golcar, RL Myers, KG Rappe, and DR Rector. 1998. *Bench-Scale Enhanced Sludge Washing and Gravity Settling of Hanford Tank S-107 Sludge*. PNNL-12010, Pacific Northwest National Laboratory, Richland, Washington.

Brooks KP, PR Bredt, GR Golcar, SA Hartley, LK Jagoda, KG Rappe, and MW Urie. 2000a. *Characterization, Washing, Leaching, and Filtration of C-104 Sludge.* BNFL-RPT-030, Battelle – Pacific Northwest Division, Richland, Washington.

Brooks KP, PR Bredt, SK Cooley, GR Golcar, LK Jagoda, KG Rappe, and MW Urie. 2000b. *Characterization, Washing, Leaching, and Filtration of AZ-102.* BNFL-RPT-038, Battelle – Pacific Northwest Division, Richland, Washington

Buck EC and BK McNamara. 2004. "Precipitation of Nitrate-Cancrinite in Hanford Tank Sludge," *Environ. Sci. Technol*. 38, pp. 4432-4438.

Buck EC, BW Arey, SK Fiskum, JGH Geeting, ED Jensen, BK McNamara, and AP Poloski. 2003. *Identification of Washed Solids from Hanford Tanks 241-AN-102 and 241-AZ-101 with X-ray Diffraction, Scanning Electron Microscopy, and Light-Scattering Particle Analysis*. PNWD-3300 (WTP-RPT-076 Rev. 0), Battelle – Pacific Northwest Division, Richland, Washington.

Bunker BC, J Liu, DR Rector, GL Graff, PA Smith, PJ Bruinsma, L Song, XS Li, JD Virden, NG Colton, JR Phillips, KD Keefer, and JM Tingey. 2000. "Fractal Colloidal Agglomerates in Nuclear Tank Wastes: Impact on Waste Properties and Processing", *Radioactive Waste Management and Env. Res.* 38, pp. 97-133.

Callaway WS. 2000. *Results of Retrieval Testing of Sludge form Tank 241-AZ-101*. HNF-7078 Rev. 0, Fluor Hanford, Inc., Richland, Washington.

CH2M HILL Hanford Group, Inc. 2003. *Aluminum Wash and Leach Factors*. RPP-11079 Rev. 0, CH2M HILL, Richland, Washington.

Cowley WL, JL Huckaby, LA Mahoney, GR Golcar, KM Krupka, DS Sklarew, and DJ Geniesse. 2003. *Chemical Source Terms for Tank Farms Safety Analyses*. RPP-8369 Rev. 2, CH2M HILL Hanford Group, Inc., Richland, Washington.

Crawford CL and CD Barnes. 2003. *Evaporation of Hanford Tank Sample AN-107 Mixed with Recycles (U)*. WSRC-TR-2003-00262 Rev. 0, Westinghouse Savannah River Co., Aiken, South Carolina.

CRC. 1975. *CRC Handbook of Chemistry and Physics, 56th Ed.,* RC Weast (Ed). CRC Press, Cleveland, Ohio.

Douglas JG. 1998. *Tank Characterization Report for Double-Shell Tank 241-SY-102*. HNF-SD-WM-ER-366, Rev. 1. Lockheed Martin Hanford Corp., Richland, WA.

Geeting JGH, RT Hallen, LK Jagoda, AP Poloski, and RD Scheele. 2002. *Filtration, Washing, and Caustic Leaching of Hanford Tank AZ-101 Sludge.* WTP-RPP-043, Battelle – Pacific Northwest Division, Richland, Washington.

Herting DL, GA Cooke, and RW Warrant. 2002. *Identification of Solid Phases in Saltcake from Hanford Site Waste Tanks*. HNF-11585 Rev. 0, Fluor Hanford, Inc., Richland, Washington.

Herting DL, GA Cooke, and RW Warrant. 2004. *Hanford Tank 241-AN-107 Solid Phase Characterization*, RPP-20018, CH2M HILL Hanford Group, Inc., Richland, Washington.

Herting DL. 1997. *Results of Dilution Studies with Waste from Tank 241-AN-105*. HNF-SD-WM-DTR-46 Rev. 0, Numatec Hanford Corporation, Richland, Washington.

Higley BA and DE Place. February 2004. *Hanford Defined Waste Model—Revision 5.0*. RPP-19822. CH2M Hill Hanford Group, Richland, Washington.

Ilievski D, P Austin, and B Whittington. 2003. "Studies into the Internal Structure of Gibbsite Agglomerates." *Chemical Engineering Technology,* 26(3):363–368.

Ilievski D and ET White. 1994. "Agglomeration During Precipitation: Agglomeration Mechanism Identification for $Al(OH)_3$ Crystals in Stirred Caustic Aluminate Solutions." *Chemical Engineering Science,* 49(19):3227–3239.

Jewett JR, SD Estey, L Jensen, NW Kirch, DA Reynolds, and Y Onishi. 2002. *Values of Particle Size, Particle Density, and Slurry Viscosity to Use in Waste Feed Delivery Transfer System Analysis*. RPP-9805. Numatec Hanford Corporation, Richland, Washington.

Jillavenkatesa A, SJ Dapkunas, and LH Lum. 2001. *Particle Size Characterization*. NIST Recommended Practice Guide. Special Publication 960-1, National Institute of Standards and Technology, Washington, D.C.

Khelifa A and PS Hill. 2006. "Models for Effective Density and Settling Velocity of Flocs." *Journal of Hydraulic Research*, 44(3):390-401.

Kim J-W and TA Kramer. 2005. "Improved Models for Fractal Colloidal Agglomeration: Computationally Efficient Algorithms." *Colloids and Surfaces A: Physicochem Engineering Aspects*, 253:33–49.

Kramer TA and MM Clark. 1999. "Incorporation of Agglomerate Breakup in the Simulation of Orthokinetic Coagulation." *Journal of Colloid and Interface Science*, 216:116–126.

Krupka KM, NJ Hess, WJ Deutsch, HT Schaef, MJ Lindberg, BW Arey, and KJ Cantrell. 2004. *Hanford Tanks 241-AY-102 and 241-BX-101: Sludge Composition and Contaminant Release Data*. PNNL-14614, Pacific Northwest National Laboratory, Richland, Washington.

Krupka KM, HT Schaef, BW Arey, SM Heald, WJ Deutsch, and KJ Lindberg. 2006. "Cantrell, Residual Waste from Hanford Tanks 241-C-203 and 241-C-204. 1. Solids Characterization." *Environ. Sci. Technol.*, 40:3749–3754.

LaFemina JP. 1995. *Tank Waste Treatment Science Task Quarterly Report for April-June 1995*. PNL-10764, Pacific Northwest Laboratory, Richland, Washington.

Lansen PP, L van Bendegom, J van den Berg, M Vries, and A Zanen. 1979. *Principles of River Engineering, The Non-Tidal Alluvial River.* Pitman Publishing, Ltd, London, United Kingdom.

Liu J, LR Pederson, and LQ Wang. 1995. *Solid-Phase Characterization in Flammable-Gas-Tank Sludges by Electron Microscopy*. PNL-10723, Pacific Northwest National Laboratory, Richland, Washington.

Lumetta GJ, BM Rapko, MJ Wagner, J Liu, and YL Chen. 1996a. *Washing and Caustic Leaching of Hanford Tank Sludges: Results of FY 1996 Studies*. PNNL-11278 Rev. 1, Pacific Northwest National Laboratory, Richland, Washington.

Lumetta GJ, MJ Wagner, FV Hoopes, and RT Steele. 1996b. *Washing and Caustic Leaching of Hanford Tank C-106 Sludge*. PNNL-11381, Pacific Northwest National Laboratory, Richland, Washington.

Lumetta GJ, IE Burgeson, MJ Wagner, J Liu, and YL Chen. 1997. *Washing and Caustic Leaching of Hanford Tank Sludge: Results of FY1997 Studies*. PNNL-11636, Pacific Northwest National Laboratory, Richland, Washington.

Lumetta GJ, BM Rapko, J Liu, DJ Temer, and RD Hunt. 1998. *Washing and Caustic Leaching of Hanford Tank Sludges: Results of FY 1998 Studies*. PNNL-12026, Pacific Northwest National Laboratory, Richland, WA.

McNown JS, J Malaika, and HR Praminak. January 1951. *Particle Shape and Settling Velocity*. Fourth Meeting of the International Association for Hydraulic Research, Bombay, India.

Meacham JE. July 2003. *Aluminum Wash and Leach Factors*. RPP-11079, CH2M Hill Hanford Group, Richland, Washington.

Onishi Y, et al. 1996. *Tank SY-102 Waste Retrieval Assessment: Rheological Measurements and Pump Jet Mixing Simulations*. PNNL-11352, Pacific Northwest National Laboratory, Richland, Washington.

Onishi Y, BE Wells, SA Hartley, and SK Cooley. 2002. *Pipeline Cross-Site Transfer Assessment for Tank 241-SY-101*. PNNL-13650, Pacific Northwest National Laboratory, Richland, Washington.

Oroskar AR and RM Turian. 1980. “The Critical Velocity in Pipeline Flow of Slurries.” *AIChE J.*, 26:550–580.

O’Rourke JF. 2000. *Results of Retrieval Studies with Waste from Tank 241-C-104*. RPP-5798 Rev. 0A, Fluor Hanford Inc., Richland, Washington.

Pacific Northwest National Laboratory (PNNL). 2006. Tank Waste Information Network (TWINS). http://twins.pnl.gov.

Poloski AP, Rapko BM and GJ Lumetta. 2000. *Status Report on Phase Identification in Hanford Tank Sludges*. PNNL-13394, Pacific Northwest National Laboratory, Richland, Washington.

Poloski AP, RC Daniel, DR Rector, PR Bredt, EC Buck, JC Berg, and AE Saez. 2006. *Characterization and Correlation of Particle-Level Interactions to the Macroscopic Rheology of Powders, Granular Slurries, and Colloidal Suspensions*. PNNL-16133, Pacific Northwest National Laboratory, Richland, Washington.

Rapko BM and MJ Wagner. 1997. *Caustic Leaching of Composite AZ-101/AZ-102 Hanford Tank Sludge*. PNNL-11580, Pacific Northwest National Laboratory, Richland, Washington.

Rector DR and BC Bunker. 1995a. *Effects of Colloidal Aggregation on the Sedimentation and Rheological Properties of Tanks Waste*. PNL-10761, Pacific Northwest Laboratory, Richland, Washington.

Rector DR and BC Bunker. 1995b. *Sedimentation Modeling*. PNL-10754, Pacific Northwest Laboratory, Richland, Washington.

Roberts WL, Campbell TJ, Rapp GR, and WE Wilson. 1990. *Encyclopedia of Minerals*, 2nd ed., Van Nostrand Reinhold, 1990.

Russell AS, JD Edwards, and CS Taylor. 1955. "Solubility and Density of Hydrated Aluminas in NaOH Solutions." *Journal of Metals*, 7:1123-1128.

Roberts WL, Campbell TJ, Rapp GR, and WE Wilson. 1990. *Encyclopedia of Minerals*, 2nd ed., Van Nostrand Reinhold, 1990.

Selomnlya C, G Bushell, R Amal, and TD Waste. 2002. "Aggregation Mechanisms of Latex of Different Particle Sizes in a Controlled Shear Environment." *Langmuir*, 18:1974–1984.

Selomnlya C, G Bushell, R Amal, and TD Waste. 2003. "Understanding the Role of Restructuring in Flocculation: The Application of a Population Balance Model." *Chemical Engineering Science*, 58:327-338.

Simons DB and F Senturk. 1977. *Sediment Transport Technology.* Water Resources Publications, Fort Collins, Colorado.

Sonntag RC and WB Russel. 1987. "Structure and breakup of flocs subjected to fluid stresses." *J. Colloid Interface Sci*. 115:378–389.

Temer DJ and R Villarreal. 1995. *Sludge Washing and Alkaline Leaching Tests on Actual Hanford Tank Sludges: A Status Report*. LAUR-95-2070, Los Alamos National Laboratory, Los Alamos, New Mexico.

Temer DJ and R Villarreal. 1996. *Sludge Washing and Alkaline Leaching Tests on Actual Hanford Tank Sludges: FY 1996 Results*. LAUR 96-2839, Los Alamos National Laboratory, Los Alamos, New Mexico.

Temer DJ and R Villarreal. 1997. *Sludge Washing and Alkaline Leaching Tests on Actual Hanford Tank Sludges: FY 1997 Results*. LAUR 97-2889, Los Alamos National Laboratory, Los Alamos, New Mexico.

Thomas AD. 1976. "The Role of Laminar/Turbulent Transition in Determining the Critical Deposit Velocity and the Operating Pressure Gradient for Long Distance Slurry Pipeline." *Proceedings of the Sixth International Conference on the Hydraulic Transport of Solids in Pipes.* Hydrotransport 6, pp 13–26.

Thomas AD. 1979. "Predicting the Deposit Velocity for Horizontal Turbulent Pipe Flow of Slurries." *International Journal of Multiphase Fluid Flow*, 55:113–129.

Vanoni AA (Ed.). 1975. *Sedimentation Engineering.* ASCE Task Committee for Preparation of the Manual on Sedimentation of the Sedimentation Committee of the Hydraulic Division, the American Society of Civil Engineers, New York.

Warrant RW. 2001. *Results of Retrieval Testing of Sludge from Tank 241-AY-102*. RPP-8909, Rev. 0. Fluor Hanford, Richland, Washington.

Warrant RW. 2002. *Results of Retrieval Testing of Sludge from Tank 241-AZ-102*. RPP-9806 Rev. 0, Fluor Hanford Inc., Richland, Washington.

Warrant RW. 2004. *Results of Retrieval Testing of Sludge from Tank 241-C-107*. RPP-18799 Rev. 0, CH2M HILL Hanford Group, Inc., Richland, Washington.

Warrant RW and GA Cooke. 2003. *Characterization of the Solids Waste in the Hanford Waste Tanks using a Combination of XRD, SEM, and PLM, Advances in X-ray Analysis*. International Centre for Diffraction Data, 46:251–256.

Wasp EJ, TJ Regan, J Withers, PAC Cook, and JT Clancey. July 1963. "Cross Country Coal Pipe Line Hydraulics." *Pipe Line News*, pp. 20-28.

Wasp EJ, PE Kenny, and RL Gandhi. 1977. *Solid-Liquid Flow Slurry Pipeline Transportation*. Series on Bulk Materials Handling, Vol. 1 (1975/77), No. 4, Trans Tech Publications, Bay Village, Ohio.

Wefers K and C Misra. 1987. *Oxides and Hydroxides of Aluminum*, Alcoa Technical Paper No. 19 revised, Alcoa Laboratories, Alcoa Center, Pennsylvania.

Wu W and SSY Wang. 2006. "Formulas for Sediment Porosity and Settling Velocity." *Journal of Hydraulic Division*, 132(8):858–862, American Society of Civil Engineers, New York.

Appendix A

List of Compiled Particle Size Data

Appendix A – List of Compiled Particle Size Data

The raw data included in the PSD are presented in this appendix. A detailed list of source references for historical particle size data used in the development of the composite particle size distribution (PSD) (described in Section 3 of the main report), outlining the instrument and test employed in each reference, can be found at the end of this appendix. These references are given more fully in Table 3.1.1 and Section 7.0 of the main body of the report.

Not all minimal disturbance and sonicated particle size data associated with reports PNNL-11278 (Lumetta et al. 1996a), PNNL-11381 (Lumetta et al. 1996b), PNNL-11636 (Lumetta et al. 1997), and PNNL-12010 (Brooks et al. 1998) were included within the reports. Raw PSD data for the sonicated and minimal disturbance data not published were obtained from Dr. Gregg J. Lumetta (PNNL). In addition, sonicated data sets for the tank wastes studied in PNNL-16133 (Poloski et al. 2006) were measured but not included. Raw PSD data for tanks B-203, T-110, T-203, and T-203 were obtained from Dr. Adam P. Poloski (PNNL).

A.1 Minimal Disturbance Data

Minimal disturbance PSDs correspond to the particle-size measurement data taken under flow conditions sufficient to suspend all of the particulate matter while minimizing and shear-induced breakage of flocs/aggregates. The goal was to evaluate the presence of flocs or soft agglomerates in the waste samples while maintaining favorable suspending flows for dense/large particles. These data would be expected to include individual primary particles and both soft and hard agglomerates. Details on the selection of data sets for inclusion in the minimal disturbance PSDs are given in Section 3.1 of the report.

Tables A.1 through A.19 give the individual data sets for all tanks considered under conditions of minimal disturbance. Reports are listed without their revision number. The Microtrac X-100, Horiba LA-910, and Malvern Mastersizer 2000 are simply referred to as the Microtrac, Horiba, and MS 2000, respectively. Of the minimal disturbance data presented below, only S-101 PSD has no corresponding ultrasonic PSD measurements.

Table A.1. AW-103 Compiled Data. All Horiba data were used "as-is" with no further computation. The 99th percentile on all Microtrac data is an interpolated value; other values were taken directly from the Microtrac data report (Bechtold et al. 2002).

Sample Description	Rep. #	PSD Percentiles (micrometers)														
		1	5	10	20	25	30	40	50	60	70	75	80	90	95	99
Sample: S01T001424. Run: AW103734-6/3/0/0. No sonication. Horiba	HNF-8862	0.19	0.34			2.7			5.7			12			55	200
Sample: S01T001425. Run: AW103741-6/3/0/0. No sonication. Horiba	HNF-8862	0.18	0.3			2.6			5.7			11			24	37
Sample: S01T001427. Run: AW103752-6/3/0/0. No sonication. Horiba	HNF-8862	0.2	0.52			3.5			7.2			16			90	220
Sample: S01T001669. Run: AW103947-6/3/0/0. No sonication. Horiba	HNF-8862	1.2	1.8			3.2			4.9			7.5			12	16
Sample: S01T001669-Dup. Run: AW103951-6/3/0/0. No sonication. Horiba	HNF-8862	1.3	1.8			3.2			5			7.4			12	15
Sample: S01T001670-Dup. Run: AW103961-6/3/0/0. No sonication. Horiba	HNF-8862	1.3	1.9			4.1			11			150			340	450
AW-103. WPAA010. 60 mL/s, No sonication. Microtrac	HNF-8862			0.94	1.2		1.4	1.8	2.3	3.1	4.1		5.4	7.5	9.6	17
AW-103 Dup. WPAA037. 60 mL/s, No sonication. Microtrac	HNF-8862			0.99	1.3		1.6	2.1	2.8	3.8	5.3		7.7	13	19	39

Table A.2. AY-101 Compiled Data. All Horiba data were used "as-is" with no further computation. The 99th percentile on all Microtrac data is an interpolated value; other values were taken directly from the Microtrac data report.

Sample Description	Rep. #	PSD Percentiles (micrometers)														
		1	5	10	20	25	30	40	50	60	70	75	80	90	95	99
Sample: S01T001489. Run: AY101830-6/3/0/0. No sonication. Horiba	HNF-8862	0.6	1.1			4.9			8.8			15			230	330
Sample: S01T001492. Run: AY101841-6/3/0/0. No sonication. Horiba	HNF-8862	0.58	1.1			4.5			8			12			20	27
Sample: S01T001490. Run: AY101851-6/3/0/0. No sonication. Horiba	HNF-8862	0.56	1.1			4.6			8.3			13			60	260
Sample: S01T001491. Run: AY101862-6/3/0/0. No sonication. Horiba	HNF-8862	0.67	1.3			5.2			9.2			17			330	450
AY-101. 101AY008. 60 mL/s, No sonication. Microtrac	HNF-8862			0.81	1.4		2.1	3	4.2	5.5	6.5		7.5	8.7	9.7	12
AY-101 Dup. 101AY019. 60 mL/s, No sonication. Microtrac	HNF-8862			0.59	1		1.5	2.9	5.2	6.6	7.8		9.2	11	14	19

Table A.3. AY-102 Compiled Data. All Horiba data were used "as-is" with no further computation.

Sample Description	Rep. #	PSD Percentiles (micrometers)														
		1	5	10	20	25	30	40	50	60	70	75	80	90	95	99
Sample: S01T001654. Run: AY102895-6/3/0/0. No sonication. Horiba	HNF-8862	0.72	0.92			1.6			4.6			18			140	200
Sample: S01T001654-Dup. Run: AY102899-6/3/0/0. No sonication. Horiba	HNF-8862	0.7	0.88			1.4			2.6			5.7			12	17
Sample: S01T001655. Run: AY102903-6/3/0/0. No sonication. Horiba	HNF-8862	0.72	0.91			1.5			3			7.2			16	22
Sample: S01T001655-Dup. Run: AY102907-6/3/0/0. No sonication. Horiba	HNF-8862	0.7	0.88			1.3			2.2			3.8			6.8	9.2

Table A.4. AZ-101 Compiled Data. Percentiles estimated from Figure 5.11 in Urie et al. (2004)

Sample Description	Rep. #	PSD Percentiles (micrometers)														
		1	5	10	20	25	30	40	50	60	70	75	80	90	95	99
AZ-101 As Received. 60 mL/s, No Sonication. Microtrac	WTP-RPT-048			0.8	1.1		1.7	2.3	3.3	4.3	5.9		8	14	19	27

Table A.5. AZ-102 Compiled Data. The 99th percentile for all Microtrac data is an interpolated value; other values were taken directly from the Microtrac data report. Horiba data from Bechtold (2002) were used “as-is” with no further computation. Some percentiles for the Horiba data from Warrant (2002) have been interpolated from raw histogram data.

Sample Description	Rep. #	PSD Percentiles (micrometers)														
		1	5	10	20	25	30	40	50	60	70	75	80	90	95	99
AZ-102. Sample CUF-AZ102-MU-R1D1 in AZ-102-MU Simulated Supernatant 60 ml/s. No Sonication. Microtrac	BNFL-RPT-038			2	3.8		5.6	7.7	11	15	20		26	35	42	61
AZ-102. Sample CUF-AZ102-MU-R2D1 in AZ-102-MU Simulated Supernatant 60 ml/s. No Sonication Microtrac	BNFL-RPT-038			1.9	3.6		5.3	7.2	10	15	20		26	34	42	60
Sample: S01T001651. Run: AZ102885-6/3/0/0. No sonication. Horiba	HNF-8862	1.3	2.6			8.4			21			63			210	310
Sample: S01T001652. Run: AZ102911-6/3/0/0. No sonication. Horiba	HNF-8862	1.7	3.1			9.7			24			110			620	770
Sample: S01T001652-Dup. Run: AZ102915-6/3/0/0. No sonication. Horiba	HNF-8862	1.3	2.2			5.4			10			16			25	30
Sample: S01T001652-Dup2. Run: AZ102919-6/3/0/0. No sonication. Horiba	HNF-8862	1.5	2.7			8.7			21			210			560	720
Sample: S01T001653. Run: AZ102923-6/3/0/0. No sonication. Horiba	HNF-8862	1.3	2.1			5.3			9.8			15			24	30
Sample: S01T001653-Dup. Run: AZ102927-6/3/0/0. No sonication. Horiba	HNF-8862	1.4	2.2			5.8			11			18			28	37
AZ-102. BOJPS7T-6/3/0/0-Dup. Analysis S01R000133, Sample 11003147. No sonication. Horiba	RPP-9806	1.4	2.4	3.2	4.8	5.7	6.7	9	12	18	75	100	120	160	190	280
AZ-102. BOJPT1T-6/3/0/0-Prim. Analysis S01R000134, Sample 11003151. No sonication. Horiba	RPP-9806	1.4	2.3	3	4.5	5.3	6.2	8.3	11	16	54	100	120	160	200	280
AZ-102. BOJPT1T-6/3/0/0-Dup. Analysis S01R000134, Sample 11003155 Horiba	RPP-9806	1.4	2.3	3	4.5	5.4	6.3	8.4	11	17	72	110	120	160	200	280
AZ-102. BOJPT5T-6/3/0/0-Prim. Analysis S01R000135, Sample 11003159. No sonication. Horiba	RPP-9806	1.6	2.9	4.1	7	9	12	21	37	53	69	78	89	120	150	230
AZ-102. BOJPT5T-6/3/0/0-Dup. Analysis S01R000135, Sample 11003163. No sonication. Horiba	RPP-9806	1.5	2.6	3.6	5.8	7.2	8.8	13	23	47	78	92	110	140	170	240

Table A.6. B-203 Compiled Data. All listed percentiles are given on the MasterSizer 2000 data report.

Sample Description	Rep. #	PSD Percentiles (micrometers)														
		1	5	10	20	25	30	40	50	60	70	75	80	90	95	99
B-203 in Water, No Sonication (19031-DL4, Averaged Runs 117-120) MS 2000	PNL-16133	0.53	1.3	1.8	2.5	2.8	3.1	3.7	4.4	5.2	6.2	6.9	7.6	9.9	12	16

Table A.7. BY-104 Compiled Data. The 99th percentile for this BY-104 data is an interpolated value; other values were taken directly from the Microtrac data report.

Sample Description	Rep. #	PSD Percentiles (micrometers)														
		1	5	10	20	25	30	40	50	60	70	75	80	90	95	99
Tank BY-104, untreated solids slurried in water. No sonication Microtrac	PNNL-11278			1.5	3.4		5.1	6.5	7.8	9.3	11		14	19	29	67

Table A.8. BY-108 Compiled Data. The 99th percentile for this BY-108 data is an interpolated value; other values were taken directly from the Microtrac data report.

Sample Description	Rep. #	PSD Percentiles (micrometers)														
		1	5	10	20	25	30	40	50	60	70	75	80	90	95	99
Tank BY-108, untreated solids slurried in water. No sonication Microtrac	PNNL-11636			0.76	1.1		1.5	2.3	3.6	5.2	7.4		11	17	23	33

Table A.9. BY-110 Compiled Data. The 99th percentile for this BY-110 data is an interpolated value; other values were taken directly from the Microtrac data report.

Sample Description	Rep. #	PSD Percentiles (micrometers)														
		1	5	10	20	25	30	40	50	60	70	75	80	90	95	99
Tank BY-110, untreated solids slurried in water. No sonication Microtrac	PNNL-11278			1	1.3		1.7	2.4	3.6	4.5	6		9.9	15	22	35

Table A.10. C-104 Compiled Data. The 99th percentile for all Microtrac data is an interpolated value; other values were taken directly from the Microtrac data report. All Horiba data were used "as-is" with no further computation.

Sample Description	Rep. #	PSD Percentiles (micrometers)														
		1	5	10	20	25	30	40	50	60	70	75	80	90	95	99
C014 Slurry; Sample CUP-C104-001 in #1 Supernatant Simulant. 60 ml sec. No Sonication Microtrac	BNFL-RPT-030			0.68	1		1.4	2	3.4	5.8	10		18	28	37	61
C014 Slurry; Sample CUP-C104-001-DUP in #1 Supernatant Simulant. 60 ml sec. No Sonication. Microtrac	BNFL-RPT-030			0.71	1.1		1.4	2.2	3.7	6.1	11		18	25	30	41
Sample: S01T001447. Run: C104781-6/3/0/0. No sonication. Horiba	HNF-8862	0.22	0.52			2.8			7.3			31			150	290
Sample: S01T001448. Run: C104792-6/3/0/0. No sonication. Horiba	HNF-8862	0.22	0.5			2.5			5.8			17			59	110
Sample: S01T001449. Run: C104802-6/3/0/0. No sonication. Horiba	HNF-8862	0.22	0.51			2.8			7.6			36			170	260
Sample: S01T001451. Run: C104815-6/3/0/0. No sonication. Horiba	HNF-8862	0.22	0.61			2.9			7.3			33			180	280
C-104. WPA038. 60 mL/s, No sonication. Microtrac	HNF-8862			0.75	1.1		1.4	1.8	2.4	3.2	4.2		5.7	10	24	39
C-104 Dup. 104C037. 60 mL/s, No sonication. Microtrac	HNF-8862			0.88	1.2		1.5	2	2.7	3.5	4.6		6.3	9.7	12	16

Table A.11. C-106 Compiled Data. The 99th percentile for this C-106 data is an interpolated value; other values were taken directly from the Microtrac data report.

Sample Description	Rep. #	PSD Percentiles (micrometers)														
		1	5	10	20	25	30	40	50	60	70	75	80	90	95	99
Tank C-106, untreated solids slurried in 1M NaNO3. No sonication Microtrac	PNNL-11381			0.72	1.6		2.9	4.5	6.5	9.7	16		25	39	50	68

Table A.12. C-107 Compiled Data. All Horiba data were used "as-is" with no further computation.

Sample Description	Rep. #	PSD Percentiles (micrometers)														
		1	5	10	20	25	30	40	50	60	70	75	80	90	95	99
Sample: S01T001673. Run: C107931-6/3/0/0. No sonication. Horiba	HNF-8862	0.91	1.3			3.4			6.2			9.5			15	19
Sample: S01T001673-Dup. Run: C107935-6/3/0/0. No sonication. Horiba	HNF-8862	0.91	1.3			3.3			5.9			9.1			14	18
Sample: S01T001673-Dup2. Run: C107939-6/3/0/0. No sonication. Horiba	HNF-8862	0.87	1.3			3.3			6.3			10			17	22
Sample: S01T001673-Dup3. Run: C107943-6/3/0/0. No sonication. Horiba	HNF-8862	0.86	1.2			3.3			6.2			9.7			15	19

Table A.13. S-101 Compiled Data. All percentiles estimated from Figure 5.3 in PNNL-11636 (Lumetta et al. 1997).

Sample Description	Rep. #	PSD Percentiles (micrometers)														
		1	5	10	20	25	30	40	50	60	70	75	80	90	95	99
Tank S-101, untreated solids slurried in water. No sonication Microtrac	PNNL-11636			0.98	1.4		2.3	3.5	4.5	5.9	9.3		13	15	18	28

Table A.14. S-107 Compiled Data. The 99th percentile for all Microtrac data is an interpolated value; other values were taken directly from the Microtrac data report.

Sample Description	Rep. #	PSD Percentiles (micrometers)														
		1	5	10	20	25	30	40	50	60	70	75	80	90	95	99
Tank S-107, untreated solids slurried in water. No sonication Microtrac	PNNL-11278			1.1	2		3.4	5.2	7.5	11	16		22	33	46	82
S-107 Retrieval Slurry, S-107 REPS DUP, 60 mL/s in 0.53M NaOH, 0.1M NaNO3. No Sonication Microtrac	PNNL-12010			1.2	1.9		3.1	5.1	6.8	8.8	12		16	23	32	60

Table A.15. SX-108 Compiled Data. The 99th percentile for this SX-108 data is an interpolated value; other values were taken directly from the Microtrac data report.

Sample Description	Rep. #	PSD Percentiles (micrometers)														
		1	5	10	20	25	30	40	50	60	70	75	80	90	95	99
Tank SX-108, untreated solids slurried in water. No sonication Microtrac	PNNL-11278			0.9	1.4		2.5	5.3	8.5	14	21		26	30	34	40

Table A.16. SY-102 Compiled Data. All Horiba data were used "as-is" with no further computation.

Sample Description	Rep. #	PSD Percentiles (micrometers)														
		1	5	10	20	25	30	40	50	60	70	75	80	90	95	99
Sample: S01T001648. Run: SY102877-6/4/0/0. No sonication. Horiba	HNF-8862	0.32	0.96			2.5			4.2			7.1			14	21
Sample: S01T001649. Run: SY102881-6/3/0/0. No sonication. Horiba	HNF-8862	0.29	0.89			2.5			4.2			7.3			15	35
SY102 s96r00511, 1M NaNO3. No Sonication. Microtrac	PNNL-11352			1.1	1.4		2.1	2.9	3.9	5.2	7.1		9.8	19	32	36

Table A.17. T-110 Compiled Data. All listed percentiles are given on the MasterSizer 2000 data report.

Sample Description	Rep. #	PSD Percentiles (micrometers)														
		1	5	10	20	25	30	40	50	60	70	75	80	90	95	99
T-110 in Water, No Sonication (19025-DL4, Averaged Runs 85-88) MS 2000	PNL-16133	0.45	1.2	2.2	4.4	5.7	7.1	11	17	30	60	83	110	190	260	410

Table A.18. T-203 Compiled Data. All listed percentiles are given on the MasterSizer 2000 data report.

Sample Description	Rep. #	PSD Percentiles (micrometers)														
		1	5	10	20	25	30	40	50	60	70	75	80	90	95	99
T-203 in Water, No Sonication (19032-DL4, Averaged Runs 133-136) MS 2000	PNL-16133	0.73	1.6	2.2	3.2	3.7	4.2	5.4	6.9	8.8	12	14	16	28	43	86

Table A.19. T-204 Compiled Data. All listed percentiles are given on the MasterSizer 2000 data report.

Sample Description	Rep. #	PSD Percentiles (micrometers)														
		1	5	10	20	25	30	40	50	60	70	75	80	90	95	99
T-204 in Water, No Sonication (19026-DL4, Averaged Runs 101-104) MS 2000	PNL-16133	0.74	1.6	2.3	3.7	4.3	5.1	6.8	9.1	13	19	24	32	57	84	150

A.2 Sonicated Data

Sonicated PSD correspond to particle-size measurement data taken under flow conditions sufficient to suspend all of the particulate matter (similar to those of minimal disturbance). The primary difference is that the sample is sonicated immediately prior to and during the measurement. The goal was to evaluate the distribution under conditions of “maximal” agitation. This data would be expected to include individual primary particles and hard agglomerates. Details regarding the selection of data sets for inclusion in the sonicated data set are given in Section 3.1.

The same shortened reporting conventions used for the instruments and reports in the minimal disturbance data are used in Tables A.20 through A.37. All PSD measurements from 7S110-WSC-03-012(a) have no corresponding minimal disturbance data.

Table A.20. AW-103 Compiled Data. All Horiba data were used “as-is” with no further computation. The 99th percentile on all Microtrac data is an interpolated value; other values were taken directly from the Microtrac data report.

Sample Description	Rep. #	PSD Percentiles (micrometers)														
		1	5	10	20	25	30	40	50	60	70	75	80	90	95	99
Sample: S01T001426. Run: AW103748 - 6/3/2/0. Sonicated 2 mins. Horiba.	HNF-8862	0.18	0.27			1.2			3.9			8.8			19	27
Sample: S01T001427. Run: AW103754 - 6/3/20/0. Sonicated 20 mins. Horiba.	HNF-8862	0.18	0.27			1			3.6			9.2			21	29
Sample: S01T001669. Run: AW103948 - 6/3/2/0. Sonicated 2 mins. Horiba.	HNF-8862	0.6	0.94			1.9			3.3			5.9			11	15
Sample: S01T001669-Dup. Run: AW103952 - 6/3/2/0. Sonicated 2 mins. Horiba.	HNF-8862	0.69	1			2.1			3.8			7.1			13	19
Sample: S01T001670-Dup. Run: AW103962 - 6/3/2/0. Sonicated 2 mins. Horiba.	HNF-8862	0.7	1.1			2.7			9.3			77			160	260
AW-103. WPAA011. 60 mL/s, Sonicated 2 mins. Microtrac.	HNF-8862			0.77	1.1		1.4	1.8	2.5	3.4	4.7		6.7	16	83	260
AW-103 Dup. WPAA045. 60 mL/s, Sonicated 2 mins. Microtrac.	HNF-8862			0.68	0.97		1.2	1.5	2	2.8	3.8		5.4	9.2	14	27

Table A.21. AY-101 Compiled Data. All Horiba data were used “as-is” with no further computation. The 99th percentile on all Microtrac data is an interpolated value; other values were taken directly from the Microtrac data report.

Sample Description	Rep. #	PSD Percentiles (micrometers)														
		1	5	10	20	25	30	40	50	60	70	75	80	90	95	99
Sample: S01T001490. Run: AY101853-6/3/2/0. Sonicated 2 mins. Horiba.	HNF-8862	0.3	0.61			2.4			5.5			8.7			15	20
Sample: S01T001491. Run: AY101864-6/3/20/0. Sonicated 2 mins. Horiba.	HNF-8862	0.26	0.56			1.8			4.1			6.8			12	16
AY-101. 101AY018. 60 mL/s, Sonicated 2 mins. Microtrac.	HNF-8862			0.55	0.98		1.5	3	5.5	6.8	7.9		9.2	11	13	19
AY-101 Dup. 101AY028. 60 mL/s, Sonicated 2 mins. Microtrac.	HNF-8862			0.42	0.78		1.2	1.8	3.6	5.7	7.1		8.5	10	12	17

(a) 7S110-WSC-03-012, “Particle Size Distribution Analysis of Samples from Tank 241-AZ-102, Core 310” (internal memo, WS Callaway to KG Carothers, December 12, 2003), CH2M HILL, Richland, Washington.

Table A.22. AY-102 Compiled Data. All Horiba data were used "as-is" with no further computation.

Sample Description	Rep. #	PSD Percentiles (micrometers)														
		1	5	10	20	25	30	40	50	60	70	75	80	90	95	99
Sample: S01T001654. Run: AY102896-6/3/2/0. Sonicated 2 mins. Horiba.	HNF-8862	0.59	0.72			1.1			2.4			7.7			15	20
Sample: S01T001654-Dup. Run: AY102900-6/3/2/0. Sonicated 2 mins. Horiba.	HNF-8862	0.59	0.73			1.1			2.2			6.3			13	18
Sample: S01T001655. Run: AY102904-6/3/2/0. Sonicated 2 mins. Horiba.	HNF-8862	0.6	0.75			1.1			2.7			7.9			16	22
Sample: S01T001655-Dup. Run: AY102908-6/3/2/0. Sonicated 2 mins. Horiba.	HNF-8862	0.57	0.7			0.99			1.6			3.6			7	9.4

Table A.23. AZ-101 Compiled Data. All percentiles estimated from Figure 5.11 (Urie et al. 2004).

Sample Description	Rep. #	PSD Percentiles (micrometers)														
		1	5	10	20	25	30	40	50	60	70	75	80	90	95	99
AZ-101 As Received. 60 mL/s, Sonicated at 40 W for 90 sec. Microtrac.	WTP-RPT-048			0.7	1.1		1.6	2.3	3.2	4.3	6		8	15	20	27

Table A.24. AZ-102 Compiled Data. Horiba percentiles from 7S110-WSC-03-012 estimated from Figure 1, Table 5. 99th percentile for Microtrac data is interpolated; other values taken directly from Microtrac data report. Horiba data from Bechtold (2002) used "as-is"; percentiles for Horiba data from Warrant (2002) interpolated from raw histogram data.

Sample Description	Rep. #	PSD Percentiles (micrometers)														
		1	5	10	20	25	30	40	50	60	70	75	80	90	95	99
Sample S03T001608, Segment 18UH-Dup, Initial (Sonicated 1 min) Horiba.	7S110-WSC-03-012	1	1.5	1.8	2.7	3.2	4	4.3	13	20	28	32	38	54	72	140
Sample S03T001608, Segment 18UH-Trip, Initial (Sonicated 1 min) Horiba.	7S110-WSC-03-012	1	1.5	1.9	2.7	3.3	3.9	6.4	11	17	23	27	30	41	49	66
Sample S03T001605, Segment 18LH-Prim, Initial (Sonicated 1 min) Horiba.	7S110-WSC-03-012	1.3	1.8	2.2	2.8	3.2	3.5	4.4	5.6	7.5	11	14	17	36	89	530
Sample S03T001605, Segment 18LH-Dup, Initial (Sonicated 1 min) Horiba.	7S110-WSC-03-012	1.4	1.8	2.2	2.9	3.3	3.7	4.6	5.8	7.9	11	14	18	39	460	670
Sample S03T001611, Segment 19UH-Dup, Initial (Sonicated 1 min) Horiba.	7S110-WSC-03-012	1.4	2	2.5	3.3	3.7	4	4.9	5.8	6.9	8.2	9	10	13	17	26
Sample S03T001635, Segment 19LH-Prim, Initial (Sonicated 1 min) Horiba.	7S110-WSC-03-012	1.1	1.7	2.4	3.7	4.4	5.1	6.7	8.4	10	13	15	17	29	120	260
Sample S03T001635, Segment 19LH-Dup, Initial (Sonicated 1 min) Horiba.	7S110-WSC-03-012	0.95	1.3	1.6	2.1	2.4	2.6	3.2	3.9	4.8	6	6.8	7.8	11	14	21
AZ-102. Sample CUF-AZ102-MU-R1D1 in AZ-102-MU Simulated Supernatant 60 ml/s, 1st Sonication 40W, 90 sec. Microtrac.	BNFL-RPT-038			1.8	3.5		5.2	7.1	9.7	14	18		23	30	37	50
AZ-102. Sample CUF-AZ102-MU-R2D1 in AZ-102-MU Simulated Supernatant 60 ml/s, 1st Sonication 40W, 90 sec. Microtrac.	BNFL-RPT-038			1.7	3.2		4.9	6.6	8.9	13	17		22	29	36	49
Sample: S01T001651. Run: AZ102886-6/3/2/0. Sonicated 2 min. Horiba.	HNF-8862	0.67	1.3			5.2			11			21			67	300
Sample: S01T001652. Run: AZ102912-6/3/2/0. Sonicated 2 min. Horiba.	HNF-8862	0.97	1.5			4.4			9.2			16			44	190
Sample: S01T001652-Dup. Run: AZ102916-6/3/2/0. Sonicated 2 min. Horiba.	HNF-8862	1	1.5			4.2			8			13			25	260
Sample: S01T001652-Dup2. Run: AZ102920-6/3/2/0. Sonicated 2 min. Horiba.	HNF-8862	0.97	1.5			4.2			8.6			15			35	220
Sample: S01T001653. Run: AZ102924-6/3/2/0. Sonicated 2 min. Horiba.	HNF-8862	1	1.6			4			7.4			11			18	23
Sample: S01T001653-Dup. Run: AZ102928-6/3/2/0. Sonicated 2 min. Horiba.	HNF-8862	1	1.6			4.3			8.1			12			20	25
AZ-102. BOJPS8T-6/3/2/0-Dup. Analysis S01R000133, Sample 11003148. Sonicated 2 min. Horiba.	RPP-9806	0.93	1.7	2.6	4.5	5.6	6.9	10	18	100	120	130	140	170	200	260
AZ-102. BOJPT2T-6/3/2/0-Prim. Analysis S01R000134, Sample 11003152. Sonicated 2 min. Horiba.	RPP-9806	0.92	1.6	2.5	4.3	5.3	6.5	9.5	17	110	130	140	150	180	200	280
AZ-102. BOJPT2T-6/3/2/0-Dup. Analysis S01R000134, Sample 11003156. Sonicated 2 min. Horiba.	RPP-9806	0.9	1.5	2.3	4	5	6	8.7	13	94	120	140	150	180	210	280
AZ-102. BOJPT6T-6/3/2/0-Prim. Analysis S01R000135, Sample 11003160. Sonicated 2 min. Horiba.	RPP-9806	1.1	2	3.1	5.8	7.4	9.4	15	23	39	65	79	93	130	160	230
AZ-102. BOJPT6T-6/3/2/0-Dup. Analysis S01R000135, Sample 11003164. Sonicated 2 min. Horiba.	RPP-9806	0.99	1.8	2.9	5.2	6.5	8.2	13	21	58	100	110	130	160	190	260

Table A.25. B-203 Compiled Data. All listed percentiles are given on the MasterSizer 2000 data report.

Sample Description	Rep. #	PSD Percentiles (micrometers)														
		1	5	10	20	25	30	40	50	60	70	75	80	90	95	99
B-203 in Water, 75% Sonication (19031-DL4, Averaged Runs 129-132) MS 2000.	PNL-16133	0.47	1	1.6	2.6	3.1	3.7	5	6.5	8.3	11	12	14	24	380	520

Table A.26. BY-104 Compiled Data. The 99th percentile on this BY-104 data is an interpolated value; other values were taken directly from the Microtrac data report.

Sample Description	Rep. #	PSD Percentiles (micrometers)														
		1	5	10	20	25	30	40	50	60	70	75	80	90	95	99
Tank BY-104, untreated solids slurried in water. 300 sec sonication. Microtrac.	PNNL-11278			0.81	1.3		2	3	4.3	5.4	6.6		8.5	15	31	48

Table A.27. BY-108 Compiled Data. The 99th percentile on this BY-108 data is an interpolated value; other values were taken directly from the Microtrac data report.

Sample Description	Rep. #	PSD Percentiles (micrometers)														
		1	5	10	20	25	30	40	50	60	70	75	80	90	95	99
Tank BY-108, untreated solids slurried in water. 300 sec sonication. Microtrac.	PNNL-11636			0.39	0.72		1	1.4	2	3	4.3		6.4	11	16	29

Table A.28. BY-110 Compiled Data. The 99th percentile on this BY-110 data is an interpolated value; other values were taken directly from the Microtrac data report.

Sample Description	Rep. #	PSD Percentiles (micrometers)														
		1	5	10	20	25	30	40	50	60	70	75	80	90	95	99
Tank BY-110, untreated solids slurried in water. 300 sec sonication Microtrac.	PNNL-11278			0.51	0.78		1.2	1.5	1.9	3.4	4.3		5.9	13	21	35

Table A.29. C-104 Compiled Data. The 99th percentile on all Microtrac data is an interpolated value; other values were taken directly from the Microtrac data report. All Horiba data were used "as-is" with no further computation.

Sample Description	Rep. #	PSD Percentiles (micrometers)														
		1	5	10	20	25	30	40	50	60	70	75	80	90	95	99
C014 Slurry; Sample CUP-C104-001 in #1 Supernatant Simulant. Sonicated at 40 W for 90 sec; 60 ml sec. Microtrac.	BNFL-RPT-030			0.59	0.96		1.3	1.9	3.3	5.4	9.4		17	26	35	59
C014 Slurry; Sample CUP-C104-001-DUP in #1 Supernatant Simulant. Sonicated at 40 W for 90 sec; 60 ml sec. Microtrac.	BNFL-RPT-030			0.65	1		1.4	2.3	3.9	6.3	11		18	25	30	40
Sample: S01T001449. Run: C104804-6/3/2/0. Sonicated 2 mins. Horiba.	HNF-8862	0.2	0.33			1.4			4.8			18			50	79
Sample: S01T001451. Run: C104817-6/3/20/0. Sonicated 20 mins. Horiba.	HNF-8862	0.2	0.3			1.1			4.9			16			34	49
C-104. WPA047. 60 mL/s, Sonicated 2 mins. Microtrac.	HNF-8862			0.41	0.66		0.91	1.1	1.4	1.9	2.6		3.6	4.9	6.2	26
C-104 Dup. 104C040. 60 mL/s, Sonicated 2 mins. Microtrac.	HNF-8862			0.68	1		1.3	1.7	2.3	3	3.9		5.3	8.1	11	14

Table A.30. C-106 Compiled Data. The 99th percentile on this C-106 data is an interpolated value; other values were taken directly from the Microtrac data report.

Sample Description	Rep. #	PSD Percentiles (micrometers)														
		1	5	10	20	25	30	40	50	60	70	75	80	90	95	99
Tank C-106, untreated solids slurried in 1M NaNO3. Sonicated 300 sec Microtrac.	PNNL-11381			0.45	1.1		1.9	2.9	3.9	5.2	6.9		9.6	14	17	23

Table A.31. C-107 Compiled Data. All Horiba data were used "as-is" with no further computation.

Sample Description	Rep. #	PSD Percentiles (micrometers)														
		1	5	10	20	25	30	40	50	60	70	75	80	90	95	99
Sample: S01T001673. Run: C107932-6/3/2/0. Sonicated 2 mins. Horiba.	HNF-8862	0.65	0.84			1.5			3.6			6.9			12	16
Sample: S01T001673-Dup. Run: C107936-6/3/2/0. Sonicated 2 mins. Horiba.	HNF-8862	0.65	0.83			1.4			3.2			5.7			9.6	12
Sample: S01T001673-Dup2. Run: C107940-6/3/2/0. Sonicated 2 mins. Horiba.	HNF-8862	0.62	0.78			1.2			2.6			4.7			7.7	9.9
Sample: S01T001673-Dup3. Run: C107944-6/3/2/0. Sonicated 2 mins. Horiba.	HNF-8862	0.62	0.79			1.3			3.3			6.7			12	15

Table A.32. S-107 Compiled Data. The 99th percentile on all Microtrac data is an interpolated value; other values were taken directly from the Microtrac data report.

Sample Description	Rep. #	PSD Percentiles (micrometers)														
		1	5	10	20	25	30	40	50	60	70	75	80	90	95	99
Tank S-107, untreated solids slurried in water. 300 sec sonication Microtrac.	PNNL-11278			0.97	1.5		2.5	3.8	5.5	7.6	11		16	26	45	69
S-107 Retrieval Slurry, S-107 REPS DUP, 40 mL/s in 0.53M NaOH, 0.1M NaNO3, 2nd Sonication 40W-90sec Microtrac.	PNNL-12010			1.1	1.7		2.8	4.5	6.2	7.9	10		14	21	28	55

Table A.33. SX-108 Compiled Data. The 99th percentile on this SX-108 data is an interpolated value; other values were taken directly from the Microtrac data report.

Sample Description	Rep. #	PSD Percentiles (micrometers)														
		1	5	10	20	25	30	40	50	60	70	75	80	90	95	99
Tank SX-108, untreated solids slurried in water. Sonicated. Microtrac.	PNNL-11278			0.4	0.82		1.2	2.2	4.3	7.5	14		21	27	31	37

Table A.34. SY-102 Compiled Data. All Horiba data were used "as-is" with no further computation.

Sample Description	Rep. #	PSD Percentiles (micrometers)														
		1	5	10	20	25	30	40	50	60	70	75	80	90	95	99
Sample: S01T001648. Run: SY102878-6/3/2/0. Sonicated 2 mins. Horiba.	HNF-8862	0.23	0.45			1.4			3.2			6			12	16
Sample: S01T001649. Run: SY102882-6/3/2/0. Sonicated 2 mins. Horiba.	HNF-8862	0.23	0.45			1.5			3.2			6.2			13	19
SY102 s96r000511. Sonicated. Microtrac.	PNNL-11352			0.8	1		1.3	1.7	2.4	3	3.7		4.9	7.4	9.8	15

Table A.35. T-110 Compiled Data. All listed percentiles are given on the MasterSizer 2000 data report.

Sample Description	Rep. #	PSD Percentiles (micrometers)														
		1	5	10	20	25	30	40	50	60	70	75	80	90	95	99
T-110 in Water, 75% Sonication (19025-DL4, Averaged Runs 97-100) MS 2000.	PNL-16133	0.34	0.61	1.1	2.4	3.1	3.9	5.9	8.5	12	20	26	32	51	70	430

Table A.36. T-203 Compiled Data. All listed percentiles are given on the MasterSizer 2000 data report.

Sample Description	Rep. #	PSD Percentiles (micrometers)														
		1	5	10	20	25	30	40	50	60	70	75	80	90	95	99
T-203 in Water, 75% Sonication (19032-DL4, Averaged Runs 145-148) MS 2000.	PNL-16133	0.44	0.87	1.4	2.3	2.8	3.3	4.6	6	7.7	9.8	11	13	20	400	510

Table A.37. T-204 Compiled Data. All listed percentiles are given on the MasterSizer 2000 data report.

Sample Description	Rep. #	PSD Percentiles (micrometers)														
		1	5	10	20	25	30	40	50	60	70	75	80	90	95	99
T-204 in Water, 75% Sonication (19026-DL4, Averaged Runs 113-116) MS 2000.	PNL-16133	0.45	0.87	1.4	2.5	3	3.6	4.8	6.3	8	10	12	13	21	300	510

The references cited in Sections A.1 and A.2 are the following:

Bechtold DB, WS Callaway, GA Cooke, JB Duncan, DL Herting, JR Jewett, JC Person, and JM Tingey. 2002. *Particle Property Analyses of High-Level Waste Tank Sludges*. HNF-8862 Rev. 0, Fluor Hanford, Inc., Richland, Washington.

Brooks KP, PR Bredt, GR Golcar, SA Hartley, LK Jagoda, KG Rappe, and MW Urie. 1998. *Bench-Scale Enhanced Sludge Washing and Gravity Settling of Hanford Tank C-107 Sludge*. PNNL-12010, Pacific Northwest National Laboratory, Richland, Washington.

Lumetta GJ, BM Rapko, MJ Wagner, J Liu, and YL Chen. 1996a. *Washing and Caustic Leaching of Hanford Tank Sludges: Results of FY 1996 Studies*. PNNL-11278 Rev. 1, Pacific Northwest National Laboratory, Richland, Washington.

Lumetta GJ, MJ Wagner, FV Hoopes, and RT Steele. 1996b. *Washing and Caustic Leaching of Hanford Tank C-106 Sludge*. PNNL-11381, Pacific Northwest National Laboratory, Richland, Washington.

Lumetta GJ, IE Burgeson, MJ Wagner, J Liu, and YL Chen. 1997. *Washing and Caustic Leaching of Hanford Tank Sludge: Results of FY1997 Studies*. PNNL-11636, Pacific Northwest National Laboratory, Richland, Washington.

Poloski AP, RC Daniel, DR Rector, PR Bredt, EC Buck, JC Berg, and AE Saez.. *Characterization and Correlation of Particle-Level Interactions to the Macroscopic Rheology of Powders, Granular Slurries, and Colloidal Suspensions*. PNNL-16133, Pacific Northwest National Laboratory, Richland, Washington.

Urie MW, PR Bredt, JA Campbell, OT Farmer, III, SK Fiskum, LR Greenwood, EW Hoppe, LK Jagoda, GM Mong, AP Poloski, RD Scheele, CZ Soderquist, RG Swoboda, MP Thomas, and JJ Wagner. 2004. *Chemical Analysis and Physical Properties Testing of 241-AZ-101 Tank Waste Supernatant and Centrifuged Solids*. WTP-RPT-048 Rev. 1, Battelle – Pacific Northwest Division, Richland, Washington.

Table A.38 lists the PSD measurement instrument and test conditions.

Table A.38. PSD Measurement Instrument and Test Conditions (MD = minimal disturbance; US = ultrasonic)

Tank	Waste Type		Particle Size Analysis				Comments	Reference
	Primary	Secondary	MD	US	Instrument	Suspending Liquid		
AN-102	No Sludge Reported		X	X	Microtrac X-100 & UPA	Diluted surrogate supernatant	PSD performed on washed solids only. Performed at multiple flow rates (40 and 60 mL/s) and with sonication at the highest flow rate. Both analyzers were used to obtain the full range of particle diameters.	WTP-RPT-076
			X	X	Microtrac X-100 & UPA	Surrogate supernatant	PSD performed on 2 wt% undissolved solids slurry of tank waste samples. Performed at multiple flow rates (40 and 60 mL/s) and with sonication at the highest flow rate. Both analyzers were used to obtain the full range of particle diameters.	WTP-RPT-021
			X	X	Horiba LA-910	Simulant solution 5.4 M NaNO$_3$ 1.2 M Na2CO$_3$ pH=12	Core 307 Segments 18 through 21 (including both segments 21A and 21B). Initial and final particle size measurements were made. Agitation of 3 (stirrer setting) and circulation of 5 (pump setting) was used for both measurements. Five minutes of sonication was performed between measurements.	Letter Report 7S110-WSC-03-002
			X	X	Horiba LA-910	ISL simulant (see reference for composition)	Core 307 Segments 18 through 21	Letter Report 7S110-WSC-05-011
AN-104	No Sludge Reported		X	X	Microtrac X-100	Slurried in water	Plots for unsonicated data only. Only minor changes in PSD observed after sonication.	PNNL-11636
			X		Brinkman PSA 2010	Not documented	Undiluted waste tank sample	HNF-3352
AN-105	No Sludge Reported		X		Brinkman PSA 2010	Not documented	PSD was reported on undiluted and 25, 50, and 75% dilutions of tank core samples.	HNF-SD-WM-DTR-046
AN-107	No Sludge Reported		X	X	Horiba LA-910	Simulant solution 5 M NaNO$_3$ 1M Na$_2$CO$_3$ pH=12	Segments 18R, 19R, 20, 21A, and 21B from Core 304. Initial and final particle size measurements were made. Agitation of 3 (stirrer setting) and circulation of 5 (pump setting) was used for both measurements. Five minutes of sonication was performed between measurements.	Letter Report B3610-WSC-02-028

Table A.38. PSD Measurement Instrument and Test Conditions (MD = minimal disturbance; US = ultrasonic)

Tank	Waste Type		Particle Size Analysis				Comments	Reference
	Primary	Secondary	MD	US	Instrument	Suspending Liquid		
AW-101	No Sludge Reported		X		Horiba LA-910	Water	Undiluted waste tank sample and an 80% dilution with water. No description was provided in the report on the conditions or the suspending liquid. The data sheet showed 0 agitation and circulation and ultrasonication was off. This may have been the conditions during the measurement, but the suspension may have been circulated, agitated, and sonicated prior to the measurement.	HNF-4964
AW-103	CWZr		X	X	Microtrac X-100	1 M NaOH 1 M $NaNO_3$	PSD performed at multiple circulation rates and sonication times including a delay in measurement from the completion of sonication. Comparison of these measurements was made with measurements in the Horiba particle size analyzer.	HNF-8862
			X	X	Horiba LA-910	1 M NaOH 1 M $NaNO_3$	PSD performed at multiple stirring speeds (step 1 and 3) and sonication times including a delay in measurement from the completion of sonication. A circulation (flow) rate of 14.4 mL/s (Step 6 pump speed) was used for all samples. Comparison of these measurements was made with measurements in the Microtrac X-100 particle size analyzer.	HNF-8862
AY-101	Unclassified		X	X	Microtrac X-100	1 M NaOH 1 M $NaNO_3$	PSD performed at multiple circulation rates and sonication times including a delay in measurement from the completion of sonication. Comparison of these measurements was made with measurements in the Horiba particle size analyzer.	HNF-8862
			X	X	Horiba LA-910	1 M NaOH 1 M $NaNO_3$	PSD performed at multiple stirring speeds (step 1 and 3) and sonication times including a delay in measurement from the completion of sonication. A circulation (flow) rate of 14.4 mL/s (Step 6 pump speed) was used for all samples. Comparison of these measurements was made with measurements in the Microtrac X-100 particle size analyzer.	HNF-8862
			X		Horiba LA-910	Water	Cores 275 and 277. Fraction cell was used for these measurements; therefore, no flow and no sonication were performed on any of the measurements.	FH-0201635
					Brinkman PSA 2010	Not documented	Data provided in an unnumbered memorandum that has not yet been obtained.	Peters 1988

Table A.38. PSD Measurement Instrument and Test Conditions (MD = minimal disturbance; US = ultrasonic)

Tank	Waste Type		Particle Size Analysis				Comments	Reference
	Primary	Secondary	MD	US	Instrument	Suspending Liquid		
AY-102	Unclassified	BL	X	X	Horiba LA-910	1 M NaOH 1 M $NaNO_3$	PSD performed at multiple stirring speeds (step 1 and 3) and sonication times including a delay in measurement from the completion of sonication. A circulation (flow) rate of 14.4 mL/s (Step 6 pump speed) was used for all samples.	HNF-8862
			X	X	Horiba LA-910	ISL simulant (see reference for composition)	Half segments (lower and upper) from each segment (segments 1 through 3) taken in Core 319. Run at various times with the circulation at 4 and agitation at 2. Performed before and after sonication.	Letter Report 7S110-WSC-06-148
			X		Horiba LA-910	Water	PSD performed in the fraction cell; therefore, minimal stirring and no circulation is performed during the measurement. No sonication was performed. Cores 289 and 290.	FH-0202392
AZ-101	P3	Unclassified	X	X	Microtrac X-100	Slurried in water	Plots for unsonicated data only. Only minor changes in PSD observed after sonication. Composite of AZ-101 and AZ-102.	PNNL-11580
			X		HIAC/ROYCO	Slurried in water	Particle size range of 5 to 225 µm. Centrifuged solids analyzed.	PNNL-13028
			X		Brinkman PSA 2010	Glycerin/water	Core 2, Segments 1 and 2 from two locations. Particle size range of 0.5 to 150 µm.	Peterson 1990 Preliminary Results
			X		Brinkman PSA 2010	Glycerin/water	Composite and washed solids. Particle size range of 0.5 to 150 µm.	Letter Report Gray 9/93
			X		Brinkman PSA 2010	Glycerin/water	Cores 1 and 2 from the HWVP process steps starting at formatting all the way to melter feed. Particle size range of 0.5 to 150 µm.	PNNL-11098 PNNL-11025
			X	X	Horiba LA-910	Water	PSD was performed on three fractions from a settling test of tank material from Cores 266 and 269. The fractions are differentiated by the rate of settling. PSD performed in the fraction cell; therefore, minimal stirring and no circulation is performed during the measurement. Sonication was performed in an external sonication bath.	HNF-7078

Table A.38. PSD Measurement Instrument and Test Conditions (MD = minimal disturbance; US = ultrasonic)

Tank	Waste Type		Particle Size Analysis				Comments	Reference
	Primary	Secondary	MD	US	Instrument	Suspending Liquid		
			X	X	Microtrac X-100 & UPA	Surrogate supernatant	PSDs were measured on as-received tank samples, samples concentrated in undissolved solids (2 times the as-received material) by filtration (CUF), and leached/washed samples. Performed at multiple flow rates (40 and 60 mL/s) and with sonication at the highest flow rate.	WTP-RPT-043
			X	X	Microtrac X-100 & UPA	Surrogate supernatant	PSD performed on as-received, concentrated, and leached tank waste samples. Performed at multiple flow rates (40 and 60 mL/s) and with sonication at the highest flow rate.	WTP-RPT-048
AZ-102	P3	SRR PL2 Unclassified	X	X	Microtrac X-100	Slurried in water	Plots for unsonicated data only. Only minor changes in PSD observed after sonication. Composite of AZ-101 and AZ-102.	PNNL-11580
			X		Brinkman PSA 2010	Glycerin/water	Composite and washed solids.	Letter Report Gray 1/93
			X		Brinkman PSA 2010	Glycerin/water	Sampled during the HWVP process steps starting at formatting all the way to melter feed.	PNNL-11098 PNNL-11025
			X	X	Horiba LA-910	5 M $NaNO_3$ 1 M Na_2CO_3 pH=12	Core 310	Letter Report 7S110-WSC-03-012
			X	X	Horiba LA-910	Water	PSD was performed on three settled fractions (upper, middle, and bottom) from a composite from cores 261, 262, and 268. PSD performed at multiple stirring (agitation) speeds (step 1 and 3) prior to and after 2 minutes of sonication. A circulation (flow) rate of 14.4 mL/s (Step 6 pump speed) was used for all samples. The samples were then rerun at a higher stirring (agitation) speed (step 6) prior to and after 2 minutes of sonication.	RPP-9806
			X	X	Microtrac X-100 & UPA	Surrogate supernatant	PSD performed on as-received, concentrated, and leached tank waste samples. Performed at multiple flow rates and with and without sonication.	BNFL-RPT-038
			X	X	Horiba LA-910	1 M NaOH 1 M $NaNO_3$	PSD performed at multiple stirring speeds (step 1 and 3) and sonication times including a delay in measurement from the completion of sonication. A circulation (flow) rate of 14.4 mL/s (Step 6 pump speed) was used for all samples.	HNF-8862

Table A.38. PSD Measurement Instrument and Test Conditions (MD = minimal disturbance; US = ultrasonic)

Tank	Waste Type		Particle Size Analysis				Comments	Reference
	Primary	Secondary	MD	US	Instrument	Suspending Liquid		
B-104	2C	1C	X		Leeds & Northrup UPA	Slurried in water	PSD measured on sludge sample and the leached sludge sample. Particle size range of this instrument is 3 nm to 6.5 µm.	LA-UR-96-2839
B-106	TBP	1C	X		Leeds & Northrup UPA	Slurried in water	PSD measured on sludge sample and the leached sludge sample. Particle size range of this instrument is 3 nm to 6.5 µm.	LA-UR-97-2889
B-111	2C	B	X		Brinkman PSA 2010	glycerin/water	PSD measured before and after sludge washing and caustic leaching.	PNL-10712
			X		Brinkman PSA 2010	50% glycerol	PSD was measured on unhomogenized material from each segment from cores 29 and 30. Original PSDs for each of these segments are in the core characterization files.	PNL-10099
B-201	224		X		Brinkman PSA 2010	Glycerin/water	PSD measured before and after sludge washing and caustic leaching.	PNL-10078
B-202	224		X		Leeds & Northrup UPA	Slurried in water	PSD measured on sludge sample and the leached sludge sample. Particle size range of this instrument is 3 nm to 6.5 µm.	LA-UR-95-2070
B-203	224		X	X	Mastersizer 2000	Slurried in water	PSDs were performed on dilutions of the tank samples at several different sonication powers including no sonication. Only the unsonicated data is reported in Revision 0. Revision 1 will include sonicated results.	PNNL-16133
BX-103	CWP	TBP	X		Leeds & Northrup UPA	Slurried in water	PSD measured on sludge sample and the leached sludge sample. Particle size range of this instrument is 3 nm to 6.5 µm.	LA-UR-97-2889
BX-105	CWP	TBP MW	X		Leeds & Northrup UPA	Slurried in water	PSD measured on sludge sample and the leached sludge sample. Particle size range of this instrument is 3 nm to 6.5 µm.	LA-UR-95-2070
BX-107	1C		X		Brinkman PSA 2010	Glycerin/water	PSD measured before and after sludge washing and caustic leaching.	PNL-10712
				X		Slurried in water	Performed at 222-S. Procedure is listed in document WHC-SD-WM-DP-028 which was not scanned and is not in RMIS. Summary of data is provided in WHC-EP-0739. Ten segments from Cores 41 and 40 were analyzed.	WHC-EP-0739 WHC-SD-WM-DP-028

Table A.38. PSD Measurement Instrument and Test Conditions (MD = minimal disturbance; US = ultrasonic)

Tank	Waste Type		Particle Size Analysis				Comments	Reference
	Primary	Secondary	MD	US	Instrument	Suspending Liquid		
BX-109	TBP		X		Leeds & Northrup UPA	Slurried in water	PSD measured on sludge sample and leached sludge sample. Particle size range of this instrument is 3 nm to 6.5 µm.	LA-UR-96-2839
BY-104	PFeCN		X	X	Microtrac X-100	Slurried in water	Plots for unsonicated data only. Decrease in fraction of larger particles observed.	PNNL-11278
			X		Brinkman PSA 2010	Water	Water digestates from saltcake. Lightly stirred solution during measurement.	WHC-SD-WM-TI-540
BY-108	PFeCN		X	X	Microtrac X-100	Slurried in water	Plots for unsonicated data only. Decrease in fraction of larger particles (> 20 µm) observed after sonication.	PNNL-11636
BY-110	PFeCN			X	Microtrac X-100	Slurried in water	Only data after 5 minutes of sonication available	PNNL-11278
C-103	CWP		X		Brinkman PSA 2010	glycerin/water	PSD measured before and after sludge washing and caustic leaching.	PNL-10712
C-104	CWP	CWZr OWW TH Unclassified	X		Leeds & Northrup UPA	Slurried in water	PSD measured on sludge sample and the leached sludge sample. Particle size range of this instrument is 3 nm to 6.5 µm.	LA-UR-97-2889
			X	X	Microtrac X-100 & UPA	Surrogate supernatant (see reference for composition)	PSD performed on the diluted tank sample, water washed sample, and caustic leached sample at a various flow rates (40 and 60 mL/s) with and without sonication.	BNFL-RPT-030
			X		Horiba LA-910	Slurried in water	No description was provided in the report on the conditions or the suspending liquid. The data sheet showed no agitation, and circulation and ultrasonication was off. This may have been the conditions during the measurement, but the suspension may have been circulated, agitated, and sonicated prior to the measurement.	RPP-5798
			X	X	Microtrac X-100	1 M NaOH 1 M $NaNO_3$	PSD performed at multiple circulation rates and sonication times including a delay in measurement from the completion of sonication. Comparison of these measurements was made with measurements in the Horiba particle size analyzer.	HNF-8862

Table A.38. PSD Measurement Instrument and Test Conditions (MD = minimal disturbance; US = ultrasonic)

Tank	Waste Type		Particle Size Analysis				Comments	Reference
	Primary	Secondary	MD	US	Instrument	Suspending Liquid		
			X	X	Horiba LA-910	1 M NaOH 1 M $NaNO_3$	PSD performed at multiple stirring speeds (step 1 and 3) and sonication times including a delay in measurement from the completion of sonication. A circulation (flow) rate of 14.4 mL/s (Step 6 pump speed) was used for all samples. Comparison of these measurements was made with measurements in the Microtrac X-100 particle size analyzer	HNF-8862
C-105	CWP	TBP	X		Leeds & Northrup UPA	Slurried in water	PSD measured on sludge sample and leached sludge sample. Particle size range of this instrument is 3 nm to 6.5 µm.	LA-UR-97-2889
C-106	Unclassified		X		Microtrac X-100	Slurried in water	PSDs were performed on leached and unleached samples.	PNNL-11381
C-107	1C	CWP SRR	X		Brinkmann PSA 2010	1:1 water:glycerine	No flow during measurement.	PNNL-11278
			X	X	Microtrac X-100 and ZetaPlus	0.1 and 1 M $NaNO_3$	Similar samples are run in the Brookhaven ZetaPlus and the Microtrac X-100.	Letter Report Brooks et. al. 9/96
			X		Leeds & Northrup UPA	Slurried in water	PSD measured on sludge sample and the leached sludge sample. Particle size range of this instrument is 3 nm to 6.5 µm.	LA-UR-96-2839
			X	X	Horiba LA-910	1 M NaOH 1 M $NaNO_3$	PSD performed at multiple stirring speeds (step 1 and 3) and sonication times including a delay in measurement from the completion of sonication. A circulation (flow) rate of 14.4 mL/s (Step 6 pump speed) was used for all samples.	HNF-8862
			X	X	Horiba LA-910	Water	PSD performed in the fraction cell; therefore, minimal stirring and no circulation is performed during the measurement. Sonication was performed in an external sonication bath. Cores 287 and 288.	FH-0201835
C-108	1C	TBP TFeCN	X		Leeds & Northrup UPA	Slurried in water	PSD measured on sludge sample and the leached sludge sample. Particle size range of this instrument is 3 nm to 6.5 µm.	LA-UR-95-2070
C-109	TFeCN	CWP 1C HS	X		Brinkmann PSA 2010	50% glycerol	Cores 47 through 49 and two simulants (INFARM-2 top and bottom). Hard copies of original data in Core Characterization Files.	PNL-10175 WHC-EP-0668
C-112	TFeCN	CWP 1C HS	X		Brinkmann PSA 2010	Not documented	Cores 34 and 36 and two simulants (INFARM-2 top and bottom). Hard copies of original data in Core Characterization Files.	PNL-10175

Table A.38. PSD Measurement Instrument and Test Conditions (MD = minimal disturbance; US = ultrasonic)

Tank	Waste Type		Particle Size Analysis				Comments	Reference
	Primary	Secondary	MD	US	Instrument	Suspending Liquid		
S-101	Unclassified		X		Microtrac X-100	Slurried in water	No mention made of sonication of these samples	PNNL-11636
S-104	R (boiling)	CWR	X		Brinkman PSA 2010	glycerin/water	PSD measured before and after sludge washing and caustic leaching.	PNL-10712
			Conditions of the measurements were not documented, but the data provided indicates that the Brinkman PSA 2010 at the 222-S Laboratory was used for these measurements.				Performed at 222-S. Procedure followed is TO44-A-01712F. Summary of data provided in WHC-SD-WM-ER-370. Particle size range for these measurements was 0.5 to 150 µm.	WHC-SD-WM-ER-370
			X		Leeds & Northrup UPA	Slurried in water	PSD measured on sludge sample and the leached sludge sample. Particle size range of this instrument is 3 nm to 6.5 µm.	LA-UR-95-2070
S-107	CWR	CWZr R (boiling)	X	X	Microtrac X-100	Slurried in water	Plots for unsonicated data only. Decrease in fraction of larger particles (> 80 µm) observed with sonication.	PNNL-11278
			X	X	Microtrac X-100	0.05 - 2 M NaOH 0.1 M $NaNO_3$	Multiple flow rates for both sonicated and unsonicated conditions. Measured at various steps through the leaching process.	PNNL-12010
S-111	R (non-boiling)	CWR	X	X	Microtrac X-100	Slurried in water	Leached samples only. Both sonicated and unsonicated data reported. Sonication appears to increase particle size. May be due to increasing the number of larger particles that were suspended.	PNNL-11636
			X		Horiba LA-910	Unknown	PSD performed in the fraction cell; therefore, minimal stirring and no circulation is performed during the measurement. Cores 237 segments 5 through 7.	HNF-1647
SX-108	R (boiling)		X	X	Microtrac X-100	Slurried in water	Plots for unsonicated data only. Only slight decrease in fraction of larger particles observed.	PNNL-11278
SX-113	Diatomaceous Earth		X		Leeds & Northrup UPA	Slurried in water	PSD measured on sludge sample and the leached sludge sample. Particle size range of this instrument is 3 nm to 6.5 µm.	LA-UR-97-2889
SY-101	No Sludge Reported		X		Horiba LA-910	Segment 16 supernatant liquid	PSD performed in the fraction cell; therefore, minimal stirring and no circulation is performed during the measurement. Cores 257 segments 2 and 7.	HNF-1666

Table A.38. PSD Measurement Instrument and Test Conditions (MD = minimal disturbance; US = ultrasonic)

Tank	Waste Type		Particle Size Analysis				Comments	Reference
	Primary	Secondary	MD	US	Instrument	Suspending Liquid		
SY-102	Unclassified	Z	X	X	Horiba LA-910	1 M NaOH 1 M $NaNO_3$	PSD performed at multiple stirring speeds (step 1 and 3) and sonication times including a delay in measurement from the completion of sonication. A circulation (flow) rate of 14.4 mL/s (Step 6 pump speed) was used for all samples.	HNF-8862
				X	Horiba LA-910	Water	PSD was performed on Pu-10 and fines fraction obtained from fractional decantation of tank waste sample. Circulation and agitation were constant (10.6 mL/s circulation and stir speed of 3). Varied sonication time (30 and 300 seconds).	CH2M-0400872
			X	X	Horiba LA-910	Water	PSD performed in the fraction cell; therefore, minimal stirring and no circulation is performed during the measurement. Sonication was performed in an external sonication bath. Core 284.	FH-0202775
			X	X	Microtrac X-100	Water 0.1 M $NaNO_3$ 1 M $NaNO_3$	PSD was measured as a function of ionic strength by varying the suspending liquid. The samples were also run sonicated and unsonicated to determine the relative effect of shearing the agglomerates.	PNNL-11352
SY-103	No Sludge Reported		X		Brinkman PSA 2010	Glycerin/water	PSD measured before and after sludge washing and caustic leaching. This tank appears to be a saltcake tank and does not appear to contain sludge waste.	PNL-10712
T-102	CWP	MW	X		Brinkman PSA 2010	50% glycerol	PSD measured on two unhomogenized samples from Core 55.	PNL-10101
T-104	1C		X		Brinkman PSA 2010	glycerin/water	PSD measured before and after sludge washing and caustic leaching.	PNL-10712
			X		Leeds & Northrup UPA	Slurried in water	PSD measured on sludge sample and the leached sludge sample. Particle size range of this instrument is 3 nm to 6.5 µm.	LA-UR-95-2070
T-107	1C	TBP CWP	X		Leeds & Northrup UPA	Slurried in water	PSD measured on sludge sample and the leached sludge sample. Particle size range of this instrument is 3 nm to 6.5 µm.	LA-UR-95-2070
T-110	2C	224	X	X	Mastersizer 2000	Slurried in water	PSDs were performed on dilutions of the tank samples at several different sonication powers including no sonication. Only the unsonicated data is reported in Revision 0. Revision 1 will include sonicated results.	PNNL-16133

Table A.38. PSD Measurement Instrument and Test Conditions (MD = minimal disturbance; US = ultrasonic)

Tank	Waste Type		Particle Size Analysis				Comments	Reference
	Primary	Secondary	MD	US	Instrument	Suspending Liquid		
T-111	224	2C	X		Brinkman PSA 2010	Glycerin/water	PSD measured before and after sludge washing and caustic leaching.	PNL-10712
T-203	224		X	X	Mastersizer 2000	Slurried in water	PSDs were performed on dilutions of the tank samples at several different sonication powers including no sonication. Only the unsonicated data is reported in Revision 0. Revision 1 will include sonicated results.	PNNL-16133
T-204	224		X	X	Mastersizer 2000	Slurried in water	PSDs were performed on dilutions of the tank samples at several different sonication powers including no sonication. Only the unsonicated data is reported in Revision 0. Revision 1 will include sonicated results.	PNNL-16133
TY-104	1CFeCN	TBP	X		Leeds & Northrup UPA	Slurried in water	PSD measured on sludge sample and the leached sludge sample. Particle size range of this instrument is 3 nm to 6.5 µm.	LA-UR-96-2839
U-110	R (boiling)	CWR 1C	X	X	Brinkman PSA 2010	glycerin/water	PSD measured before and after sludge washing and caustic leaching. Sonication was performed on the leach solutions to determine if sonication improved leachability.	PNL-10078
			X		Brinkman PSA 2010	Water 75% glycerin/ 25% ethanol	Particle size analysis was performed on every segment delivered to the laboratory. Water was used as a dispersant for cores 5 through 7 and segments 2 through 4 of core 14. Glycerine/ethanol was used as a dispersant for cores 8, 12, 13, 15, and segment 1 of core 14.	WHC-EP-0643

The following list contains the documents cited in Table A.38.

7S110-WSC-03-002, October 7, 2003, "Particle Size Distribution Analysis Results: Tank-241-AN-102, Core 307." Internal memorandum from WS Callaway to KG Carothers. CH2M Hill Hanford Group, Inc., Richland, Washington.

7S110-WSC-05-011, March 18, 2005, "Particle Size Measurements in Support of the Tank 241 AN 102 Chemistry Control Recovery Plan." Internal memorandum from W. S. Callaway, G. A. Cooke, and D. L. Herting to K. G. Carothers. CH2M HILL Hanford Group, Inc., Richland, Washington.

7S110-WSC-03-012, December 12, 2003, "Particle Size Distribution Analysis of Samples from Tank 241 AZ 102, Core 310." Internal memorandum from W. S. Callaway to K. G. Carothers. CH2M HILL Hanford Group, Inc., Richland, Washington.

7S110-WSC-06-148, January 24, 2006, "Particle Size Distribution Measurements on Samples from Tank 241-AY-102 Core 319." Internal memorandum from W. S. Callaway to K. G. Carothers. CH2M HILL Hanford Group, Inc., Richland, Washington.

B3610-WSC-02-028, December 26, 2002, "Particle Size Distribution Analysis Results: Tank 241 AN 107, Core 304." Internal memorandum from W. S. Callaway to H. L. Baker. Fluor Hanford, Inc., Richland, Washington.

BNFL-RPT-030, 2000, "Characterization, Washing, Leaching, and Filtration of C-104 Sludge." Prepared by Battelle – Pacific Northwest Division, Richland, Washington.

BNFL-RPT-038, 2000, "Characterization, Washing, Leaching, and Filtration of AZ-102." Prepared by Battelle – Pacific Northwest Division, Richland, Washington.

Brooks et al. 1996. "Sludge Pretreatment Studies Using Hanford Tank C-107." Letter report prepared for Westinghouse Hanford Company by Pacific Northwest National Laboratory, Richland, Washington.

CH2M-0400872, May 17, 2004, "Distribution of Plutonium-Rich Particles in Tank 241-SY-102 Sludge." External letter from W. S. Callaway and G. A. Cooke to K. H. Abel, BNI. CH2M HILL Hanford Group, Inc., Richland, Washington.

FH-0201635, April 9, 2002, "Particle Size Distribution Analysis Results: Tank 241-AY-101, Cores 275 and 277." External letter from W. S. Callaway to J. H. Baldwin, CH2M HILL. Fluor Hanford, Inc., Richland, Washington.

FH-0201835, April 24, 2002, "Particle Size Distribution Analysis Results: Tank 241-C-107, Cores 287 and 288." External letter from W. S. Callaway to J. H. Baldwin, CH2M HILL. Fluor Hanford, Inc., Richland, Washington.

FH-0202392, May 28, 2002, "Particle Size Distribution Analysis Results: Tank 241-AY-102, Cores 289 and 290." External letter from W. S. Callaway to J. H. Baldwin, CH2M HILL. Fluor Hanford, Inc., Richland, Washington.

FH-0202775, June 18, 2002, “Particle Size Distribution Analysis Results: Tank 241-SY-102, Core 284.” External letter from W. S. Callaway to J. H. Baldwin, CH2M HILL. Fluor Hanford, Inc., Richland, Washington.

Gray et al., 1993, “Characterization of the First Core Sample of Neutralized Current Acid Waste from Double-Shell Tank 102-AZ,” (unnumbered report), Pacific Northwest National Laboratory, Richland, Washington.

Gray et al., 1993, “Characterization of the Second Core Sample of Neutralized Current Acid Waste from Double-Shell Tank 101-AZ.” Unnumbered report, Pacific Northwest National Laboratory, Richland, Washington.

HNF-1647, 1999, Tank 241-S-l11, Core 237 Analytical Results for the Final Report, Rev. 0A, Waste Management of Hanford, Inc., for Fluor Daniel Hanford, Inc., Richland, Washington.

HNF-1666, 1999, “Tank 241-SY-101, Cores 255, 256, and 257, Analytical Results for the Final Report” (Rev. 0A). Waste Management of Hanford, Inc., for Fluor Daniel Hanford, Inc., Richland, Washington.

HNF-3352 Rev. 0, 1998, “Results of Dilution Studies with Waste from Tank 241 AN 104.” Fluor Daniel Hanford Inc., Richland, Washington.

HNF-4964 Rev. 0A, 2000, “Results of Dilution Studies with Waste from Tank 211-AW-101.” Fluor Hanford Inc., Richland, Washington.

HNF-7078 Rev. 0A, 2002, “Results of Retrieval Testing of Sludge from Tank 241-AZ-101.” Fluor Hanford, Inc., Richland, Washington.

HNF-8862 Rev. 0, 2002, “Particle Property Analyses of High-Level Waste Tank Sludges.” Fluor Hanford, Inc., Richland, Washington.

HNF-SD-WM-DTR-046 Rev. 0, 1999, “Results of Dilution Studies with Waste from Tank 241-AN-105.” Fluor Daniel Hanford Inc., Richland, Washington.

LA-UR-95-2070, 1995, “Sludge Washing and Alkaline Leaching Tests on Actual Hanford Tank Sludge: A Status Report.” Los Alamos National Laboratory, Los Alamos, New Mexico.

LA-UR-96-2839, 1996, “Sludge Water Washing and Alkaline Tests on Actual Hanford Tank Sludge: FY 1996 Results.” Los Alamos National Laboratory, Los Alamos, New Mexico.

LA-UR 97-2889, 1997, “Sludge Water Washing and Alkaline Tests on Actual Hanford Tank Sludge: FY 1997 Results.” Los Alamos National Laboratory, Los Alamos, New Mexico.

Peters, July 22, 1988, “Tank 101-AY Sludge Particle Size Analysis.” Unnumbered memorandum to R.S. Edrington. Westinghouse Hanford Company, Richland, Washington.

Peterson, February 28, 1990, “Preliminary Results—Analysis of Waste Layers from DST 101-AZ Core #2.” Letter 9001040 to A.J. DiLiberto and L.M. Sasaki. Pacific Northwest National Laboratory, Richland, Washington.

PNL-10078, 1995, “Washing and Alkaline Leaching of Hanford Tank Sludges: A Status Report.” Pacific Northwest National Laboratory, Richland, Washington.

PNL-10099, 1994, “Tank Characterization Report for Single-Shell Tank B-111.” Pacific Northwest National Laboratory, Richland, Washington.

PNL-10101, 1994, “Tank Characterization Report for Single-Shell Tank T-102.” Pacific Northwest National Laboratory, Richland, Washington.

PNL-10175, 1994, “Ferrocyanide Safety Project: Comparison of actual and simulated ferrocyanide waste properties.” Pacific Northwest National Laboratory, Richland, Washington.

PNL-10712, 1995, “Washing and Caustic Leaching of Hanford Tank Sludges: Results of FY 1995 Studies.” Pacific Northwest National Laboratory, Richland, Washington.

PNNL-11025, 1996, “Comparison of simulants to actual neutralized current acid waste: process and product testing of three NCAW core samples from Tanks 101-AZ and 102-AZ.” Pacific Northwest National Laboratory, Richland, Washington.

PNNL-11098, 1996, “Comparison of simulants to actual neutralized current acid waste: Process and product testing of three NCAW core samples from Tanks 101-AZ and 102-AZ.” Pacific Northwest National Laboratory, Richland, Washington.

PNNL-11278 Rev. 1, 1996, “Washing and Leaching of Hanford Sludges: Results of FY 1996 Studies.” Pacific Northwest National Laboratory, Richland, Washington.

PNNL-11352, 1996, “Tank SY-102 Waste Retrieval Assessment: Rheological Measurements and Pump Jet Mixing Simulations.” Pacific Northwest National Laboratory, Richland, Washington.

PNNL-11381 Rev. 1, 1996, “Washing and Caustic Leaching of Hanford Tank C-106 Sludge.” Pacific Northwest National Laboratory, Richland, Washington.

PNNL-11580, 1997, “Caustic Leaching of Composite AZ-101/AZ-102 Hanford Tank Sludge.” Pacific Northwest National Laboratory, Richland, Washington.

PNNL-11636, 1997, “Washing and Leaching of Hanford Sludges: Results of FY 1997 Studies.” Pacific Northwest National Laboratory, Richland, Washington.

PNNL-12010, 1998, “Bench-Scale Enhanced Sludge Washing and Gravity Settling of Hanford Tank C-107 Sludge.” Pacific Northwest National Laboratory, Richland, Washington.

PNNL-13028, 1999, “Characterization of the First Core Sample of Neutralized Current Acid Waste from Double-Shell Tank 101-AZ.” Pacific Northwest National Laboratory, Richland, Washington.

PNNL-16133, 2006, “Characterization and Correlation of Particle-Level Interactions to the Macroscopic Rheology of Powders, Granular Slurries, and Colloidal Suspensions.” Pacific Northwest National Laboratory, Richland, Washington.

RPP-5798 Rev. 0, 2002, “Results of Retrieval Studies with Waste from Tank 241-C-104.” Fluor Hanford, Inc., Richland, Washington.

RPP-9806 Rev. 0, 2002, “Results of Retrieval Testing of Sludge from Tank 241-AZ-102.” Fluor Hanford, Inc., Richland, Washington.

WHC-EP-0643, 1993, Tank characterization report for single-shell tank 241-U-110, Westinghouse Hanford Company, Richland, Washington.

WHC-EP-0668, 1993, “Tank characterization report: Tank 241-C-109.” Westinghouse Hanford Company, Richland, Washington.

WHC-EP-0739, 1994, “Tank characterization report for Single-Shell Tank 241-BX-107.” Westinghouse Hanford Company, Richland, Washington.

WHC-SD-WM-ER-370, “Tank characterization report for single-shell tank 241-S-104.” Westinghouse Hanford Company, Richland, Washington.

WHC-SD-WM-TI-540, 1992, “Analysis report for 241-BY-104 auger samples.” Westinghouse Hanford Company, Richland, Washington.

WTP-RPT-021 Rev. 1, 2002, “Chemical and Physical Properties Testing of 241-AN-102 Tank Waste Blended with 241-C-104 Wash/Leachate Solutions.” Battelle – Pacific Northwest Division, Richland, Washington.

WTP-RPT-043 Rev. 1, 2003, “Filtration, Washing, and Caustic Leaching of Hanford Tank AZ-101 Sludge.” Battelle – Pacific Northwest Division, Richland, Washington.

WTP-RPT-048 Rev. 1, 2004, “Chemical Analysis and Physical Properties Testing of 241-AZ-101 Tank Waste Supernatant and Centrifuged Solids.” Battelle – Pacific Northwest Division, Richland, Washington.

WTP-RPT-076, 2003, “Chemical Analysis and Physical Properties Testing of 241-AZ-101 Tank Waste Supernatant and Centrifuged Solids.” Battelle – Pacific Northwest Division, Richland, Washington.

Appendix B

List of Waste Type Acronyms and Their Meanings

Appendix B – List of Waste Type Acronyms and Meanings

The list of waste type definitions in Table B.1 was adapted from Meacham (2003) with some additions from Higley and Place (2004) as identified in TWINS.(a)

Table B.1. List of Waste Type Definitions

Waste Type	Definition
1C	$BiPO_4$ first cycle decontamination waste (1944-1956)
1C1	$BiPO_4$ first cycle decontamination waste and coating waste (1944-1949). Note: In this document and in TWINS 1C1 and 1C2 were combined to form waste type 1C.
1C2	$BiPO_4$ first cycle decontamination waste and coating waste (1950-1956). Note: In this document and in TWINS 1C1 and 1C2 were combined to form waste type 1C.
1CFeCN	ferrocyanide sludge from in-farm scavenging of 1C supernatants in TY-Farm (1955-1958)
224	lanthanum fluoride process “224 Building” waste (1944-1956)
224-1	lanthanum fluoride process 224 Building waste (1944-1949). Note: In this document 224-1 and 224-2 were combined to form waste type 224.
224-2	lanthanum fluoride process 224 Building waste (1950-1956). Note: In this document 224-1 and 224-2 were combined to form waste type 224.
2C	$BiPO_4$ second cycle decontamination waste (1944-1956)
2C1	$BiPO_4$ second cycle decontamination waste (1944-1949). Note: In this document and in TWINS 2C1 and 2C2 were combined to form waste type 1C.
2C2	$BiPO_4$ second cycle decontamination waste (1950-1956) and low activity cell 5-6 drainage waste (June 1951–1956). Note: In this document and in TWINS 2C1 and 2C2 were combined to form waste type 1C.
A1-SltCk	saltcake from first 242-A Evaporator campaign using 241-A-102 feed tank (1977-1980).
A2-SltSlr	saltcake from the second 242-A Evaporator campaign (1981-1994).
AR	washed PUREX sludge (1967-1976)
B	high-level acid waste from PUREX processed at B Plant for Sr recovery (1967-1972)
B-SltCk	Saltcake from 242-B Evaporator operation (1951-1953)
BL	low-level waste from B Plant Sr and Cs recovery operations (1967-1976)
BY-SltCk	Saltcake from in-tank solidification (ITS) in BY-Farm (1965-1974)
CEM	Portland cement
CWP	PUREX cladding waste (1956-1960 and 1961-1972)
CWP1	PUREX cladding waste, aluminum clad fuel (1956-1960). Note: In this document CWP1 and CWP2 are combined into a single waste type (CWP).
CWP2	PUREX cladding waste, aluminum clad fuel (1961-1972). Note: In this document CWP1 and CWP2 are combined into a single waste type (CWP).
CWR	REDOX cladding waste, aluminum clad fuel (1952-1960 and 1961-1972)
CWR1	REDOX cladding waste, aluminum clad fuel (1952-1960). Note: In this document CWR1 and CWR2 are combined into a single waste type (CWR).
CWR2	REDOX cladding waste, aluminum clad fuel (1961-1966). Note: In this document CWR1 and CWR2 are combined into a single waste type (CWR).
CWZr	zirconium cladding waste (PUREX and REDOX)
CWZr1	PUREX (and REDOX) zirconium cladding waste, (1968-1972) Note: In this document

---

(a) TWINS database (http://twinsweb.pnl.gov).

	CWZr1 and CWZr2 are combined into a single waste type (CWZr).
CWZr2	PUREX zirconium cladding waste, (1983-1989) Note: In this document CWZr1 and CWZr2 are combined into a single waste type (CWZr).
DE	diatomaceous earth
HS	hot semi-works ^{90}Sr recovery waste (1962-1967)
MW	$BiPO_4$ process metal waste (1944-1956)
MW1	$BiPO_4$ metal waste (1944-1949) Note: In this document MW1 and MW2 are combined in a single waste type (MW).
MW1	$BiPO_4$ metal waste (1950-1956) Note: In this document MW1 and MW2 are combined in a single waste type (MW).
OWW3	PUREX organic wash waste (1968-1972)
P2	PUREX high-level waste (1963-1967)
P3	PUREX high-level waste (1983-1990)
P3AZ1	PUREX high-level waste to AZ-101 (1983-March 13, 1986) Note: In this document P3AZ1 and P3AZ2 are combined in a single waste type (P3).
P3AZ1	PUREX high-level waste to AZ-102 (March 13, 1986-1990) Note: In this document P3AZ1 and P3AZ2 are combined in a single waste type (P3).
PFeCN	ferrocyanide sludge from in-plant scavenged supernatant
PL2	PUREX low-level waste (1983-1988)
R (boiling)	boiling REDOX high-level waste
R (non-boiling)	non-boiling REDOX high-level waste
R1	REDOX high-level waste (1952-1958) Note: Depending on the thermal history of the waste, this waste type was classified as R (boiling) or R (non-boiling) in this document.
R2	REDOX high-level waste (1959-1966) Note: Depending on the thermal history of the waste, this waste type was classified as R (boiling) or R (non-boiling) in this document.
R-SltCk	saltcake from self-concentration in S- and SX-Farms (1952-1966)
S1-SltCk	saltcake from the first 242-S Evaporator campaign using 241-S-102 feed tank (1973-1976)
S2-SltCk	saltcake from the second 242-S Evaporator campaign using 241-S-102 feed tank (1977-1980)
SRR	high-level waste transfers (late B Plant operations)
T2-SltCk	Saltcake from the last 242-T Evaporator campaign (1965-1976)
TBP	tributyl phosphate waste (from solvent based uranium recovery operations)
TFeCN	ferrocyanide sludge produced by in-tank or in-farm scavenging
TH	PUREX waste from processing of thoria targets
TH1	thoria process wastes (1966). In this document TH1 and TH2 were combined in a single waste type (TH).
TH2	thoria process wastes (1970). In this document TH1 and TH2 were combined in a single waste type (TH).
Z	Z Plant waste

References

Higley BA and DE Place. 2004. *Hanford Defined Waste Model – Revision 5*. RPP-19822, CH2M HILL Hanford Group, Inc., Richland, Washington.

Meacham JE. 2003. *Aluminum Wash and Leach Factors*. RPP-11079, CH2M Hill Hanford Group, Richland, Washington.

Appendix C

Summary of Non-Salt Compounds Observed in Sludge Layers

Appendix C – Summary of Non-Salt Compounds Observed in Sludge Layers

Table C.1 is included to illustrate the extent to which various waste types were represented in the samples that have been used in this study. The table is qualitative to some extent; it indicates only which tanks the observed samples came from, not which layer or layers. Many of the samples were composites and therefore were potentially mixtures of layers, making it difficult to be more specific about which layer was present.

The first column of Table C.1 shows the sludge type, as defined in the November 2006 BBI, and the fraction of the total bulk solid waste (whether salt or sludge) that consists of that sludge type (as of November 2006). The sludge types are listed in order of decreasing volume that is present in Hanford waste; the most common types first. The second column gives the tanks that contain each type of waste. Within each sludge type, tanks are listed in order of decreasing volume of the sludge type, the tanks containing the largest volumes of the sludge type first. Note that many tanks appear under more than one category because they contain more than one type of sludge.

The observations listed in the final two columns of the table are of two types. First are the images used to derive size-distribution information. The observed compounds and number of images are given; the references are as listed in Appendix D. The last column lists any additional compounds that have been observed in samples from the tank[a,b] (LaFemina 1995; Temer 1995; Lumetta 1996a, 1996b, 1997, 1998; Temer 1996, 1997; Rapko and Lumetta 2000; Herting et al. 2002, 2004; Buck et al. 2003; Buck and McNamara 2004; Warrant and Cooke 2003; Krupka et al. 2006). The data in the table may include compounds observed in either unleached or caustic-leached samples or both. Though leaching can create new compounds that are not representative of the original waste, it can also make pre-existing compounds more observable by concentrating them in the leached residuum.

Images of non-salt particles that were taken from tanks that contain only salt layers (e.g., AN-102 and AN-107) were also used in this study. These images were noted in Section 3.2.2 and are not included here.

(a) Herting DL. 8/28/2003. "Caustic Demand Test Results, Tank 241-AN-102 Sludges." FH-0303343, Fluor Hanford, Inc., Richland, Washington.

(b) Herting DL. 7/28/2005. "Tank 241-AN-102 Process Chemistry Test Results." 7S110-DLH-05-028, CH2M HILL Hanford Group, Inc., Richland, Washington.

Table C.1. Summary of Non-Salt Compounds Observed in Sludge Layers

Waste Type	Tank Name	Images Used to Set PSD Parameters	Other Identified Non-Salt Compounds
1C (7.1% of bulk solids volume)	TX-109 (no obs.)[a]		
	BX-107	---[b]	$AlPO_4$, $Al(OH)_3$, aluminosilicate, $Bi/FePO_4$, Bi_2O_3, $Fe_2Bi(SiO_4)_2OH$
	T-104	---	$AlPO_4$, $Al(OH)_3$, aluminosilicate, $Na_2Fe_2Al(PO_4)_3$, $Fe_2Bi(SiO_4)_2OH$, Bi_2O_3, $Bi_{24}Al_2O_{39}$, $Bi^{38}CrO^{60}$, Cr phosphate, UO_2 phosphate hydrate, $FeFe_2(PO_4)_2(OH)_2$, $Na_2Fe_2Al(PO_4)_3$, $Bi_{36}Fe_2O_{57}$, Bi metal
	C-110, BX-112 (no obs.)		
	T-107	---	gibbsite, aluminosilicate, $AlPO_4$, $NaAlCO_3(OH)_2$, NO_3-cancrinite, Al or Al/Fe
	C-107	1 image: $BiPO_4$	$Al(OH)_3$, $(Al_2O_3)_x$•$(H_2O)_y$, clays, $Pb_5OH(PO_4)_3$, Fe_3O_4, FeOOH, $Al(OH)_3$, cancrinite, ZrO_2
	B-104	---	$KMg_3(Si_3AlO)\cdot 10H_2O$, mixed Fe-Bi-Si-Al-U-Ca-Cr-Na phase
	TX-113, B-107, B-106, TX-111 (no obs.)		
	BX-110	---	$Fe_2Bi(SiO_4)_2OH$, $Bi_2Fe_4O_9$, Bi metal
	TX-110, BX-111 (no obs.)		
	U-110	---	gibbsite, boehmite
	C-108	---	gibbsite, $Ca_3(PO_4)_2$, $Ca_5OH(PO_4)_3$, $Ca_5F(PO_4)_3$; $Ca(PO_3)_2$, $Ca_{10}(PO_4)_6S$
	C-112	---	gibbsite, SiO_2, CaU_2O_7, $Na_2U_2O_7$, boehmite, aluminosilicate
	C-111, U-111, U-112, B-105, BX-108 (no obs.)		
	C-109	---	gibbsite, SiO_2, boehmite, Ni aluminum oxide, $Ni(OH)_2$, UO_3
	T-106, T-108, TX-114, T-105 (no obs.)		
2C (4.2% of bulk solids volume)	T-110 (no obs.)		
	B-110	---	aluminosilicate, $BiPO_4$
	B-111	---	aluminosilicate, $Bi_{38}CrO_{60}$, $Fe(OH)_3$, Bi_2O_3, $Fe_2Bi(SiO_4)_2OH$
	T-111	---	$La_4(P_2O_7)_3$, $Ca_5OH(PO_4)_3$, $Bi/FePO_4$, $Fe(OH)_3$, Mn_2MnO_4, Fe_2MnO_4, FeOOH, Bi/Fe silicate hydroxide
	B-104	---	$KMg_3(Si_3AlO)\cdot 10H_2O$, mixed Fe-Bi-Si-Al-U-Ca-Cr-Na phase
	T-105, T-112, B-105, B-112 (no obs.)		
R (boiling) (3.6% of bulk solids volume)	SX-104, SX-114 (no obs.)		
	S-107	---	boehmite. clays, ZrO_2, FeOOH, UO_3
	S-104	1 image: boehmite 1 image: U_3O_8 1 image: $UO_3\cdot 2H_2O$	aluminosilicate, $FeMnO_4$, $Al_{45}O_{45}(OH)_{44}Cl$
	U-110	---	gibbsite, boehmite
	SX-111, SX-107, SX-103, S-110, SX-112 (no obs.)		
	SX-108	---	boehmite, FeOOH, β-U_3O_8, clays, $(Al_2O_3)_x$•$(H_2O)_y$, $Ca_3Al_2O_6$, $(Mn,Fe)_3O_4$
	SX-109, SX-115, SX-113 (no obs.)		
TBP	TY-105 (no obs.)		

Waste Type	Tank Name	Images Used to Set PSD Parameters	Other Identified Non-Salt Compounds
(2.4% of bulk solids volume)	BX-109	---	nordstrandite ($Al(OH)_3$), $Na_2U_2O_7$
	B-106, TY-103 (no obs.)		
	C-101	1 image: gibbsite 1 image: Fe_2O_3 1 image: $Na_2U_2O_7$	---
	C-108	---	gibbsite, $Ca_3(PO_4)_2$, $Ca_5OH(PO_4)_3$, $Ca_5F(PO_4)_3$, $Ca(PO_3)_2$, $Ca_{10}(PO_4)_6S$
	BX-108, BX-102 (no obs.)		
	T-107	---	gibbsite, aluminosilicate, $AlPO_4$, $NaAlCO_3(OH)_2$, NO_3-cancrinite, Al or Al/Fe
	C-102, BX-101 (no obs.)		
	BX-105	---	gibbsite
	BX-104 (no obs.)		
	C-105	---	gibbsite, $UO_3 \bullet H_2O$, $Na_2U_2O_7$
	TY-104, TX-115 (no obs.)		
	BX-103	---	gibbsite, $Na_2U_2O_7$
	BX-106, TX-108, TY-106 (no obs.)		
Unknown sludge (2.0% of bulk solids volume)	AP-108, AP-106 (no obs.)		
	AY-102	2 images: gibbsite 1 image: $LaPO_4 \bullet 2H_2O$ 1 image: Fe_2O_3 1 image: $NaAlCO_3(OH)_2$ 1 image: ZrO_2 1 image: Ag_2CO_3	cancrinite,
	AY-101 (no obs.)		
	SY-102	1 image: $Na_2U_2O_7$ 1 image: ZrO_2 1 image: $CaCO_3$ 1 image: Fe_2O_3 1 image: Ag_2CO_3 11 images: Pu oxide 5 images: Pu/Bi rich 2 images: Pu/Bi/P rich	gibbsite
	C-104, TX-118 (no obs.)		
	BX-110	---	$Fe_2Bi(SiO_4)_2OH$, $Bi_2Fe_4O_9$, Bi metal
	AP-102, AP-103, AN-106 (no obs.)		
	AZ-101	1 image: Fe_2O_3 1 image: $Mn(OH)_2$ 2 images: U oxide	gibbsite, boehmite, $FeZrPO_4.4H_2O$, $FeCr_2O_4$, Pb
	AW-102 (no obs.)		
	C-106	1 image: gibbsite 1 image: Fe_2O_3 1 image: $NaAlCO_3(OH)_2$ 1 image: Ag_2CO_3 2 images: $Na_4(UO_2)(CO_3)_3$ 1 image: $Mn_3(PO4)_2$ 1 image: $MnCO_3$	cancrinite, FeOOH, Ag_2O, ZrO_2, $Na_3MnPO_4CO_3$
	AZ-102	1 image: gibbsite	aluminosilicate
CWP2 (1.9% of bulk solids volume)	C-102, C-104 (no obs.)		
	BX-103	---	gibbsite, $Na_2U_2O_7$
	B-109, B-108 (no obs.)		
	BX-105	---	gibbsite

Waste Type	Tank Name	Images Used to Set PSD Parameters	Other Identified Non-Salt Compounds
	BY-109	---	$Na_2U_2O_7/U_3O_8$, $(Ca,Sr)_3(Cr,Al)_2(OH)_2$
	C-107	1 image: $BiPO_4$	$Al(OH)_3$, $(Al_2O_3)_x \cdot (H_2O)_y$, clays, $Pb_5OH(PO_4)_3$, Fe_3O_4, FeOOH, $Al(OH)_3$, cancrinite, ZrO_2
	BX-102, T-102, T-103, BX-104, BX-101, B-107, BY-103 (no obs.)		
	T-107	---	gibbsite, aluminosilicate, $AlPO_4$, $NaAlCO_3(OH)_2$, NO_3-cancrinite, Al or Al/Fe
	BX-106 (no obs.)		
R1 (1.8% of bulk solids volume)	SX-101, TX-101, SX-102, S-111, SX-105, U-102, TX-104, U-101, S-102, U-112, S-109, U-111, U-103, S-103, S-108, TX-106, S-105, (no obs.)		
	S-112	---	$(Ca,Sr)_3(Cr,Al)_2(OH)_2$
224-2 (1.5% of bulk solids volume)	T-111	---	$La_4(P_2O_7)_3$, $Ca_5OH(PO_4)_3$, $Bi/FePO_4$, $Fe(OH)_3$, Mn_2MnO_4, Fe_2MnO_4, FeOOH, Bi/Fe silicate hydroxide
	B-203, B-204, T-203, T-204 (no obs.)		
	B-202	---	mixed Fe-Bi-Si-Al-U-Ca-Cr-Na phase
	T-112, T-202 (no obs.)		
	T-110	---	$BiPO_4$
CWZr2 (1.4% of bulk solids volume)	AW-103 (no obs.)		
	AW-105	---	$Al(OH)_3$, aluminosilicate
CWR1 (1.2% of bulk solids volume)	S-107	---	boehmite. clays, ZrO_2, FeOOH, UO_3
	U-110	---	gibbsite, boehmite
	U-105, BX-104, U-109, T-105 (no obs.)		
	S-104	1 image: boehmite 1 image: U_3O_8 1 image: $UO_3 \cdot 2H_2O$	aluminosilicate, $FeMnO_4$, $Al_{45}O_{45}(OH)_{44}Cl$
	S-110, U-112, U-107 (no obs.)		
	S-111	---	α-$Al(OH)_3$ (bayerite), boehmite, $FeCr_2O_4$, Mn_2CrO_4, $Mn_{1.5}Cr_{1.5}O_4$, UO_3
	T-106, T-103, U-201, U-202, U-203, U-204 (no obs.)		
CWP1 (1.1% of bulk solids volume)	C-105	---	gibbsite, $UO_3 \cdot H_2O$, $Na_2U_2O_7$
	C-104 (no obs.)		
	C-101	1 image: gibbsite 1 image: Fe_2O_3 1 image: $Na_2U_2O_7$	---
	C-102, C-111 (no obs.)		
	C-112	---	gibbsite, SiO_2, CaU_2O_7, $Na_2U_2O_7$, boehmite, aluminosilicate
	C-109	---	gibbsite, SiO_2, boehmite, Ni aluminum oxide, $Ni(OH)_2$, UO_3
	C-103	1 image: gibbsite 1 image: Fe_2O_3	cancrinite---
PFeCN (0.78% of bulk solids volume)	BY-104	---	$Ni(OH)_2$, $(Al_2O_3)_x \cdot (H_2O)_y$, aluminosilicate, $Fe(Fe,Cr)_2O_4$, $Ca_5OH(PO_4)_3$, β-U_3O_8, $Ni_3O_2(OH)_4$, FeOOH
	BY-110	---	$Ca_5OH(PO_4)_3$, CrOOH, β-U_3O_8, $Ni_3O_2(OH)_4$, γ-Fe_2O_3, Fe/Si phase
	BY-105 (no obs.)		
	BY-108	---	$Ca_xSr_{10-x}(PO_4)_6(OH)_2$, β-U_3O_8, γ-Fe_2O_3, FeOOH,
	BY-101, BY-106, BY-107 (no obs.)		

Waste Type	Tank Name	Images Used to Set PSD Parameters	Other Identified Non-Salt Compounds
Unknown (boiling) (0.72% of bulk solids volume)	S-101	1 image: boehmite	diaspore (AlOOH), aluminosilicate, Mn/FeOOH
DE (0.66% of bulk solids volume)	TX-116, U-104, BX-102, TX-117, SX-113, TY-106 (no obs.)		
Unknown (0.48% of bulk solids volume)	S-102 (no obs.)		
1CFeCN (0.45% of bulk solids volume)	TY-101, TY-103, TY-104 (no obs.)		
SRR (0.45% of bulk solids volume)	C-107	1 image: $BiPO_4$	$Al(OH)_3$, $(Al_2O_3)_x$•$(H_2O)_y$, clays, $Pb_5OH(PO_4)_3$, Fe_3O_4, FeOOH, $Al(OH)_3$, cancrinite, ZrO_2
	A-106 (no obs.)		
	AZ-102	1 image: gibbsite	aluminosilicate
	AX-101 (no obs.)		
TFeCN (0.43% of bulk solids volume)	C-112	---	gibbsite, SiO_2, CaU_2O_7, $Na_2U_2O_7$, boehmite, aluminosilicate
	C-109	---	gibbsite, SiO_2, boehmite, Ni aluminum oxide, $Ni(OH)_2$, UO_3
	C-111 (no obs.)		
	C-108	---	gibbsite, $Ca_3(PO_4)_2$, $Ca_5OH(PO_4)_3$, $Ca_5F(PO_4)_3$, $Ca(PO_3)_2$, $Ca_{10}(PO_4)_6S$
CWR2 (0.38% of bulk solids volume)	S-107	---	boehmite. clays, ZrO_2, FeOOH, UO_3
	T-101, U-108, T-106 (no obs.)		
PL2 (0.23% of bulk solids volume)	AW-104 (no obs.)		
	AW-105	---	$Al(OH)_3$, aluminosilicate
	AZ-102	1 image: gibbsite	aluminosilicate
P3AZ2 (0.22% of bulk solids volume)	AZ-102	1 image: gibbsite	aluminosilicate
R2 (0.19% of bulk solids volume)	SX-110, SX-105 (no obs.)		
224-1 (0.18% of bulk solids volume)	B-201, T-201 (no obs.)		
BL (0.18% of bulk solids volume)	B-101 (no obs.)		
	AY-102	2 images: gibbsite 1 image: $LaPO_4$•$2H_2O$ 1 image: Fe_2O_3 1 image: $NaAlCO_3(OH)_2$ 1 image: ZrO_2 1 image: Ag_2CO_3	cancrinite
	BX-101 (no obs.)		
CWZr1 (0.18% of bulk solids volume)	S-107	---	boehmite. clays, ZrO_2, FeOOH, UO_3
	C-104, C-102 (no obs.)		
P2 (0.17% of bulk solids volume)	A-105, AX-103, AX-104, A-101 (no obs.)		
MW1 (0.16% of bulk solids volume)	BX-104, C-102, B-101 (no obs.)		
	BX-105	---	gibbsite
	B-103 (no obs.)		
AR (0.15% of bulk solids volume)	A-104, A-106, A-103 (no obs.)		
Z (0.15% of bulk solids volume)	SY-102	1 image: $Na_2U_2O_7$ 1 image: ZrO_2 1 image: $CaCO_3$	gibbsite

Waste Type	Tank Name	Images Used to Set PSD Parameters	Other Identified Non-Salt Compounds
		1 image: Fe_2O_3 1 image: Ag_2CO_3 11 images: Pu oxide 5 images: Pu/Bi rich 2 images: Pu/Bi/P rich	
	TX-101 (no obs.)		
P3AZ1 (0.14% of bulk solids volume)	AZ-101	1 image: Fe_2O_3 1 image: $Mn(OH)_2$ 2 images: U oxide	gibbsite, boehmite, $FeZrPO_4.4H_2O$, $FeCr_2O_4$, Pb
B (0.13% of bulk solids volume)	B-111	---	aluminosilicate, $Bi_{38}CrO_{60}$, $Fe(OH)_3$, Bi_2O_3, $Fe_2Bi(SiO_4)_2OH$
	AX-102, B-101 (no obs.)		
	B-110	---	aluminosilicate, $BiPO_4$
OWW3 (0.084% of bulk solids volume)	C-104 (no obs.)		
TH1 (0.080% of bulk solids volume)	C-102 (no obs.)		
MW2 (0.070% of bulk solids volume)	TX-105, TX-101, BY-112, T-102, TX-102, TX-108, T-103, TX-106, U-104 (no obs.)		
TH2 (0.065% of bulk solids volume)	C-104 (no obs.)		
HS (0.044% of bulk solids volume)	C-109	---	gibbsite, SiO_2, boehmite, Ni aluminum oxide, $Ni(OH)_2$, UO_3
	C-111 (no obs.)		
	C-204	---	$Na_4(UO_2)(CO_3)_3$
	C-112	---	gibbsite, SiO_2, CaU_2O_7, $Na_2U_2O_7$, boehmite, aluminosilicate
	C-202, C-201 (no obs.)		
	C-203	---	$Na_4(UO_2)(CO_3)_3$
Portland cement (0.024% of bulk solids volume)	BY-105 (no obs.)		
P1 (0.003% of bulk solids volume)	A-104 (no obs.)		
No solids layer in BBI; sample was evaporated	AP-101	1 image: NO_3-cancrinite	---

(a) No observations for the tank(s).
(b) No observations of this kind.
All BBI data were taken from TWINS in November 2006. In tanks where boiling REDOX waste had been added, R1 and R2 waste types are referred to simply as R waste; R1 and R2 are added together in those boiling tanks in which both are present. The relevant tanks are listed in Section 3.2.1.3.

References

Buck EC and BK McNamara. 2004. "Precipitation of Nitrate-Cancrinite in Hanford Tank Sludge." *Environ. Sci. Technol*. 38, pp. 4432-4438.

Buck EC, BW Arey, SK Fiskum, JGH Geeting, ED Jensen, BK McNamara, and AP Poloski. 2003. *Identification of Washed Solids from Hanford Tanks 241-AN-102 and 241-AZ-101 with X-ray Diffraction, Scanning Electron Microscopy, and Light-Scattering Particle Analysis*. PNWD-3300 (WTP-RPT-076 Rev. 0), Battelle – Pacific Northwest Division, Richland, Washington.

Herting DL, GA Cooke, and RW Warrant. 2002. *Identification of Solid Phases in Saltcake from Hanford Site Waste Tanks*. HNF-11585 Rev. 0, Fluor Hanford, Inc., Richland, Washington.

Herting DL, GA Cooke, and RW Warrant. 2004. *Hanford Tank 241-AN-107 Solid Phase Characterization*, RPP-20018, CH2M HILL Hanford Group, Inc., Richland, Washington.

Krupka KM, HT Schaef, BW Arey, SM Heald, WJ Deutsch, and KJ Lindberg. 2006. "Cantrell, Residual Waste from Hanford Tanks 241-C-203 and 241-C-204. 1. Solids Characterization." *Environ. Sci. Technol.*, 40:3749–3754.

LaFemina JP. 1995. *Tank Waste Treatment Science Task Quarterly Report for April-June 1995*. PNL-10764, Pacific Northwest Laboratory, Richland, Washington.

Lumetta GJ, BM Rapko, MJ Wagner, J Liu, and YL Chen. 1996a. *Washing and Caustic Leaching of Hanford Tank Sludges: Results of FY 1996 Studies*. PNNL-11278 Rev. 1, Pacific Northwest National Laboratory, Richland, Washington.

Lumetta GJ, MJ Wagner, FV Hoopes, and RT Steele. 1996b. *Washing and Caustic Leaching of Hanford Tank C-106 Sludge*. PNNL-11381, Pacific Northwest National Laboratory, Richland, Washington.

Lumetta GJ, IE Burgeson, MJ Wagner, J Liu, and YL Chen. 1997. *Washing and Caustic Leaching of Hanford Tank Sludge: Results of FY1997 Studies*. PNNL-11636, Pacific Northwest National Laboratory, Richland, Washington.

Lumetta GJ, BM Rapko, J Liu, DJ Temer, and RD Hunt. 1998. *Washing and Caustic Leaching of Hanford Tank Sludges: Results of FY 1998 Studies*. PNNL-12026, Pacific Northwest National Laboratory, Richland, WA.

Rapko BM and GJ Lumetta. 2000. *Status Report on Phase Identification in Hanford Tank Sludges*. PNNL-13394, Pacific Northwest National Laboratory, Richland, Washington.

Temer DJ and R Villarreal. 1995. *Sludge Washing and Alkaline Leaching Tests on Actual Hanford Tank Sludges: A Status Report*. LAUR-95-2070, Los Alamos National Laboratory, Los Alamos, New Mexico.

Temer DJ and R Villarreal. 1996. *Sludge Washing and Alkaline Leaching Tests on Actual Hanford Tank Sludges: FY 1996 Results*. LAUR 96-2839, Los Alamos National Laboratory, Los Alamos, New Mexico.

Temer DJ and R Villarreal. 1997. *Sludge Washing and Alkaline Leaching Tests on Actual Hanford Tank Sludges: FY 1997 Results*. LAUR 97-2889, Los Alamos National Laboratory, Los Alamos, New Mexico.

Warrant RW and GA Cooke. 2003. *Characterization of the Solids Waste in the Hanford Waste Tanks using a Combination of XRD, SEM, and PLM, Advances in X-ray Analysis*. International Centre for Diffraction Data, 46:251–256.

Appendix D

Solid-Phase Compound Images

Appendix D – Solid-Phase Compound Images

Particle sizes were determined by measuring particles on calibrated images.

Example from Gibbsite Determination:

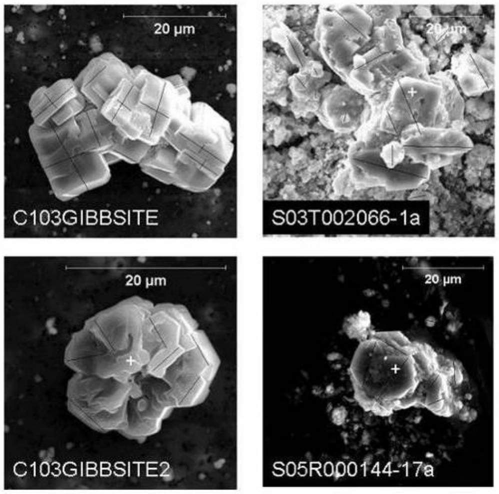

Figure D.1. Images of Gibbsite Showing Location of Measurements of Crystal Sizes.

Example from Phosphate Particle determination:

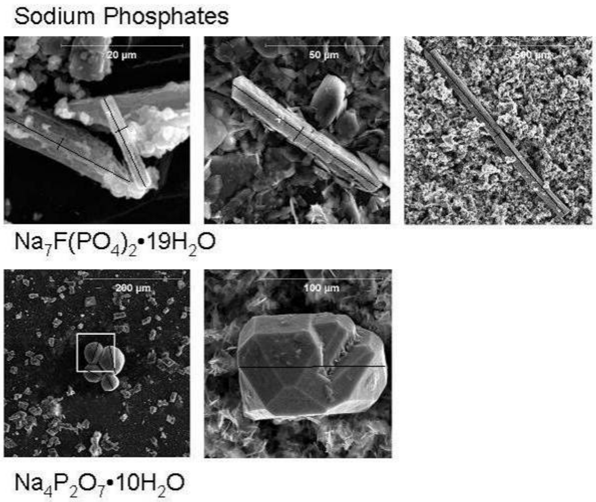

Figure D.2. Images of Sodium Phosphates Showing Particle Size Measurement Lines

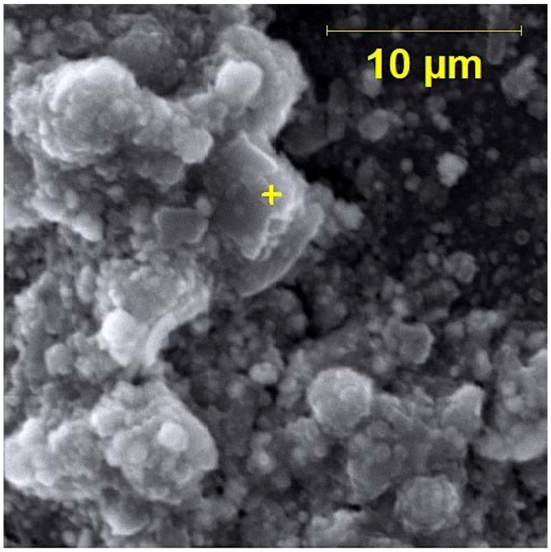

Figure D.3. Gibbsite/Al$(OH)_3$, from Tank AY-102[(a)]

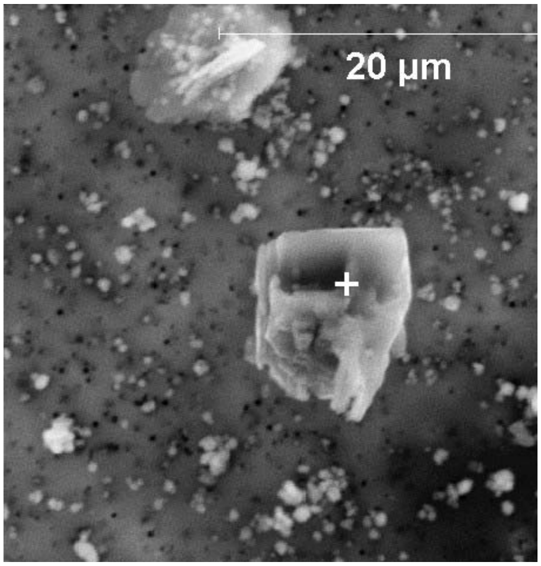

Figure D.4 Gibbsite/Al$(OH)_3$, from Tank C-106 (Bechtold et al. 2003)

(a) Warrant RW. "Results of Caustic Testing of Tank 241-AY-102 Core 319 Sludge Solids." 7S110-RWW-06-080, November 2006, CH2M HILL Hanford Group Inc., Richland, Washington.

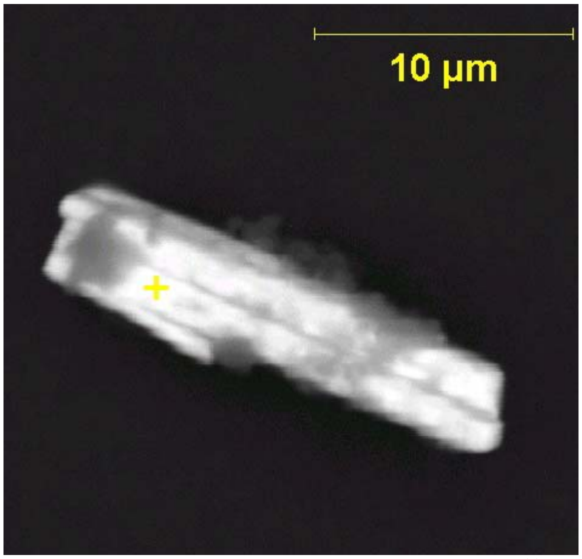

Figure D.5. Pu-Rich from Tank SY-102[(a)]

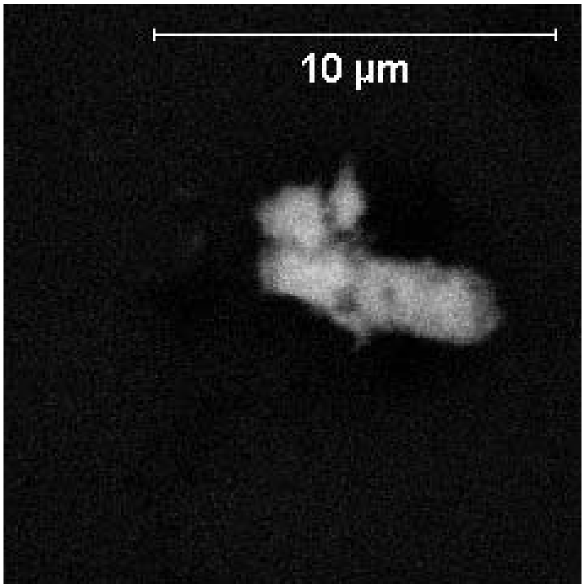

Figure D.6. $CaCO_3$, from Tank SY-102[(a)]

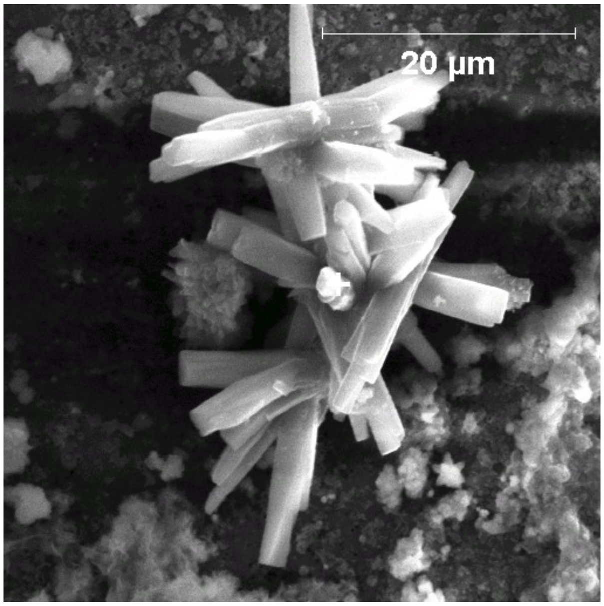

Figure D.7. Gibbsite/$Al(OH)_3$ from Tank AN-102b[(b)]

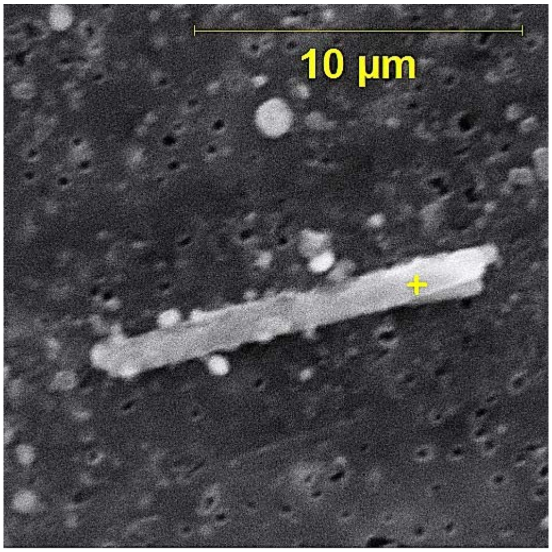

Figure D.8. $NaAlCO_3(OH)_2$ from Tank AY-102[(c)]

(a) Callaway WS and GA Cooke. "Distribution of Plutonium-Rich Particles in Tank 241-SY-102 Sludge." CH2M-0400872, 5/17/2004, CH2M HILL Hanford Group, Inc., Richland, Washington.

(b) Callaway WS, GA Cooke, and DL Herting. "Particle Size Measurements in Support of the Tank 241-AN-102 Chemistry Control Recovery Plan." 7S110-WSC-05-011, 3/18/2005, CH2M HILL Hanford Group Inc., Richland, Washington.

(c) Warrant RW. "Results of Caustic Testing of Tank 241-AY-102 Core 319 Sludge Solids." 7S110-RWW-06-080, November 2006, CH2M HILL Hanford Group Inc., Richland, Washington.

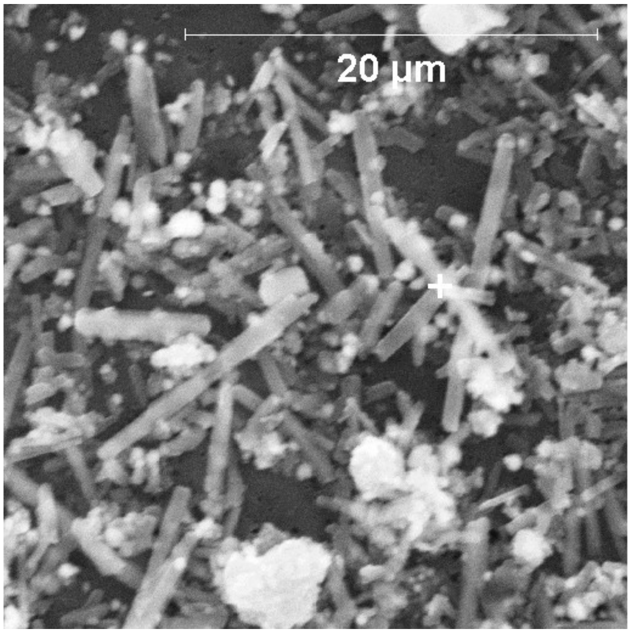

Figure D.9. $NaAlCO_3(OH)_2$ from Tank C-106 (Bechtold et al. 2003)

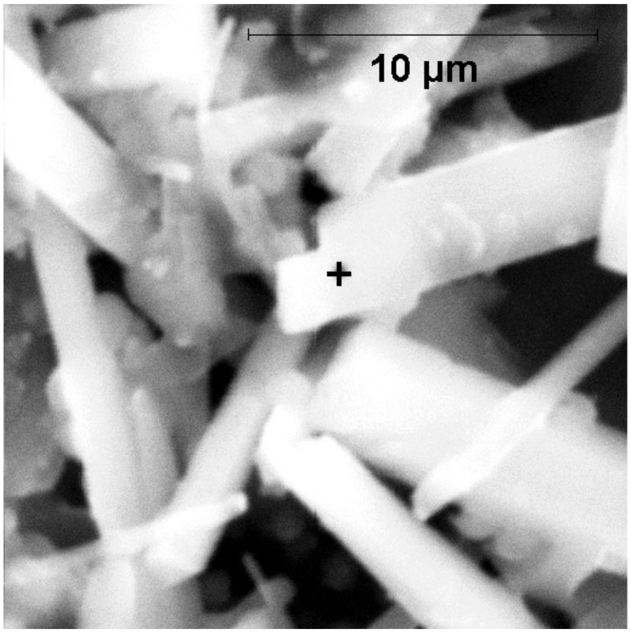

Figure D.11. $NaAlCO_3(OH)_2$, from Tank AN-107 (Herting et al. 2004)

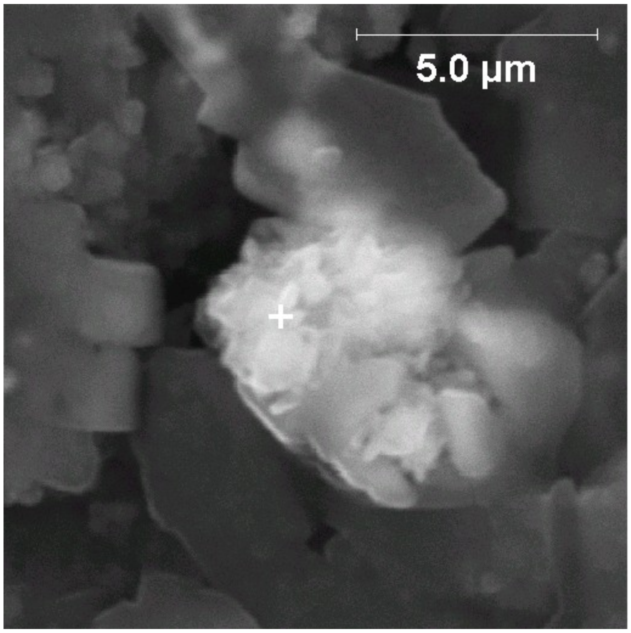

Figure D.10. $NaAlCO_3(OH)_2$, from Tank AN-102a[a]

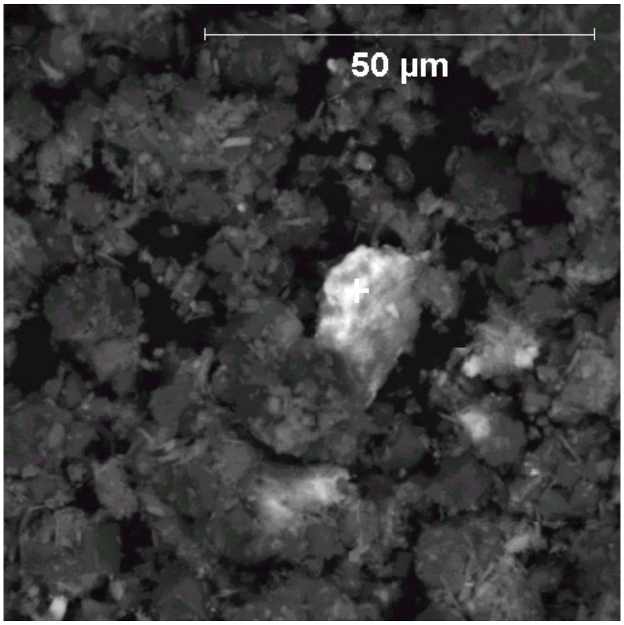

Figure D.12. $Na_2U_2O_7$, from Tank C-101[b]

---

[a] Herting DL. "Caustic Demand Test Results, Tank 241-AN-102 Sludges." FH-0303343, 8/28/2003, Fluor Hanford, Inc., Richland, Washington.

[b] Frye JM. "Results of Caustic Testing of 241-C-101 & 241-C-107." 7S110-JMF-05-015, 4/29/2005, CH2M HILL Hanford Group Inc., Richland, Washington.

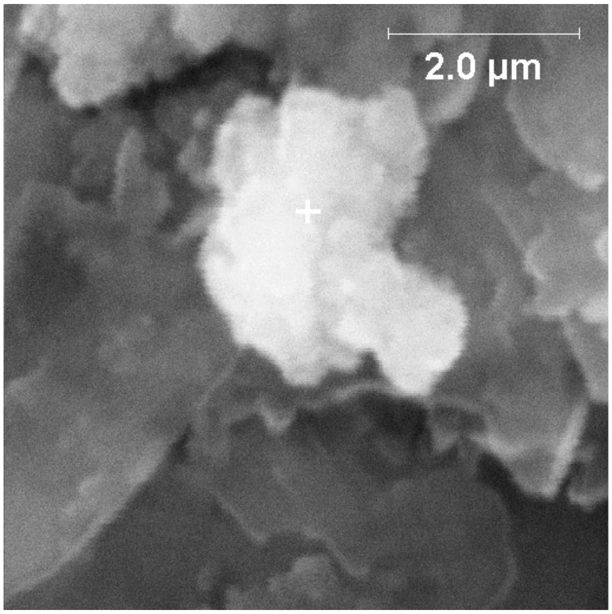

Figure D.13. $NaAlCO_3(OH)_2$ from Tank AN-107 (Herting et al. 2004)

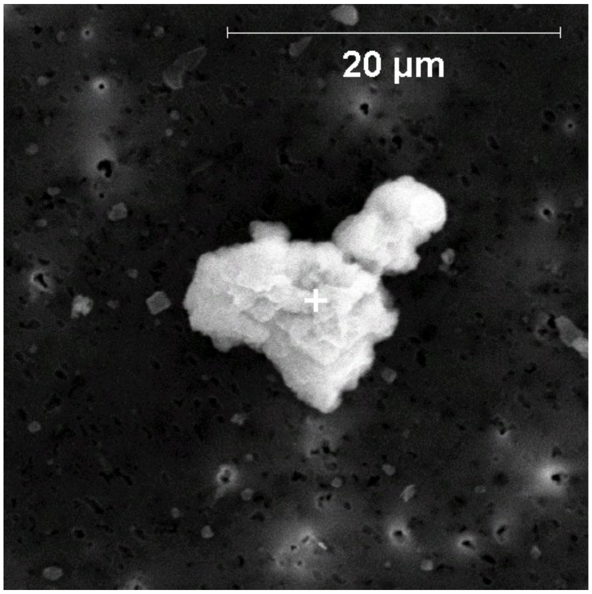

Figure D.14. $Na_2U_2O_7$ from Tank SY-102(a)

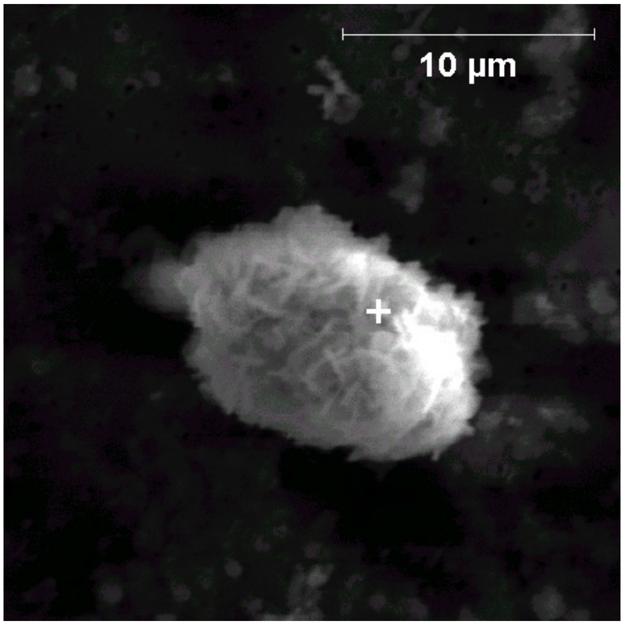

Figure D.15. $Na_2U_2O_7$ from Tank AN-102b(b)

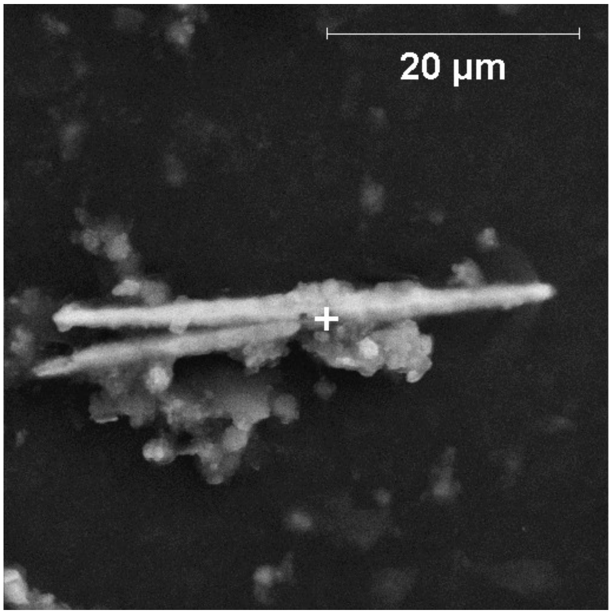

Figure D.16. $Na_2U_2O_7$ from Tank AN-107 (Herting et al. 2004)

(a) Callaway WS and GA Cooke. "Distribution of Plutonium-Rich Particles in Tank 241-SY-102 Sludge." CH2M-0400872, 5/17/2004, CH2M HILL Hanford Group, Inc., Richland, Washington.

(b) Callaway WS, GA Cooke, and DL Herting. "Particle Size Measurements in Support of the Tank 241-AN-102 Chemistry Control Recovery Plan." 7S110-WSC-05-011, 3/18/2005, CH2M HILL Hanford Group Inc., Richland, Washington.

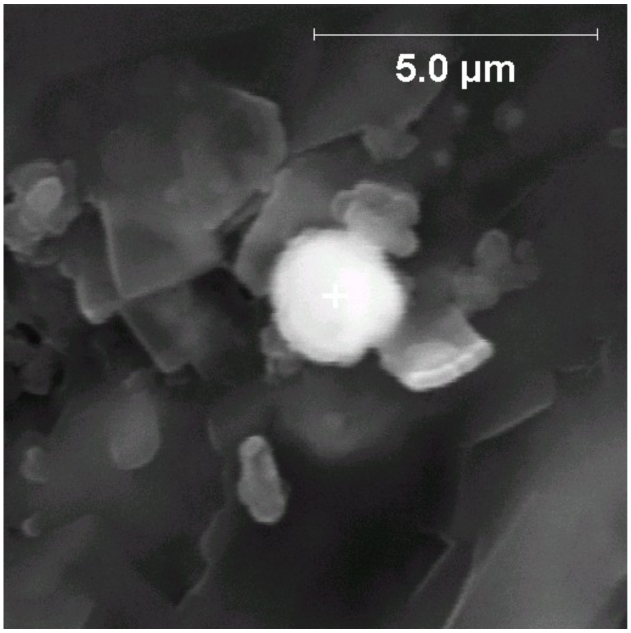

Figure D.17. $Na_2U_2O_7$ from Tank AN-102a[a]

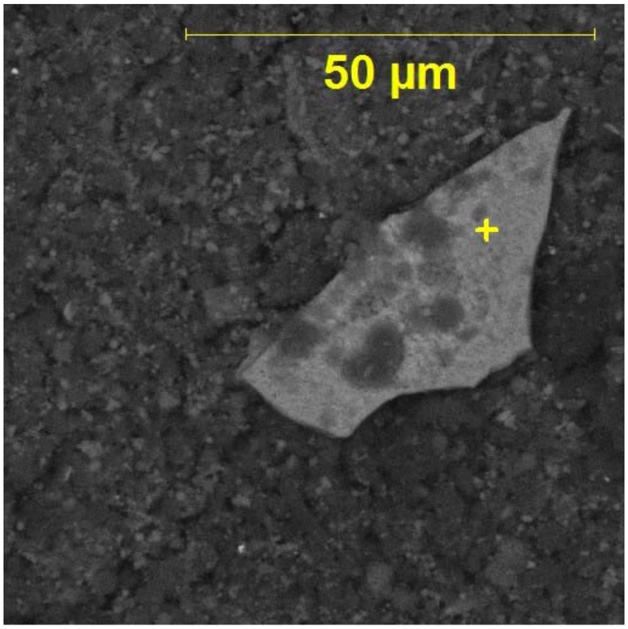

Figure D.19. ZrO_2 from Tank AY-102[b]

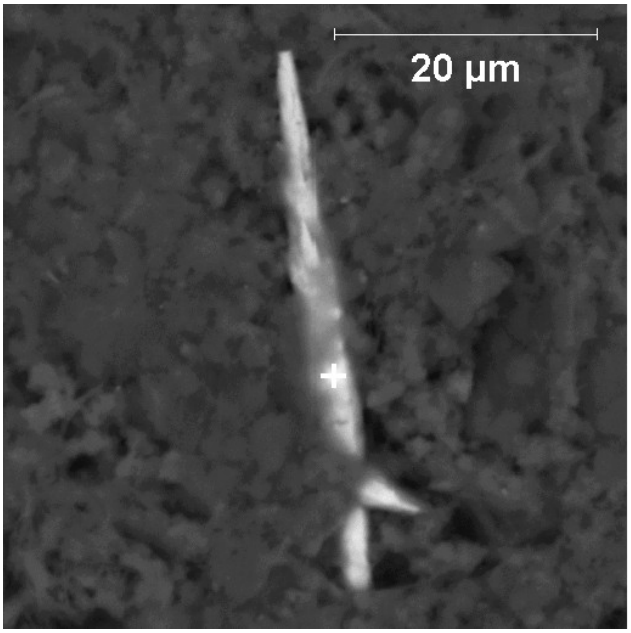

Figure D.18. $Na_2U_2O_7$ from Tank AN-107 (Herting et al. 2004)

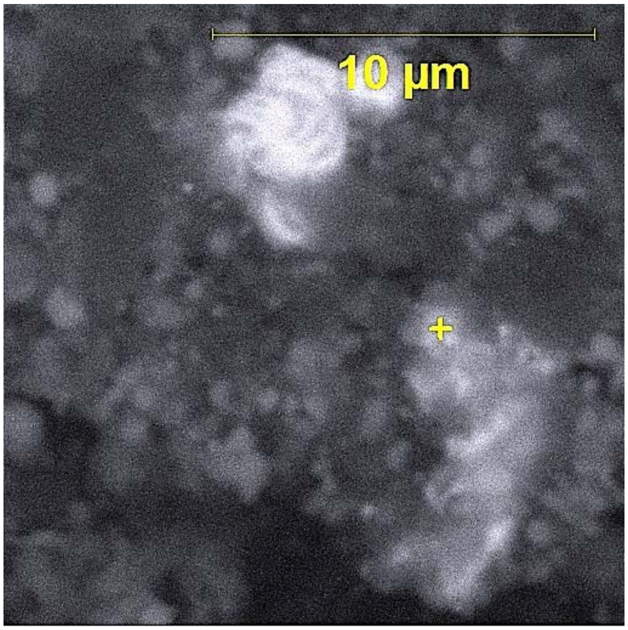

Figure D.20. Ag_2CO_3 from Tank AY-102[c]

---

[a] Herting DL. "Caustic Demand Test Results, Tank 241-AN-102 Sludges." FH-0303343, 8/28/2003, Fluor Hanford, Inc., Richland, Washington.

[b] Warrant RW. "Results of Caustic Testing of Tank 241-AY-102 Core 319 Sludge Solids." 7S110-RWW-06-080, November 2006, CH2M HILL Hanford Group Inc., Richland, Washington.

[c] Warrant RW. "Results of Caustic Testing of Tank 241-AY-102 Core 319 Sludge Solids." 7S110-RWW-06-080, November 2006, CH2M HILL Hanford Group Inc., Richland, Washington.

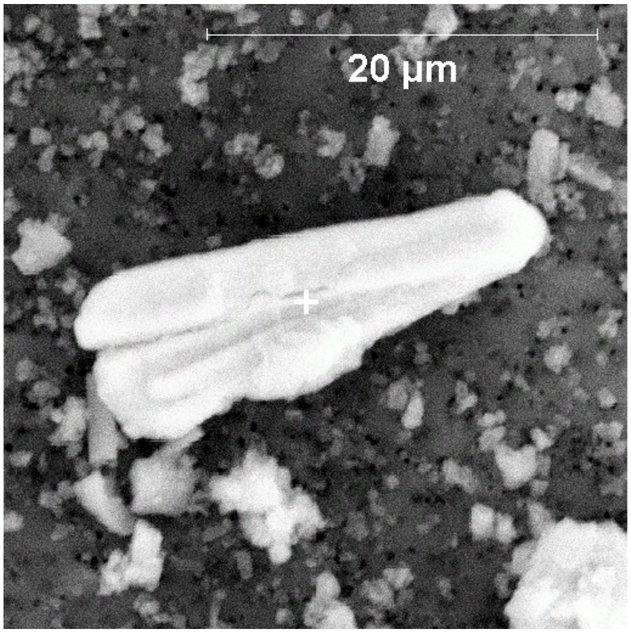

Figure D.21. ZrO_2, from Tank SY-102[a]

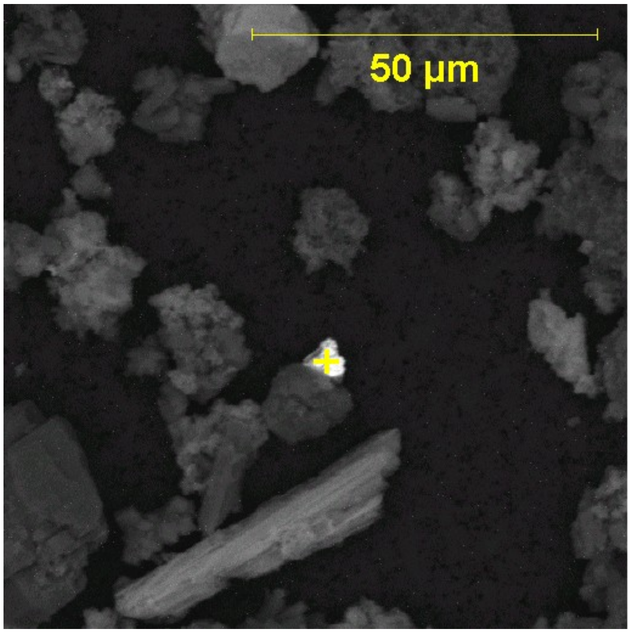

Figure D.22. Ag_2CO_3 from Tank SY-102[b]

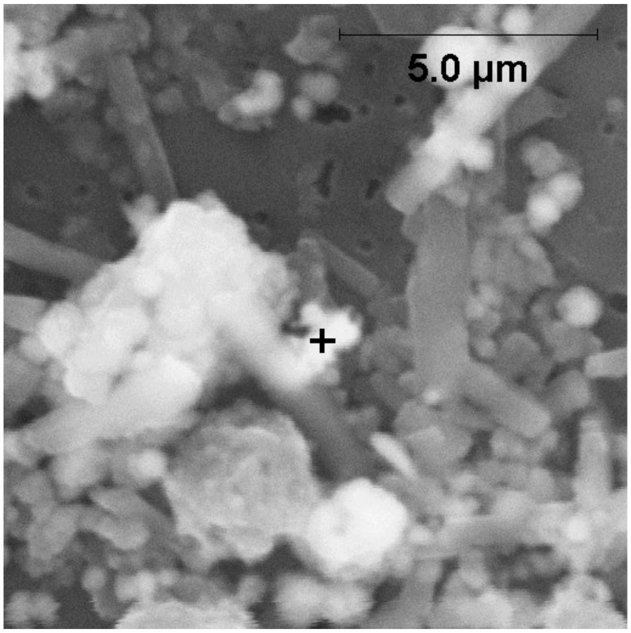

Figure D.23. Ag_2CO_3 from Tank C-106 (Bechtold et al. 2003)

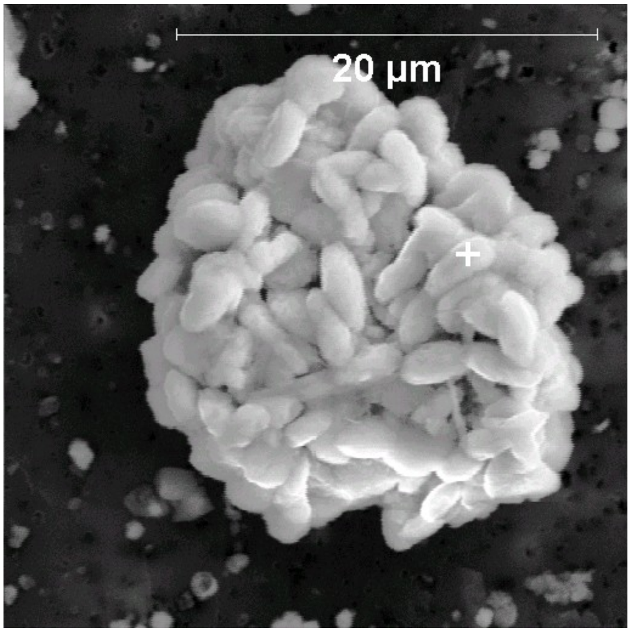

Figure D.24. Fe_2O_3 from Tank C-103[c]

---

[a] Callaway WS and GA Cooke. "Distribution of Plutonium-Rich Particles in Tank 241-SY-102 Sludge." CH2M-0400872, 5/17/2004, CH2M HILL Hanford Group, Inc., Richland, Washington.

[b] Callaway WS and GA Cooke. "Distribution of Plutonium-Rich Particles in Tank 241-SY-102 Sludge." CH2M-0400872, 5/17/2004, CH2M HILL Hanford Group, Inc., Richland, Washington.

[c] Herting DL and GA Cooke. "Caustic Demand Test Results for Tank 241-C-103 Sludge." 7S110-DLH-04-015, 5/5/2004, CH2M HILL Hanford Group, Inc., Richland, Washington.

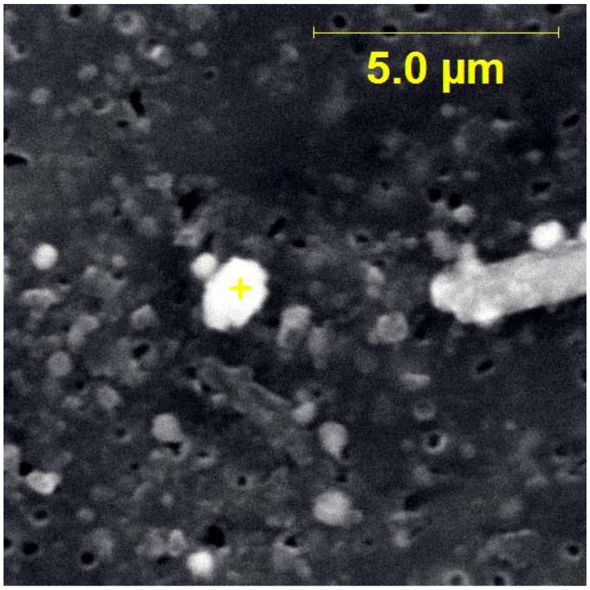

Figure D.25. Fe_2O_3 from Tank AY-102[(a)]

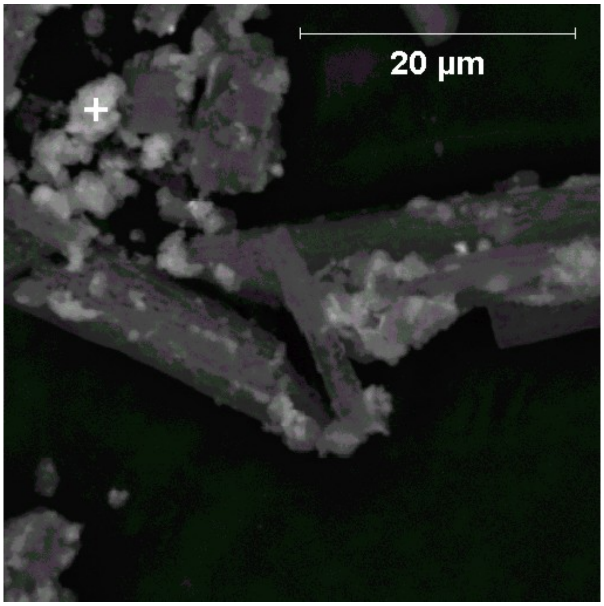

Figure D.26. Fe_2O_3 from Tank C-101[(b)]

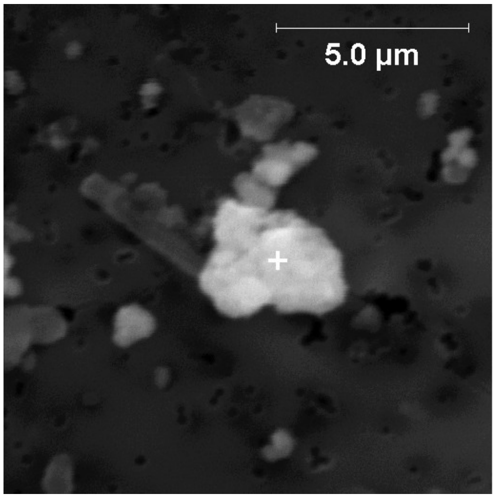

Figure D.27. Fe_2O_3 from Tank C-106 (Bechtold et al. 2003)

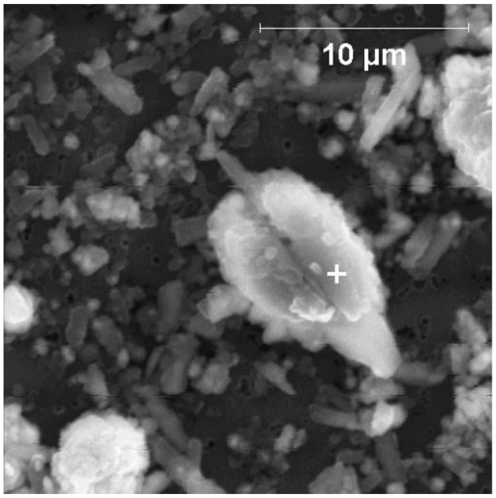

Figure D.28. $Mn_3(PO_4)_2$ from Tank C-106 (Bechtold et al. 2003)

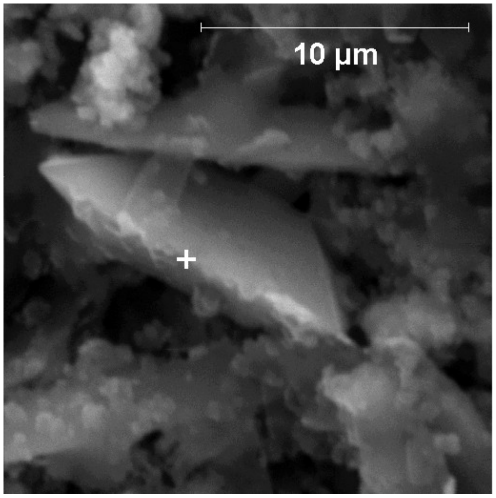

Figure D.29. $CaCO_3$ from Tank AN-107 (Herting et al. 2004)

(a) Warrant RW. "Results of Caustic Testing of Tank 241-AY-102 Core 319 Sludge Solids." 7S110-RWW-06-080, November 2006, CH2M HILL Hanford Group Inc., Richland, Washington.

(b) Frye JM. "Results of Caustic Testing of 241-C-101 & 241-C-107." 7S110-JMF-05-015, 4/29/2005, CH2M HILL Hanford Group Inc., Richland, Washington.

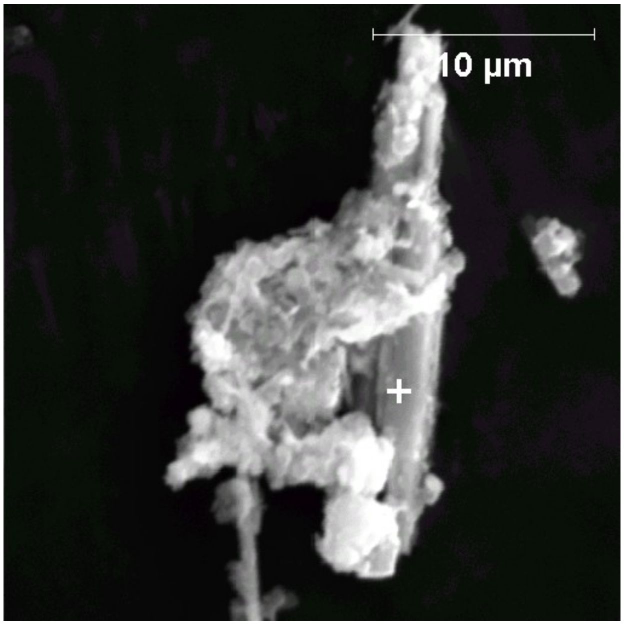

Figure D.30. $BiPO_4$ from Tank C-107[a]

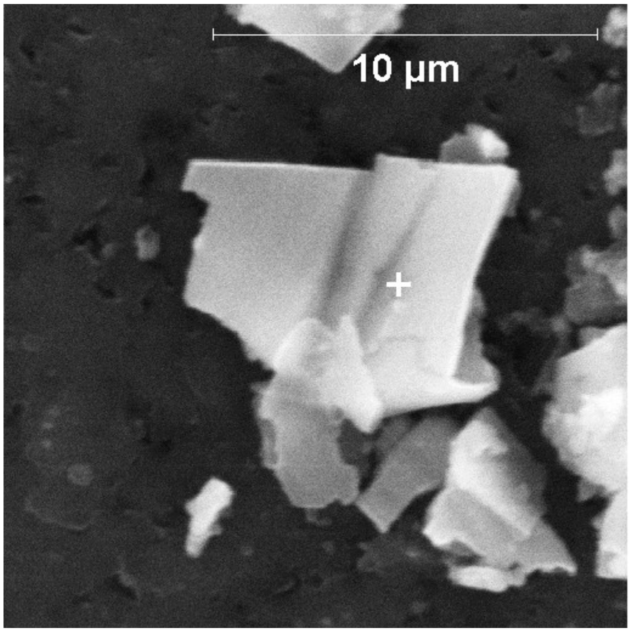

Figure D.31. $MnCO_3$ from Tank C-106 (Bechtold et al. 2003)

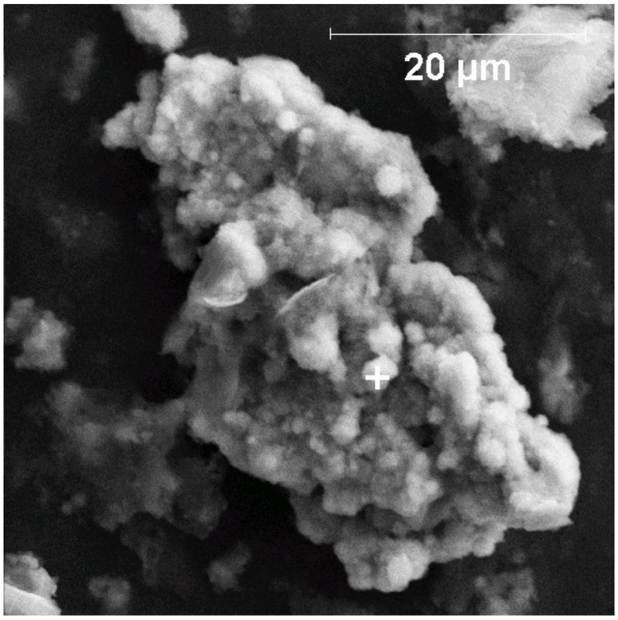

Figure D.32. Fe_2O_3 from Tank AN-107 (Herting et al. 2004)

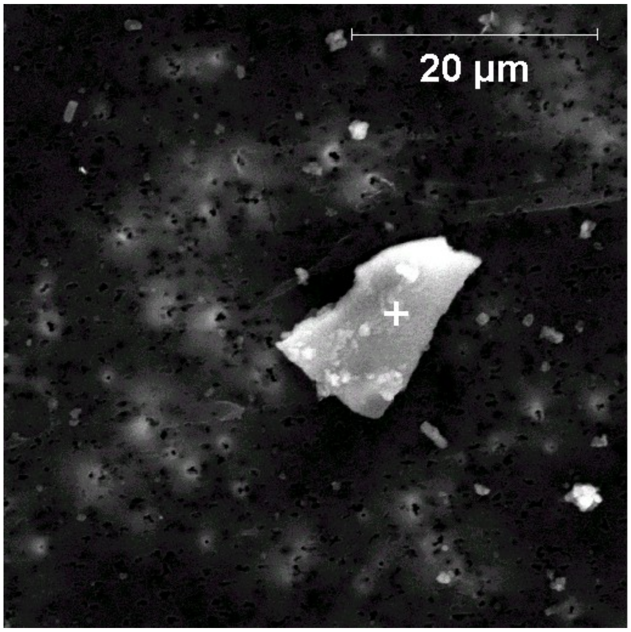

Figure D.33. Fe_2O_3 from Tank SY-102[b]

---

[a] Frye JM. "Results of Caustic Testing of 241-C-101 & 241-C-107." 7S110-JMF-05-015, 4/29/2005, CH2M HILL Hanford Group Inc., Richland, Washington.

[b] Callaway WS and GA Cooke. "Distribution of Plutonium-Rich Particles in Tank 241-SY-102 Sludge." CH2M-0400872, 5/17/2004, CH2M HILL Hanford Group, Inc., Richland, Washington.

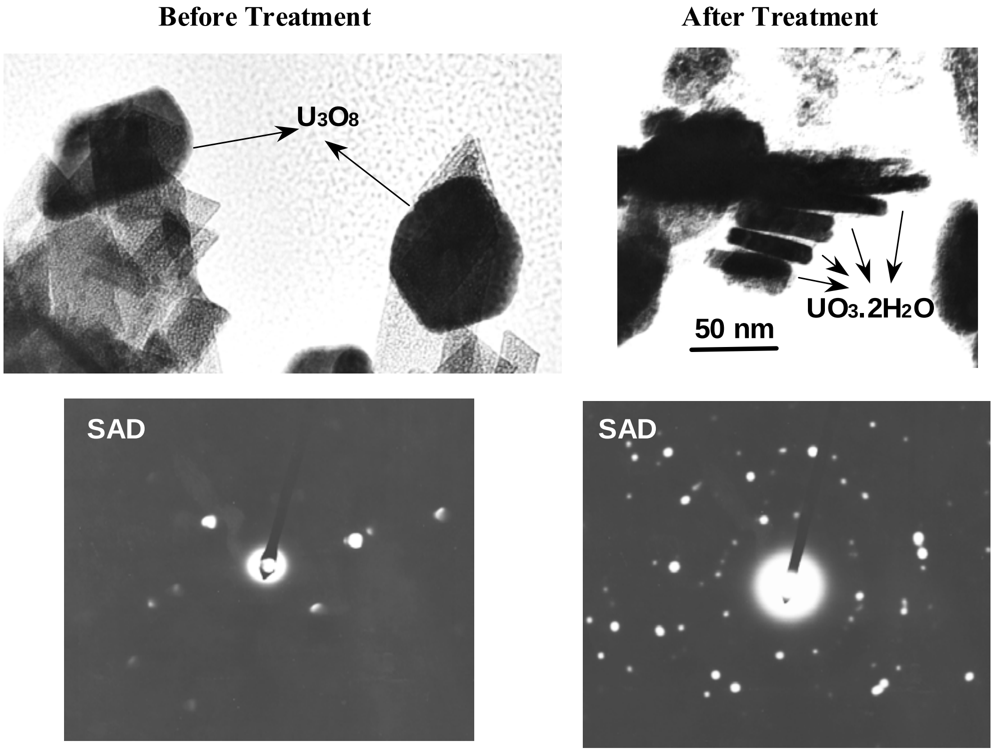

Figure D.34. Uranium Oxide Species Before and After Leaching S-104 Sludge (Lumetta et al. 1997)

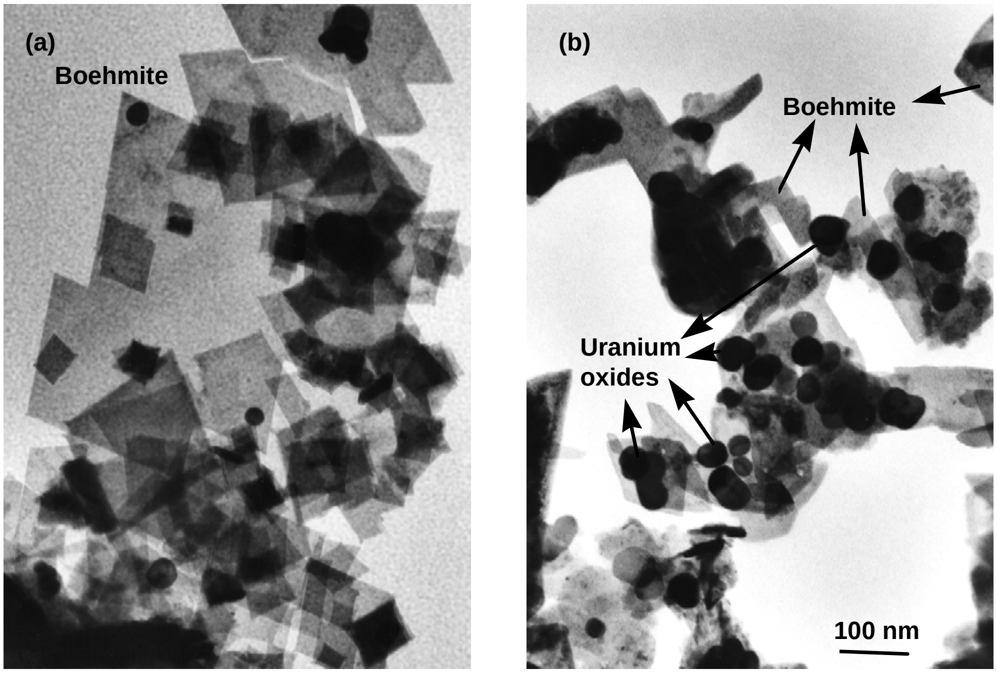

Figure D.35. Micrograph of S-101 Sludge Boehmite Particles Before (a) and After (b) Leaching (Lumetta et al. 1997)

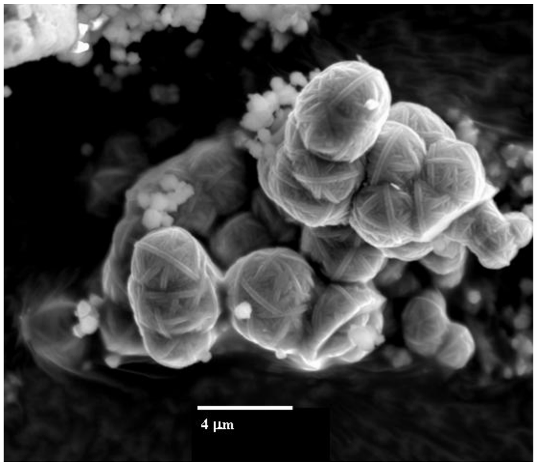

Figure D.36. Cancrinite from Tank AP-101 (Buck and McNamara 2004)

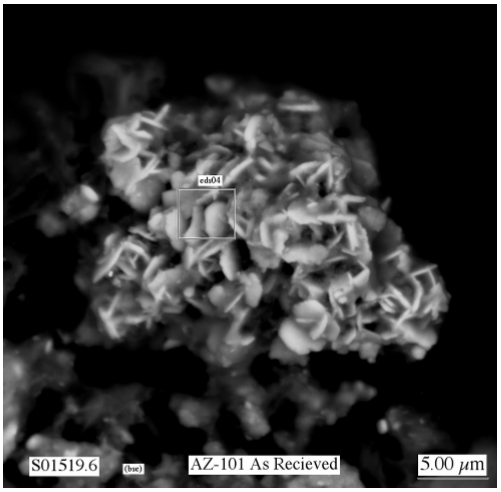

Figure D.37. Hematite from Tank AZ-101 (Buck et al. 2003)

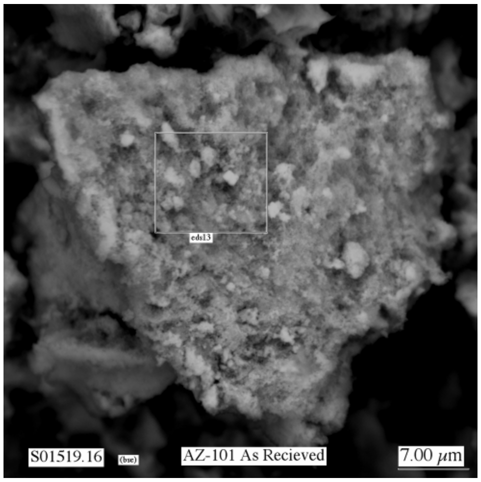

Figure D.38. $Mn(OH)_2$ from Tank AZ-101 (Buck et al. 2003)

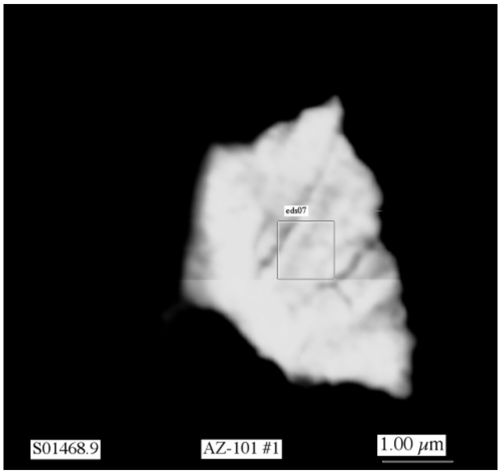

Figure D.39. Uranium Oxide Phase from Tank AZ-101 (Buck et al. 2003)

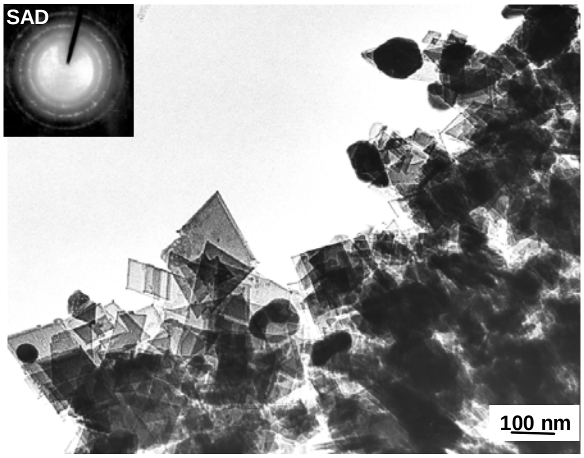

Figure D.40. Boehmite Particles from Tank S-104 (Lumetta et al. 1997)

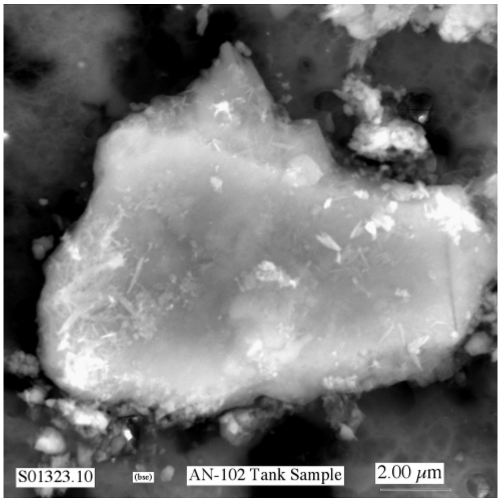

Figure D.41. Zeolite Phase from Tank AN-102 (Buck et al. 2003)

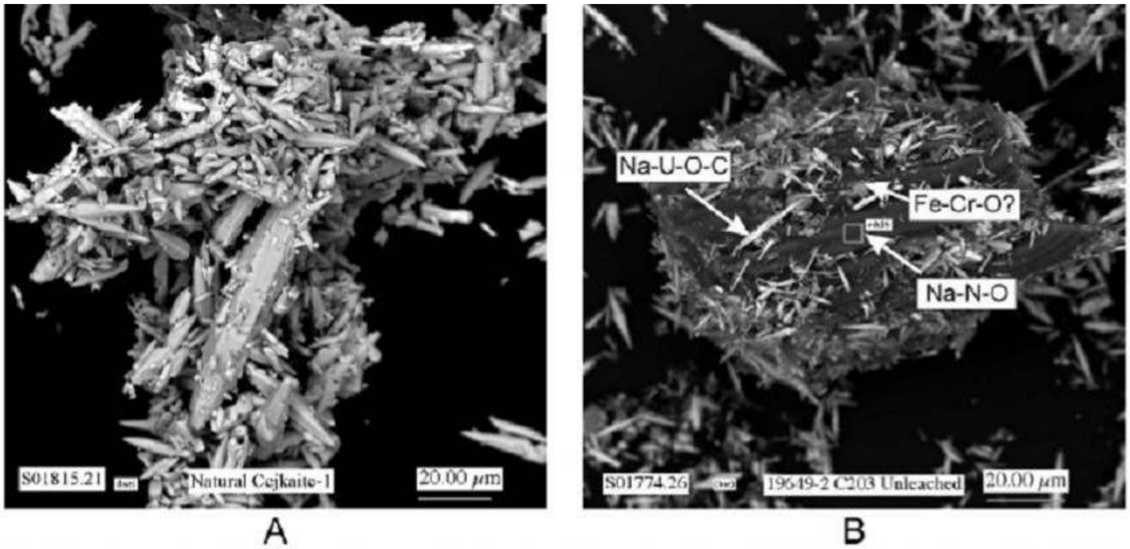

Figure D.42. Uranium Carbonate Phase from Tank C-106 (Krupka et al. 2006)

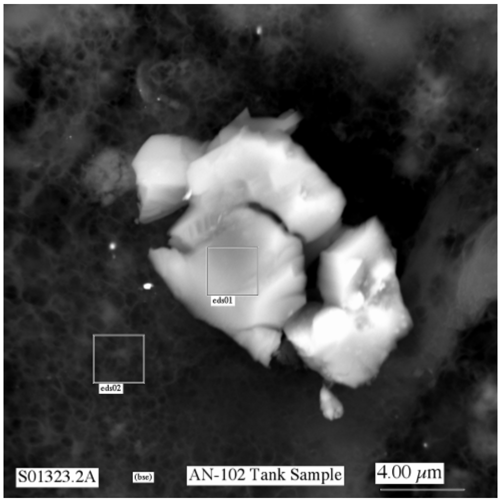

Figure D.43. Zeolite Phase from Tank AN-102 (Buck et al. 2003)

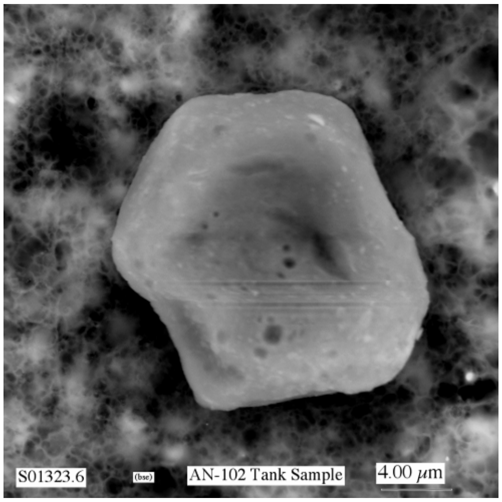

Figure D.44. Zeolite Phase from Tank AN-102 (Buck et al. 2003)

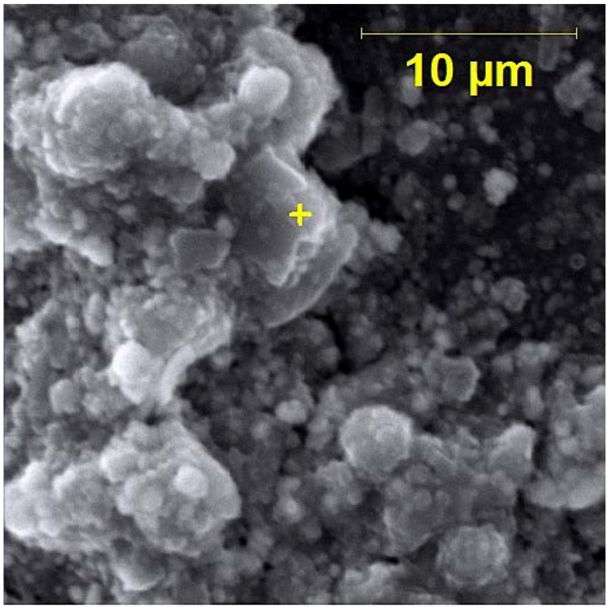

Figure D.45. Gibbsite/Al(OH)$_3$ from Tank AY-102[a]

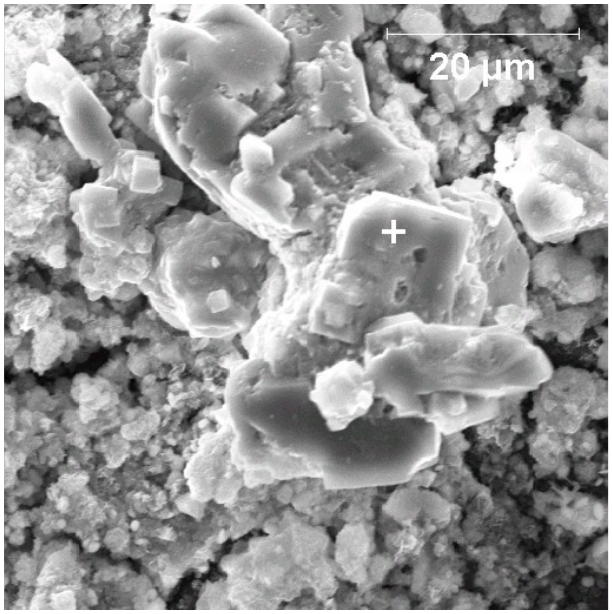

Figure D.46. Gibbsite/Al(OH)$_3$ from Tank AZ-102 (Warrant 2002)

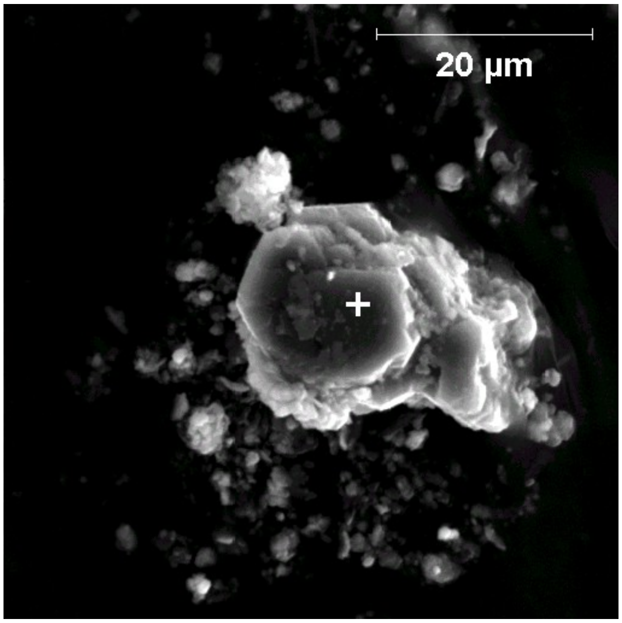

Figure D.47. Gibbsite/Al(OH)$_3$ from Tank C-101[b]

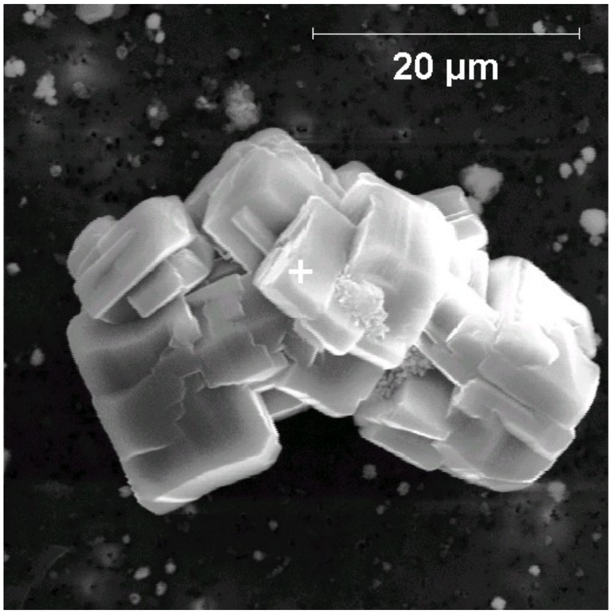

Figure D.48. Gibbsite/Al(OH)$_3$ from Tank C-103a[c]

---

[a] Warrant RW. "Results of Caustic Testing of Tank 241-AY-102 Core 319 Sludge Solids." 7S110-RWW-06-080, November 2006, CH2M HILL Hanford Group Inc., Richland, Washington.

[b] Frye JM. "Results of Caustic Testing of 241-C-101 & 241-C-107." 7S110-JMF-05-015, 4/29/2005, CH2M HILL Hanford Group Inc., Richland, Washington.

[c] Herting DL and GA Cooke. "Caustic Demand Test Results for Tank 241-C-103 Sludge." 7S110-DLH-04-015, 5/5/2004, CH2M HILL Hanford Group, Inc., Richland, Washington.

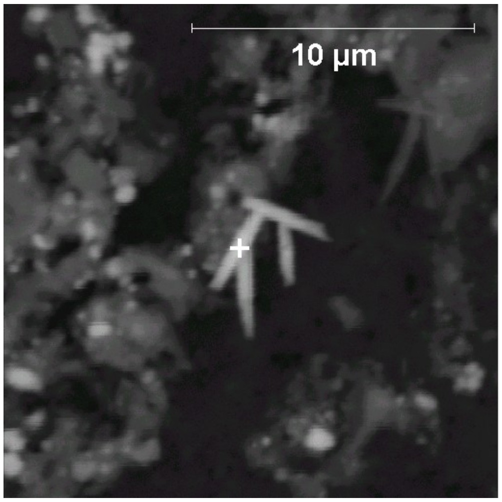

Figure D.49. $LaPO_4 \cdot 2H_2O$ from Tank AY-102[a]

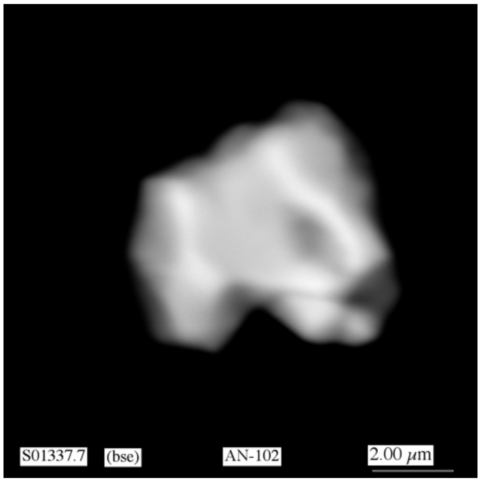

Figure D.50. Uranium Oxide Phase from Tank AZ-101 (Buck et al. 2003)

---

[a] Frye JM. "Results of Caustic Testing of 241-C-101 & 241-C-107." 7S110-JMF-05-015, 4/29/2005, CH2M HILL Hanford Group Inc., Richland, Washington.

}

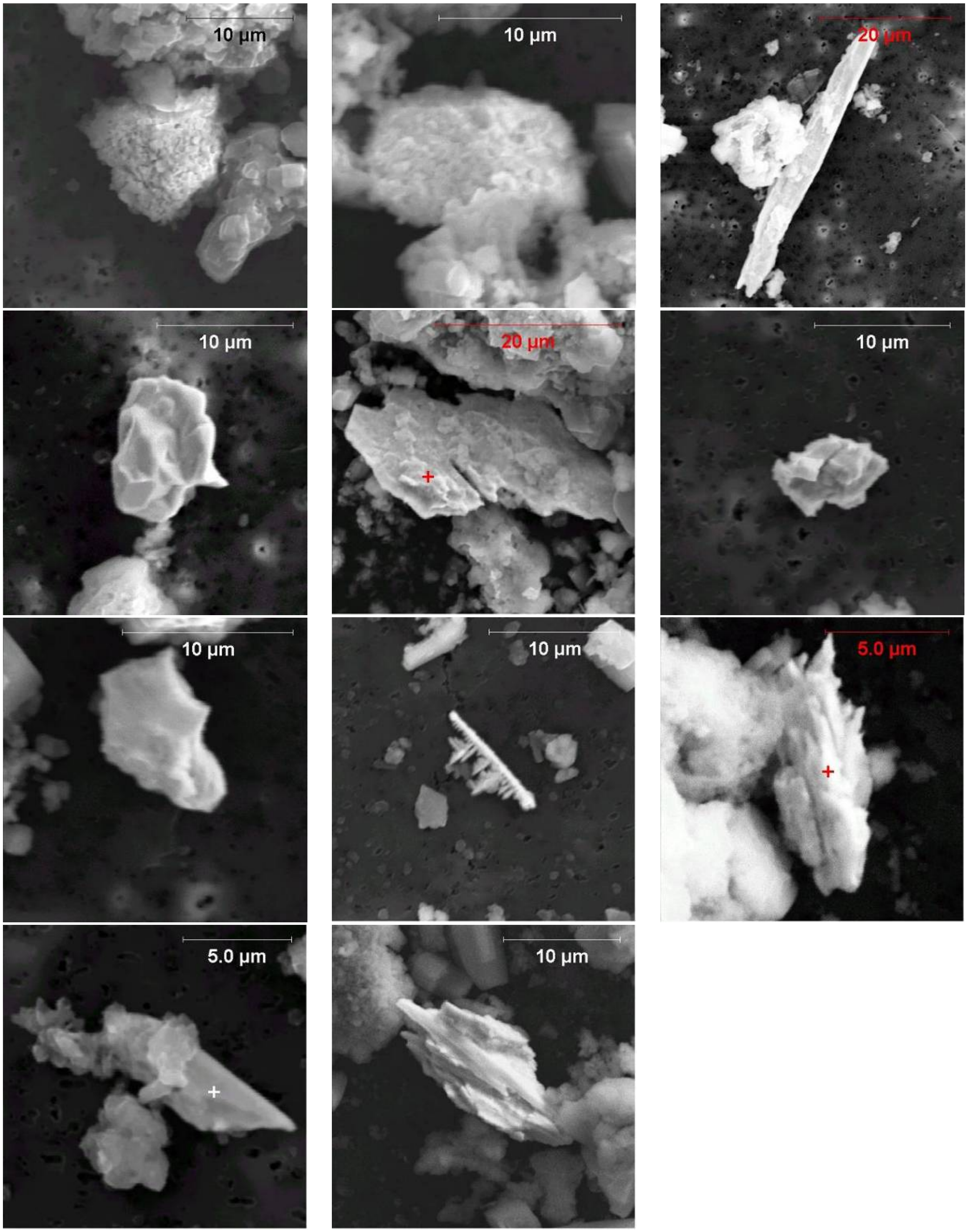

Figure D.51. Pu Oxide from Tank SY-102[a]

---

[a] Callaway WS and GA Cooke. "Distribution of Plutonium-Rich Particles in Tank 241-SY-102 Sludge." CH2M-0400872, 5/17/2004, CH2M HILL Hanford Group, Inc., Richland, Washington.

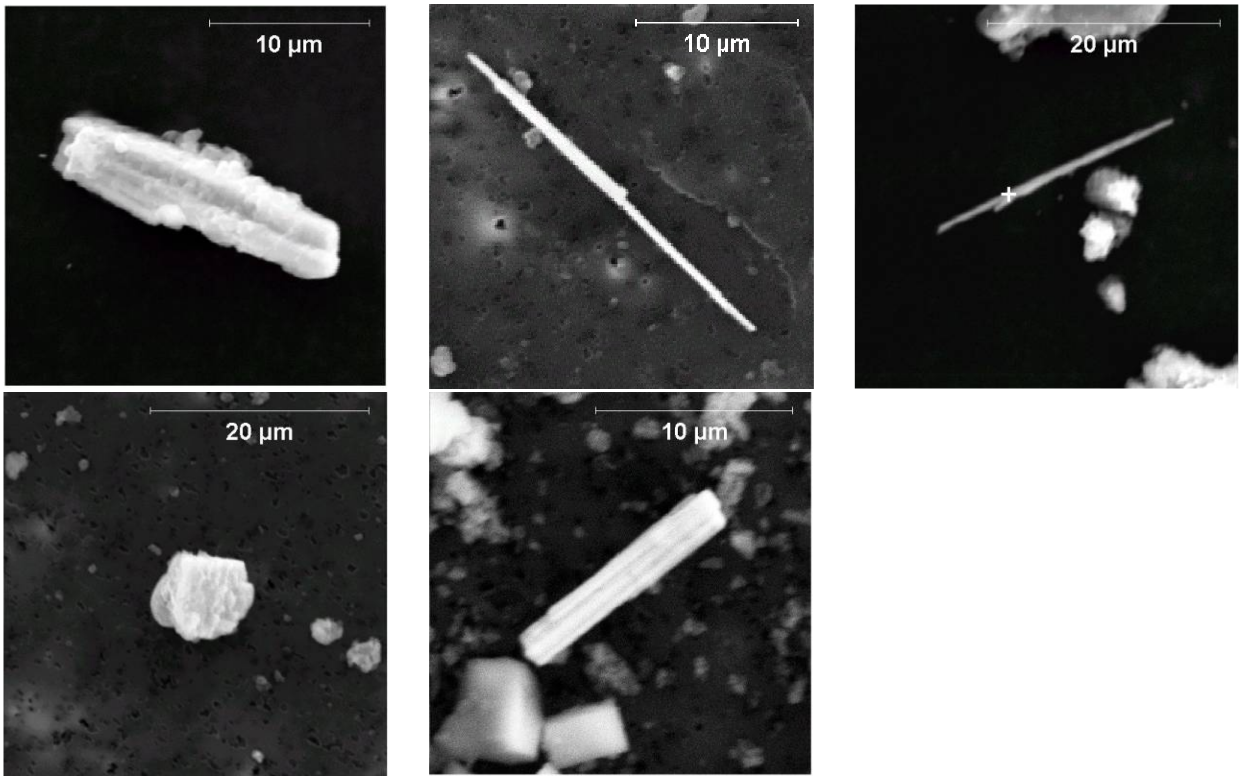

Figure D.52. Pu-Bi-Rich Particulate from Tank SY-102[a]

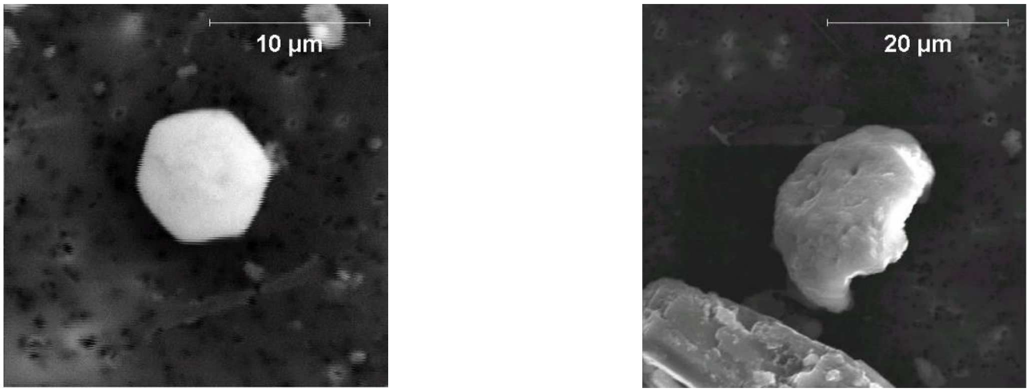

Figure D.53. Pu-Bi-P-Rich Particulate, From Tank SY-102[b]

---

[a] Callaway WS and GA Cooke. "Distribution of Plutonium-Rich Particles in Tank 241-SY-102 Sludge." CH2M-0400872, 5/17/2004, CH2M HILL Hanford Group, Inc., Richland, Washington.

[b] Callaway WS and GA Cooke. "Distribution of Plutonium-Rich Particles in Tank 241-SY-102 Sludge." CH2M-0400872, 5/17/2004, CH2M HILL Hanford Group, Inc., Richland, Washington.

References

Bechtold DB, GA Cooke, DL Herting, JC Person, RS Viswanath, and RW Warrant. 2003. *Laboratory Testing of Oxalic Acid Dissolution of Tank 241-C-106 Sludge.* RPP-17158 Rev. 0, Fluor Hanford, Inc., Richland, Washington.

Buck EC and BK McNamara. 2004. "Precipitation of Nitrate-Cancrinite in Hanford Tank Sludge," *Environ. Sci. Technol.* 38, pp. 4432-4438.

Buck EC, BW Arey, SK Fiskum, JGH Geeting, ED Jensen, BK McNamara, and AP Poloski. 2003. *Identification of Washed Solids from Hanford Tanks 241-AN-102 and 241-AZ-101 with X-ray Diffraction, Scanning Electron Microscopy, and Light-Scattering Particle Analysis.* PNWD-3300 (WTP-RPT-076 Rev. 0), Battelle – Pacific Northwest Division, Richland, Washington.

Herting DL, GA Cooke, and RW Warrant. 2004. *Hanford Tank 241-AN-107 Solid Phase Characterization*, RPP-20018, CH2M HILL Hanford Group, Inc., Richland, Washington.

Krupka KM, HT Schaef, BW Arey, SM Heald, WJ Deutsch, and KJ Lindberg. 2006. "Cantrell, Residual Waste from Hanford Tanks 241-C-203 and 241-C-204. 1. Solids Characterization." *Environ. Sci. Technol.*, 40:3749–3754.

Lumetta GJ, IE Burgeson, MJ Wagner, J Liu, and YL Chen. 1997. *Washing and Caustic Leaching of Hanford Tank Sludge: Results of FY1997 Studies*. PNNL-11636, Pacific Northwest National Laboratory, Richland, Washington.

Warrant RW. 2002. *Results of Retrieval Testing of Sludge from Tank 241-AZ-102.* RPP-9806 Rev. 0, Fluor Hanford Inc., Richland, Washington.

Appendix E

Expert Elicitation

Appendix E – Expert Elicitation

Teams of experts relevent to this study were assembled. These experts included:

E. C. Buck	PNWD
R. C. Daniel	PNWD
W. S. Callaway III	CH2M HILL
G. A. Cooke	CH2M HILL
S. K. Cooley	PNWD
J. J. Davis	DOE - ORP
M. N. Hall	BNI
DL Herting	CH2M HILL
M. E. Johnson	CH2M HILL
M. A. Knight	CH2M HILL
G. J. Lumetta	PNWD
L. A. Mahoney	PNWD
J. E. Meacham	CH2M HILL
P. A. Meyer	PNWD
A. P. Poloski	PNWD
J. G. Reynolds	BNI
S. L. Thomson	BNI
M. G. Thien	CH2M HILL
J. M. Tingey	PNWD
G. L. Smith	BNI
Y. Onishi	Yasuo Onishi Consulting, LLC
D. R. Rector	PNWD
D. J. Washenfelder	CH2M HILL
B. E. Wells	PNWD

Distribution

No. of
Copies

OFFSITE

1 Savannah River National Laboratory
Richard Edwards
Savannah River National Laboratory
Westinghouse SA
Aiken, SC 29808-0001

1 Yasuo Onishi Consulting, LLC
Y. Onishi
144 Spengler St.
Richland, WA 99354

No. of
Copies

ONSITE

13 Battelle – Pacific Northwest Division

E. C. Buck	P7-27
R. C. Daniel	P7-22
S. K. Cooley	K6-08
D. E. Kurath	P7-28
G. J. Lumetta	P7-22
L. A. Mahoney	K7-15
P. A. Meyer	K7-15
A. P. Poloski	P7-25
D. R. Rector	K7-15
C. W. Stewart	K7-15
J. M. Tingey	P7-25
B. E. Wells	K7-15
Project Office (1)	P7-28

12 Bechtel National, Inc.

R. A. Brouns	H4-02
G. Duncan	H4-02
P. A. Fisher (2)	H4-02
M. N. Hall	H4-02
J. G. Reynolds	H4-02
S. A. Saunders	H4-02
G. L. Smith	H4-02
E. L. Strieper	H4-02
S. L. Thomson	H4-02
S. W. Vail	H4-02
R. Voke	H4-02

7 CH2M HILL Hanford Group, Inc.

W. S. Callaway III	T6-07
G. A. Cooke	T6-07
M. E. Johnson	H6-19
M. A. Knight	R2-58
J. E. Meacham	R2-58
M. G. Thien	H6-03
D. J. Washenfelder	R2-58